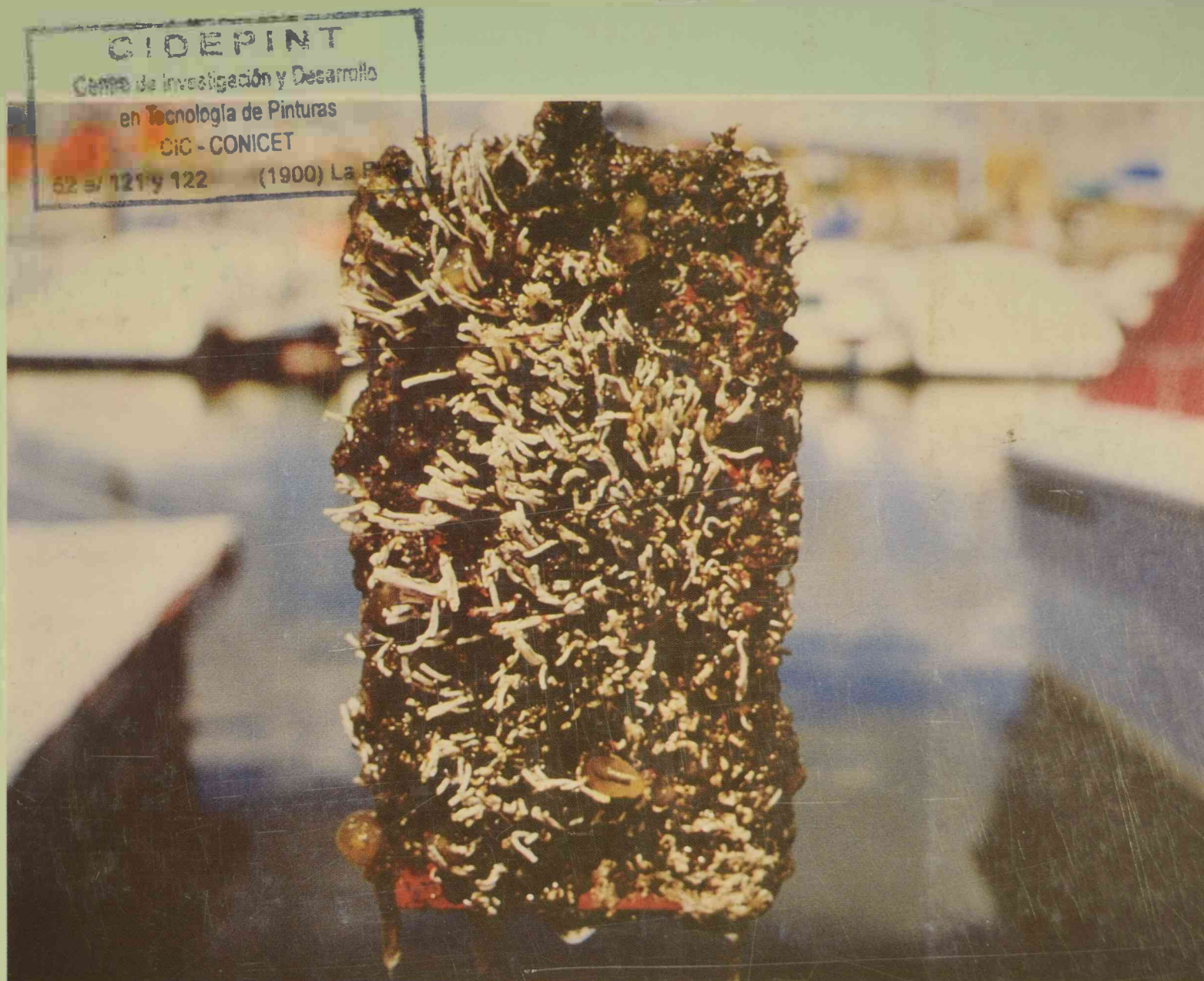


cidepint

ISSN - 0325 - 4186



CENTRO DE INVESTIGACION Y DESARROLLO
EN TECNOLOGIA DE PINTURAS
CIC - CONICET

ANALES 1996

El Centro de Investigación y Desarrollo en Tecnología de Pinturas es patrocinado actualmente por la Comisión de Investigaciones Científicas de la Provincia de Buenos Aires (CIC) y por el Consejo Nacional de Investigaciones Científicas y Técnicas (CONICET).

Los objetivos fundamentales de su creación fueron los siguientes: obtener nuevos desarrollos tecnológicos relativos a pinturas y revestimientos protectores, particularmente en aquellos aspectos que puedan resultar de mayor interés desde el punto de vista nacional; formar y perfeccionar investigadores y técnicos; y finalmente, asesorar y prestar asistencia técnica a entidades estatales y privadas, realizar peritajes y efectuar estudios especiales y tareas de control de calidad en los temas de su especialidad.

Desarrolla sus actividades en las siguientes áreas de investigación: estudios electroquímicos aplicados a problemas de corrosión y anticorrosión; análisis electroquímico; propiedades fisicoquímicas de películas de pintura; propiedades protectora de películas de pintura; planta piloto; análisis orgánico; química analítica general, cromatografía e inscrustaciones biológicas.

Durante los últimos treinta años los trabajos realizados se han publicado en diferentes revistas nacionales e internacionales: Anales de la Asociación Química Argentina, Revista de Ingeniería, Revista Latinoamericana de Ingeniería Química y Química Aplicada y Revista del Museo de Ciencias Naturales Bernardino Rivadavia (Argentina); Revista Iberoamericana de Corrosión y Protección (España); Journal of Coatings Technology, Industrial Engineering Chemistry Research, Journal of Solution Chemistry, Journal of Chromatography, Journal of Chromatographic Science, Journal of Colloid and Interface Science y Journal of Physical Chemistry (EE.UU.); Marine Biology, European Coatings Journal (Alemania Occidental); Journal of the Oil and Colour Chemists Association y Journal of Chemical Technology and Biotechnology (Gran Bretaña); Progress in Organic Coatings (Suiza); Pitture e Vernice (Italia); Revista de la Sociedad Química de México (México); Peintures, Pigments, Vernis y Corrosion Marine Fouling (Francia).

Organismos de "fouling" fijados sobre un panel experimental. Puerto de Mar del Plata, un mes de inmersión.

(05)
PINT
C37
2007

CIDEPINT

Centro de Investigación y Desarrollo
en Tecnología de Pinturas

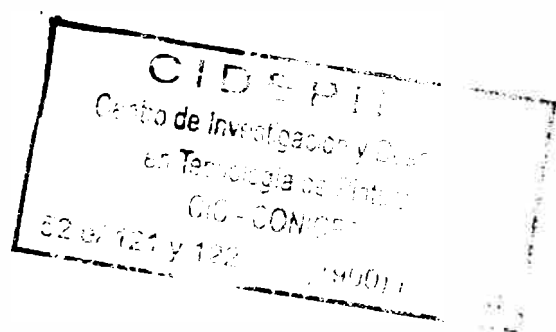
CIC - CONICET

52 e/ 121 y 122 (1900) La Plata

CIDEPINT agradece expresamente el apoyo económico que los organismos promotores (Comisión de Investigaciones Científicas de la Provincia de Buenos Aires y Consejo Nacional de Investigaciones Científicas y Técnicas) prestaron para la realización de los trabajos que constituyen el presente volumen.

**Editor: CENTRO DE INVESTIGACION Y DESARROLLO EN
TECNOLOGIA DE PINTURAS**

**Dirección: 52 entre 121 y 122
1900 La Plata - Argentina
Teléfonos: (021) 831141/44 y (021) 216214
Fax: 54-21-271537**



CIDEPINT-Anales es indizado periódicamente en:

**Aquatic Sciences and Fisheries Abstracts (México)
Centre de Documentation CNRS (Francia)
Chemical Abstracts (EE.UU.)
Referativnyi Zhurnal (Rusia)
World Surface Coatings Abstracts (Gran Bretaña)**

Diagramación: Prof. Viviana M. Segura

COMITE DE REPRESENTANTES

Comisión de Investigaciones Científicas de la Provincia de Buenos Aires (CIC)

Ing. Carlos Mayer (Titular)
Ing. Carlos Gigola (Alternó)

Consejo Nacional de Investigaciones Científicas y Técnicas (CONICET)

Dra. Noemí Walsöe de Reca (Titular)
Dr. José María Carella (Alternó)

DIRECTOR

Dr. Vicente J. D. Rascio

SUBDIRECTOR

Ing. Quím. Alejandro R. Di Sarli

JEFES DE AREA

Ing. Quím. Ricardo A. Armas
Propiedades Fisicoquímicas de Películas de Pintura

Ing. Quím. Juan J. Caprari
Propiedades Protectoras de Películas de Pintura

Dr. Ing. Carlos A. Giúdice
Estudios en Planta Piloto

Dr. Vicente F. Vetere
Estudios Electroquímicos Aplicados a Problemas
de Corrosión y Anticorrosión

Ing. Quím. Alejandro R. Di Sarli
Análisis Electroquímico de Pinturas y Revestimientos

Dr. Javier I. Amalvy
Materiales Poliméricos

Dr. Reynaldo C. Castells
Cromatografía

Tco. Quím. Rodolfo R. Iasi
Absorción Atómica

Ing. Quím. Silvia Zicarelli
Espectrofotometría

Lic. Mirta E. Stupak
Incrustaciones Biológicas

COMENTARIOS DE LA DIRECCION DEL CIDEPINT

En este volumen (el número vigésimo noveno de la serie iniciada en 1969 en el ámbito del LEMIT, y que fue seguida, a partir de 1976 por CIDEPINT-Anales) este comentario de la Dirección incluirá primero algunas reflexiones acerca del momento que vive el sistema científico, se pondrá énfasis sobre los problemas que enfrenta la investigación y desarrollo y los fabricantes de pintura en función de las regulaciones vigentes en cuanto a toxicidad y contaminación del medio ambiente y, finalmente, se cerrará con un breve resumen de las actividades académicas y técnicas.

Son perfectamente conocidas las dificultades por las que atraviesan los Institutos de Investigación ante la insuficiencia de los presupuestos de funcionamiento y la falta de apoyo para lograr un reequipamiento acorde con los últimos desarrollos existentes a nivel mundial.

Partiendo de la base de que la investigación y desarrollo debe tener, por lo menos en el mediano plazo, un efecto favorable en la economía general del país, en las condiciones de vida de sus habitantes o en el logro de determinados objetivos políticos y/o económicos como Nación, esto resulta muy difícil de alcanzar con las estrategias y recursos disponibles en la actualidad.

En relación con lo primero (estrategias) no existe un Plan (así, con mayúscula) que apunte a un objetivo preestablecido y que determine cuales son las metas a alcanzar y los tiempos en que ello debe concretarse. Así, pequeños planes a nivel personal (investigadores) o institucional (Centros de ID) se van formulando en forma aislada, por lo cual puede haber superposiciones que nunca, sumadas, podrán considerarse como un **Plan Nacional (y Racional) de Investigación y Desarrollo**. Si ello no es bueno para la ciencia en general, es particularmente grave en el área tecnológica.

Algunos anuncios se han realizado a través de la SECYT y del CONICET, al instrumentar los PIA, PIP y PIR y los proyectos de transferencia tecnológica inmediata. El manejo inconexo y poco claro de la información en relación con fechas y plazos, así como el desconocimiento, en la mayoría de los casos, de las pautas que se van a aplicar para la evaluación, llevan a confusión y ocasionan una enorme pérdida de tiempo, tiempo que debe, necesariamente, restarse a los objetivos específicos de cada Instituto.

La investigación y desarrollo tecnológico plantea problemas de estructura, de infraestructura y, además, de coyuntura. En el caso de los Centros Tecnológicos los esfuerzos se concentran en la optimización del uso de materias primas, procesos de fabricación y, como complemento, se efectúan servicios en función de los conocimientos desarrollados y del equipamiento existente. Se apunta así a lograr nuevas tecnologías, teniendo en cuenta todas las medidas que en la actualidad tienden a evitar la contaminación del medio ambiente. Todos los problemas inherentes a estos objetivos deben ser resueltos rápidamente en el caso particular de cada proyecto, con el objeto de cumplir con los cronogramas propuestos.

La estructura de Ciencia y Técnica, tanto Nacional como Provincial, se caracterizó, desde la creación del CONICET y de la CIC hasta hace unos pocos años, por una tendencia a la desburocratización, lo cual permitió el cumplimiento de los objetivos fijados con

presupuestos bajos. Se vislumbra actualmente la tendencia opuesta, por la supresión de presupuestos globales y la necesidad de discriminar los gastos según rubros. Esto, que es relativamente factible en el caso de organismos estatales que trabajan con estructuras y planes fijos, es imposible a nivel investigación; en este caso el propio desarrollo de los proyectos es el que fija el camino a seguir, que puede ser diferente del proyectado. Se debe trabajar con una dinámica acorde con la posibilidad de resolver cada situación coyuntural. La necesidad de materiales sólo puede ser prevista en forma general, pero muchos casos particulares deben ser resueltos en forma rápida y por adquisición directa, comprando el producto de la calidad y pureza requerida en forma inmediata. En esta simplificación, la descentralización es el componente substancial. En caso contrario no tiene sentido la preparación de cronogramas y tampoco es posible prever todas las materias primas, materiales y repuestos necesarios para cubrir todas las eventualidades y los “imprevistos no previstos”. Además es la forma de operar con el menor costo posible.

En lo que se refiere a documentación científica, el CONICET, en los últimos años, ha creado un Programa de Bibliotecas con el objeto de “racionalizar” las adquisiciones de libros y revistas. Este programa ha vuelto engorrosa y lenta la renovación de los libros y, fundamentalmente, la de las publicaciones periódicas que, usualmente deben ser pagadas al inicio del año calendario, pues en caso contrario se producen discontinuidades en la recepción de las revistas. En el caso del CIDEPINT, a través de un mecanismo más ágil, que se implementó por CIC y empleando en parte recursos propios, se ha conseguido superar esta situación. La adquisición se hace directamente a las respectivas editoriales, lo cual, al eliminar intermediarios, abarata notablemente los costos.

Es importante que el investigador tenga a su alcance, en forma inmediata, el material necesario para la revisión bibliográfica, a fin de no incurrir en superposición de temas, por una parte, y para aprovechar los avances realizados por otros. La biblioteca de un centro de investigación debe estar además equipada de equipos informáticos a fin de ubicar rápidamente los diferentes temas en base a las palabras claves que se incluyen en la actualidad en los trabajos que se publican. Esto requiere equipamiento y personal especializado.

El problema no se restringe a lo expuesto precedentemente, sino que se extiende al pago de servicios tales como gas, electricidad, teléfono, fax, el mantenimiento de computadoras y equipos de alta complejidad, pago de fotocopias, combustibles, viáticos, concurrencia a congresos, etc. En el caso del CIDEPINT, los tres primeros son soportados por la CIC, mientras que los restantes son pagados fundamentalmente con recursos propios y, eventualmente, por algún subsidio.

Otro aspecto importante está constituido por los escasos presupuestos a nivel nacional y provincial destinados a la formación de becarios internos y externos, que siempre resultó el procedimiento más idóneo para la generación de grupos de trabajo en las diferentes especialidades. El número de becas debe crecer en función de las necesidades de los Institutos, ya que en caso contrario se produce un estancamiento en el crecimiento, que lleva a la inmovilidad en un mundo de permanente avance científico y tecnológico. Además, deben proporcionarse remuneraciones que atraigan a los profesionales jóvenes y los recursos necesarios para que los mismos puedan realizar normalmente sus tareas.

La insuficiencia de las remuneraciones de los investigadores facilita su éxodo o conduce a desvirtuar las condiciones de dedicación exclusiva en que se debe trabajar para lograr una producción y capacitación adecuadas que permitan, luego de transcurrida la etapa inicial y contribuir también a la formación de recursos humanos. En la situación actual se corre el riesgo que el investigador pueda comenzar a realizar tareas extraoficiales para obtener ingresos adicionales, lo que lo aparta de su objetivo fundamental, con una evidente disminución de eficiencia y creatividad.

En relación con los planes de investigación y desarrollo del Centro y también con los problemas que enfrenta la industria de la pintura, se ha puesto énfasis en la necesidad de adecuarse a las regulaciones existentes para el control de la contaminación ambiental que se están implementando en el mundo. En particular, la reducción de disolventes orgánicos volátiles, uno de los más claros objetivos desde el punto de vista de dichas reglamentaciones, constituye un claro desafío para el futuro inmediato. Muchos disolventes utilizados en la industria de la pintura son fotoquímicamente activos y en algunos casos particularmente agresivos, afectando la piel, mucosas, ojos, etc. Siendo el disolvente un componente importante de las formulaciones, ya que actúan solubilizando la resina, facilitando la dispersión de los pigmentos, proporcionando un producto fácilmente aplicable, regulando el tiempo de secado y la tendencia al escurrimiento en superficies verticales entre otros aspectos, su eliminación o reemplazo por otros menos agresivos no es un problema menor. En el CIDEPINT actualmente se está trabajando activamente en pinturas emulsionadas diluibles con agua aun cuando el sólo reemplazo del disolvente por agua no resuelve totalmente el problema pues se deben utilizar biocidas para proteger el producto de la acción de microorganismos, tanto en el envase como luego de formada la película. Investigaciones relacionadas con pinturas de alto contenido de sólidos y de pinturas en polvo constituyen también un objetivo a corto plazo y realizable con el equipamiento disponible.

Durante 1995 se participó en diversos Congresos y Reuniones Científicas en el país y en el exterior, a saber: Congreso IRAM 1995 - ISO 9000, VII Congreso Argentino de Microbiología, Jornadas SAM'95, I Taller Argentino sobre Materiales Magnéticos y sus Aplicaciones, First Argentine-USA Bilateral Symposium on Materials Science and Engineering, IV Jornadas Geológicas y Geofísicas Bonaerenses, Simposio Argentino de Polímeros, CORROSION/95 - NACE Meeting, Symposium on Marine Corrosion, 4º Congreso Internacional de Tintas, V Congreso Iberoamericano de Corrosión y Protección, 18º Congreso Brasileiro de Corrosión y II Simposio de Electroquímico de Superficies.

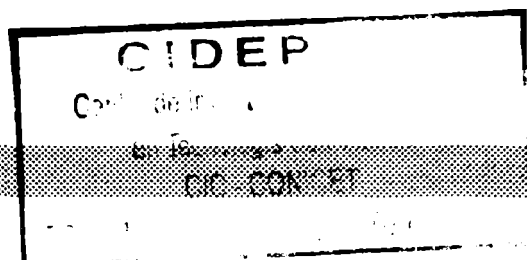
En el curso de 1996 el CIDEPINT presentó trabajos y/o conferencias plenarias en: Jornadas SAM'96, VII Jornadas Argentinas de Corrosión y Protección, XXI Congreso Argentino de Química, Jornadas Especializadas sobre la Corrosión, III Congreso de Exploración de Hidrocarburos, XII Congreso Iberoamericano de Electroquímica - IX Encuentro Venezolano de Electroquímica, IUPAC 2nd International Symposium on Free Radical Polymerization: Kinetics and Mechanisms, Simposio 13 del International Materials Research Congress, 2nd NACE Latin American Region Corrosion Congress y 16th Conference on Waterborne, High Solids and Radcure Technologies.

Entre 1995 y 1996 el CIDEPINT ha publicado 43 trabajos de investigación sobre pinturas y temas afines en las revistas científicas más importantes de la especialidad; otros varios se encuentran en trámite de publicación.

Simultáneamente se han efectuado peritajes, asesoramientos y tareas de control de calidad para un significativo número de usuarios (empresas y organismos privados, organismos de la Provincia de Buenos Aires, organismos Nacionales, Universidades y Empresas del Estado).

A handwritten signature in black ink, appearing to be 'VR', is positioned above the printed name and title.

Dr. Vicente J. D. Rascio
Director del CIDEPIINT

**INDICE****CONTENTS**

- pág. 1 **Effect of the paint application method on adhesion and corrosion resistance of an alkyd coated steel¹**
(Efecto del método de pintado en la adhesión y resistencia a la corrosión de aceros recubiertos con pintura alquídica)

P.R. Seré
D.M. Santágata
C.I. Elsner
A.R. Di Sarli
- pág. 17 **Study of formulation variables of thermoplastic reflecting materials for traffic marking²**
(Estudio de variables de la formulación de materiales termoplásticos para uso vial)

A.C. Aznar
J.J. Caprari
J.F. Meda
O. Slutzky
- pag. 27 **Chemical and electrochemical assessment of tannins and aqueous primers containing tannins³**
(Evaluación química y electroquímica de taninos y de imprimaciones acuosas a base de taninos)

V.F. Vetere
R. Romagnoli
- pag. 41 **Dilute-solution viscosimetry and solution properties of colloidal polymers**
(Estudio por viscosimetría de las propiedades de polímeros en solución)

J.I. Amalvy
- pag. 53 **Recent developments in miniemulsion polymerization⁴**
(Desarrollos recientes en polimerización de miniemulsiones)

I. Aispurua
J.I. Amalvy
M.J. Barandiaran
J.C. de la Cal
J.M. Asua
- pag. 63 **Thermodynamic consideration of the retention mechanism in a poly(perfluoroalkyl ether) gas chromatographic stationary phase used in packed columns⁵**
(Consideraciones termodinámicas acerca del mecanismo de retención en un poli(perfluoroalquil eter) utilizado como fase estacionaria en columnas rellenas para cromatografía gaseosa)

R.C. Castells
L.M. Romero
A.M. Nardillo

- pag. 77 **Activity coefficients of hydrocarbons at infinite dilution in di-n-octyltin dichloride. Comparison with results obtained in other alkyltin solvents⁶**
(Medición por cromatografía gaseosa de coeficientes con actividad de hidrocarburos a dilución infinita en dicloro dioctilestaño. Comparación con resultados obtenidos en otros solventes alquilestannicos)
- A.M. Nardillo
D.B. Soria
C.B.M. Castells
R.C. Castells
- pag. 83 **Thermodynamics of solutions of hydrocarbons in low molecular weight poly(isobutylene). A gas chromatographic study⁷**
(Termodinámica de soluciones de hidrocarburos en poli(isobutileno) de bajo peso molecular. Un estudio por cromatografía gaseosa)
- R.C. Castells
L.M. Romero
A.M. Nardillo
- pag. 95 **Revisión sobre los aspectos biológicos del “fouling”**
(Biofouling: An overview)
- M.C. Pérez
M.E. Stupak
- pag. 155 **New trends in industrial painting⁸**
(Nuevas tendencias en pinturas industriales)
- V.J.D. Rascio
- pag. 175 **Comparative corrosion behaviour of 55aluminium-zinc alloy and zinc hot-dip coatings deposited on low carbon steel substrates⁹**
(Comportamiento frente a la corrosión de acero recubierto con cinc o aluminio-cinc aplicados por inmersión)
- P.R. Seré
M. Zapponi
C.I. Elsner
A.R. Di Sarli
- pag. 197 **Reactive surfactants in heterophase polymerization of high performance polymers. VIII. Emulsion polymerization of alkyl sulfopropyl maleate polymerizable surfactants (surfmers) with styrene¹⁰**
(Surfactantes reactivos en la heterofase de la polimerización de polímeros de alta resistencia)
- H.A.S. Schoonbrood
M.J. Unzué
J.I. Amalvy
J.M. Asua
- pag. 209 **Gas chromatography of aliphatic amines on diatomaceous solid supports modified by adsorption and crosslinking of polyethyleneimines¹¹**
(Cromatografía gaseosa de aminas alifáticas sobre soportes sólidos derivados de diatomeas modificadas por adsorción y entrecruzamiento de poli(etileniminas)
- A.M. Nardillo
R.C. Castells

- pag. 217 **Excess enthalpies of nitrous oxide + pentane at 308.15 and 313.15 K from 7.64 to 12.27 MPa¹²**
(*Entalpias de exceso de óxido nitroso + pentano a 308,15 y 313,15 K desde 7,64 hasta 12,2 MPa*)

J.A.R. Renuncio
C. Pando
C. Menduiña
R.C. Castells

- pag. 225 **Excess molar enthalpies of nitrous oxide-toluene in the liquid and supercritical regions¹³**
(*Entalpias molares de exceso de óxido nitroso-tolueno en las regiones correspondientes a líquido y a fluido supercrítico*)

R.C. Castells
C. Menduiña
C. Pando
J.A.R. Renuncio

- pag. 235 **Separation of low-boiling pyridine bases by gas chromatography¹⁴**
(*Separación de bases piridínicas de bajo punto de ebullición por cromatografía gaseosa*)

M.C. Titon
A.M. Nardillo

- pag. 243 **Evaluation of the surface treatment effect on the corrosion performance of paint coated carbon steel**
(*Evaluación del efecto del tratamiento superficial sobre el comportamiento frente a la corrosión de acero al carbono pintado*)

D.M. Santágata
P.R. Seré
C.I. Elsner
A.R. Di Sarli

Algunos de los trabajos de investigación incluidos en este volumen han sido publicados, aceptados o remitidos para su publicación en revistas científicas de difusión internacional de la especialidad (*Some of the research papers issued in this volume have been published, accepted or submitted for publication to international journals on the speciality*).

¹ Surface Coatings International - JOCCA. Remitido para su publicación, mayo 1996.

² Journal of Coatings Technology. Aceptado para su publicación, noviembre 1996.

³ Corrosion Science. Remitido para su publicación, octubre 1996.

⁴ Macrom. Chem. Phys. Macrom. Symp. Aceptado para su publicación, setiembre 1996.

⁵ Journal of Chromatography, 715, 299 (1995).

⁶ Journal of Solution Chemistry, 25, 369 (1996).

⁷ Macromolecules, 29, 4278 (1996).

⁸ Presentado como Conferencia Plenaria Invitada en el 2nd NACE Latin American Region Corrosion Congress, Rio de Janeiro, Brasil, 9-13 de setiembre de 1996.

⁹ Corrosion Science. Remitido para su publicación, agosto 1996.

¹⁰ European Union Programme "Human Capital and Mobility". Aceptado para su publicación.

¹¹ Anales de la Asociación Química Argentina, 82 (5), 337 (1994).

¹² Journal of Chemical Engineering Data, 40, 642 (1995).

¹³ Journal of the Chemical Society, Faraday Transactions, 90, 2677 (1994).

¹⁴ Journal of Chromatography, 699, 403 (1995).

EFFECT OF THE PAINT APPLICATION METHOD ON ADHESION AND CORROSION RESISTANCE OF AN ALKYD COATED STEEL

EFEECTO DEL METODO DE PINTADO EN LA ADHESION Y RESISTENCIA A LA CORROSION DE ACEROS RECUBIERTOS CON PINTURA ALQUIDICA

P. R. Seré¹, D. M. Santágata², C. I. Elsner³, A. R. Di Sarli⁴

SUMMARY

The influence of the paint application method (spinning (Sn), rollering (R), brushing (B) and spraying (Sy)) on the behaviour of steel/alkyd coating/aqueous aggressive medium systems was analized. Experimental results obtained from electrochemical and standardized tests allowed to conclude that: a) all intact coated samples showed a high resistance to the strong aggressive medium of the salt spray cabinet; b) cross scribed ones only show corrosion at and close to the cross; c) from the electrochemical point of view, the corrosion potential, ionic and charge transfer resistance evolution on immersion time suggests that the alkyd paint applied by the four different methods used have relatively good protective properties, in the order $Sy > R \cong Sn > B$, at the present environmental conditions.

Keywords: *paint application methods, adhesion, corrosion resistance, alkyd paint, carbon steel, salt spray test, electrochemical impedance.*

INTRODUCTION

Paints have been used for many years to protect steel against corrosion. The effectiveness of the coating depends upon many factors. Some of them provide relatively little protection even under rather mild exposure conditions. Others will provide complete protection for many years even under severe conditions.

Until about 30 years ago, it was assumed that the mechanism by which coatings protect steel was acting as a barrier keeping water and oxygen away from the surface of the steel and so that preventing the occurrence of the corrosion process. Then, based on the paint film's water and oxygen permeability values, it was confirmed that the uptake of these species into the interface was higher than its rate of consumption in the corrosion process of the uncoated steel [1]. Since this means that the mechanism of protection could not be the barrier effect of

¹ Becario CIC, UNLP

² Becario CIC

³ Miembro de la Carrera del Investigador del CONICET, UNLP

⁴ Miembro de la Carrera del Investigador de la CIC

the coating, it was proposed that the electrical conductivity of the coating must be the controlling variable of the corrosion process. Therefore, presumably, high conductivity coatings would have less protective performance than low conductivity ones. In practice, that is truth except for very low conductivity coatings which present no relationship between conductivity and corrosion protection [2,3].

Funke et al [4-7] found that an important factor which had not been sufficiently considered was the adhesion of the coating to the steel in presence of water. They proposed that water permeating through an intact film could detach some films from the steel, that is, the film could have poor "wet adhesion". In such a case, water and oxygen, dissolved in the water, after they permeated through the film, would be in direct contact with the steel surface. In this way, all the elements necessary for corrosion would be present in the water layer, and in direct contact with the anodic and cathodic areas on the surface of the steel. Therefore, if the wet adhesion is poor, corrosion protection will be poor in any case; however, if the wet adhesion is quite good, a low rate of water and oxygen permeation may delay the loss of adhesion and then, for many practical conditions, an adequate corrosion protection level was obtained.

On the other hand, a paint or coating, as supplied, is not a finished product. It fulfils its function only when applied to the substrate. In a most basic sense, coating application can be described as getting the paint from the can to the surface being coated. There are a number of ways of accomplishing this, and often the type of paint material determines the selection of the most appropriate method. Besides, proper application is a critical point of the paint system. The proper use of an application method utilized to apply the paint or coating, can have a definite effect on the time required, the appearance of the finished job, the performance of the applied product and the total cost of the job.

With regard to the performance of the applied coating the application method can have a marked effect, especially when it is subsequently exposed to adverse environments. The choice of the application method may, in general, be dependent on some of the following considerations: 1) where the coating is applied; 2) the object being painted; 3) the objects' location; 4) the objects' configuration; 5) the number of units being coated; 6) the time available to do the job; 7) the surrounding environment; 8) the type of paint used; 9) the skill of the applicator and 10) the budget of the job.

A survey of the literature showed that it is difficult to find specific information about the effect of the paint application method on the behaviour of steel/organic coating/aqueous medium systems, at least from an electrochemical point of view. Consequently, the objective of the present work was to begin its study by using four (brushing, rolling, spraying and spinning) application methods of a commercial alkyd paint on carbon steel sheets. The painted electrodes, exposed to NaCl solutions, were assessed with respect to water and oxygen permeability as well as impedance and corrosion potential evolution as a function of immersion time. Besides, the pull-off and tape adhesion tests as well as salt spray cabinet standardized procedures were also performed.

EXPERIMENTAL PROCEDURE

Each sample substrate consisted of a (10x10x0.3 cm) carbon steel test panel, whose percentual chemical composition was: C (0.16); Mn (0.54); Si (0.05); S (0.01); P (0.01), Fe

being the difference. The surface was sandblasted to ASa 2^{1/2}-3 (Swedish Standard SIS 05 59 00/67); its roughness, measured with a Hommel Tester mod. T 1000, was 2.04±0.24 µm. Then, the steel sheets were cleaned with toluene to ensure surface uniformity and coated with a commercially available alkyd paint using either the brushing, rollering, spraying or spinning method. During the drying period the coated plates were kept in a desiccator at a constant temperature (30±2 °C). The dry film thickness was measured with an Elcometer instrument mod. 300, using a bare plate and standards of known thickness as reference; its mean values are shown in **Table 1**.

Table 1
Average thickness of the tested alkyd films

Paint Application Method	Average thickness (µm)
BRUSHING (B)	24±3
ROLLERING (R)	27±3
SPINNING (S _n)	24±1
SPRAYING (S _y)	28±2

For all the electrochemical measurements, two acrylic tubes were attached to each coated panel (working electrode) with an epoxy adhesive in order to get good adhesion. The geometrical area for each cell exposed to the electrolyte was 15.9 cm². A large area Pt-Rh mesh of negligible impedance and a saturated calomel (SCE) were employed as auxilliary and reference electrodes, respectively. The electrolyte solution was 3% NaCl solution at a pH of 8.2.

All impedance spectra in the frequency range 10⁻³ Hz ≤ f ≤ 6.10⁴ Hz were performed in the potentiostatic mode at the corrosion potential, as a function of the exposure time to the electrolyte solution, using the 1255 Solartron Frequency Response Analyzer and the 1286 Solartron Electrochemical Interface, the amplitude of the applied AC voltage was 10 mV peak to peak. Data processing was accomplished with an Olivetti PC and a set of programs developed by Boukamp [8].

The value of the water permeability coefficient of the coated steel/electrolyte solution systems above described was determined from measurements of the dielectric capacitance performed in the potentiostatic mode at a frequency of 2.10⁵ Hz and the calculus method showed elsewhere [9] while the oxygen one was obtained applying a DC electrochemical technique developed at the CIDEPINT [10]. In it, the samples in contact with a 3% NaCl solution saturated with either oxygen, air or nitrogen were polarized cathodically at a potential value which assures a mass transport control of the oxygen reduction reaction. All the electrochemical experiments were carried out at laboratory temperature (20±2 °C).

Besides the mentioned electrochemical techniques, the **anticorrosive** behaviour of these systems was also evaluated by the salt spray cabinet method (ASTM Standard B-117/85) (exposure time: 750 hours for non-scratched samples and 300 hours for cross scribed ones). On the other hand, before and after exposure tests, the adhesion strength of the four

steel/alkyd paint systems was determined through the **Pull-off strength** (Elcometer mod. 106 tester, ASTM D-4541/85) and the **Tape test** (ASTM D-3359/92a, Method B) standardized procedures. The porosity of the paint films was determined by means of the ASTM Standard D-3258-80 (1992)⁶¹.

RESULTS

Electrochemical tests

Fig. 1 shows the changes observed in the DC corrosion potential (E_{corr}) of the coated electrodes for a 45 days immersion period. It is evident that initially samples B (brushing), S_n (spinning) and R (rollering) exhibited corrosion potentials which became more negative (active) as time elapsed, while that corresponding to sample S_y (spraying) remained almost unvariable. In essence, the more negative the measured potential becomes, the more susceptible to corrosion is the underlying steel surface.

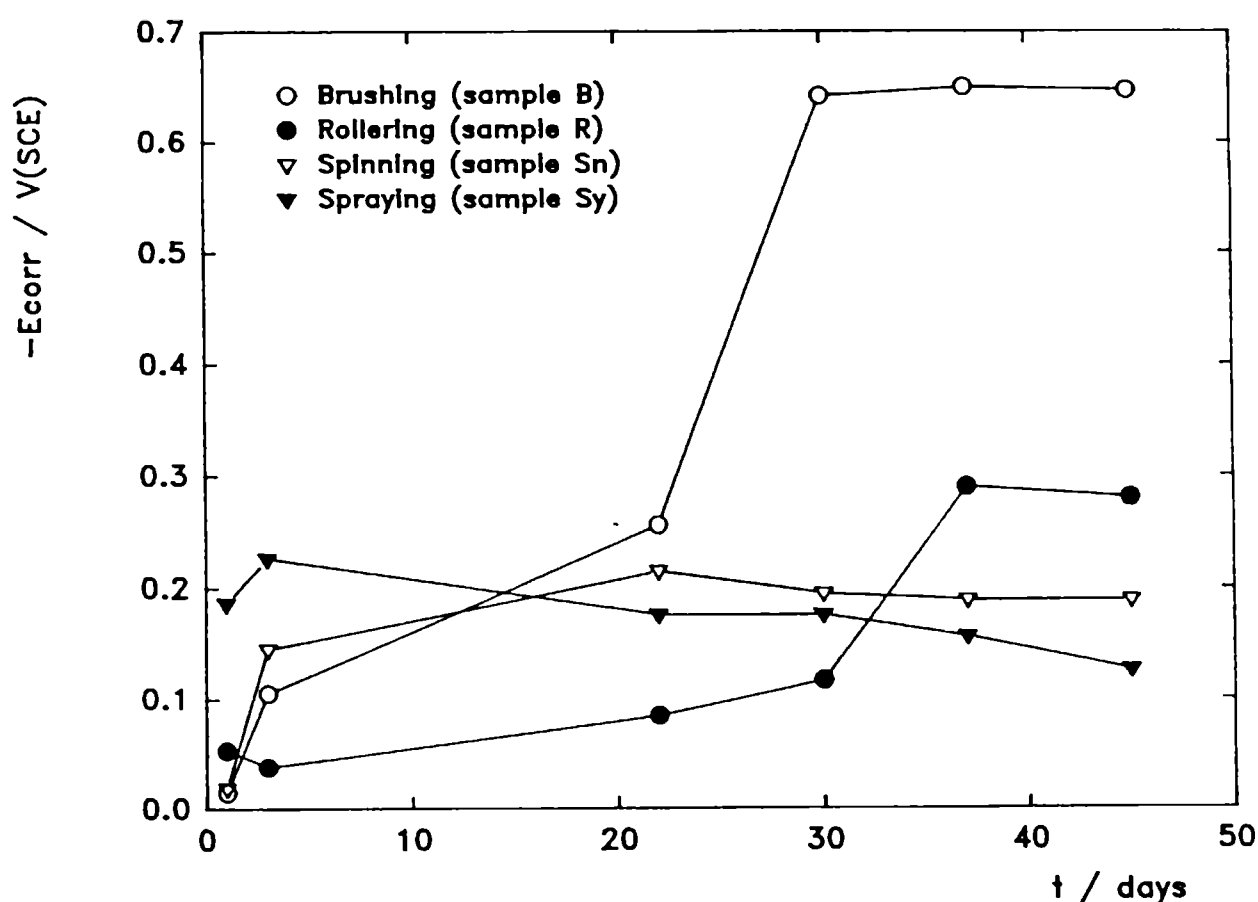


Fig. 1.- Corrosion potential (E_{corr}) vs. immersion time (t).

The samples B assumed a limiting value in the order of ca. -0.68 V/SCE after only 30 days immersion. This approaches the value expected to be taken up by uncoated carbon steel if measured under similar circumstances. In contrast, samples S_n and R appear to approach, or in the case of sample S_y , remained at much more noble potentials, but after an initial period of rapid deterioration.

The impedance spectra were analyzed using the analogous circuit shown in **Fig. 2**. In this circuit, as the exponent $n \rightarrow 1$ in all tests, it was assumed that the corresponding passive component was a dielectric capacitance C ; likewise, the solution resistance was not drawn

because its value was compensated by the measurement equipment in each run. **Figs. 3 - 4** illustrate the impedance results as a function of the immersion time for the four steel/alkyd/3% NaCl solution systems investigated in this work, which differ according to the paint application method employed.

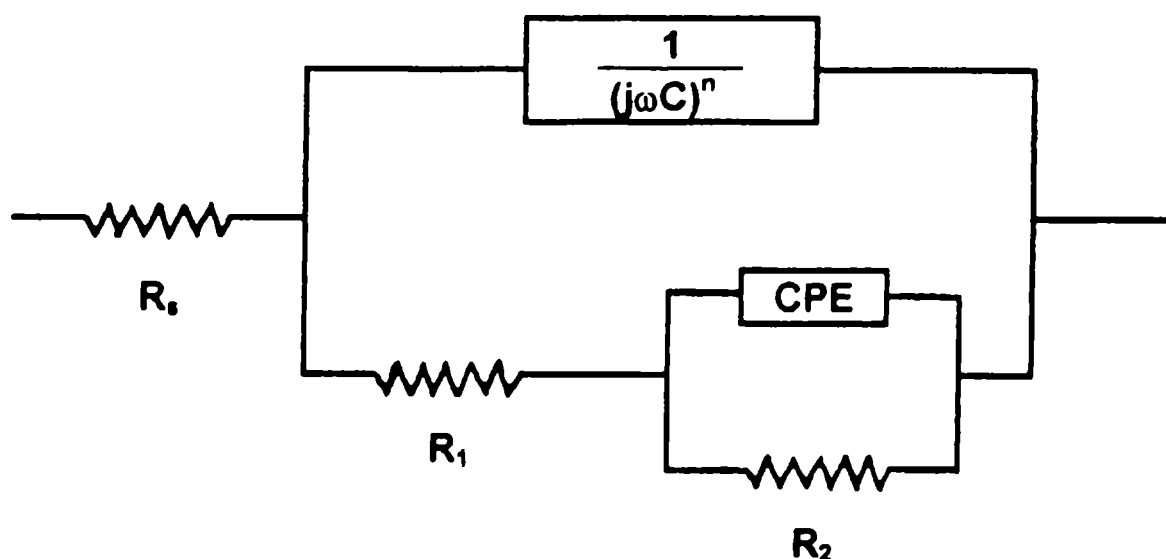


Fig. 2.- Analogous circuit used for EIS modelling.

Due to the small alkyd film thickness as well as to its water, oxygen and ionic permeability, just after few hours immersion in the electrolyte, the coating conductivity increased. Thus, the resistance R_1 (which describes paths filled with electrolyte solution of lower resistance shortcircuiting the organic coating) associated with the dielectric capacitance C (whose value is related to the water uptake), can be obtained applying non-linear squares fitting algorithms to the impedance data. Almost simultaneously, the permeating species reached the metallic substrate causing the emergence of the electrochemical double layer capacitance (Q) and the charge transfer resistance (R_2) characteristics of the faradaic process and assumed to be inversely proportional to the coated steel corrosion rate.

Information derived from impedance data suggests that both ionic resistance R_1 (**Fig. 3a**) and dielectric capacitance C (**Fig. 3b**) dependence on exposure time indicate that a constant deterioration took place in the case of samples B but R_1 values remained either oscillating in the 10^7 - $10^5 \Omega\text{cm}^2$ range for samples S_n and R and grown up just to stabilization at the same order of magnitude for samples S_y ; coupled to this parameter through the time constant R_1C , corresponding to the alkyd coating relaxation, the dielectric capacitance (C) evolution shows either fluctuations between 10^{-8} - 10^{-10}Fcm^{-2} for samples S_n and R, a significant decrease up to stability at the same range for the sample S_y , and finally a continuous increase up to 10^{-6}Fcm^{-2} for sample B. Assuming that the capacitance change is due to the water uptake, the application of the Brasher and Kingsbury equation [11] gives about 7-9 % water absorption in the alkyd samples after 3 hours immersion, **Fig. 5**.

Fig. 4a illustrates the highly fluctuating behaviour of the charge transfer resistance (R_2) with the immersion time. Changes of R_2 values between 10^6 and 10^3 for samples B denotes either a progress or a blockage of the active metal surface beneath the alkyd paint film as R_2 decreases or increases, respectively. Correspondingly, as it is shown in **Fig. 4b**, the electrochemical response of the double layer capacitance (which was best fitted using a constant phase element, Q) follows an undulating evolution as the time elapsed.

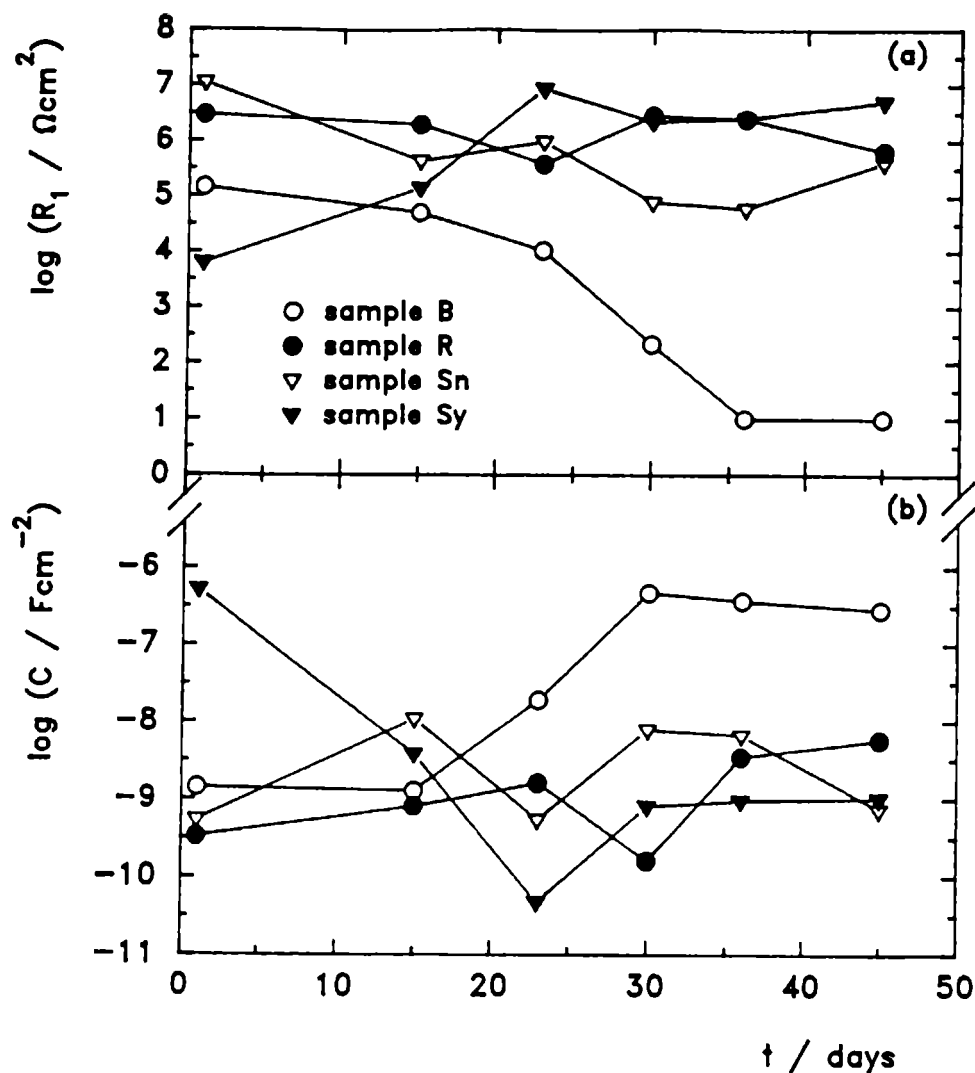


Fig. 3.- a) Ionic resistance (R_1) vs. immersion time (t); b) Dielectric capacitance (C) vs. immersion time (t).

Concerning the effect of the paint application method on the coating paint water and oxygen permeability the results are included in **Table 2**. The values of the water permeability coefficient in the alkyd coatings were calculated from measurements of the parallel capacitance as a function of immersion time and using a linear regression of the Carpenter equation [9], while the oxygen ones were determined polarizing cathodically the coated steel, exposed to the electrolyte solution saturated with either nitrogen, air or pure oxygen, and measuring the limiting current for each case [10]. Thus obtained, the values of the water permeability coefficients ranged from a minimum of $3.92 \times 10^{-11} \text{ cm}^2 \text{ s}^{-1}$ for sample B to a maximum of $7.03 \times 10^{-11} \text{ cm}^2 \text{ s}^{-1}$ for sample R, whilst the oxygen ones from 3.56×10^{-7} for sample B to $7.98 \times 10^{-7} \text{ cm}^2 \text{ s}^{-1}$ for sample S_y .

Table 2

**Average water and oxygen permeability coefficients
of the tested alkyd films**

Sample	$P_{\text{H}_2\text{O}} \times 10^{11} (\text{cm}^2 \text{ s}^{-1})$	$P_{\text{O}_2} \times 10^7 (\text{cm}^2 \text{ s}^{-1})$
B	3.92	3.56
R	7.03	4.40
Sn	5.80	7.69
Sy	6.88	7.98

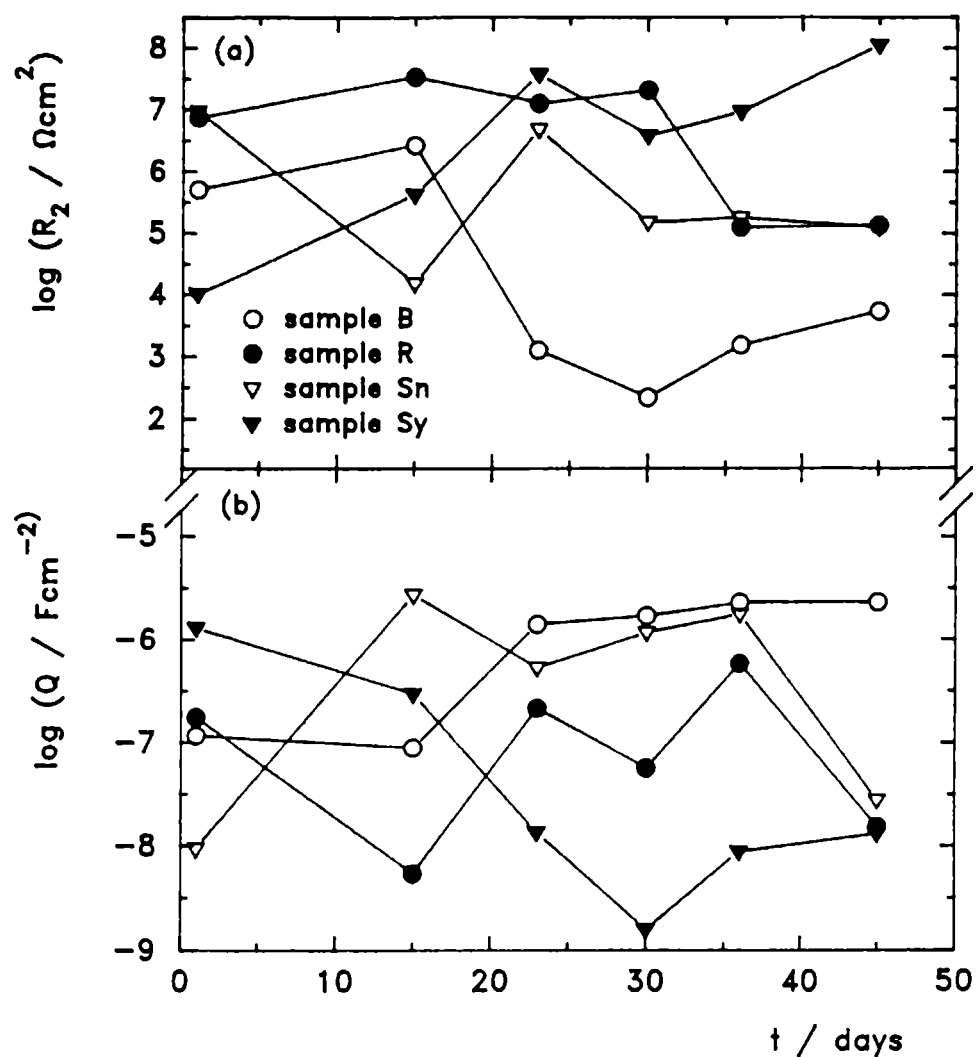


Fig. 4.- a) Charge transfer resistance (R_2) vs. immersion time (t); b) Double layer capacitance (Q) vs. immersion time (t).

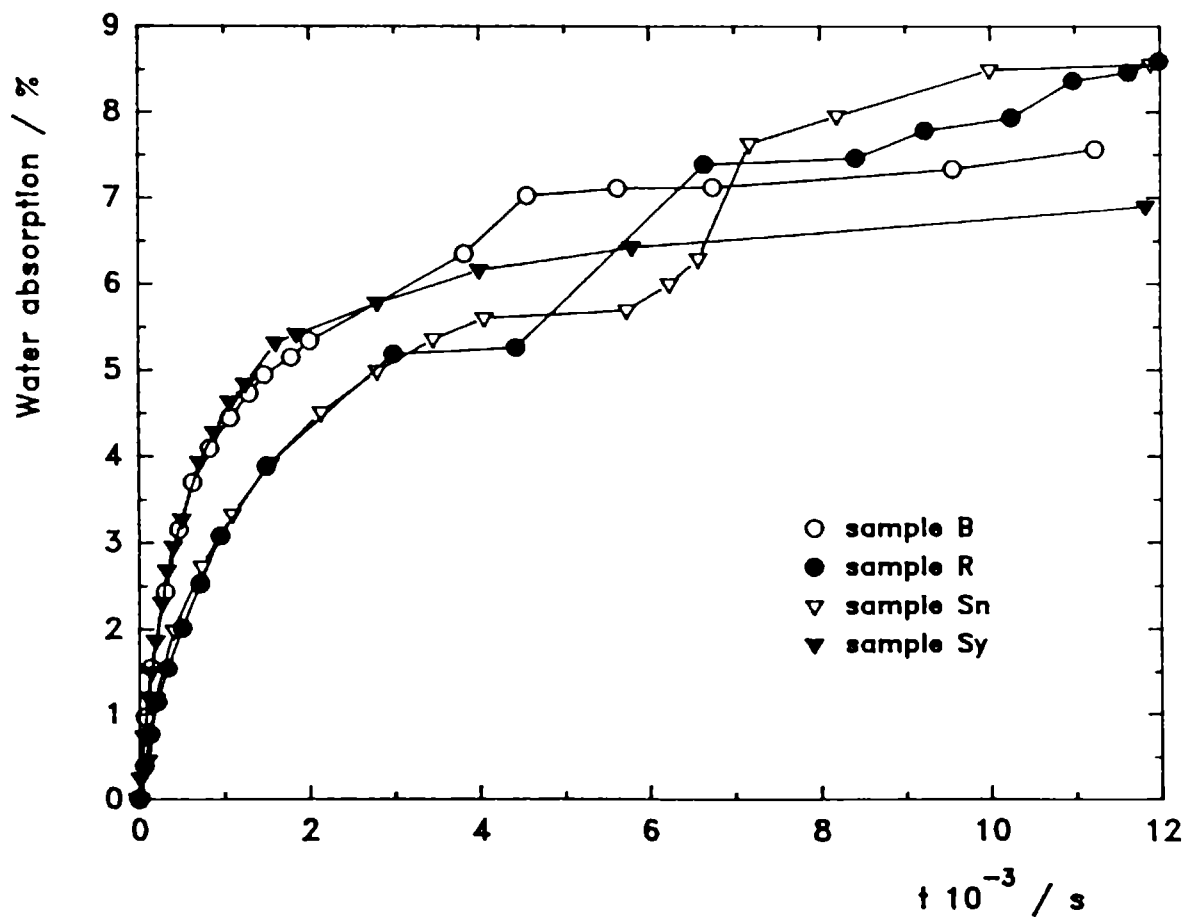


Fig. 5.- Evolution of water uptake for 3 h. immersion.

Salt spray cabinet and Adhesion Tests

Fig. 6a shows steel panels coated by the different application methods with the alkyd paint after an exposure time of 750 h in the salt spray chamber. The intact films show neither corrosion products nor coating defects on the main body of the panels. Slight rusting and blistering were noticeable at the vertical edges of the panels; this was due to a defective wax used there. **Fig. 6b** shows similar panels but with a cross scribe in the coating through the steel substrate. After 300 h in the salt cabinet chamber, the photographs illustrate that areas with intact paint coating have no corrosion, while those at and close to the cross scribe have been corroded severely.

Fig. 7 and **Tables 3 - 4** give the average level of the steel/alkyd film adhesion strength before and after the salt spray cabinet test carried out for 750 h for intact coatings and 350 h for scribed ones. Such values were obtained using the pull-off (**Figs.7 a-b**) and the tape test (**Tables 3 - 4**) standardized procedures. In both cases it can be seen that except for the corroded areas, i.e. at and close to scratched zones, where adhesion ranged from poor to bad, the adhesion strength show neither meaningful changes nor corrosion after exposure (see **Fig. 6**).

Table 3

Tape test adhesion results (ASTM D 3359-92a, Method B) after the salt spray cabinet test for non scratched samples

	sample B	sample R	sample Sn	sample Sy
before testing	5B	5B	5B	5B
non corroded areas	5B	5B	4B	4B
nearby corroded areas	1B	1B	1B	1B
corroded areas	0B	0B	0B	0B

Table 4

Tape test adhesion results (ASTM D 3359-92a, Method B) after the salt spray cabinet test for scratched samples

	sample B	sample R	sample Sn	sample Sy
on the scratch	0B	0B	0B	0B
5mm from the scratch	1B	0B	0B	0B
10mm from the scratch	4B	0B	0B	0B
15mm from the scratch	4B	4B	0B	1B
20mm from the scratch	4B	4B	0B	4B
30mm from the scratch	4B	4B	0B	4B
40mm from the scratch	4B	4B	1B	4B

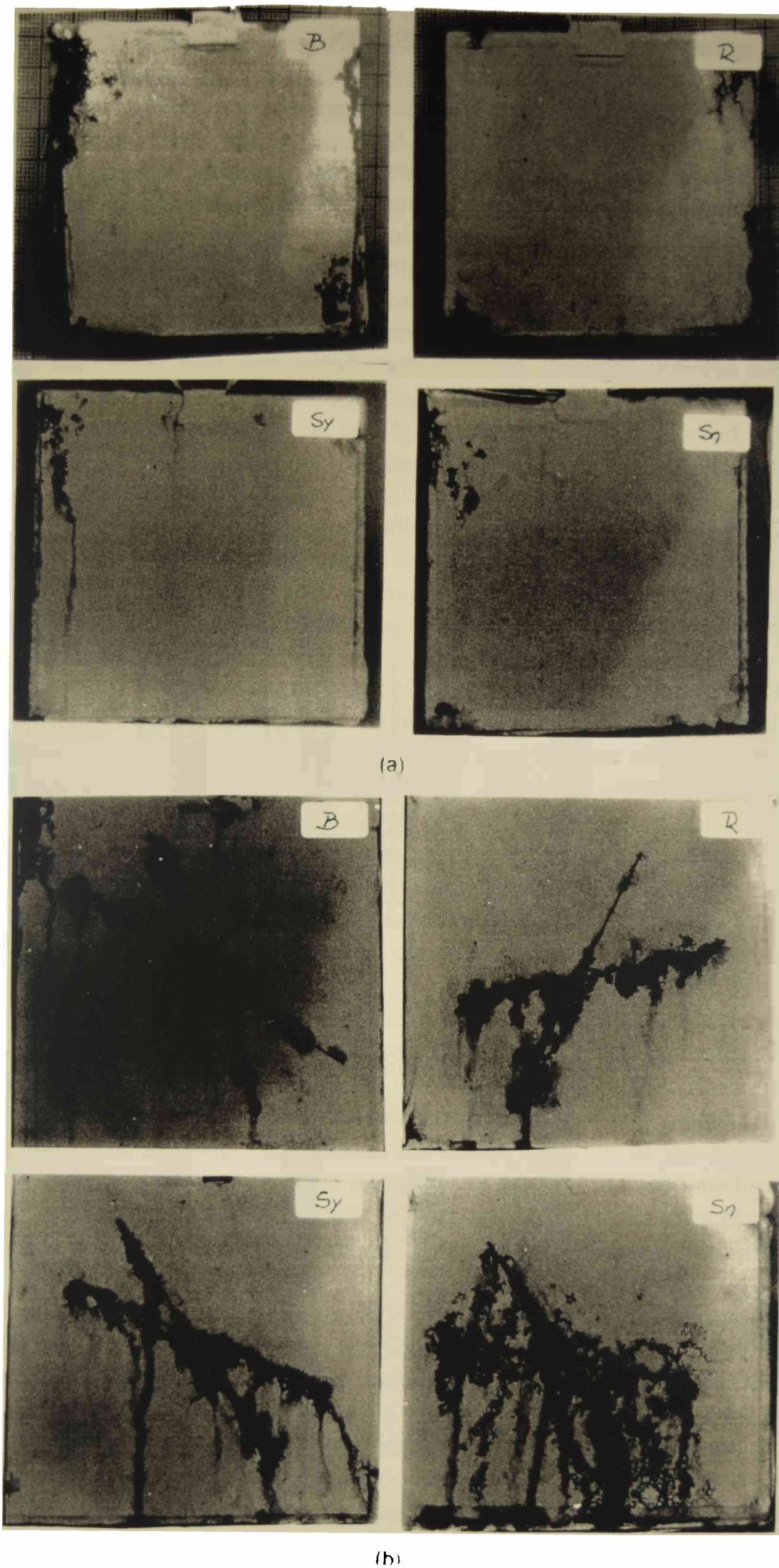


Fig. 6.- Visual inspection after exposure in the salt spray cabinet a) intact samples; b) scratched samples.

DISCUSSION

Electrochemical measurements

This work is part of a continuous investigation of electrochemical phenomena under paint coatings, clasping defects in films, porous films, metal/coating adhesion, surface preparation and/or pretreatments, blistered coatings and cathodic protection. The coating used here was a commercially available alkyd paint. In spite of the fact that in practice this paint is only a part of a painting scheme, it was considered interesting to use it individually to evaluate if the paint application method has any effect on the protective properties of carbon steel/alkyd/NaCl solution systems. Besides, the choice was also supported by the rapid electrochemical response of such a system.

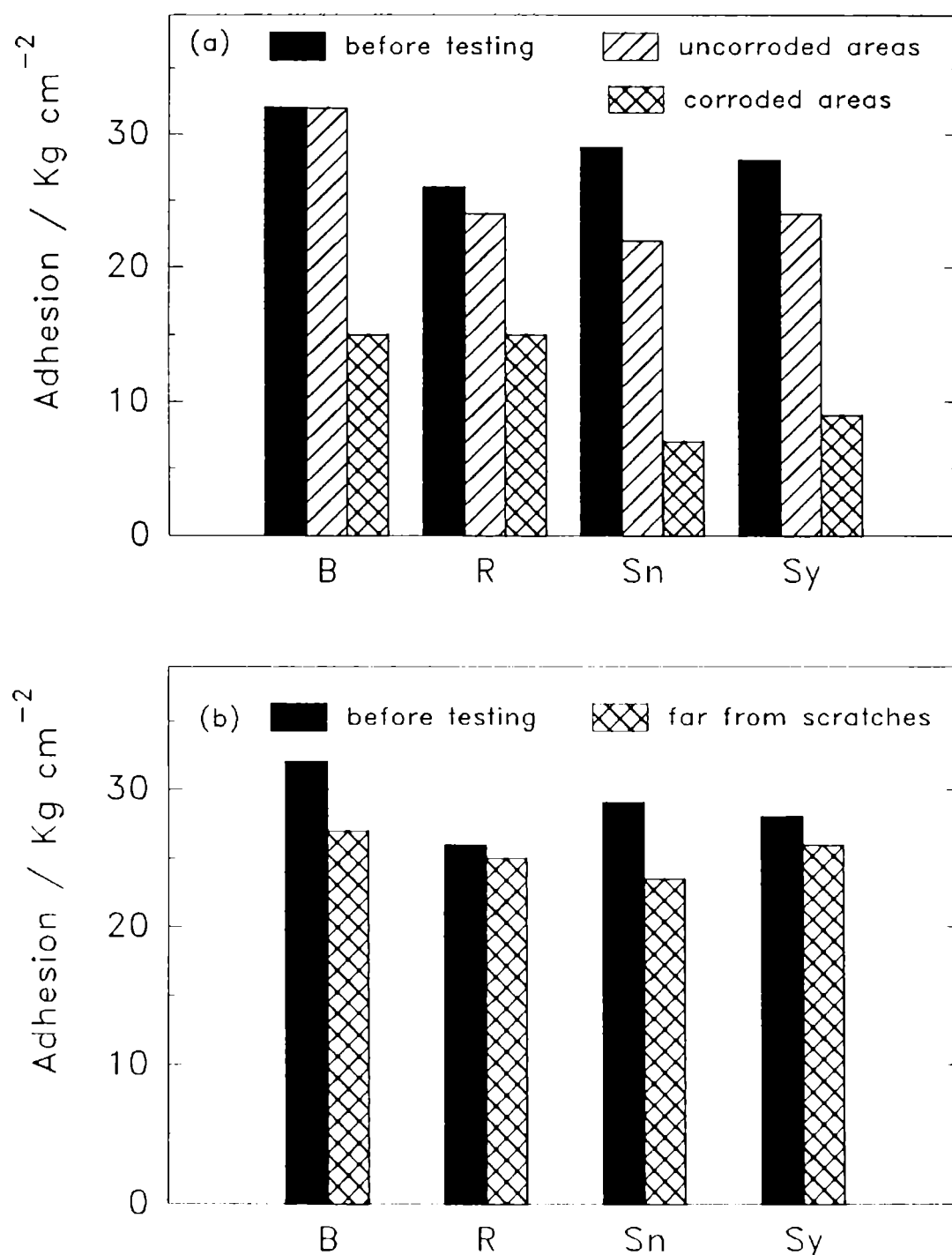


Fig. 7.- Adhesion strength for a) non scratched and b) scratched samples before and after exposure in the salt spray cabinet.

According to Ritter and Kruger [12], it may be supposed that during the first stage of immersion in NaCl containing solutions, different amounts of water, oxygen, Na^+ and Cl^- can permeate the paint coating. In the systems used here, such a process could be attributed to the fact that the air dried alkyd coating contained some unreacted polar groups which developed hydrophilic characteristics when exposed to aqueous solutions; consequently, this condition facilitated permeation. Besides, the relatively great amount of water absorbed by the alkyd paint coating has some plasticizing effect on the internal structure with consequent easy movement of molecules through the coating film.

Thus, during the first hours of immersion in 3% NaCl solution the corrosion potential (E_{cor}) for the four alkyd/steel systems was between 0.018 and 0.18 V/SCE, **Fig. 1**. The more noble values for samples B, S_n and R than for sample S_y were attributed to an initial higher barrier effect, presumably added by the significant adhesion forces, afforded by these samples. As the test goes on, however, it is evident the sample's B potentials approach values close to the free corrosion potential characteristic of uncoated carbon steel under equivalent environmental conditions. Such a trend support the assumption of an increasing electrochemical activity at the steel surface along the test, caused by the water, oxygen and ionic species diffusion through the coating paint with a rate and to an extent determined by the physicochemical characteristics of the painting scheme/metallic substrate interactions.

The amount of water absorption by alkyd paint films, obtained from the electric capacitance measurements, against immersion time is illustrated in **Fig. 5**; this shows that sample S_y gives the lowest value. The other samples have a higher water uptake in the order of $R \approx S_n > B$ after about 3 h immersion. In particular, samples' B values increased rapidly as the paint film began to deteriorate and peel-off from the metal and the corrosion process progressed. Although the water uptake for sample S_y was less than for samples R and S_n , it can be observed in **Fig. 8** that the adhesion force on the metal surface became weak, causing the paint film peel-off but no steel corrosion. Consequently, the steep increase of water absorption in samples S_n and R seems to be due to water collected at the steel/alkyd paint interface.

Impedance spectra contain valuable information about the electrical coating paint parameters and kinetics of the corrosion process taking place on the metallic substrate. Due to the dynamic character of corrosion products formation and the metal/coating paint interaction forces, the impedance spectra of carbon steel/alkyd film/3% NaCl solution systems change throughout the exposure time. Nevertheless, the complex nature of the interfacial processes have been studied through mathematical and physical models that account for the impedance data measured at such interfaces. Basically, a good description of the experimental impedance can be obtained in terms of a transfer function analysis using non-linear fit routines.

The analogous circuit model used in order to explain the impedance data is shown in **Fig. 2**. A first interpretation of the complex plain plot establishes that it may be described by a transfer function corresponding to an equivalent circuit built up by the electrolyte resistance (R_s) in series with the parallel combination taking into account the high frequency time constant due to the coating paint capacitance (C) and the ionic resistance (R_1) interaction, while the low frequency relaxation time would be given by the charge transfer resistance (R_2) and the electrochemical double layer capacitance (Q). The distortions occurred in the resistive-capacitive contribution at low frequency (reason by which the double layer capacitance was best fitted using a constant phase element (CPE), Q), indicate a deviation from the ideal behaviour in terms of a distribution of time constants due to tangential penetration of

electrolyte at the metal/paint interface, surface inhomogeneities and/or roughness effects [13,14]. By fitting the transfer function associated to the most probable circuit, these factors were taken into consideration through the CPE.

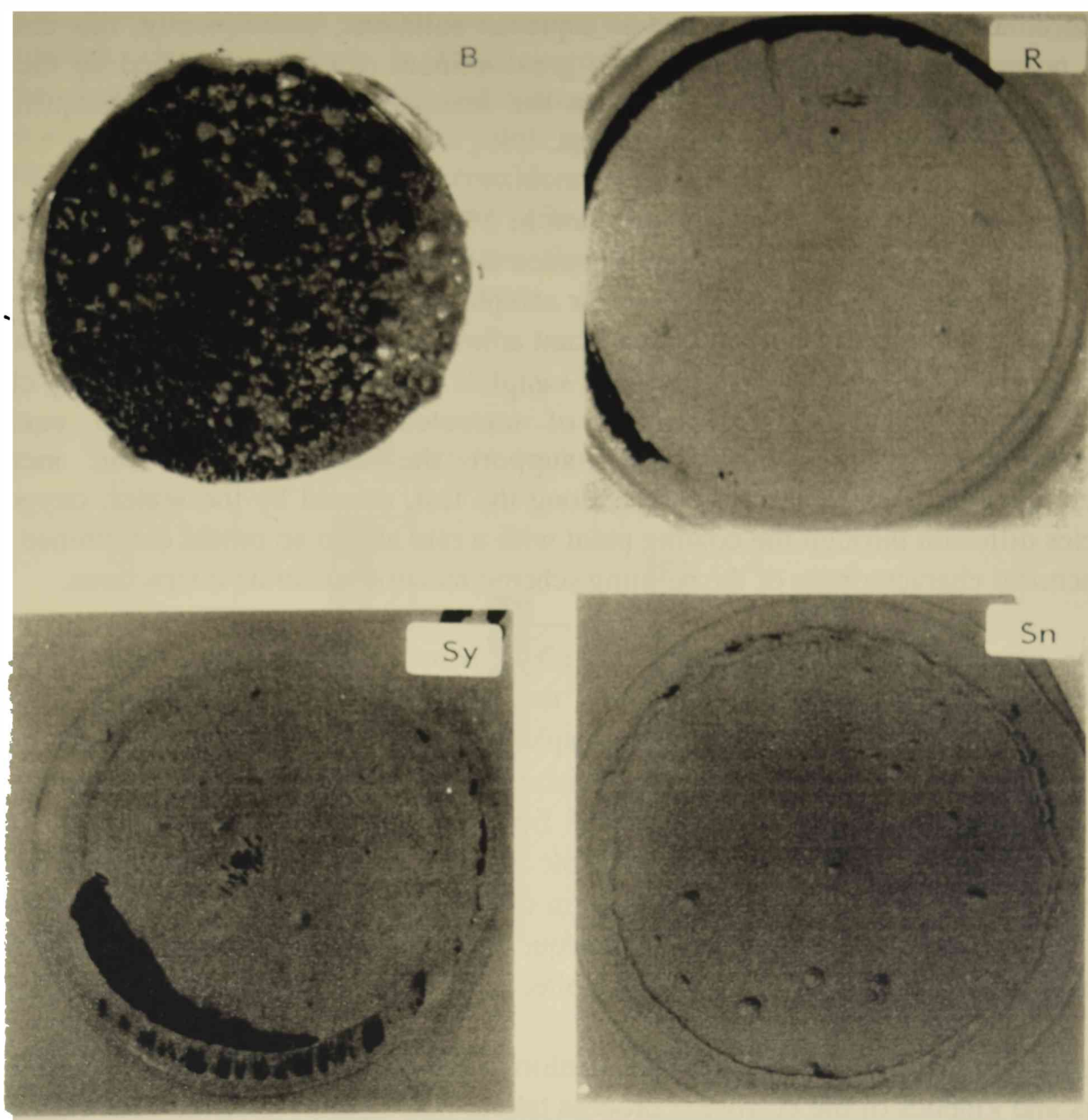


Fig. 8.- Visual inspection after EIS measurements

As can be seen from **Fig. 3**, the ionic resistance for sample B decreased with the exposure time; since its value is mainly determined by the geometric size of the defects filled with the electrolyte solution and the specific conductivity of the test solution, these results suggest that the electrolyte paint film penetration increased with exposure time and confirm those shown in **Fig. 5**. Recognizing that the coating is free from corrosion inhibitors, it is assumed that the very low R_1 values obtained for these samples, agree with the appearance of large corrosion spots on the coated specimens (**Fig. 8**), prove of their poor protective properties under the present environmental conditions. Such a behaviour is particularly attributable to one disadvantage of the brushing application method, it does not produce a very uniform film thickness nor low pores density; both of these factors allow the Cl^- concentration threshold for steel corrosion be rapidly attained at the base of the paint defects causing an initial localized corrosion which, in turn, promotes a local coating delamination. As the immersion time increases, these areas grow and coalesce until the overall area in contact with the electrolyte shows substrate corrosion and coating disbonding.

The remaining samples (R, S_n and S_y) exhibited a well differentiated performance. For samples S_y, the increase of the ionic resistance (R_i) values up to about 25 days immersion indicates an increase of the barrier effect afforded by the organic coating presumably enhanced by the formation of an underfilm and, therefore no visually identified, blocking layer due to reaction products (soaps) of the alkyd film. On the other hand, the R_i values for samples R and S_n does not greatly differ showing certain stabilization in the range 10⁵-10⁷ Ωcm² for 45 days immersion. The relatively good anticorrosive protection of these samples was also attributed to the mechanism described by the barrier and insulating model (i.e., the film capacity for delaying the diffusion of aggressive ions to the steel/alkyd paint interface).

Referring to the paint dielectric capacitance (C) dependence on the immersion time **Fig. 3b**, the results document that, in general, there was an undulating performance, which depends on the coating deterioration degree. For sample B the capacity (C) increases gradually to attain the normal value range of an electrochemical double layer (between ≈ 3 and 30×10^{-6} Fcm⁻²) when the protective properties are totally lost (sample B) and for the other samples C remains oscillating within the range 10⁻⁸-10⁻¹⁰ Fcm⁻², which is characteristics of somewhat deteriorated organic coatings.

Changes in R₂ (**Fig. 4a**) denote the progress of the active (corroding) metal surface under the alkyd film when either R₂ decreases (due to an increase of the steel/electrolyte solution contact area) or increases (which is caused by the insulating effect due to the accumulation of corrosion and paint degradation products). Again, the protective properties, in the order S_y > S_n \approx R, were higher than those corresponding to sample B, although differences between S_n-R and B tend to diminish as the test proceed. Correspondingly, the parameter (Q) representing the double layer capacitance followed an undulating evolution as the time elapsed, **Fig. 4b**. Such evolution can provide information about the extent of the underfilm steel/aqueous solution contact area as a consequence of the progressive coating disbonding [15].

With respect to delamination without corrosion in the case of samples S_y, S_n and R, it may envision that the initial oxygen and water permeation through the coating develop small localized regions where local delamination of the paint film takes place. As the continuous exposure to the electrolyte goes on, these zones grow leading to their coalescence into larger units until the total exposed area became delaminated. Likewise, the visual evidence of corrosion absence (**Fig. 8**) on these samples could be explained taking into account that spinning, rollering and spraying methods give smoother, more uniform and non-porous films than brushing does. It was assumed, therefore, that the slower rate of Cl⁻ permeation due to the development of negative charges in the paint structure, which restricts the permeation of ions with the same charge sign when exposed to aqueous electrolytes, added to the lack of direct pathways (pores, pinholes, etc) through the paint film, avoids that the chloride concentration threshold for the underlying steel corrosion would be reached [16-18].

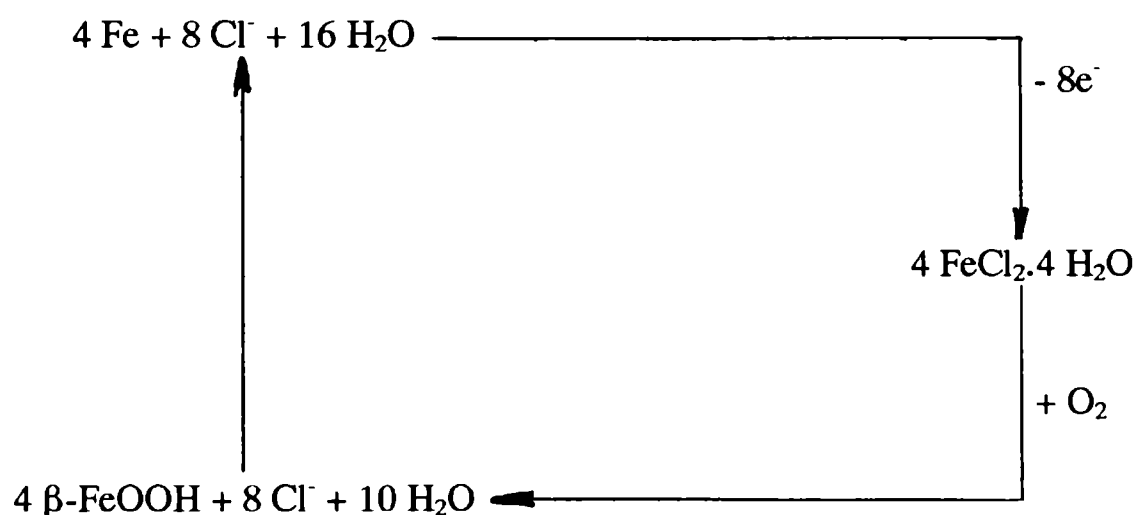
Salt spray cabinet and adhesion tests

Fig. 7 shows the dry adhesion values as a function of the film application method, brushing samples have the highest adhesion strength (> 30 kgcm⁻²) and the rollering ones the lowest (about 24 kgcm⁻²); the others (spinning and spraying) do not greatly differ since they have an average value of 28 and 26 kgcm⁻², respectively.

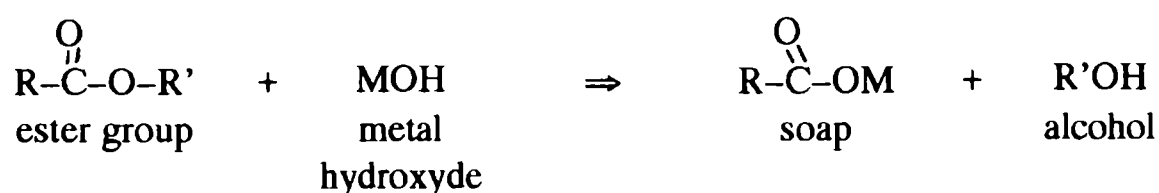
The amount of adhesion loss is dependent on the severity of the exposure and the strength of the specific paint/metal interactions. Thus, different studies have shown an adhesion loss coincident with the presence of water at the metal/coating interface [19-23]. The pull-off and the cross cut tape tests applied on the exposed areas immediately after withdrawing the samples from the salt spray chamber produce the results shown in Fig. 7 and Tables 3 - 4. These indicate that the major shift in adhesive strength occurs in the order $S_n > S_y > R > B$ for non-scratched samples and $B > R \approx S_n > S_y$ for the scratched ones.

As it was quoted before, the adhesion values are reduced on exposure to aqueous solution. However, the interesting fact is not this reduction but the finite level of adhesion remaining after immersion. The adhesion loss is thought as molecules of water reaching the metal/paint coating interface and the hydrogen bonding with the available hydrophilic groups of the polymer. It might be surprising that this water does not cause rapid underfilm corrosion. Taking into account the water permeability data given in Table 2, and assuming that the water vapour could be still lower, the possible explanation is that where the paint film remained intact the amount of water necessary to cause interfacial disbonding is substantially less than the amount required to form a discrete aqueous phase, therefore, it would not be able to support the charge transfer process associated with corrosion nor to avoid that adhesion settles to an acceptable and consistent value. Besides, this fact is also supported by the above mentioned restriction of the Cl^- diffusion through the paint film.

On the other hand, for cross scribed samples all tests have shown a direct relationship between adhesion loss and corrosion attack neighbor to the scratch. In this region, the cross scribe becomes an anode where Fe dissolves as Fe^{+2} , in principle, according to the following reaction mechanism [24].



and the metal under the paint film becomes the cathode. An electric circuit is formed throughout the paint film. At the cathode, OH^- ions are formed by the oxygen reduction reaction; the alkaline medium, created as the steel corrosion progress, rapidly attack the oil base of the alkyd film, saponifying it, according to:



where R and R' are alkyl groups. As a result of this coating degradation, paint adhesion weakens facilitating the metal/coating disbonding and, consequently, the lateral access of electrolyte to the paint/steel interface which feedbacks the process.

CONCLUSIONS

- AC together with DC and standardized procedures have considerable value in assessing the protective ability of a paint film from scientific and methodic studies of anticorrosion problems. Knowledge about the changes in permeability, conductivity and adhesion properties of coatings when exposed to aggressive environments is important, not only because it indicates how the coating may behave in practice, but also because it gives an insight into its protective properties in prevention of corrosion of the metal substrate.
- From the values of corrosion potencial, ionic and charge transfer resistance on immersion time, the alkyd paint applied by means of four different methods showed relatively good protective properties in the order $S_y > R \approx S_n$ but very poor ones for sample B. On the other hand, when submitted to the salt spray cabinet test, all the steel sheets coated with intact alkyd films have shown high resistance to the strongly aggressive medium (5% NaCl). Likewise, the cross scribed samples only shown corrosion at and close to the cross.

Taking into account the overall results, the more effective application method was spraying followed by rollering, spinning and, in last term brushing, also further work needs to be done to confirm some of the assumptions made here.

ACKNOWLEDGEMENTS

The authors would like to thank the Comisión de Investigaciones Científicas de la Provincia de Buenos Aires (CIC) and the Consejo Nacional de Investigaciones Científicas y Técnicas (CONICET) for their financial support of this research work.

REFERENCES

- [1] J.E.O. Mayne, *Official DIGEST*, **24**(235), 127 (1952).
- [2] J.E.O. Mayne, "Corrosion", L.L. Shreir de., Butterworth (Boston), vol.2, 15:24 (1976).
- [3] H. Leidheiser, Jr., *Prog. Org. Coat.*, **7**, 79 (1979).
- [4] W. Funke, U. Zorll & B.G.K. Murth, *J. Paint Technol.*, **41**(530), 210 (1969).
- [5] W. Funke & H. Haagen, *Ind. Eng. Chem. Prod. Res. Dev.*, **17**, 50 (1978).
- [6] W. Funke, *J. Coat. Technol.*, **55**(705), 31 (1983).
- [7] W. Funke, *J. Oil Col. Chem. Assoc.*, **68**, 229 (1985).
- [8] B.A. Boukamp, *Report CT88/265/128, CT89/214/128*, University of Twente, The Netherlands (1989).
- [9] E.E. Schwiderke & A.R. Di Sarli, *Prog. Org. Coat.*, **14**, 279 (1980).
- [10] C.I. Elsner, R.A. Armas & A.R. Di Sarli, *Portugalæ Electrochim. Acta*, **13**, 5 (1995).
- [11] D:M: Brasher & A.H. Kingsbury, *J. Appl. Chem.*, **4**, 62 (1954).
- [12] J.J. Ritter & J. Kruger, *Corrosion Control by Organic Coating*, H. Leidheiser, Jr. ed., NACE, Houston, Tx, 28 (1981).

- [13] T. Szauer & A. Brandt, *J. Oil Col. Chem. Assoc.*, **67**, 13 (1981).
- [14] D.J. Frydrych, G.C. Farrington & H.E. Townsend, *Corrosion Protection by Organic Coatings*, M.W. Kendig & H. Leidheiser, Jr. eds., vol. 87-2, p. 240, The Electrochem. Soc., Pennington, NJ, (1987).
- [15] L.M. Callow & J.D. Scantlebury, *J. Oil Col. Chem. Assoc.*, **64**, 119 (1981).
- [16] C.I. Elsner, R.A. Armas & A.R. Di Sarli. In press.
- [17] A.L. Glass and J. Smith, *J. Paint Technol.*, **39**, 490 (1967).
- [18] H. Corti, R. Fernandes Prini and D. Gómez, *Prog. Org. Coat.*, **10**, 5 (1982).
- [19] J.W. Watt & J.E. Castle, *J. Materials Sci.*, **18**, 2987 (1983).
- [20] H. Leidheiser, Jr. & W. Funke, *J. Oil Col. Chem. Assoc.*, **70**(5), 121 (1987).
- [21] H. Hansman, *Ind. Eng. Chem. Prod. Res. Dev.*, **24**, 252 (1982).
- [22] W. Schwenk, *Corrosion Control by Organic Coatings*, H. Leidheiser, Jr. de., NACE, Houston, Tx, 103, (1981).
- [23] P. Walter, *Off. Digest*, **37**, 1561 (1965).
- [24] W. Funke, *J. Oil Col. Chem. Assoc.*, **62**, 63 (1979).

STUDY OF FORMULATION VARIABLES OF THERMOPLASTIC REFLECTING MATERIALS FOR TRAFFIC MARKING

ESTUDIO DE VARIABLES DE LA FORMULACION DE MATERIALES TERMOPLASTICOS PARA USO VIAL

A.C. Aznar, J.J. Caprari¹, J.F. Meda and O. Slutzky

SUMMARY

Nine formulations of thermoplastic materials for traffic marking were prepared using a resin based on maleic anhydride modified with rosin in different proportions (18, 22 and 26%). As plasticizer a liquid coconut long oil alkyd resin (100% solids) was employed.

Hiding pigment was titanium dioxide; calcium carbonate and micronized talc were used as extenders. Coarse marble powder is used to facilitate the incorporation of glass beads. The operation was made employing a double Z mixer oil heated to obtain a mass temperature of 180-190 °C. The mixer was provided with two asynchronous arms rotating at 46 rpm.

Dry and wet abrasion tests were carried out and the obtained results indicated that wearing values are three times greater in the case of the wet test.

It is demonstrated that plasticization degree controls hardness variation as a function of temperature, determining a critical point which is the beginning of an abrupt reduction of hardness. Water absorption increases when plasticizer content increases. Matrix correlation of tests results was used to analyze the obtained numeric values.

Keywords: *thermoplastic materials, reflecting properties, agglutinant, dry abrasion test, wet abrasion test, bond strength, water elimination rate.*

INTRODUCTION

Frequently reflecting thermoplastics applied in city streets, roads or highways lost their efficiency due to the wearing or to the partial detachment of the used materials. The appearance and physical characteristics were modified.

The adequate life-time is a function of different variables [1], acting individually or as a whole: adhesion to the surface where they were applied on (asphalt or concrete), resistance to abrasion and weathering (moisture due to rain, dew remaining long time in contact with

¹ Miembro de la Carrera del Investigador del CONICET

thermoplastic marks), high temperatures producing deformation or low temperatures diminishing elasticity and favouring checking or cracking of the coat.

An important aspect is related to the influence of traffic intensity and the rolling action of tires, specially the pressure when the tire takes contact with the line or the suction when rolling over them. A high quality result is related to the components of the formulation and to the adequate cleaning of the surface before application. A best performance was always obtained in asphalt pavements [2].

The objective of this research is to determine the influence of composition variables (pigment/binder ratio, resin content, plasticizer type and content, fillers employed, and PVC) on the adhesion or wearing resistance of the thermoplastic applied on a concrete surface.

EXPERIMENTAL

Nine samples of thermoplastics reflecting materials were formulated, containing as agglutinant a resin based on maleic anhydride and modified with rosin (A.I.= 14; melting point 114 °C). The modified resin was used in 18, 22 or 26% on the total formulation. As plasticizer a coconut oil alkyd resin was employed (without organic solvents) in a proportion between 2.7 and 6.5 per cent.

As hiding pigment titanium dioxide rutile type was employed, to obtain a white colour with high luminosity ($Y > 80$). Pigment formulation was completed using fillers as calcium carbonate and talc, which are of good wearing resistance. Samples formulation were indicated in Table 1.

TABLE 1

Composition of the thermoplastic materials*

Material	IA	IB	IC	IIA	IIB	IIC	IIIA	IIIB	IIIC
Maleic resin	18.0	22.0	26.0	18.0	22.0	26.0	16.0	22.0	26.0
Alkyd resin	2.7	3.3	3.9	3.6	4.4	5.2	4.5	5.5	6.5
Titanium dioxide	10.0	10.0	10.0	10.0	10.0	10.0	10.0	10.0	10.0
Glass beads	20.0	20.0	20.0	20.0	20.0	20.0	20.0	20.0	20.0
Marble	22.4	20.3	18.2	22.0	19.8	17.6	21.6	19.3	17.0
Calcium carbonate	22.4	20.3	18.2	22.0	19.8	17.6	21.6	19.3	17.0
Talc	4.5	4.1	3.6	4.4	4.0	3.6	4.3	3.9	3.5

* g.100 g

A double Z mixer (Fig. 1) was used for the thermoplastic preparation, having the mixer two asynchrone arms, one of them rotating at 46 rpm. For heating a mineral thermic fluid which circulates in the heating jacket was employed (maximum temperature 300 °C).

Titanium dioxide, fillers and glass beads were incorporated at 180-190 °C. The operation at this temperature lasts 30 minutes. After that, the product obtained was casted in special molds.



Fig. 1.- Double Z mixer for test samples preparation.

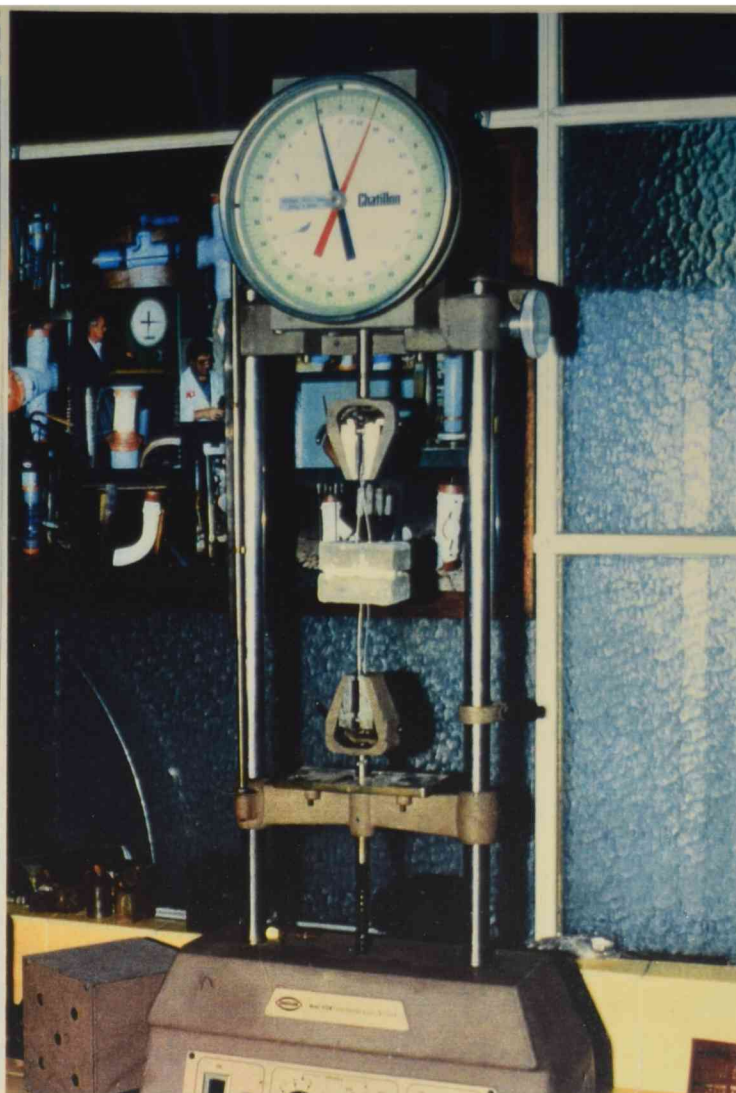


Fig. 2.- Adhesion-strength determination by CIDEPINT method.

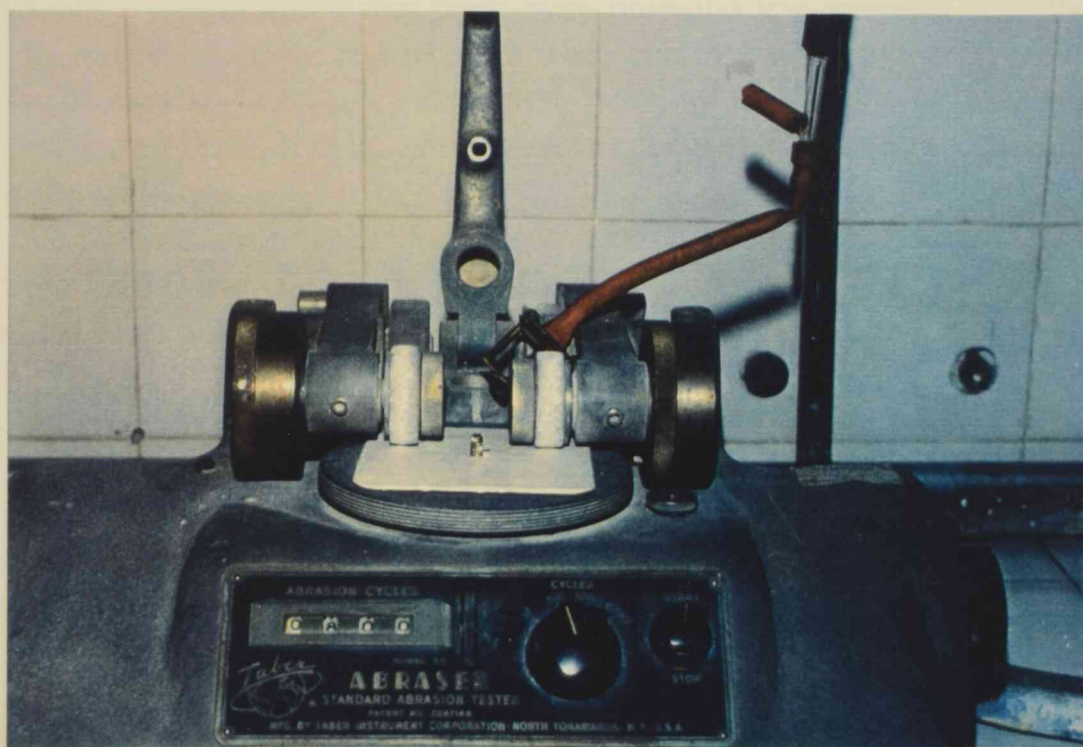


Fig. 3.- Wet and dry abrasion test equipment.

The samples tests were performed at different temperatures; wet and dry abrasion, Shore A hardness, adhesion-cohesion, water absorption and water elimination rate were determined.

For the **wet and dry abrasion test** [3], circular specimens were employed (80 mm diameter and 3 mm thick). After 24 hours samples were abraded using a Taber Abraser equipment, with a H-22 abrasive and 1000 g load (ASTM D 4060). The dust produced by the wearing operation was eliminated constantly by flowing pressurized air. When a track is formed as a consequence of wearing, the sample is weighed with an exactitude of 1 mg. After that, the wearing operation is continued along 100 revolutions of the equipment and newly weighed. The difference between the two values obtained is expressed as dry wearing (**Fig. 2**).

After finishing the previous test, distilled water is added to the track and the operation continued during 100 revolutions more. The sample is now conditioned for water elimination and weighed. The difference with the previous value is expressed as wet wearing.

Shore A hardness [4] at temperatures between 40 and 70 °C was determined each 5 °C, according to DIN 53505. In this case test plates are 50 mm diameter and 3 mm thick; the value was registered after 15 seconds. Samples were stabilized during 1 hour at test temperature before hardness determination.

To obtain adhesion and cohesion strength values a method developed at CIDEPINT was employed [5,6]. The melted material was put in the midst of concrete probes (3 mm thick), previously primed with an acrylic varnish and preheated at 40 °C. An iron flexible wire was inserted in test probes to allow the clamps of a dinamometer. The traction effort was performed at a velocity of 200 mm.min⁻¹ and at a temperature of 20 °C (**Fig. 3**).

For the determination of **water absorption** and **water elimination rates** [7,8,9], specimens of 50 mm diameter and 3 mm thick were prepared and weighed with the precision of 1 mg. Hung by means of a copper wire, they were completely submerged in distilled water at 20 ± 1 °C for 24 hours. After that, they were dried with filter paper and weighed; the operation was made after 48 and 72 h. **Absoption values** were obtained by difference with the initial weight of the samples .

Afterwards the probes were conditioned at 20 °C and 50 % HR. By weighing, **water elimination values** were obtained.

DISCUSSION

The maleic resin is the agglutinant used in the formulation of thermoplastic traffic materials. The modification of physical properties (reduction of melting point and adequate elasticity characteristics) by means of an alkyd resin improved the system wetting, facilitating the incorporation of the hiding pigment (TiO₂), fillers and glass beads. In those conditions a homogeneous distribution of glass beads was obtained. This is a very important aspect in field behaviour; in wearing, an adequate distribution of beads in the mass assures adequate night visibility, during a long period.

A certain correlation was observed between the thermoplastic traffic materials composition and the values of the obtained physical properties (**Table 2**).

TABLE 2

Correlation between materials composition variables and physical properties

	R	P	M	C	T	W ⁺	AS	D	Δ	PVC	W ⁻
R	1.00	0.58	-0.97	-0.93	-0.98	-0.92	0.98	-0.31	-0.89	-0.97	-0.90
P	0.58	1.00	-0.75	-0.77	-0.72	-0.71	0.43	-0.94	-0.73	-0.76	-0.75
M	-0.97	-0.75	1.00	0.97	0.99	0.95	-0.91	0.51	0.93	1.00	0.94
C	-0.93	-0.77	0.97	1.00	0.97	0.98	-0.85	0.55	0.93	0.97	0.98
T	-0.98	-0.72	0.99	0.97	1.00	0.95	-0.91	0.48	0.91	1.00	0.94
W ⁺	-0.92	-0.71	0.95	0.98	0.95	1.00	-0.87	0.50	0.84	0.95	1.00
AS	0.98	0.43	-0.91	-0.85	-0.91	-0.87	1.00	-0.15	-0.83	-0.91	-0.84
D	-0.31	-0.94	0.51	0.55	0.48	0.50	-0.15	1.00	0.46	0.52	0.55
Δ	-0.89	-0.73	0.93	0.93	0.91	0.84	-0.83	0.46	1.00	0.92	0.84
PVC	-0.97	-0.76	1.00	0.97	1.00	0.95	-0.91	0.52	0.92	1.00	0.95
W ⁻	-0.90	-0.75	0.94	0.98	0.94	1.00	-0.84	0.55	0.84	0.95	1.00

Key of the table

R:	resin	P:	Plasticizer
M:	marble powder	C:	calcium carbonate
T:	micronized talc	W ⁺ :	water absorption
AS:	adhesion-strength	D:	hardness at 55°C
Δ:	abrasion	PVC:	PVC
		W ⁻ :	water elimination

In the dry abrasion test the trend of wearing is determined by pigment volume concentration of the different samples. Two series of wearing values were obtained (Fig. 4).

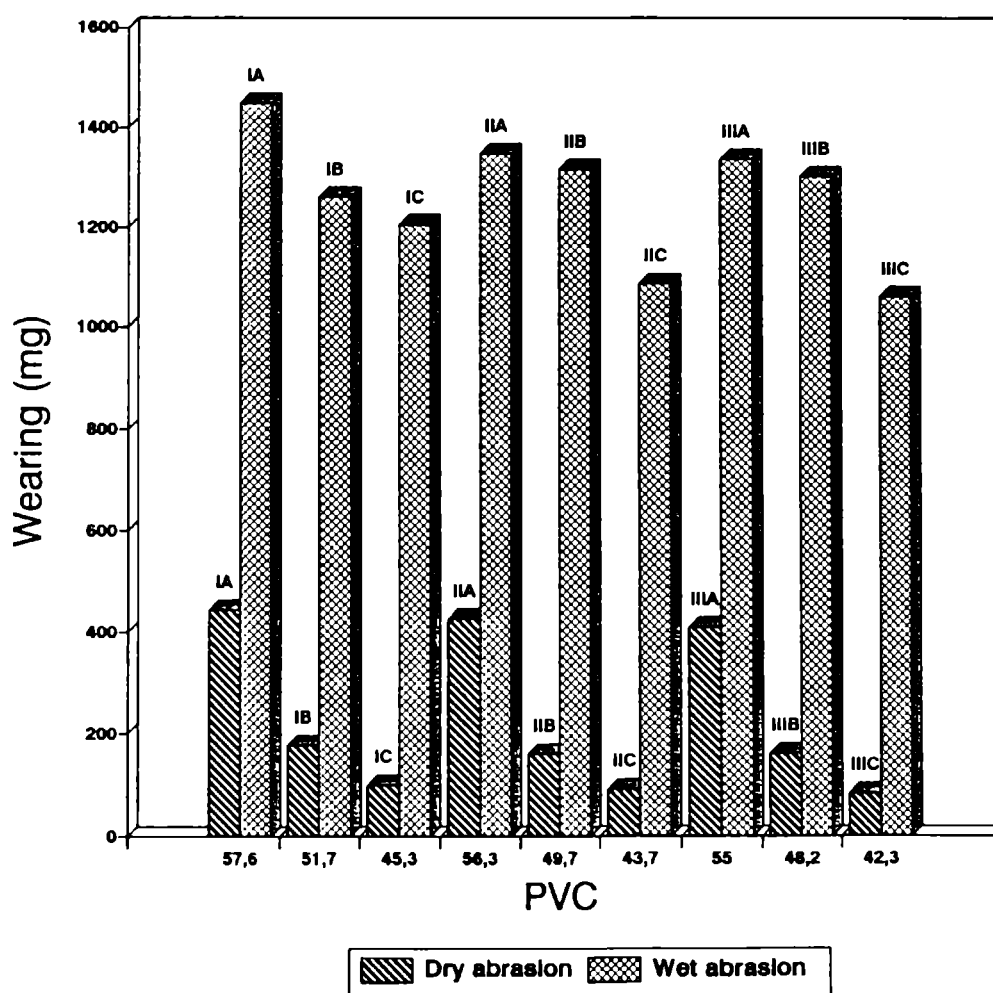


Fig. 4.- Comparative result of dry and wet abrasion test.

The wet abrasion test shows greater wearing values than those obtained in the dry abrasion test.

Results of hardness test, as a function of temperature, are related to the plasticization degree of the agglutinant resin. This is particularly observed over a temperature of 55 °C, which is considered critical; over this temperature value, hardness disminishes abruptly in practically all the samples. This characteristics is independent of plasticizer level and PVC values (Fig. 5).

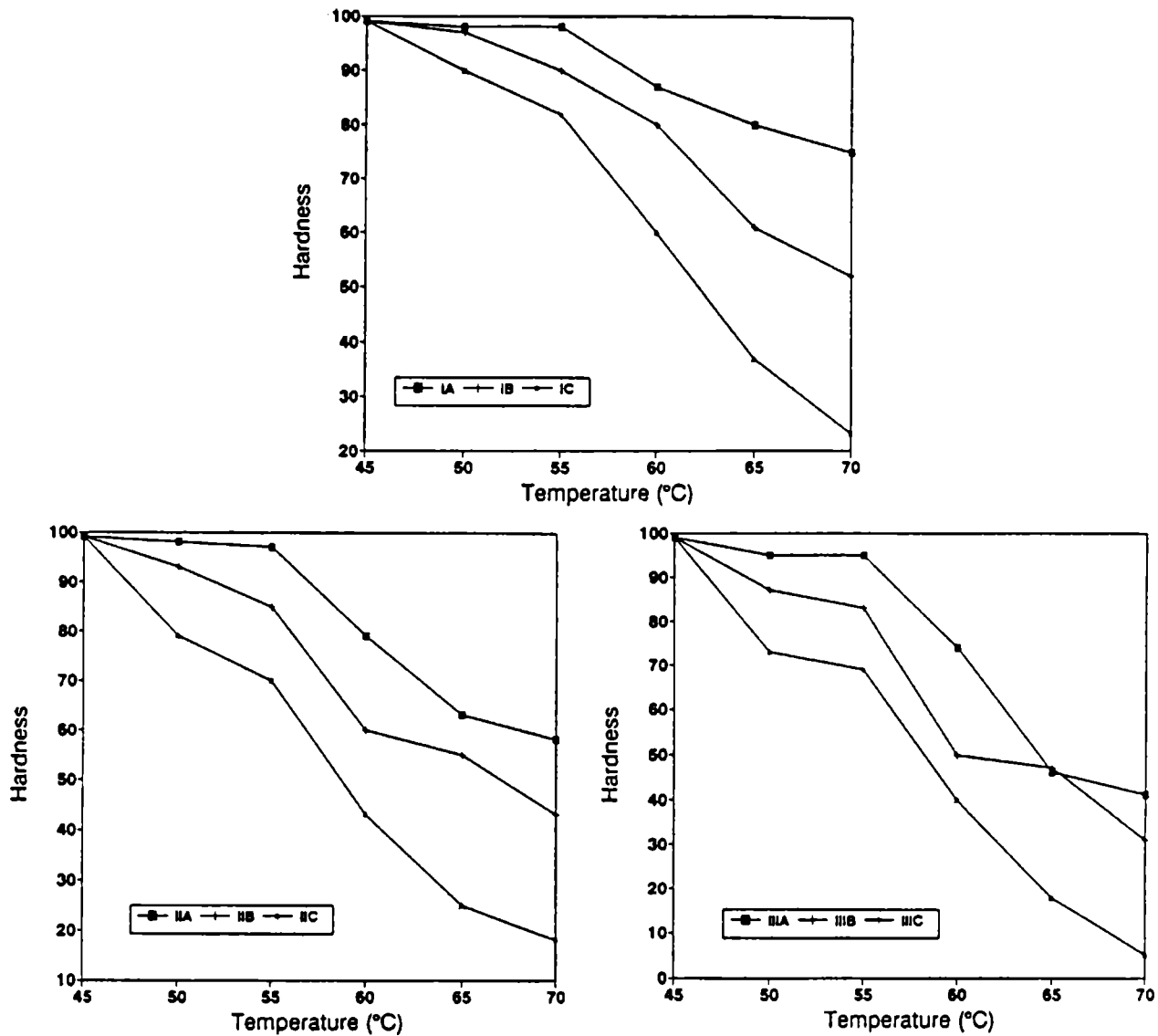


Fig. 5.- Variations of hardness as a function of the temperature.

The indicated critical temperature is a harmful interactive factor in the material application.

Adhesion-tension values are lineally dependent on the employed resin (Fig. 6) and not related with the plasticizer level; the obtained values expressed in kg.cm^{-2} are of the same order than those of the standards used to qualify this type of materials.

In the results of water absorption (Fig. 7) and water elimination (Fig. 8) tests, the increase of weight of the termoplastic mass during immersion is faster than the elimination value.

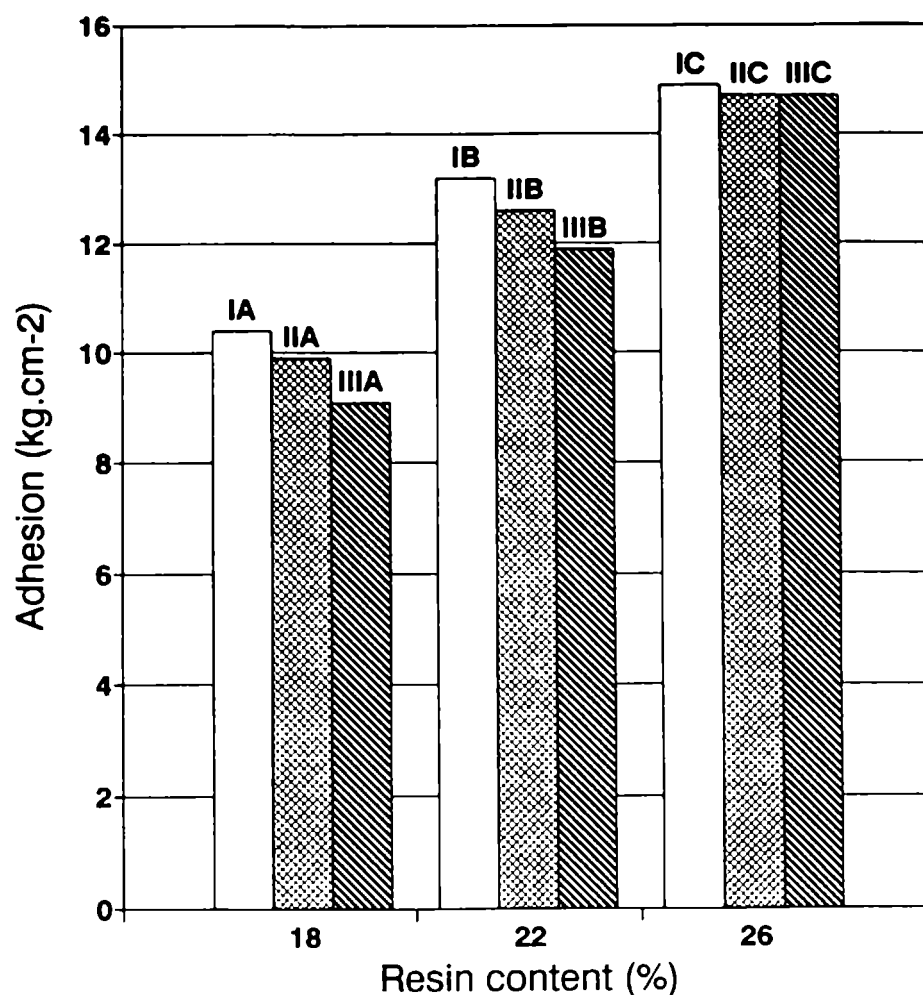


Fig. 6.- Variations in adhesion-strength as a function of resin content.

CONCLUSIONS

- 1.- The wet abrasion wearing values are higher than those obtained in the dry abrasion test. Wearing is directly dependent on the plasticizer level but independent of the maleic resin content.
- 2.- Plasticization degree has a high influence on hardness variation as a function of temperature. A critical point appears at 55 °C with a sudden reduction of hardness values.
- 3.- Adhesion strength is dependent on the resin content, a higher content increases adhesion strength. This parameter is independent of the plasticization degree.
- 4.- Water absorption decreases when plasticizer increases, independently of the resin content. Water elimination rate decreases too.
- 5.- The retained moisture of the thermoplastic traffic material after immersion must be considered as a harmful property in relation to the wearing resistance in service.

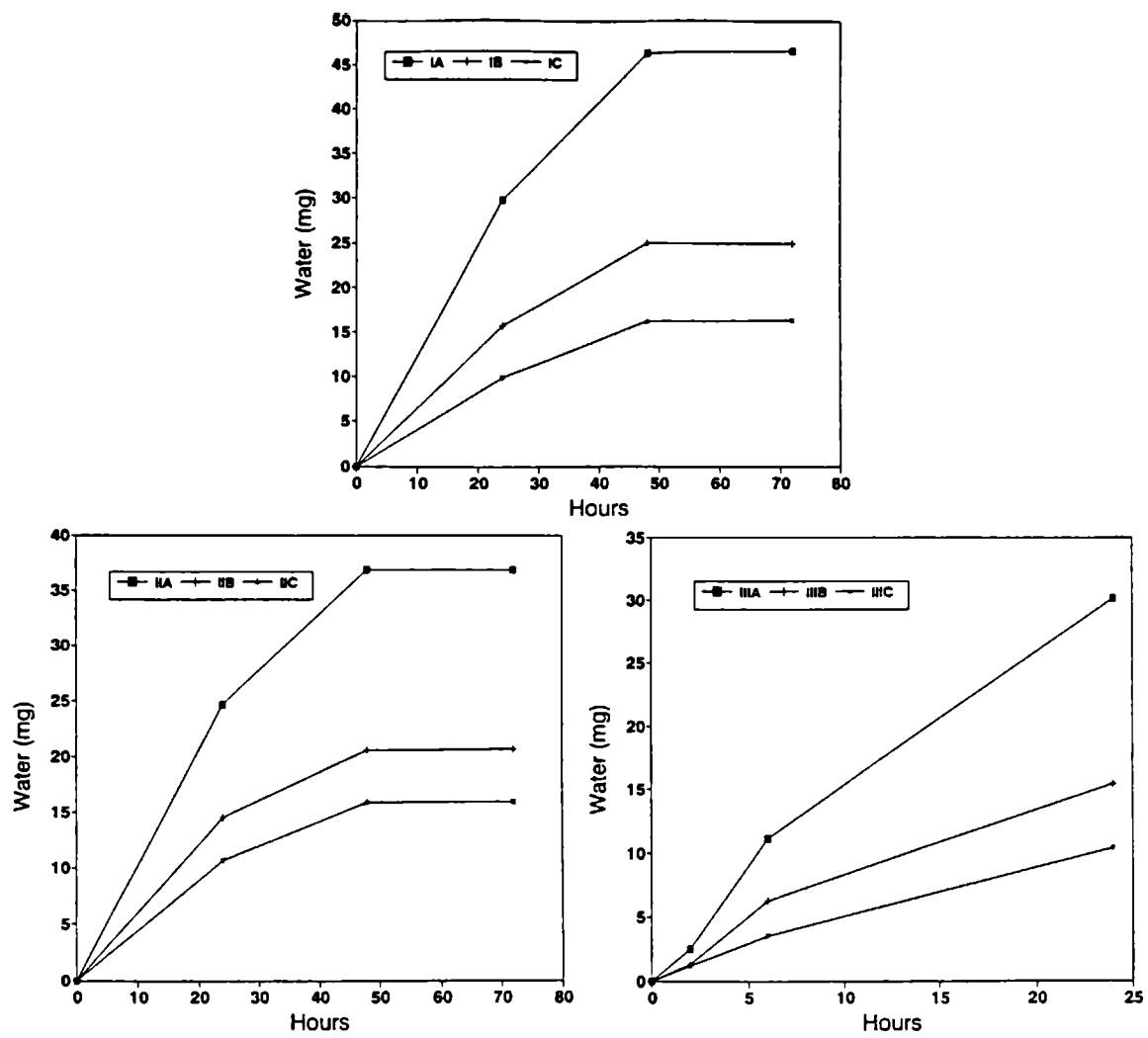


Fig. 7.- Water absorption values as a function of time.

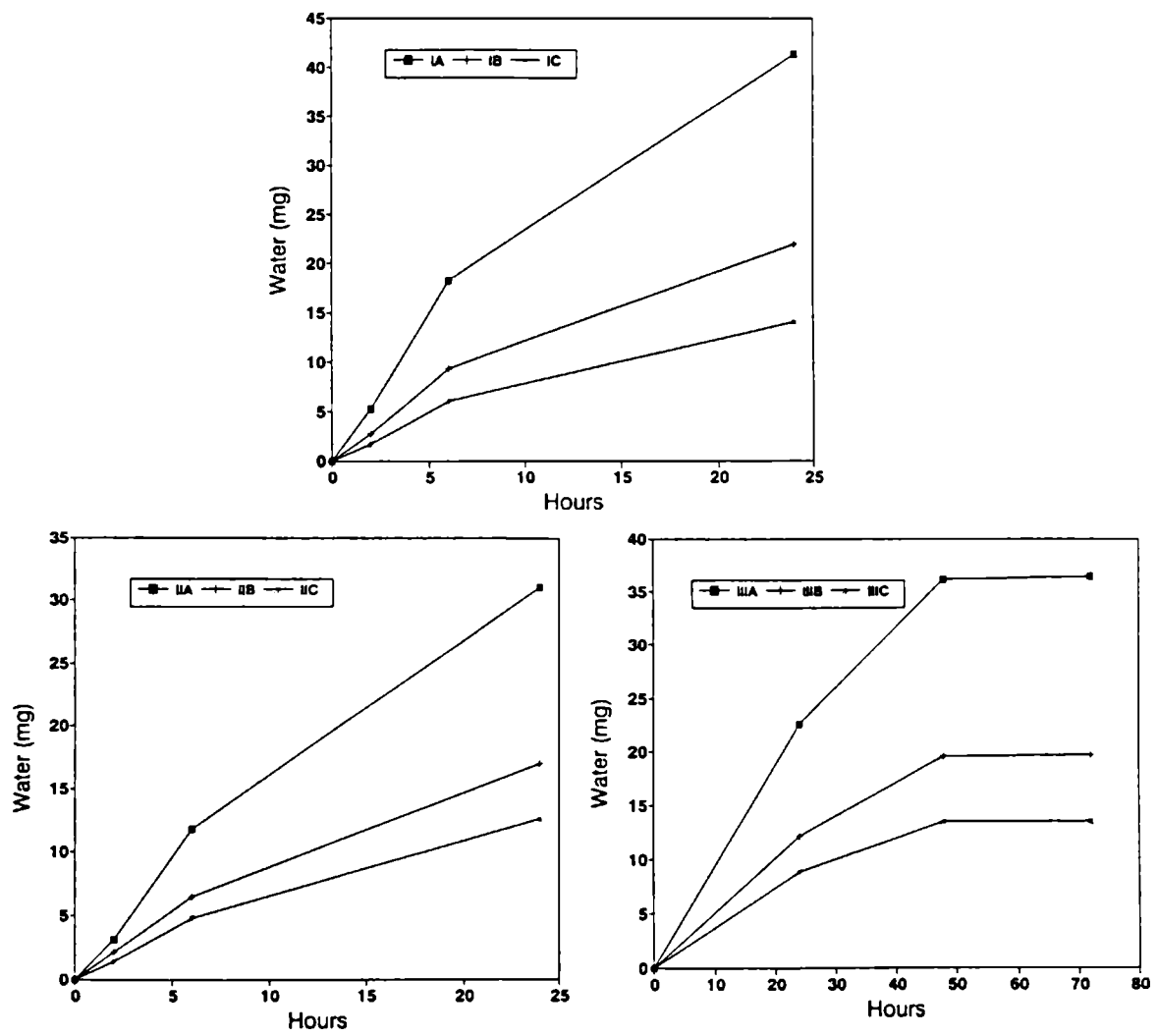


Fig. 8.- Water elimination values as a function of time.

REFERENCES

- [1] Lindberg, B., "Painting Concrete", J. Oil. Col. Chem. Assoc., **57**, 100-113 (1974).
- [2] Nutt, N.O., "A Quantitative Method for Determining the Adhesion of Coatings to Plastics", J. Oil Col. Chem. Assoc., **75**, 53-58 (1992).
- [3] Departamento de Entradas Rodagen de Estado de Sao Pablo. Especificacoes e metodos de ensaios de materiais de sinalizacao rodoviaria, 1990.
- [4] ASTM D-2240. Rubber property - Durometer Hardness, test 35, 702-705 (1980).
- [5] ASTM D-4796. Standard test method for bond strength of thermoplastic traffic marking materials, Vol. 06.01, 846-849 (1980).
- [6] Aznar, A.C., "Proposal for a method to determine the cohesive and adhesive bond strength of traffic marking thermoplastic materials", CIDEPINT-Anales, 215-226 (1994).
- [7] Norma IRAM 1211. Recubrimientos termoplásticos para la demarcación de pavimentos (1981).
- [8] Norma IRAM 1212. Recubrimientos termoplásticos reflectantes para la demarcación de pavimentos (1981).
- [9] Koleske, J.V. (De.), "Paint and Coating Testing Manual", Chapter 66, Fourteenth Edition of the Gardner-Sward Handbook, ASTM Manual Series MNL17 (1995).

CHEMICAL AND ELECTROCHEMICAL ASSESSMENT OF TANNINS AND AQUEOUS PRIMERS CONTAINING TANNINS

EVALUACION QUIMICA Y ELECTROQUIMICA DE TANINOS Y DE IMPRIMACIONES ACUOSAS A BASE DE TANINOS

V. F. Vetere, R. Romagnoli¹

SUMMARY

When the mechanical cleaning of metallic surfaces is not possible, some chemical treatments are an important possibility. The benefit of using acidified aqueous suspensions of tannins in this field has been recognized for more than thirty years. However, little is known about the action of these substances on rusted surfaces. Thus, the chemical reaction of tannins with soluble and precipitated ferric species was studied. The influence of the phosphate anion was also considered.

At the same time, cleaned and oxidized steel surfaces, treated with tannin suspensions were analyzed by microscopy and scanning electron microscopy (SEM) to observe the surface film morphology.

Four tannins were selected to carry out this investigation: quebracho, sulphitated quebracho, mimosa and chestnut.

The experimental results show that each tannin reacts with soluble and precipitated ferric species in a different way. This reaction depends on the pH of the solution. The tannate film formed on the steel surfaces had a plate morphology which also depended on the tannin. The presence of phosphoric acid contributed to the tannate film building.

Keywords: *tannins, phosphoric acid, surface conversion, ferric tannate, plate morphology.*

INTRODUCTION

The performance of an organic coating mainly depends on the metallic surface condition as well as the environment aggressiveness. The application of a good paint on a contaminated or rusted surface results in early failure of the coating. The complete removal of rust is a very important condition to enhance the coating durability.

¹ Miembro de la Carrera del Investigador del CONICET, UNLP

A metallic surface may be prepared either by chemical or mechanical methods. Recently, metallic surfaces derusting by fungi has been reported [1]. The sealing of metal-oxide structures with plastics cured in-situ was also proposed [2].

In some cases, an exhaustive surface cleaning is impossible and chemical treatments are an important alternative. Thomas [3] registered more than 100 commercial products to be applied on poorly prepared steel substrates. They work by different mechanisms: oxide impregnation, stabilization, conversion and inertization. According to the author, the best results were obtained with barrier paints or with red lead pigmented primers. These paints also perform well in surfaces contaminated with chloride and/or sulphate ions.

The usefulness of anticorrosive primers and pretreatments based on aqueous suspensions of tannins acidified with phosphoric acid has been recognized during the last 30 years. In order to convert surface oxide films, tannins are employed in three different forms.

Acid aqueous suspensions of tannins may be used directly on rusted surface after wire brushing; the remaining material is generally removed by washing [4]. These formulations have, as a general rule, bad wettability and surfactants must be used together with low evaporation rate solvents to achieve good brushability. The phosphoric acid and tannin concentrations may reach 55 % and 10 % respectively [5].

Wash primers are formulated adding a water soluble resin to fix the non-adherent products resulting from the oxide layer conversion. This would also help further painting of the metallic surface.

The penetration rate of the above mentioned formulations depends on the solvent employed, the tannin concentration and the oxide layer structure; thus, a 10 % butanol solution proved to be the best solvent and 10% is the recommended concentration level. The highest the tannin concentration the lowest the penetration rate. The optimum phosphoric acid concentration is 10 %. Free resins formulations penetrate deeper inside the oxide layer [6, 7].

According to the results obtained with mimosa tannin [8], these pretreatments are useful in the following conditions:

- a) when the substrate preparation is poor,
- b) when it is necessary to wait some days, after cleaning of the surface, to paint it,
- c) when the thickness of the anticorrosive primer is reduced, and
- d) when it is necessary to paint in wet ambients.

In the case of an oxide layer contaminated with chloride, sulphate, etc., the employment of rust converters combined with an anticorrosive primer is mandatory [8-10].

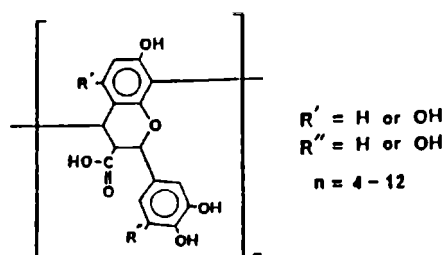
DesLauriers [4] claims that the performance of these systems depends on both the amount of oxide present on the surface and the barrier properties of the complete painting scheme. This is true despite of the ability of the particular tannin to form ferric tannate. Commercial formulations, tested by other researchers, failed in all laboratory tests [11].

Tannins may be also employed as anticorrosive coats. Bruzzoni et al [12] investigated several commercial rust converters in comparison with a conventional alkyd

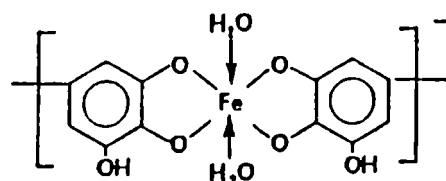
anticorrosive paint. All formulations showed similar protective action when applied on cleaned substrates. The presence of magnetite was not detected among the oxides present on the metallic surface. As time elapsed, oxides evolved to the most harmful lepidocrosite. These paints must be used in combination with either zinc chromate or red lead primer when the converter film thickness is low (20-25 μm) [13].

Anticorrosive paints with ferric tannate were proposed in the literature, for poorly prepared substrates, with promising results [14, 15].

From a chemical point of view, the term tannin is applied to an extract of certain plants which contains polyhydric phenols within its structure. According to DesLauriers [4], they may be represented by the next formula:



Tannins react with the oxide layer giving a black ferric tannate film, 10 μm in thickness and highly reticulated. Ferric tannate is a non crystalline substance. The film would also contain free tannin. The iron content in the film is about 2.5 % [8]. The structure of the complex ferric tannate may be represented as follows [4]:



The formation of magnetite could not be demonstrated. Joseph and Vallejos [16] detected the interaction between tannin and the extender pigment present in the formulation. Converted oxide layers contain ferrous cation coming from the reducing action of tannins on $\gamma\text{-FeOOH}$ [13, 17].

The time for tannins to react with iron oxides is 3 hours as minimum, however, 12-24 hours is waited before painting. Tannins yield 20-30 $\text{m}^2\cdot\text{l}^{-1}$ and are compatible with red lead, zinc chromate and zinc phosphate primers. Tannins may be employed with: alkyd, chlorinated rubber, epoxy, phenolic, polyurethane and polyester resin [9].

Tannins suspensions are more corrosive than distilled water. However, ferric tannate films formed on a steel substrate have some protective properties, depending on the surface chloride concentration [19].

Phosphoric acid is usually incorporated to formulations containing tannins. Several researchers suggested that phosphoric acid would yield to the formation of a passive layer of ferric phosphate. Likewise, Mössbauer spectroscopy demonstrated that ferric phosphate is not formed for phosphoric acid concentrations below 8.5 M [20].

Other substances than tannins able to stabilize iron oxide films has been reported [21-24].

Rust converters based on a resin and phosphoric acid, without tannins, which can act on cleaned and rusted substrates have been developed. In some cases, they showed a performance similar to that of zinc chromate and red lead primers [25-28].

The purpose of this paper is to study the reaction among tannins and cleaned and rusted steel. It attempts to specify some features of the iron oxides-tannins interaction for optimizing current rust converters formulations. Four tannins were chosen to carry out this research: "quebracho", sulphitated "quebracho", mimosa and chestnut. The employment of other less diffused tannins such as pine [29], oak [30] eucalyptus saligna [31], etc. have been reported, but they are not considered here.

The first stage of this investigation comprised the study of the reaction among the selected tannins and the ferric cation at 2.0, 4.0, 6.0 and 8.0 pH values. The mass of tannin precipitated for a given amount of ferric cation, in every case, the influence of the phosphate anion on the complexing capacity of tannins, at the same pH values as well as the reactivity of the four tannins with ferric hydroxide were investigated.

During the second stage, the morphology of the products formed on cleaned and rusted steel surfaces by tannins was determined employing optical microscopy and SEM.

The steel corrosion rate in tannins suspensions was also evaluated. Finally, a primer containing tannin was formulated and its anticorrosive performance evaluated through corrosion potential measurements.

EXPERIMENTAL AND RESULTS

Reactivity among tannins and ferric cation as a function of pH

A solution of each one of the four tannins employed ("quebracho" (*Schinopsis* sp), sulfitated "quebracho", mimosa and chestnut) was prepared as follows: 10 g of tannin was placed in a 400 ml beaker and suspended in 400 ml of hot water (90 °C); then, 50 ml of 1 M potassium nitrate was added to coagulate colloidal substances and the system was left 24 hours in repose, filtered and transferred to a 500 ml volumetric flask.

10 ml of a 10 g.l⁻¹ ferric nitrate solution and 10 ml of the 1 M potassium nitrate solution were placed in a 250 ml beaker. Afterwards, 100 ml of the tannin solution was added and the pH value adjusted to 2, 4, 6 or 8. After 24 hours the pH value was controlled and adjusted to the original ones. 24 hours later, the pH was measured again and the suspensions filtered. The amount of both the tannin and the iron precipitated were determined by drying at 100 °C and calcination at 1000 °C, respectively.

The working temperature was 20 ± 1 °C.

The precipitated form of tannin and ferric species is a ferric tannate whose IR spectrum coincides with the spectrum of tannin alone.

The results plotted in **Fig. 1** show that the maximum reaction capacity of tannins with soluble ferric species increased together with pH, this is the mass of tannin precipitated for a given amount of iron increased as pH did. The highest the amount of precipitated tannin the best the quality of the obtained film [8].

Chestnut tannin showed higher reaction capacity at low pH values; which was exceeded by mimosa tannin as pH increases. Finally at alkaline pH values such a capacity for sulphitated tannin exceeded the corresponding to the other tannins.

From data in **Fig. 1**, at pH = 4, it may be calculated that chestnut precipitated the highest amount of tannin per mmole of ferric cation, 700 mg; while mimosa, "quebracho" and sulfited "quebracho" 560, 500 and 195 mg, respectively. Those amounts represent the highest amount of each tannin reacting with a given amount of ferric cation in the conditions of the experiment.

As it was stated in the literature [33], ferric tannates resulted insoluble compounds, which precipitated from tannins suspensions when ferric cation was added. They are non adherent compounds and surfaces treated with acid aqueous suspensions of tannins must be washed to eliminate loose reaction products. Instead, primers are formulated with resins in order to fix the loose tannates resulting from the conversion of the steel surface [4]. Ferrous tannates are soluble in water, colourless and easily oxidable [33].

Reactivity among tannins and ferric cation as a function of pH in the presence of phosphate anion

The procedure employed in this case was similar to the former one with the exception of 2.0 g of phosphoric acid added to the beaker containing the ferric cation. The precipitated was analyzed to determine the amount of tannin, iron and phosphate present. Phosphate content was determined by a gravimetric technique [32] and the results plotted in **Fig. 2**.

Phosphate anion and tannins compete for the ferric cation; therefore, the presence of that anion diminishes the amount of tannin precipitated for a given amount of iron. Chestnut tannin is the less affected by such competition because it precipitated 87.3% (at pH = 4) of the amount of tannin consigned in the preceeding paragraph; while mimosa, "quebracho" and sulfited "quebracho" 49.5, 7.80 and 5.70% respectively. These calculations were made from data in **Fig. 2**. However, the presence of phosphoric acid is necessary because it acts on clean steel surfaces contributing to iron oxides dissolution, generating the ions to form the ferric tannate film. Likewise, it improves the wetting properties of tannins suspensions.

Reactivity among tannins and precipitated ferric hydroxide as a function of pH

10 ml of a 10 g.l⁻¹ ferric nitrate solution and 10 ml of the 1 M potassium nitrate solution were placed in a 250 ml beaker. The pH value was adjusted to 2.0, 4.0, 6.0 and 8.0, respectively. The system was allowed to repose for 24 hours. The same procedure was performed but employing the solution of each tannin in water. After 24 hours the content of each beaker was mixed and the pH adjusted. The pH adjustment was repeated 24 hours later and the systems allowed to repose one day more. Finally, the solids present in each beaker

were filtered and both tannin and ferric contents determined according to the procedure described in the first paragraph of this section. Results are shown in Fig. 3.

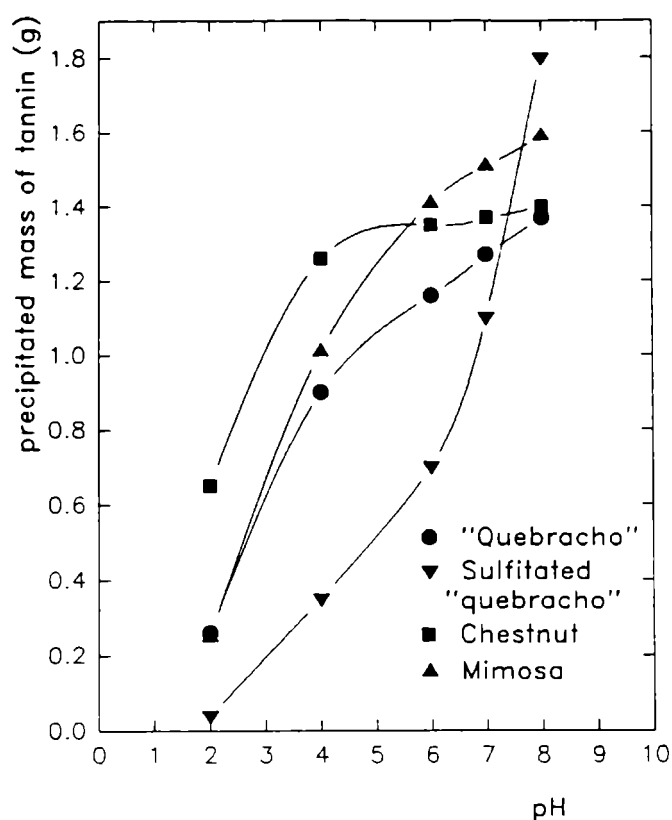


Fig. 1.- Mass of tannin precipitated from 1.79 mmoles of soluble ferric cation as a function of pH, for the different tannins.

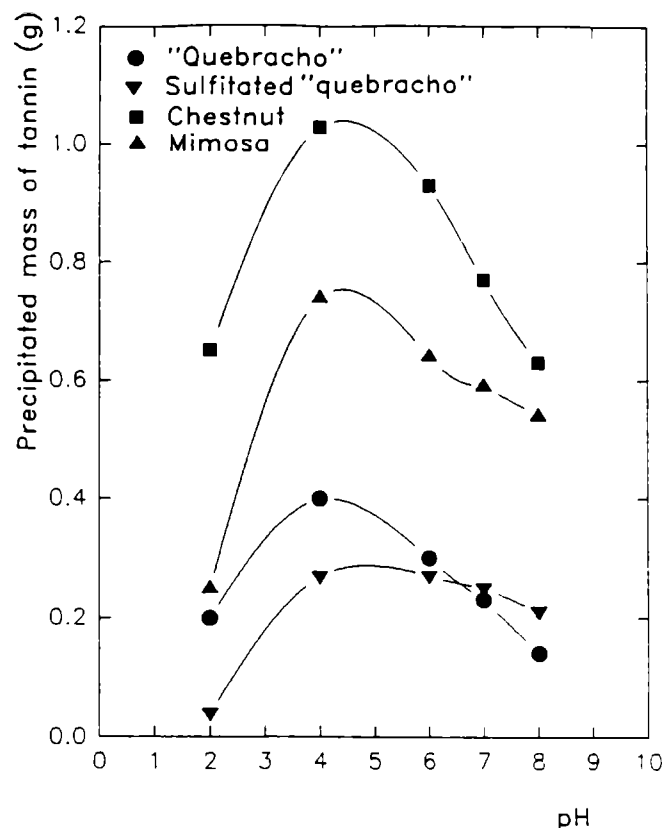


Fig. 2.- Mass of tannin precipitated from 1.79 mmoles of soluble ferric cation in the presence of 20.0 mmoles of phosphoric acid as a function of pH, for the different tannins.

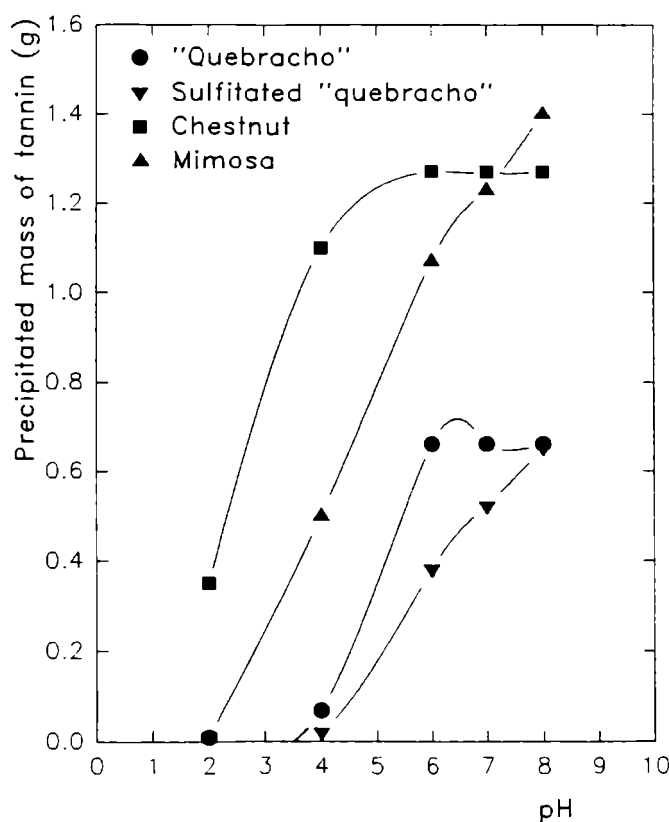


Fig. 3.- Mass of tannin precipitated from 1.79 moles of precipitated ferric hydroxide as a function of pH, for the different tannins.

Comparing Figs. 1 and 3, it may be seen that the reaction capacity of tannins with precipitated ferric hydroxide is less than the one observed with soluble ferric cation. It also depends on the tannin tested. Chestnut tannin is the most reactive while "quebracho" and sulphitated "quebracho" are the less reactive tannins. From data in Fig. 3, at pH = 4, it may be calculated that chestnut precipitated 81.8% of the precipitable tannin per mmole of ferric

cation; while mimosa, "quebracho" and sulfitated "quebracho" 73.3, 44.4 and 77.1 %, respectively.

The curves in **Fig. 3** have a similar shape. The amount of tannin reacting with iron increased as pH did up to the interval 3.0-5.0; in this zone the curve presents a maximum. The initial increase is attributed to the tannin deprotonization which favours ferric cation complexation. At higher pH values the ferric hydroxide precipitation competes with the formation of ferric tannate reason by which the amount of precipitated tannin diminished. The pH interval 3.0 - 5.0 is the optimum zone to form the ferric tannate film. As tannins react with precipitated iron hydroxide in a lesser extent, unreacted tannin may combine with soluble ferric species formed lately by corrosion.

Morphology of surface compounds formed by tannins on pickled AISI 1010 steel panels

This study was carried out employing pickled AISI 1010 steel panels (C: 0.12 %, Si: 0.01 %, Mn: 0.35 %, S: 0.02 %, P: 0.02 %). Panel dimensions were 10.0 x 1.5 x 0.1 cm. They were degreased with calcium hydroxide and washed with distilled water.

The panels were treated with 5 % tannin suspensions keeping their natural pH (**Table 1**) or modifying their pH to 2.0 and 4.0 with nitric and phosphoric acid, respectively. Time reaction was 48 hours.

TABLE 1

Corrosion rate of pickled AISI 1010 panels in aqueous suspensions of tannins

Tannin	pH	Corrosion rate mg.cm⁻².day⁻¹
"Quebracho"	3.83	0.227
Sulphitated "Quebracho"	4.14	0.402
Mimosa	4.40	0.227
Chestnut	3.09	0.505
Blank	7.00	0.140

NOTE: pH values measured in a suspension containing 0.5 g of tannin in 50 ml of distilled water

Once the reaction took place, the panels were observed by means of a microscope (40X). The morphology was studied by SEM (350X in most cases). Then, loose reaction products were removed by brushing and the observations repeated. Aqueous suspensions of tannins react with ferric ions produced by steel corrosion generating a black iron tannate film.

"Quebracho" tannin showed the best spreading ability on steel surfaces while chestnut and sulphitated "quebracho" tannins the worst. The spreading ability is highly improved when phosphoric acid is added to the formulation. Corrosion of the base metal was observed in sites

when the liquid film did not cover the metal surface. By this reason many commercial products incorporate surfactants in their formulation [5].

For tannin suspensions at their natural pH, a microscopic analysis (40X) showed that "quebracho" tannin formed the best film on the steel surface. It also showed good adherence to the substrate. Underfilm corrosion was observed in the case of chestnut and sulphitated "quebracho" tannins. For the sake of simplicity, photographs and micrographs of panels treated with mimosa tannin (**Fig. 4**) are included in this paper.

SEM analysis of treated surfaces revealed a plate morphology of tannate film, aspect which varied for the different tannins (**Fig. 5**, 350X). "Quebracho" tannin produced small plates and a highly reticulated surface; sulphitated "quebracho" originated a film with bigger plates and less cracks. All the films appeared to be loose-leaf films.

Some of the ferric tannate film remained strongly adhered to the steel substrate when the treated panel was brushed with a hard brush. The tannate film in contact with the metallic surface appeared to be more compact and less cracked. **Fig. 6** (3500X) shows the adherent film remaining after brushing.

The reactivity of tannins with cleaned steel surfaces ensures the adherence of the tannate film to the base metal [34].

"Quebracho" and mimosa tannins generated the best films due to their spreading properties and highest reactivity for pH values close to neutrality (**Fig. 1**).

Tannins suspensions in nitric medium (pH = 2) also form a ferric tannate film with a plate morphology (**Fig. 7**, 40X). However, in all the cases, underfilm corrosion at the base metal took place. Chestnut tannin treated panels showed the lowest degree of corrosion. By this the reason studies employing tannin suspensions acidified with nitric acid did not go on.

When phosphoric acid was used instead of nitric acid, it was observed that the tannate film seemed to be less cracked (**Fig. 8**, 350X). The presence of phosphoric acid diminished markedly the base metal corrosion. Both, nitric and phosphoric acids, favoured the tannate film formation. Acids allowed the dissolution of the base metal causing a homogeneous precipitation throughout the metal surface and, consequently a tannate layer of better quality.

Chestnut tannin produced the best films from suspensions acidified with phosphoric acid. In diminishing the natural pH of tannin suspensions, it may be seen that chestnut tannin reacts with ferric cation in a greater proportion (**Figs. 2-3**), generating a better quality film.

After brushing, it was observed the existence of a strongly adhered tannate film on the metal surface.

Morphology of the surface compounds formed on rusted AISI 1010 steel panels by tannins

Rusted panels were prepared from pickled AISI 1010 steel panels exposed in a chamber at 40 ± 1 °C, wetting them periodically with distilled water, during 3 weeks. The oxide film

obtained by this technique was 150 μm thick being FeOOH the most important product, which is normally found in atmospheric exposures [4]. The rusted panels were brushed with a wire brush to remove weak and not adhered corrosion products. The thickness of the remaining layer was 30 μm .

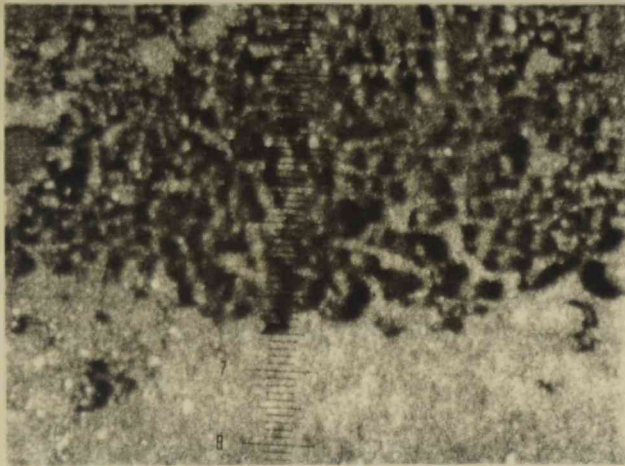


Fig. 4.- Photograph of the ferric tannate film formed on a clean AISI 1010 steel surface by mimosa tannin suspension at its natural pH (40 X).



Fig. 5.- SEM micrograph of the ferric tannate film formed on a clean AISI 1010 steel surface by mimosa tannin suspension at its natural pH (350X).



Fig. 6.- SEM micrograph of the remaining of the ferric tannate film formed on a clean AISI 1010 steel surface by mimosa tannin suspension, at its natural pH, after brushing (3500X).



Fig. 7.- Photograph of the ferric tannate film formed on a clean AISI 1010 steel surface by mimosa tannin suspension at pH = 2 of nitric acid (40X).

The panels were treated with 5 % tannin suspensions keeping their natural pH value (Table 1) or modifying it to either 2.0 or 4.0 with phosphoric acid. Time reaction was 48 hours. Once the reaction took place, the panels were observed in the same way as pickled ones did.

When rusted steel panels were treated with tannins suspensions at their natural pH, the oxide morphology (Fig. 9, 350X) is replaced by a plate morphology (Fig. 10, 350X). The oxide present on the surface supported the tannate film leading to a less cracked film. A significant amount of non-converted rust was encountered under the tannate film formed by sulphitated "quebracho" or chestnut tannins. However, these react strongly with outer oxides. Mimosa and "quebracho" tannins produced films of higher quality; this could be attributed to their better spreading properties. Besides, the mimosa variety is highly reactive with ferric hydroxide (Fig. 3). Again, the presence of phosphoric acid improved film quality and reduced the base metal corrosion (Fig. 11, 350X).

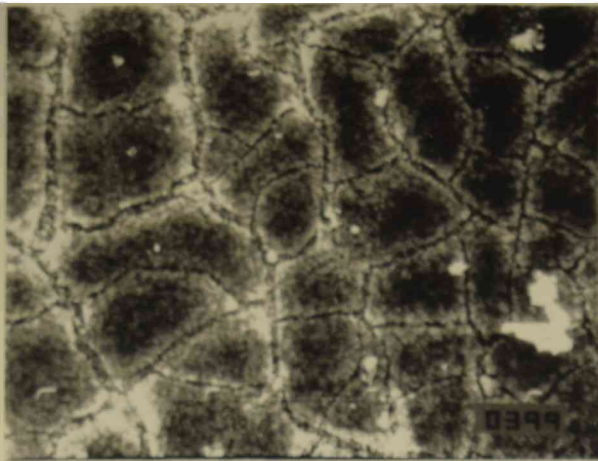


Fig. 8.- SEM micrograph of the ferric tannate film formed on a clean AISI 1010 steel surface by mimosa tannin suspension at pH = 2 of phosphoric acid (350 X).



Fig. 9.- SEM micrograph of the untreated ferric oxide morphology (350X).



Fig. 10.- SEM micrograph of the ferric tannate film formed on a rusted AISI 1010 steel surface by mimosa tannin suspension at its natural pH (350X).

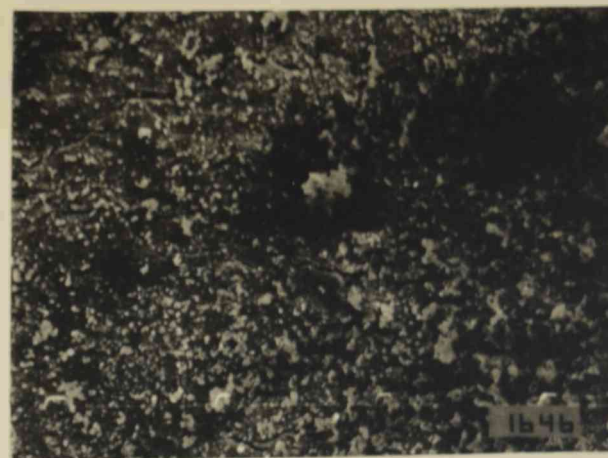


Fig. 11.- SEM micrograph of the ferric tannate film formed on a rusted AISI 1010 steel surface by mimosa tannin suspension at pH = 2 of phosphoric acid (350X).

For phosphoric acid suspensions, chestnut gave very good films while "quebracho" and Mimosa tannins produced films of fair quality. This behaviour could be explained, partially, considering the curves in **Fig. 3**.

Adherence to the steel substrate and replacement of the iron oxides morphology by a plate one, indicate that tannins: a) actually convert the steel surface, b) stabilize the rusted steel surface and c) may be employed as pre-treatments on rusted steel surfaces.

Determination of AISI 1010 steel corrosion rate in tannins suspensions

This step was performed in order to know if the steel corrosion was avoided by the tested tannins. For corrosion rate determinations, 10.0 x 1.5 x 0.1 cm steel panels were placed in a 2 g tannins suspensions for 5 days, stirring them periodically. After 5 days, the panels were taken off and the total amount of dissolved iron determined colorimetrically. No adherent films formed on the steel surface kept in contact with tannin suspensions. Tannate films adhere on such a surface only when solvents are completely evaporated; these films have some corrosion resistance [19, 35]. Results displayed in **Table 1**, show that tannins suspensions are more

corrosive than distilled water (blank), as it was stated in the literature [18]. The corrosion rate also varied for the different tannins; thus chestnut suspensions are the most corrosive, probably due to the more acidic properties of this tannin.

Finally, an aqueous primer containing tannin was formulated and its anticorrosive performance evaluated through open circuit potential measurements. The composition of the primer was as follows: acrylic resin 20% by v/v, tannin 6% w/v phosphoric acid 3% w/v and corrosion inhibitor 0.3% w/v. The inhibitor to stifle flash rusting was selected among: butyraldehyde, benzaldehyde, cyclohexanone, as it is suggested in the literature [36]. The primer was applied by brushing on a slightly rusted steel panel up to a thickness of 10 μm and allowed to cure for 7 days. The measurements were carried out following a procedure previously described [37]. The variation of the open circuit potential as a function of time is presented in Fig. 12 together with the curves of the primer without tanning and the naked steel electrode.

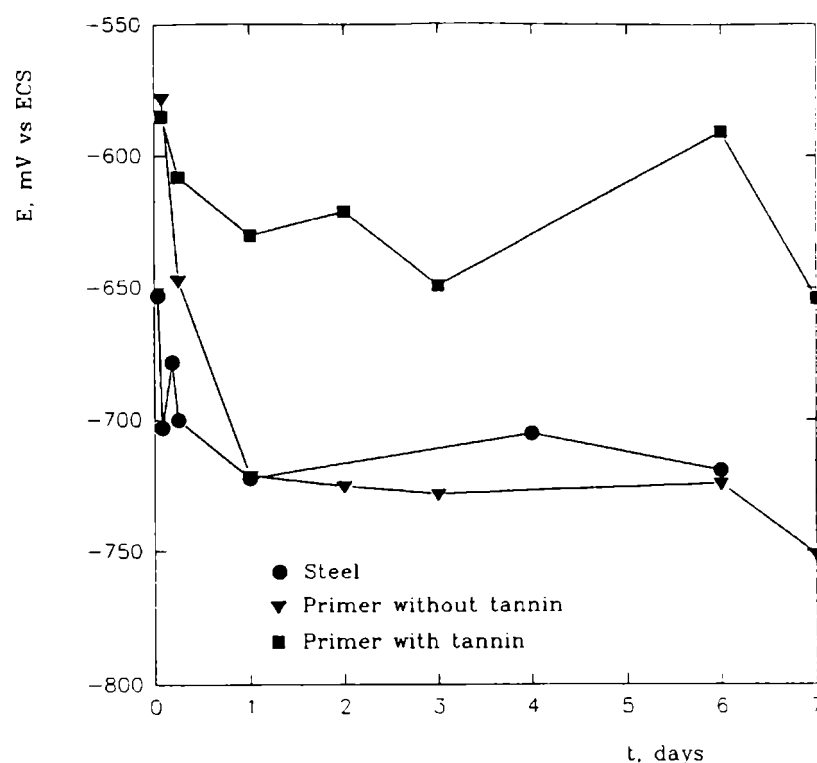


Fig. 12.- Corrosion potential variation as a function of time for steel coated with an aqueous primer containing tannin. Electrolyte: sodium perchlorate 0.5 M.

It may be seen that the primer containing tannin protected steel from corrosion because the electrode potential was shifted to the more noble values during a week. In the other cases, the electrode potential derived quickly to the steel corrosion potential. This protection was due to the presence of tannin, the sole addition of phosphoric acid was not enough to stop corrosion.

CONCLUSIONS

1. The analytical procedure previously outlined is recommended to evaluate the interaction of tannins with iron species. Previous to formulation, each tannin must be evaluated by a similar procedure to assess its usefulness in formulating anticorrosive primers.

2. The determination of pH and corrosivity of tannin suspensions may help in understanding its interaction with steel. The more acidic and the more corrosive the suspension, the greatest the interaction with steel will result.

3. The optimum pH for the tannate film to develop is comprised in the range 3.0-5.0. The values are close to the natural tannins suspensions pH.

4. The presence of phosphoric acid in the formulations passivates steel surfaces and favours the tannate film formation on cleaned steel surfaces. It also assists oxides dissolution and further reaction with tannins.

5. Tannins react with cleaned and rusted steel surfaces generating a layer with a plate morphology replacing the globular one of iron oxides.

6. Aqueous primers containing tannins do inhibit steel corrosion as it was revealed by potential corrosion measurements.

ACKNOWLEDGEMENTS

The authors thank to CIC (Comisión de Investigaciones Científicas de la Provincia de Buenos Aires) and to CONICET (Consejo Nacional de Investigaciones Científicas y Técnicas) for their sponsorship to do this investigation and thank to Lic. Mirta Stupak and Tco. Químico Pedro Luis Pesi for their help in photographic registers.

BIBLIOGRAFIA

- [1] Winkel P.- Galvanotechnik, **83** (9), 3095-97 (1992).
- [2] White J.- Corrosion Reviews, **7** (2 & 3), 235-257 (1987).
- [3] Thomas N. L.- J. Protect. Coat. & Lin., 63-71 (Dec, 1989).
- [4] DesLauriers P. J.- Mat. Perf., **26** (11), 35-40 (1987).
- [5] Alvarez Z. E., Callozo I., Valdés D.- Rev. Iber. Corros. y Prot., **XVIII** (1), 35-38 (1987).
- [6] González M. I., Corvo F.- Rev. Iber. Corros. y Prot., **XVIII**, 39-41 (1987).
- [7] Kurkurs O.- Produkti atmosfernoi korrozii zheleza i obraska porzhauchine, Ed. Zinatne, Riga, 83-86 (1980).
- [8] Seavell A. J.- J. Oil Col. Chem. Assoc., **61** (12), 439-462 .
- [9] Gianelli R.- Memorias del II Congreso Iberoamericano de Corrosión y Protección, Venezuela, 253-257 (1986).
- [10] Morcillo M., Feliú S., Simancas J.- Farbe + Lack, **95** (10), 726-(1989).

- [11] Emeric D. A., Miller C. E.- Proc. ADV MAT/91 (NACE, Houston), San Diego, 212 (1991).
- [12] Bruzzoni W. O., Aznar A., Iñiguez Rodríguez A.- Rev. Iber. Corros. y Prot. **6** (2), 3-10 (1975).
- [13] Morcillo M., Gracia M., Gancedo J. R., Feliú S.- Memorias del II Congreso Iberoamericano de Corrosión y Protección, Venezuela, (1986).
- [14] Seavell A. J.- J. Oil Color Chem. Assoc, (8) 293-306 (1992).
- [15] Draper, P. A.- J. Oil Color. Chem. Assoc., 68 (10), 243-250.
- [16] Joseph G., Vallejos R.- Rev Iber. Corros. y Prot., **XIX** (6), (1988).
- [17] Kuzniecowa J. I., Iwanow J.- Ochrona Przed Koroz. 33 (8-9) (1990).
- [18] Morcillo M., Feliú S., Simancas J., Bastidas J. M., Galvan J., Feliú S. (Jr.), Almeida E. M.- Corrosion (NACE), 48 (12) (1992).
- [19] González M. I., Abreu A.- Revistas de Ciencias Químicas, **15** , 315-317 (1984).
- [20] Nigam A. M., Tripathi R. P., Dhoot K.- Corr. Sci., **30** (8-9), (1990).
- [21] NIPPON OILS & FATS CO.- Jap. Pat. Abs. 92 (21) Gp G, 54. Patent Number 04/110357.
- [22] PENZOIL PRODUCTS CO.- United States Patent 5015507: Off. Gaz. (2) 1036 (1991).
- [23] Balmforth B.- Proc. "Corrosion 91", Cincinnati, Paper 561.
- [24] Balmforth B.- Chemicals for the Automotive Industry, Drake J. G. (Ed.), Royal Society of Chemistry, 38-46 (1991).
- [25] Guruviah S., Sundaram M.- Proc. Adv. Surf Treatment Metals, Bombay, 216-20 (1987).
- [26] Lin Ch., Lin P., Hsiao M.- Meldrum D. A., Martin F. L.- Ind. Eng. Chem. Res., **31** (1), 424-430 (1992).
- [27] Watanabe T., Kanda, S., Oono H.- JP 62,260,866 [87,260,866] (Cl. C09D3/58) (1987).
- [28] Szego F., Szego F. M., Patel Szego K.- Hung. Teljes HU 43,100 (Cl C08L33/08) 28SEP1987.
- [29] Matamal A. G., Smeltzer W., Benavente, R.- Proc. "Surface Modification Technologies III" (Minerals, Metals and Materials Society, USA), Neuchatel, 403-411 (1989).
- [30] Gust J.- Ochrona Przed Koroz., 34 (7), 151-154 (1991).

- [31] González M. I., López Planes, R.- Rev. Iber. Corros. y Prot., **XIX** (6), 374-376 (1988).
- [32] Bermejo Martínez F., Prieto Bouza A.- Aplicaciones analíticas del AEDT y similares, Imprenta del Seminario Conciliar, Santiago de Compostela, 268 (1960).
- [33] Noller C. R.- Química de los Compuestos Orgánicos, López Libreros Editores S. R. L., Buenos Aires, 758-759 (1968).
- [34] Brandau, A. H., Introduction to coatings technology, Federation Series for Coatings Technology, U.S.A., 40, 1990.
- [35] Ross, T. K., Francis, R. A.- Corros. Sci., 18, 351-361.
- [36] Uhlig, H. H.- The Corrosion Handbook, John Wiley & sons, Inc., N. Y. 910-912 (1948).
- [37] del Amo, B., Romagnoli, R., Vetere, V. F.- Corrosion Reviews, 121-134 (1996).

DILUTE-SOLUTION VISCOSIMETRY AND SOLUTION PROPERTIES OF COLLOIDAL POLYMERS

ESTUDIO POR VISCOSIMETRIA EN SOLUCION DILUIDA Y PROPIEDADES EN SOLUCION DE POLIMEROS COLOIDALES

J.I. Amalvy¹

SUMMARY

The intrinsic viscosities of a terpolymer of methyl methacrylate, ethyl acrylate and methacrylic acid, prepared by semicontinuous emulsion polymerization (latex) were measured in acetone and THF at different temperatures. Data were analyzed with the aid of the equations of Huggins, Kraemer, Martin, Schulz-Blaschke and an equation recently suggested by Rao. Relationships between different parameters were also considered. The effects of low-molecular weight and water-soluble compounds on the intrinsic viscosities were observed for uncleaned samples of latex as compared to samples purified, by single precipitation or by dissolution and precipitation from THF. Solvent powers and effects of degree of purification and temperature on viscosity are discussed. Polymer-solvents interactions are discussed in terms of the acceptor / donor properties of the solvents.

It is concluded that purification of functionalized latices can lead to modifications of the original systems, through the elimination of different polymer chains.

Keywords: DSV; solution properties; colloidal polymers; latices.

INTRODUCTION

In latex synthesis by emulsion polymerization, the molecular weight (M) of the colloid polymer reaches relatively high values. Several methods for determination of molecular weight are available, such as GPC, osmometry or dilute solution viscosimetry (DSV). DSV is based on the measurements of the increase in viscosity of a dilute polymer solution and allows determination of the intrinsic viscosity ability of a polymer to increase the viscosity of a particular solvent at a given temperature. This quantity provides a wealth of information relating to the size of the polymer molecule in solution, including the effects of polymer structure, molecular shape and degree of polymerization and polymer-solvent interactions upon chain dimensions. There are several equations that relate the intrinsic viscosity and other parameters reflecting solution properties, and relations between these parameters of these equations have also been suggested.

¹ Miembro de la Carrera del Investigador de la CIC

DSV also provides information on polymer - solvent interaction, which is of importance for systems used in products like paints and coatings. Understanding the interactions between polymers and solvents is therefore of practical importance.

If absolute molecular weight determination is not possible, the intrinsic viscosity determination can be used as a relative method to characterize polymers.

Berger [1] in his determination of molecular weight by viscosimetry, found that the presence of additives does not substantially affect the intrinsic viscosity of polymer solutions. However, Anzur et al. [2] studied the solution properties of acrylic emulsion copolymers and concluded that determination of Mw by viscosity measurement (as well as GPC) of uncleaned emulsion polymer samples is questionable due to the influence of residual emulsifier.

Most studies of DSV have been performed with homopolymers and the presence of a second or third type of repeat unit causes the dilute solution behaviour of copolymers and terpolymers to be more complex than in the homopolymer case. The most obvious factors which affect the intrinsic viscosities of co- or terpolymers are composition, composition distribution and the sequence length distributions.

In most practical applications of latices, a few percent of an acidic monomer (methacrylic acid for example) are commonly added during the synthesis to improve the freeze-thaw and mechanical stability of the final product. In functionalized latices the way and timing of functional monomer addition could have an important effect in the latex structure. Even in non-functionalized latices the surface of particles acquire carboxylic groups due to the hydrolysis of the ester linkage during the polymerization and storage [3]. This part of the latex particle could be of a hydrophilic nature and even water-soluble. The solution properties of cleaned samples should be different when compared with uncleaned samples, due to the elimination of the water-soluble fraction during the purification process.

The present study deals with the solution properties of a terpolymeric system composed of methyl methacrylate, ethyl acrylate and methacrylic acid in two common solvents used in DSV, acetone and tetrahydrofuran (THF), with and without purification and at different temperatures. In this work we also test the available relations between different parameters relating to polymer solution properties.

EXPERIMENTAL

The latex was prepared by a semicontinuous emulsion polymerization method with a variable monomer feed rate. Details of synthesis can be found in a previous paper [4].

The solvents for viscosity of polymer solutions used in this work were acetone and tetrahydrofuran (THF) of analytical grade.

Samples of uncleaned latex were prepared by air drying, and dissolving in the solvent. Cleaned samples were prepared by coagulation from the latex, by adding isopropanol drop-by-drop to the emulsion and shaking. The polymer was then filtered, washed exhaustively with water and dried to constant weight. Further purifications were carried out by solubilizing the polymer in THF, precipitating with water and drying it.

The viscosities of polymer solutions were determined in most cases at 15, 20, 25, 30 and 35 °C, by means of a commercial, calibrated Ubbelöhde-type viscometer. Triplicate measurements usually agreed within 0.3 seconds. Initial polymer concentrations were between 0.20-0.45 g of polymer per 100 ml of solution, prepared at 20 °C. The concentration at the other temperatures were calculated taking into account the density of the solvents at each temperature. Calibration of the viscometer was performed using flow times measured and reported viscosity of chloroform, acetone, THF and toluene at different temperatures.

For the calculations, the following relation was used:

$$\frac{\eta}{\eta_o} = \frac{\left(A \cdot t - \frac{B}{t^2} \right)}{\left(A \cdot t_o - \frac{B}{t_o^2} \right)} \quad (1)$$

where η and η_o are the viscosities and t and t_o the flow times of the solution and pure solvent respectively, and A and B are the constants of the viscometer.

In some cases the intrinsic viscosity were close to or even higher than 4 dL/g and a correction for non-Newtonian behaviour should have been applied [5], but for the purpose of this work this was not performed.

RESULTS AND DISCUSSION

Data from the polymer solutions were analyzed using least-squares analysis with the following mathematical equations:

- relationships for very dilute solutions:

Huggins
$$\left(\frac{\eta_{sp}}{C} \right) = [\eta] + K_H \cdot [\eta]^2 \cdot C \quad (2)$$

Kraemer
$$\left(\frac{\ln \eta_r}{C} \right) = [\eta] + K_K \cdot [\eta]^2 \cdot C \quad (3)$$

- relationships over a large concentration range:

Martin
$$\ln \left(\frac{\eta_{sp}}{C} \right) = \ln [\eta] + K_M \cdot [\eta] \cdot C \quad (4)$$

Schulz-Blaschke (SB)
$$\left(\frac{\eta_{sp}}{C} \right) = [\eta] + K_\eta \cdot [\eta] \cdot \eta_{sp} \quad (5)$$

- relationship for moderate to concentrated solution

Rao [6]

$$\left(\frac{1}{2(\eta_r^{1/2} - 1)} \right) = \left[\frac{1}{[\eta] \cdot C} \right] - \left[\frac{a-1}{2.5} \right] \quad (6)$$

where C is the concentration (grams of polymer per 100 ml), $\eta_r = \eta/\eta_o$ is the reduced viscosity, $\eta_{sp} = (\eta - \eta_o)/\eta_o$ is the specific viscosity, $[\eta]$ the intrinsic viscosity, K_i are coefficients and $a = 1/\phi_m$, where ϕ_m is the maximum volume fraction to which particles of polymers can pack in the solution.

For the determination of constants using Huggins' equation, an improved method suggested by Nagy et al. [7] was used. This method gives intrinsic viscosities and Huggins constants with lower standard deviations.

Whether a certain high molecular weight polymer solution falls into dilute, semi-dilute or concentrated regimes depends not only on its actual concentration, but also on temperatures, polymer type and solvent properties and only the appropriate equations for those conditions will describe the polymer-solvent behaviour correctly: the same polymer in different solvents and at different temperatures can be described by different equations. For these reasons it is useful to consider several equations and choose the most appropriate one.

The best fit results were obtained by using the equations of Huggins with the method of Nagy et al. [7] and Rao, with C and Schulz-Blaschke with η_{sp} as independent variable. The intrinsic viscosities determined by Rao's equation were comparable with those obtained by the Martin equation, both being able to describe the viscosity of polymer solutions over a large concentration range. In particular, the equation suggested by Rao⁶ takes into account the solvent-polymer interaction effects. The $[\eta]$ values determined by the equation of Schulz-Blaschke were the highest.

Typical plots of the above mentioned equations are shown in **Fig. 1**. The method suggested by Nagy et al. [7] is also included, where the parameter α is $C_m + C_M$, being C_m and C_M the minimum and maximum concentrations.

Intrinsic viscosity coefficients and their temperature dependence

In a good solvent where the energy of interaction between a polymer segment and a solvent molecule adjacent to it exceeds the mean of the energies of interaction between the polymer-polymer and solvent-solvent pairs, the polymer will tend to expand further so as to reduce the number of contacts between pairs of polymer elements. Therefore, the polymer molecule will be in a very extended form in a very good solvent. The value of the intrinsic viscosity will be high in a good solvent, as the molecule is very extended. In a poor solvent, on the other hand, where the energy of interaction is unfavourable, a small configuration in which polymer-polymer contacts occur more frequently will be favoured, and the polymer will tend to occupy a tightly coiled form, resulting in a lowering of the intrinsic viscosity.

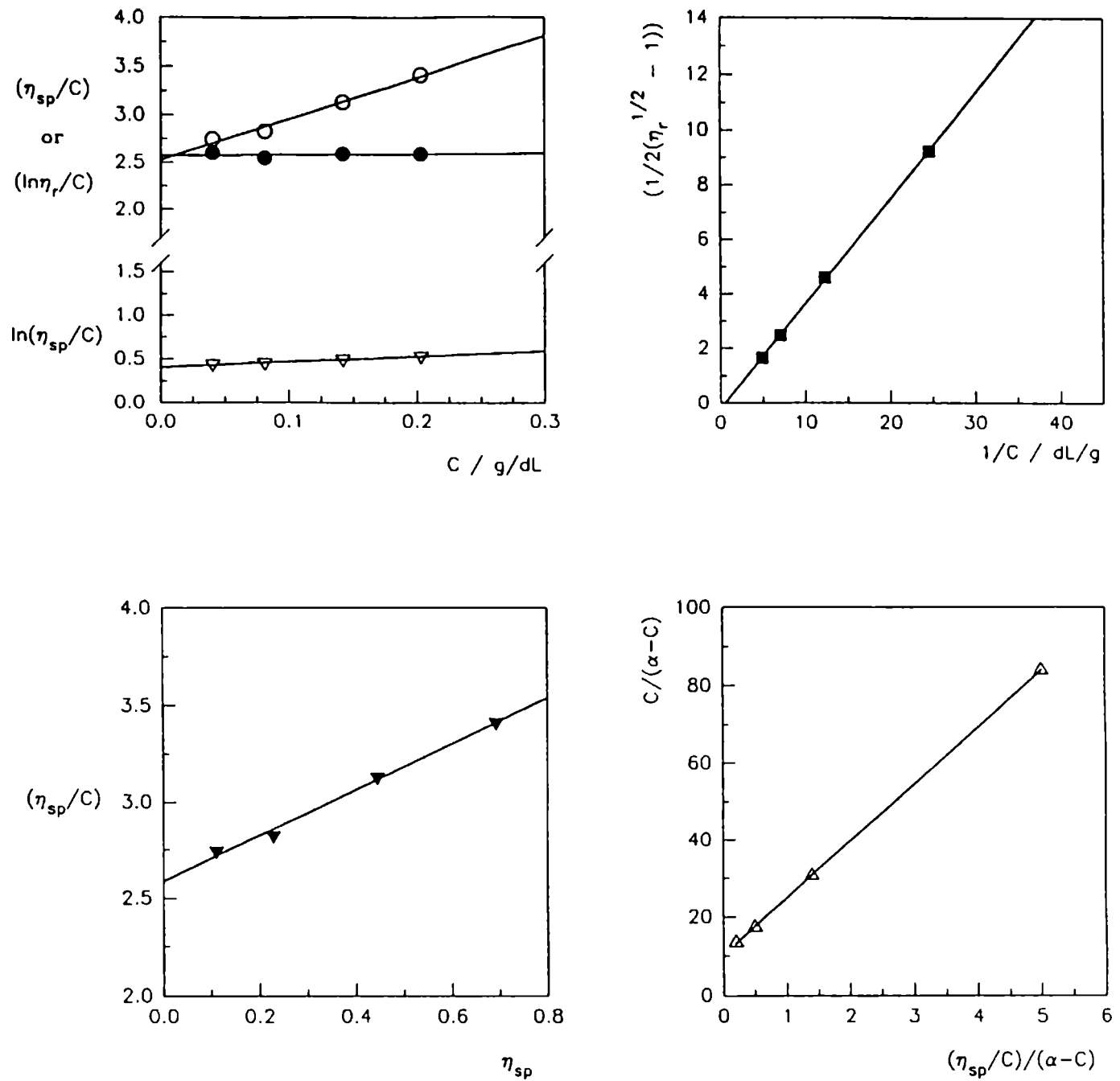


Fig. 1.- Huggins (O), Kraemers (●), Martin (V), Schulz-Blaschke (◆) and Rao's (▼) plots for isopropanol precipitate samples in acetone at 20 °C. The plot method by Nagy et al. [7] is also shown (Δ).

In good solvents the plots given by equations 2 and 3 are linear and K_H is about 0.34 to 0.40 and in poor solvents the value of K_H increases [8]. For most random chain polymer systems $K_H \leq 0.5$, but if there is association of macromolecules in the solution, an effective Huggins coefficient $K_{eff} > 0.5$ is obtained [9].

The intrinsic viscosity is given as follows [10]:

$$[\eta] = K \cdot M^{1/2} \cdot \alpha^3 \quad (7)$$

where K is a constant independent of the polymer molecular weight M , and of the solvent and α is the isotropic swelling factor given by:

$$\left(\overline{r^2}\right)^{1/2} = \alpha \left(\overline{r_0^2}\right)^{1/2} \quad (8)$$

and $\left(\overline{r^2}\right)^{1/2}$ is the root-mean-square end to end distance of the polymer chain and $\left(\overline{r_0^2}\right)^{1/2}$ indicates unperturbed conditions.

The root-mean-square end to end distance is related to the molecular expansion and the greater the value, the better the solvent and the "swelling" of the molecule [10]. The intrinsic viscosity is a measure of the shape and size of the isolated macromolecule and a measure of the solvent power and K_H is a measure of the hydrodynamic interaction.

A change of temperature affects $[\eta]$ and the coefficient values [10], due to modifications in the polymer-polymer and polymer-solvents interactions. Thus the interpretation of different temperature data provides a useful way to obtain information about the interactions particularly.

Although the temperature dependence on $[\eta]$ is not very well-defined, it is possible to conclude from the effect of this variable on the coefficients (in particular K_H) how the solubilizing power changes.

A maximum in the $[\eta]$ - T relation seems to be a general phenomenon for polymer solutions [11-12]. Kawai and Ueyama [11] found this behavior for PMMA in acetone and they concluded that there is a T_m for a given polymer-solvent combination and the polymer molecules take on the most expanded conformation. T_m is affected by the chain flexibility and its measurement will provide a characteristic parameter of the polymer. Radic and Gargallo [12] found that intrinsic viscosities of several fractions of poly(4-ter-butylcyclohexyl methacrylate) in cyclohexane present a maximum at $T_m \approx 25^\circ\text{C}$ and fractions of poly(pentachlorophenyl methacrylate) in o-dichlorobenzene at $T_m \approx 30^\circ\text{C}$. They concluded that this behaviour should be observed generally for polymer solutions.

Fig. 2a shows the dependence of the intrinsic viscosity with temperature for the evaporated latex (uncleaned sample) in acetone and THF.

For acetone, the intrinsic viscosity has a maximum value at about 20°C , which is in agreement with the observations of Kawai and Ueyama [11]. The solution properties are described correctly by all equations, but in particular by those of Kraemer and Schulz-Blaschke.

In THF, it can be seen that no maximum is observed, in the range of temperature covered here, and the intrinsic viscosity decreases slightly with temperature. This behaviour is characteristic of solvents with low theta temperature [10].

Except at 20°C , where the K_H values are about 0.4 and K_K about 0.13, the values of K_H are higher than 0.5, and the plots of equations 2 and 3, become slightly curved indicating the contribution of higher terms in these equations [13] or association. Equation 6 describes

the behaviour better indicating that in this case the system is in the moderately to concentrated regime.

When the polymer samples obtained by coagulation of latex with isopropanol were tested, the dependence of the intrinsic viscosities with temperature were those shown in **Fig. 1b**.

In THF, the $[\eta]$ values are the highest and there is a minimum at 20 °C. The appearance of a minimum in the $[\eta]$ vs. T curve is rather peculiar and was also reported by Vasudevan and Santappa [14]. It may be noted that in this region the value of the Huggins constant decreased with decreasing temperature and at 20 °C had the maximum value. Equation 6 is the best to describe the solution properties. For acetone the behaviour is different and the $[\eta]$ values decrease slightly with temperature. In this case, equations 5 and 6 are able to describe the behaviour. Equations 2 and 3 show a slightly curve up at $\eta_{sp} \sim 0.7$, indicating again a contribution of higher terms.

In THF, the Huggins coefficients change between 0.23 and 0.38 and the Kraemer coefficients between 0.11 and 0.20, indicating that THF is a good solvent for this polymer. The K_H value for acetone rises with temperature and varies between 0.56 and 0.81, therefore the quality of solvent decreases with temperature and the polymer-polymer interaction is higher than the polymer-solvent interaction.

When the terpolymer was purified by solubilization in THF and precipitation with water, the behaviour of the intrinsic viscosities with temperature, are those in **Fig. 1c**. In THF the intrinsic viscosity decreases slightly with temperature and the K_H values range between 0.32 and 0.42 and K_K between 0.11 - 0.16. These values indicate that for this case THF is a good solvent. For acetone the intrinsic viscosity increases with temperature and the Huggins coefficients decrease. The higher temperature improves the solvent quality.

When an additional purification of the sample is performed, the intrinsic viscosity in THF at 20 °C rises to 4.45 dL/g, and the coefficients are $K_H = 0.37$ and $K_K = 0.14$.

The removal of low molecular weight compounds and water soluble fractions resulted in changes of the intrinsic viscosity values, and in the solution properties behaviour. In acetone, the change in the intrinsic viscosity is smaller compared with THF. In the first case, the purifications cause a decrease and in the second case, the values increase notably.

In the purification process, as the low molecular weight portion is eliminated, the average value of M should increase. According to eq. 7, the α value should decrease by a similar amount, so that $[\eta]$ did not change very much. In THF, the intrinsic viscosity value increases in the purified samples Therefore acetone is a poorer solvent than THF.

The $[\eta]$ values of the samples without purification in acetone and THF, are rather similar, but when the terpolymer was purified, the higher $[\eta]$ value corresponds to THF, which indicates that the polymer-solvent interaction is the highest in this case, and therefore it is a better solvent.

In the evaporated sample case, as acetone is an amphoteric molecule, both types of polymers are able to interact with the solvent and the $[\eta]$ value is the highest.

In THF as a predominant electron-donor solvent, the water soluble component will not interact efficiently. The high value of $K_H \sim 0.9$ could indicate some association of the macromolecules.

When comparing the linearity of experimental data of equations 2 - 6, it was found that in the evaporated and isopropanol precipitated samples, some departure from linearity is observed, especially in the low concentration region, due to the fact that these equations are valid for non-ionic polymers and not for the water-soluble components.

In samples with one or two purification cycles the linearity of those equations is notably improved, due perhaps to the elimination of the ionic component.

The observations outlined above are in agreement with the nature of the terpolymer. The latex was prepared by a semicontinuous method with the MAA monomer added in the second part of the feed. The relatively concentrated addition of MAA results in the formation of water-soluble polymer blocks, heavily enriched with acid and of a hydrophilic nature. Purifications of terpolymer by dissolving in THF and precipitation from water, left a less enriched acidic polymer. When solutions of these fractions (with and without purification) are prepared in THF and acetone, different situations occur, due to the different acid-base characteristics of solvents; THF is a predominant basic (proton acceptor) solvent and acetone acts both as acidic (proton donor) and basic (proton acceptor) i.e. an amphoteric solvent.

When the polymer is further purified with THF, the $[\eta]$ value increases again and this considerable increment should correspond to the elimination of the additional low molecular weight components, leaving only the highest molecular weight fraction.

The different behaviour of latex samples with and without purifications described above indicates the inhomogeneity of the original latex sample, due to the presence of water-soluble components, and of SDS in the unpurified samples and to a lesser extent in singly precipitated samples. The presence of these polymers and surfactant should be treated as a mixture of components. In our case, the non-linear trend of equations 2 and 3 observed in some cases, does not seem to follow the ideal condition that each component contributes to the η of the mixture. A further contribution due to some interaction should be taken into account.

Relation between K_H and $[\eta]$

Stern [15] proposed an empirical relation for the Huggins' constant and the intrinsic viscosities in the form:

$$K_H = D + E \cdot [\eta]^{-2} \quad (9)$$

where D and E are empirical constants independent of molecular weight.

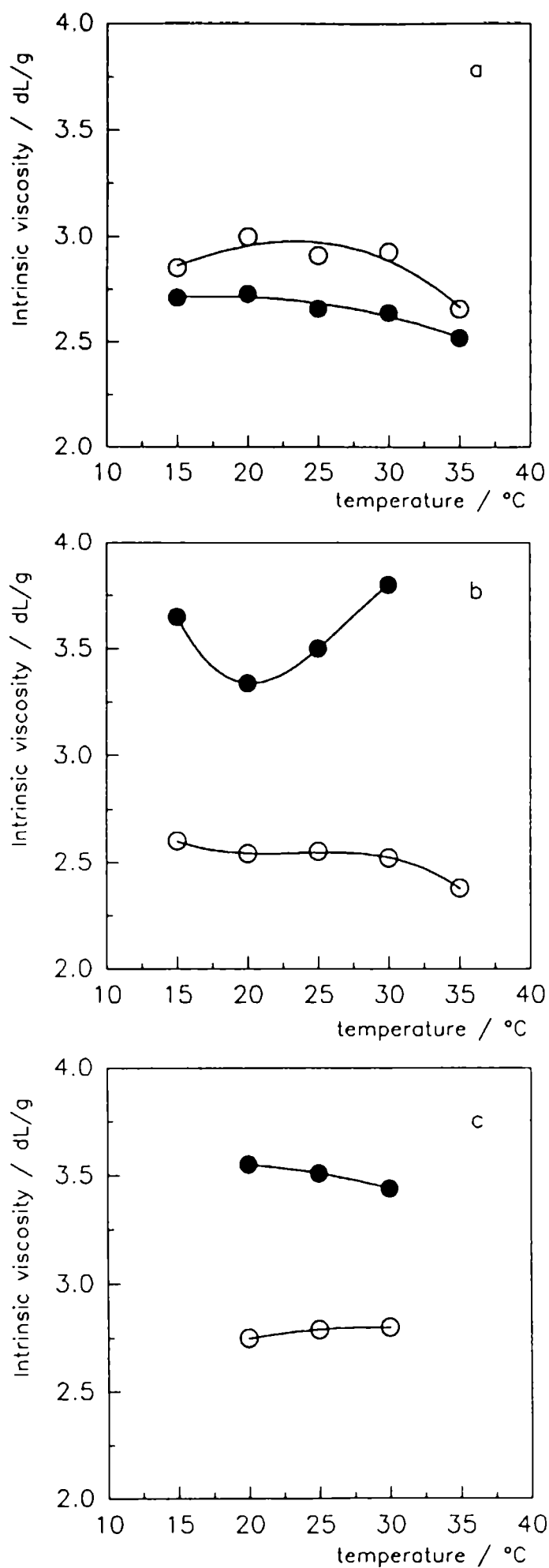


Fig. 2.- Dependence of intrinsic viscosity on temperature for solutions of uncleaned samples (a), isopropanol precipitated fraction (b) and samples with one purification cycle (c); in acetone (open circles) and THF (closed circles).

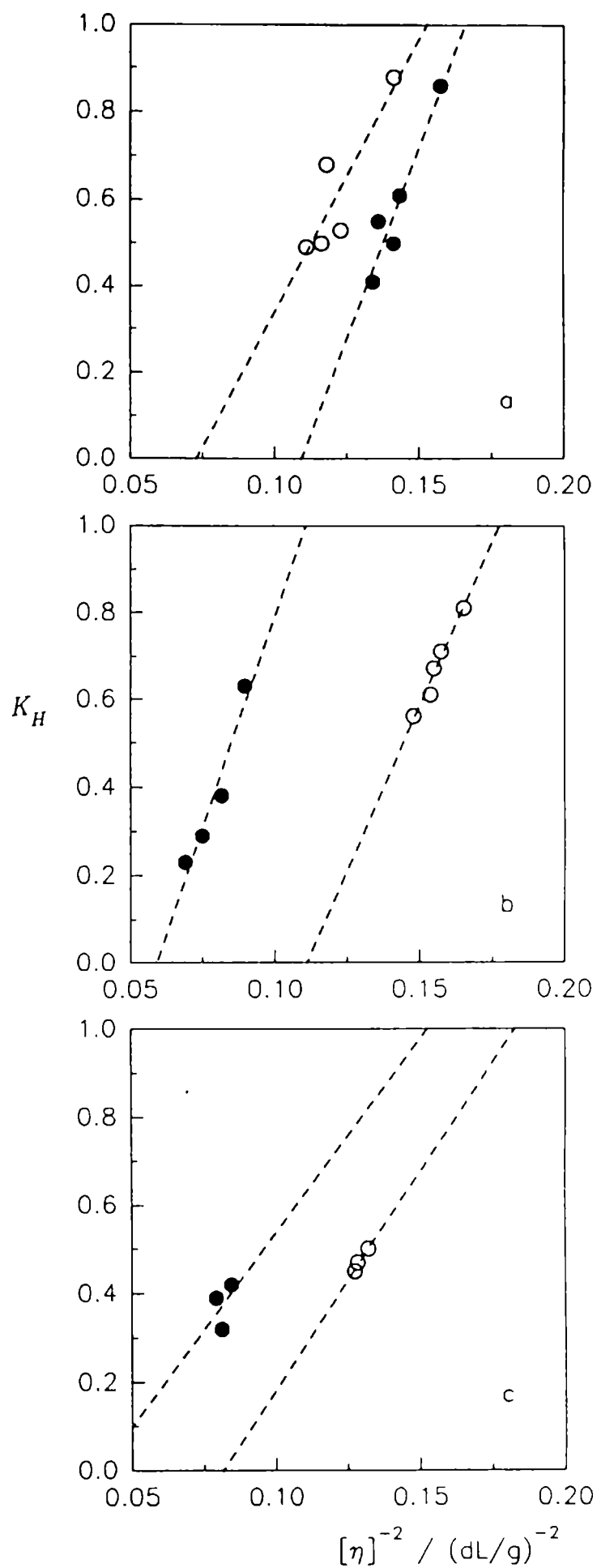


Fig.3.- Relation between K_H and $[\eta]$. See Figure 2 for explanation.

The data available from this work were used to test this equation. **Fig. 3** shows the relation for the systems studied. From this figure it was concluded that the relation is suitable in our case.

Relation between ϕ_m and K_H

Rao [6] found that the ϕ_m value of equation 6 is always less than unity and that a polymer-solvent system having lower K_H tends to give higher values of ϕ_m . For those polymer-solvent systems having $K_H = 0.25$ the value of ϕ_m should be near to or equal to unity. As this is possible only in dilute solutions and good solvents, Rao concluded that ϕ_m can be taken as a good measure of solvent quality.

Fig. 4 shows the relation of ϕ_m and K_H for the polymer-solutions systems studied in this work. A good negative correlation can be seen between the two variables, supporting the observations of Rao.

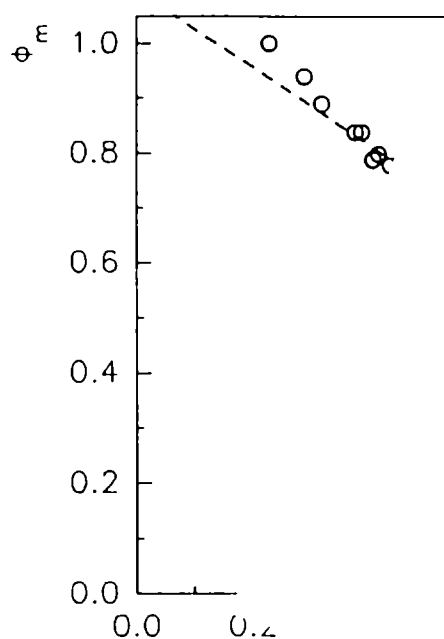


Fig. 4.- Relation between ϕ_m and K_H .

By comparing the values of the ϕ_m parameters it appears that for the uncleaned polymer latex, acetone and THF at 20 °C with $\phi_m \approx 0.8$ are good solvents. When latex was precipitated with isopropanol, THF seemed to be the best solvent. With ϕ_m values in THF ranging between 0.8 - 0.9 and those in acetone ca. 0.75, THF is the best solvent for samples purified by solubilizing the polymer in THF and precipitated with water.

CONCLUSIONS

Different fractions of an acrylic copolymer prepared by a semicontinuous emulsion polymerization method with a variable monomer feed and functionalized with an acidic acrylic monomer, were studied by solution viscosimetry. Results were interpreted using different equations for cases with different degrees of purification.

Different behaviours were observed in each case and no general rules can be given to choose the best conditions (solvent and temperatures) to perform a study of solution properties.

From the above results, it can be concluded that care must be taken when dilute solution viscometry or another technique depending on the polymer-solvent interactions is used to characterize functionalized latex samples. The most appropriate model for describing solution properties of this type of latices seems to be that for polymer mixtures with interactions.

It should be taken into account that purification of functionalized latices can lead to modifications of the original systems, through the elimination of different polymer chains, modified by the presence of functional monomers added during the synthesis.

A detailed study of solution properties including their variations with temperature, together with the knowledge of the synthesis characteristics of samples, should give the best method and working conditions.

Further study with similar compounds might help to clarify the various polymer properties differences, arising from the different synthesis procedures.

Acknowledgements

The author wishes to thank Comisión de Investigaciones Científicas de la Provincia de Buenos Aires and CONICET for financial support, and the technical assistance of O.R. Pardini and C.A. Lasquibar.

REFERENCES

- [1] Berger H.W.- **J. Paint Technol**, **39**, 310 (1967).
- [2] Anzur I., Osredkar U., Ukmar I. and Vizovisek I.- **Makromol. Chem. Suppl**, **10/11**, 311 (1985).
- [3] Fitch, R.M. Gajria, C and Tarcha, P.J.- **J. Colloid Interface Sci.**, **71**, 107 (1979).
- [4] Amalvy, J.I.- **J. Appl. Polym. Sci.**, **59**, 339 (1996).
- [5] Lovell P.A.- In "Comprehensive Polymer Science", Allen G. and Bevington J.C. (eds.), Pergamon Press, Oxford, 1989, Ch. 1 Vol. 9, page 179.
- [6] Rao, M.V.S.- **Polymer**, **34**, 592 (1993).
- [7] Nagy, T.T., Kelen, T. and Tüdös, F.- **Polymer**, **19**, 1360 (1978).

- [8] Fox T.G. and Flory P.J.- **J. Am. Chem. Soc**, **73**, 1909 (1951).
- [9] Wolff C., Silberberg A., Priel Z., Layec-Raphalen M.N.- **Polymer**, **20**, 281 (1979).
- [10] Flory, P.J.- *Principles of Polymer Chemistry*, Cornell University, Press, Ithaca, NY (1953).
- [11] Kawai, T. and Ueyama, T.- **J. Appl. Polym. Sci**, **8**, 227 (1960).
- [12] Radic, D. and Gargallo, L.- **Polymer**, **22**, 410 (1981).
- [13] Berry G.C.- **J. Chem. Phys**, **46**, 1338 (1967).
- [14] Vasudevan P. and Santappa M.- **Makromol. Chem**, **137**, 261 (1970).
- [15] Stern M.D.- Paper presented at the 142nd National Meeting of the American Chemical Society, Atlantic City, N.J. September 1962, see also Stobayashi H. **Makromol. Chem.**, **73**, 235 (1964).

RECENT DEVELOPMENTS IN MINIEMULSION POLYMERIZATION

DESARROLLOS RECIENTES EN POLIMERIZACION EN MINIEMULSIONES

I. Aizpurua¹, J.I. Amalvy², M.J. Barandiaran¹, J.C. de la Cal¹ and J.M. Asua¹

SUMMARY

Some developments in miniemulsion polymerization aiming at taking advantage of its unique mechanisms minimizing the drawbacks of this technique are discussed. The discussion includes preparation of highly concentrated latexes, miniemulsion polymerization in continuous stirred tank reactors (CSTRs), and elimination of the low molecular weight hydrophobe.

INTRODUCTION

Miniemulsions are finely divided oil-in-water dispersions stabilized against coagulation by conventional emulsifiers (usually anionic emulsifiers) and containing a highly water-insoluble compound (hydrophobe) to minimize the Ostwald ripening effect, namely, the diffusion of oil phase from small to large droplets to minimize the interfacial free energy of the system. Monomer miniemulsions can be polymerized upon addition of either water-soluble or oil-soluble initiators leading to a dispersed polymer, similar to a latex produced by conventional emulsion polymerization [1-19]. Nevertheless, miniemulsion polymerization follows a mechanism different from emulsion polymerization. The main difference is that, in miniemulsion polymerization, particle nucleation occurs in the submicron monomer droplets. The fraction of the monomer droplets that is nucleated depends on both the rate of nucleation and on the stability of the monomer droplets against monomer diffusion to growing particles and collision. Any operational variable affecting these processes will have a significant influence on the particle size distribution of the resulting latex, and hence on both the kinetics of the process and the properties of the final product. Thus, Miller et al. [14] reported that in the batch miniemulsion polymerization of styrene, the fraction of miniemulsion droplets that are nucleated could be greatly increased with the addition of a small amount of polymer to the monomer phase. A drawback of miniemulsion polymerization is that the water-insoluble compound remains in the polymer particle after polymerization and may have a deleterious effect on the properties of the polymer.

This paper considers some developments in miniemulsion polymerization aiming at taking advantage of the miniemulsion polymerization mechanisms whilst minimizing the drawbacks of this technique. Comparisons with conventional emulsion polymerization are presented.

¹ Grupo de Ingeniería Química, Departamento de Química Aplicada, Facultad de Ciencias Químicas, Universidad del País Vasco, España.

² Centro de Investigación y Desarrollo en Tecnología de Pinturas (CIDEPINT). Miembro de la Carrera del Investigador de la CIC.

HIGHLY CONCENTRATED LATEXES

High solids contents offer numerous advantages for most commercial applications, e.g. low shipping costs and no need to remove water. In practice, the solids content of a latex is limited by its viscosity. For a monodisperse latex, the viscosity approaches infinity as the volume fraction of the polymer particles approaches 0.62. On the other hand, polydisperse latexes show a lower viscosity, because the small particles fit within the voids of the array of large particles. Polydispersity is associated with long nucleation periods which are typical of miniemulsion polymerization. For the semicontinuous seeded emulsion polymerization of butyl acrylate in which the monomer was added as a miniemulsion, Tang et al. [8] showed that monomer droplet nucleation took place continuously during the feeding period. Masa et al. [9] compared the emulsion and miniemulsion polymerization of styrene, 2-ethylhexyl acrylate and methacrylic acid (34/60/6 wt/wt) at 55 wt % solids content finding that the viscosities of the neutralized final latexes were 4.5 Pa·s for the emulsion and only 0.7 Pa·s for the miniemulsion. This suggests that highly concentrated latexes can be obtained through miniemulsion polymerization.

A 65 wt % solids content latex was obtained by means of the semicontinuous miniemulsion polymerization of methyl methacrylate (MMA), butyl acrylate (BuA) and vinyl acetate (VAc) (monomer molar ratio MMA/BuA/VAc=35/50/15) using a mixed emulsifier system Alipal CO 436 (2 wt % based on monomers) (ammonium salt of sulfated nonylphenoxy (polyethyleneoxy) ethanol (4 ethyleneoxide), Rhône Poulenc) and Brij 98 (2 wt %) (C₁₆H₃₁-O-(C₂H₄O)₁₈, ICI), and hexadecane (HD) (2 wt %) as the hydrophobe [10]. Polymerizations were carried out at 80°C initiated by potassium persulfate (1.04 wt %) by using miniemulsions for both the initial charge and the feed. The partition of the monomer between the initial charge and the feed was the key operational variable. When a high solids content miniemulsion (>55 wt %) was used as initial charge, coagulum was formed during the batch polymerization of the initial charge, whereas when a low solids content initial charge was employed, the solids content of the feed was excessive and the sonication cell, where the feed was continuously miniemulsified, plugged. A compromise between these situations was achieved using a 55 wt % solids content initial charge and a 66.1 wt % solids content feed. Under these conditions a highly concentrated latex (65 wt %) of low viscosity (0.44 Pa·s) was obtained.

MINIEMULSION POLYMERIZATION IN CSTRs

Conventional emulsion polymerizations in continuous stirred tank reactors often show oscillations in conversion and number of polymer particles, N_p . The oscillatory behavior is due to the role of the surfactant in particle nucleation. At the beginning of the process, a large number of small polymer particles is formed, their number being controlled by the amount of emulsifier available in the system. These polymer particles grow by polymerization, and hence their surface area increases, depleting the aqueous phase of emulsifier. Therefore, new particles are not formed and, as the reaction mixture is continuously withdrawn from the reactor, N_p decreases. After some time, this process counteracts the increase in size of the particles and the amount of free emulsifier increases, allowing nucleation of new particles. The oscillatory behavior is disadvantageous for both control of the production and product properties. This phenomenon is more acute for low emulsifier concentrations and for polymerizing systems in which the volumetric growth rate of the polymer particles is strongly nonlinear with particle diameter (usually systems with high radical desorption rates). Barnett and Schork [4] reported a case in which the miniemulsion polymerization of MMA in a CSTR did not show oscillations whereas

the conventional emulsion polymerization exhibited decaying oscillatory transients. Surprisingly, the authors reported that the particle size distribution of the latex resulting from the miniemulsion was indistinguishable from the corresponding conventional emulsion latex.

A more stringent test for the miniemulsion process would be to work with a monomer that gives higher radical desorption rates. Vinyl acetate has this characteristic because of its large monomer chain transfer rate and high water-solubility. Both conventional emulsion and miniemulsion polymerizations of VAc (30 wt % solids content) were carried out in a 0.47 L jacketed CSTR at 60°C. The feed flow rates were controlled by means of weight-based flow controllers, and there was no head space in the reactor to ensure that a constant reactor volume was maintained during the experiments. The residence time was $q = 20$ min. Sodium lauryl sulfate (SLS) was used as emulsifier and potassium persulfate (KPS) as initiator. Hexadecane, HD, (2 wt % based on monomer) was used in the miniemulsion polymerization. In this case, the feed was continuously miniemulsified in a sonication cell before entering the reactor.

Figures 1 and 2 present the evolution of the monomer conversion, particle size (d_p) - measured by dynamic light scattering (DLS)-, and number of polymer particles per cm^3 of water for both miniemulsion and conventional emulsion polymerizations for two different emulsifier concentrations. It can be seen that at low emulsifier concentrations (**Fig. 1**) the particle size of the conventional emulsion latex showed severe oscillations, whereas that of the miniemulsion was constant. In addition, the particle size of the miniemulsion was smaller, i. e. larger number of polymer particles. On the other hand, the oscillations in the monomer conversions were less noticeable. At high emulsifier concentration (**Fig. 2**) neither the particle size of the conventional emulsion latex nor that of the miniemulsion presented oscillations. The monomer conversions were also constant.

The sustained oscillations of particle diameter at the low emulsifier concentration found in the emulsion polymerization resulted from intermittent nucleation. On the other hand, at the high emulsifier concentration the system never became depleted of emulsifier and hence an almost constant nucleation rate was obtained, maintaining the number of polymer particles in the reactor constant. The low sensitivity of the monomer conversion to the particle number oscillations was due to the fact that, because of the large particle size, the system was under Smith-Ewart case III kinetics ($\bar{n} \sim 3$) [20]. At the high emulsifier concentration, the particle size decreased making the polymerization rate sensitive to the number of polymer particles ($\bar{n} \sim 0.4$) and hence monomer conversion increased with N_p . For both emulsifier concentrations, the miniemulsion process does not present oscillations. The reason for this behavior is that, in this process, a stable (as proved by creaming experiments) monomer miniemulsion was continuously fed into the reactor, and hence the total interfacial surface area of the system was quite constant throughout the process preventing oscillations of free emulsifier level. In addition, the monomer droplets are much larger than the particle precursors formed during nucleation in conventional emulsion polymerization, and for these sizes, the nonlinearity of the volumetric growth rate vs particle size is greatly reduced. Comparison between **Figures 1 and 2** shows that for both emulsion and miniemulsion polymerizations, N_p increased with the amount of emulsifier, this effect being more acute for the conventional emulsion polymerization. In the emulsion process, the number of stabilized particle precursors increased when the surfactant level increased. On the other hand, in the case of miniemulsion polymerization, at higher emulsifier concentration the monomer droplet diameter decreased [18], and therefore, a higher number of droplets could be nucleated. **Figure 3** presents the molecular weight distribution (MWD) of samples collected at $t/q = 10$ in the miniemulsion and conventional emulsion polymerizations carried out at low

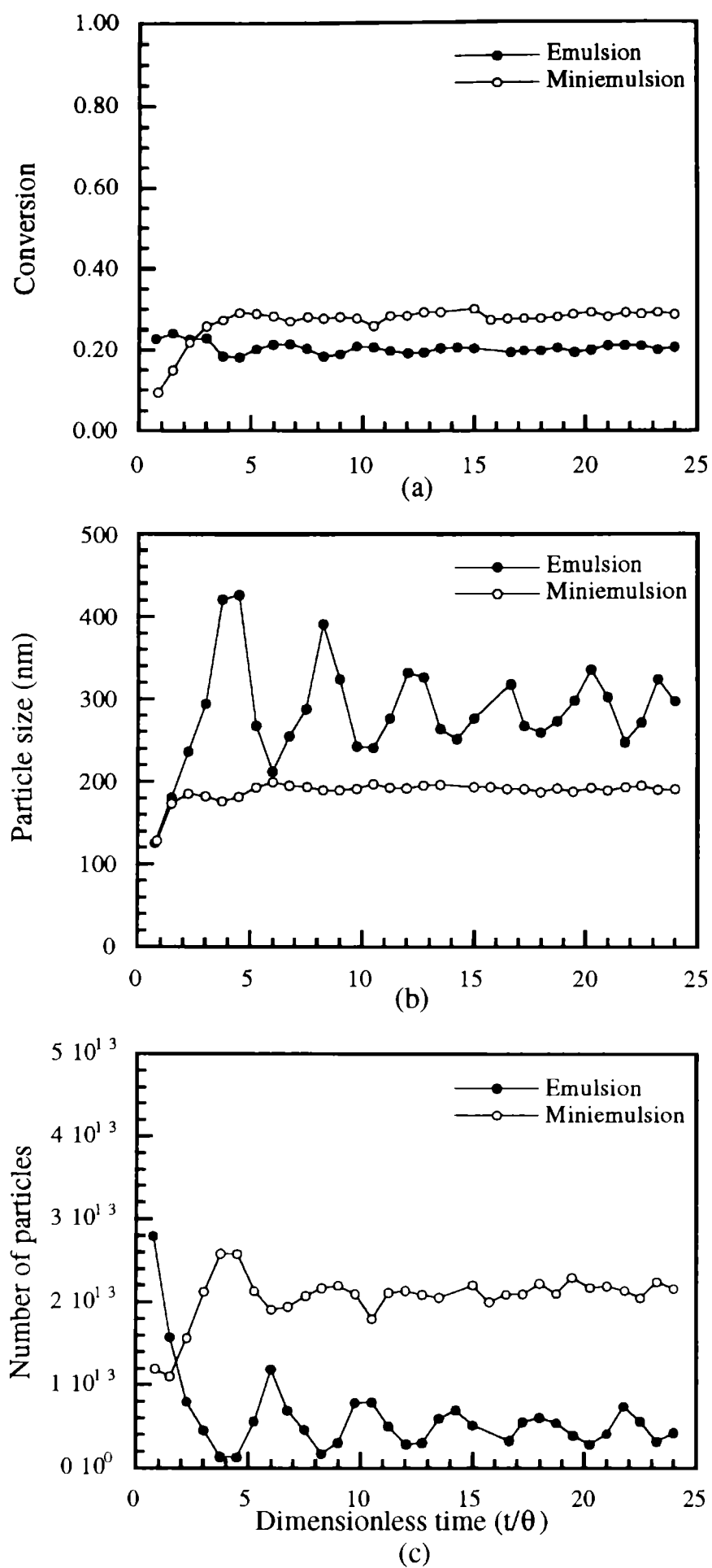


Fig. 1.- Evolution of conversion (a), particle size (b) and number of polymer particles (c) for the miniemulsion and conventional emulsion polymerization of VAc in a CSTR. [KPS] = 0.4 wt %; [SLS] = 0.6 wt % (both based on monomer).

emulsifier concentration. It can be seen that the MWD was not affected by the process used suggesting that the MWD was controlled by chain transfer to monomer.

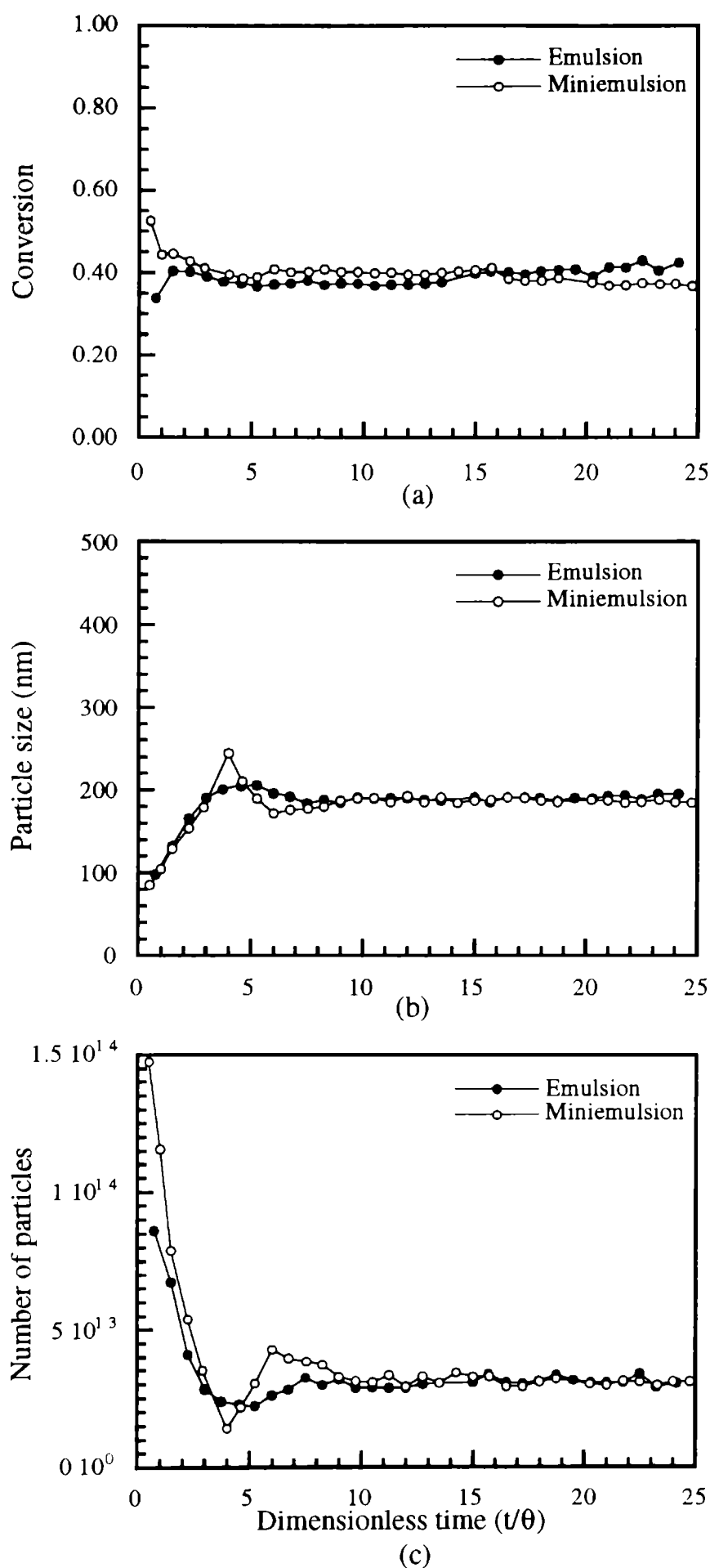


Fig. 2.- Evolution of conversion (a), particle size (b) and number of polymer particles (c) for the miniemulsion and conventional emulsion polymerization of VAc in a CSTR. [KPS] = 0.4 wt %; [SLS] = 4.8 wt % (both based on monomer).

ELIMINATION OF THE LOW MOLECULAR WEIGHT HYDROPHOBE

Fatty alcohols [15-17] and long chain alkane [5] have commonly been used to stabilize the miniemulsion droplets against monomer diffusion. These are low molecular weight compounds that remain in the particles after polymerization plasticizing the polymer, and hence affecting its properties. This effect may be reduced if the hydrophobe becomes covalently bonded to the polymer during polymerization or if a preformed polymer is used as hydrophobe.

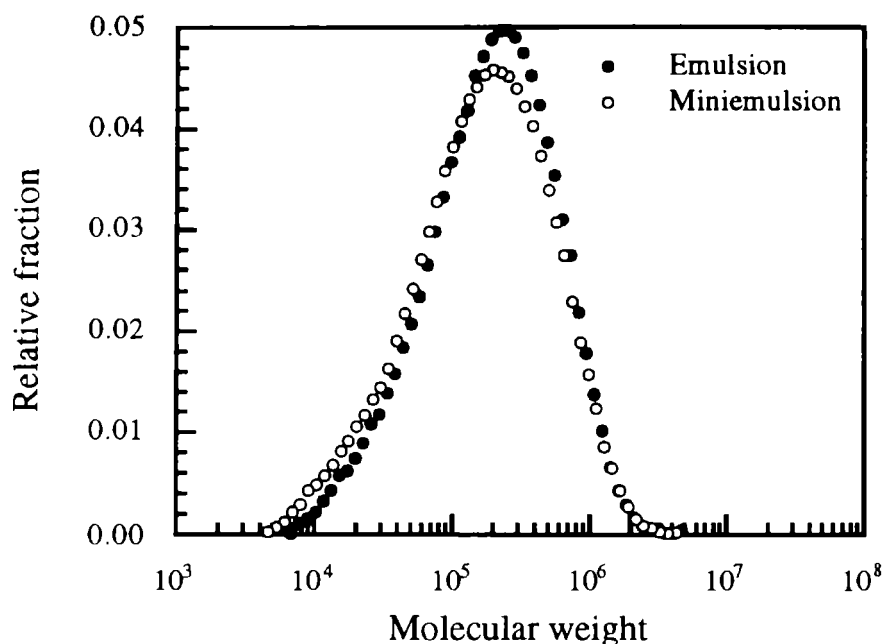


Fig. 3. -Molecular weight distribution for the miniemulsion and conventional emulsion polymerization of VAc in a CSTR. [KPS] = 0.4 wt %; [SLS] = 0.6 wt % (both based on monomer).

Covalently Bonded Hydrophobe

This might, in principle, be achieved by using water-insoluble macromonomers, initiators or chain transfer agents. Alduncin et al. [12] studied the ability of a series of initiators with different water solubilities (lauroyl peroxide (LPO), benzoyl peroxide (BPO), and azobis(isobutyronitrile) (AIBN)) in stabilizing monomer droplets against degradation by molecular diffusion in the batch miniemulsion polymerization of styrene. A 2.5 wt % of initiator based on monomer was used. For the sake of comparison, another series of miniemulsion polymerizations was carried out, in which the stability of the monomer droplets was ensured by using hexadecane in addition to the oil-soluble initiators. **Figure 4** presents the particle size distribution (PSD) of the final latexes. It can be seen that, in the absence of HD, only the LPO was sufficiently water-insoluble to avoid extensive monomer droplet degradation, yielding a PSD similar to that of the miniemulsion polymerization costabilized with HD. On the other hand, BPO and AIBN are not water-insoluble enough to avoid the Ostwald ripening effect, and extensive monomer droplet degradation occurred. **Figure 4** also shows that the type of initiator had only a limited effect on the PSDs obtained in the miniemulsions costabilized with HD. However, the process yielded a rather low molecular weight polymer ($\overline{M}_n \sim 40,000$) [13]. Therefore, the application of this type of process should be restricted to systems in which the MWD is controlled by chain transfer to monomer (for example PVC production).

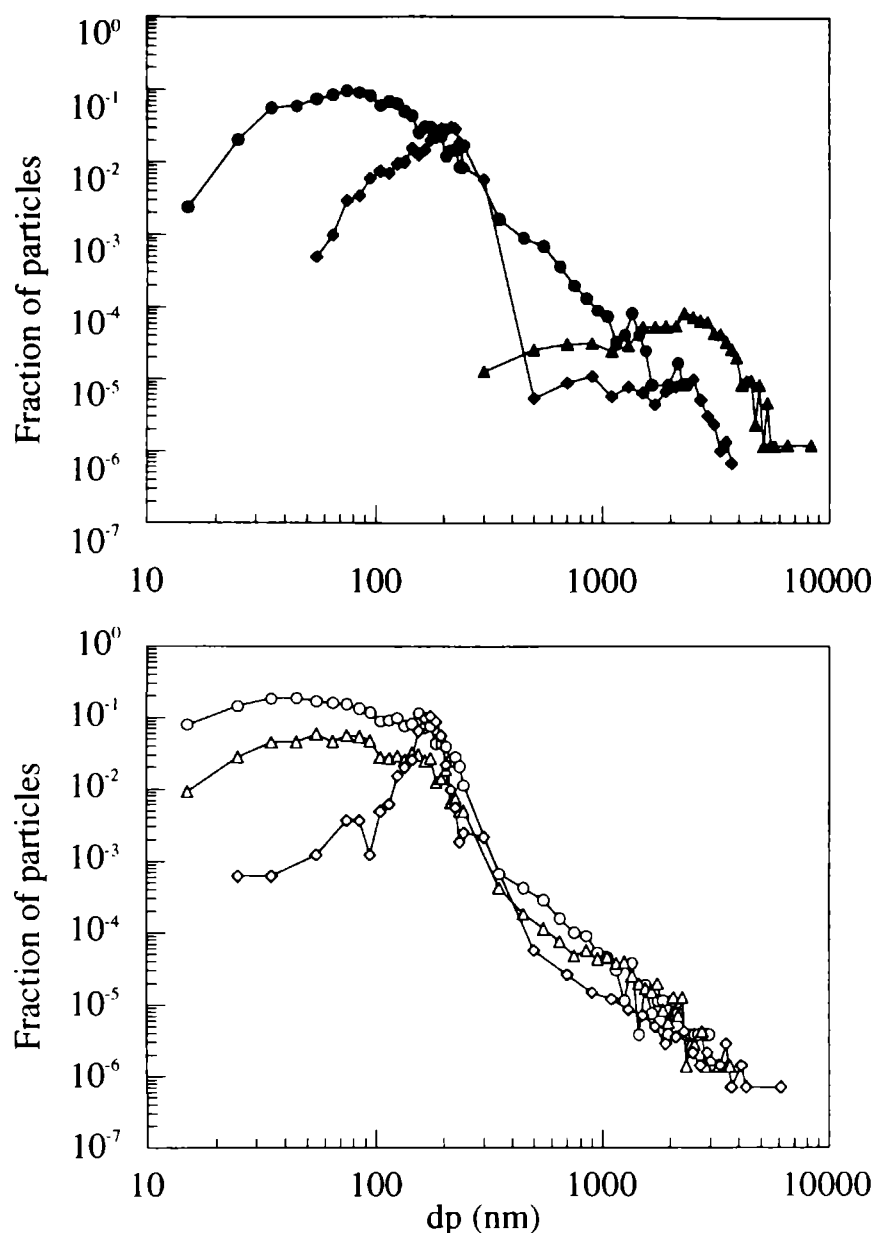


Fig. 4. Particle size distributions of the final latexes obtained in miniemulsion polymerizations initiated by oil-soluble initiators. Legend: (●) LPO; (▲) BPO; (◆) AIBN; (○) LPO + HD; (Δ) BPO + HD; (◇) AIBN + HD.

Polymeric Hydrophobe

The presence of polymer in the miniemulsion droplets has been reported to increase significantly the polymerization rate by increasing the rate of particle nucleation [14-19]. For the batch miniemulsion polymerization of styrene, Miller et al. [15] found that the larger increase was obtained using a combination of polystyrene and cetyl alcohol although a significant increase was also achieved using only polystyrene. Similar results were obtained by Reimers and Schork [19] in the study of the batch miniemulsion polymerization of methyl methacrylate when poly(methyl methacrylate) was used as hydrophobe. On the other hand, Wang and Schork [18] did not obtain stable vinyl acetate miniemulsions using poly(vinyl acetate) as hydrophobe and polyvinyl alcohol as surfactant. Vinyl acetate miniemulsions (55 wt % solids content stabilized with pVAc, HD and HD+pVAc (hydrophobe) and SLS (emulsifier) have been prepared in our laboratories. The miniemulsions containing HD were stable for several days, whereas that using only pVAc as hydrophobe suffered phase separation after some minutes. Nevertheless, these miniemulsions were polymerized in batch, minimizing the time elapsed between emulsification and polymerization. Conventional emulsion polymerization was carried out as a reference. Coagulum

free latexes were obtained in all cases with the following particle diameters (measured by DLS): $d_p(\text{emulsion}) = 104 \text{ nm}$; $d_p(\text{HD}) = 229 \text{ nm}$; $d_p(\text{HD+pVAc}) = 219 \text{ nm}$; $d_p(\text{pVAc}) = 165 \text{ nm}$.

These results suggest that the pVAc was able to stabilize the miniemulsion droplets long enough for them to be nucleated. In order to test this point, a 55 wt % solids content miniemulsion (using pVAc as the sole hydrophobe) and a conventional emulsion polymerization were carried out in a 0.47 L CSTR. Polymerization conditions were as follows: $T = 60 \text{ }^\circ\text{C}$; $q = 20 \text{ min}$; [Arkopal N 230] = 1 wt %; [Alipal CO436] = 0.75 wt %; [Hydroxyethyl cellulose] = 0.1 wt %; [pVAc] = 1 wt %; [KPS] = 1.05 wt % (all of them based on monomer). The results are presented in Fig. 5. It can be seen that a stable operation was achieved using the miniemulsion process whereas severe oscillations occurred in the conventional emulsion polymerization. This is a proof that nucleation occurred in monomer droplets. It is interesting to notice that N_p for the miniemulsion process was larger than for the emulsion polymerization, while the opposite was found in a batch reactors. Work is in progress to clarify this point using a complete mathematical model.

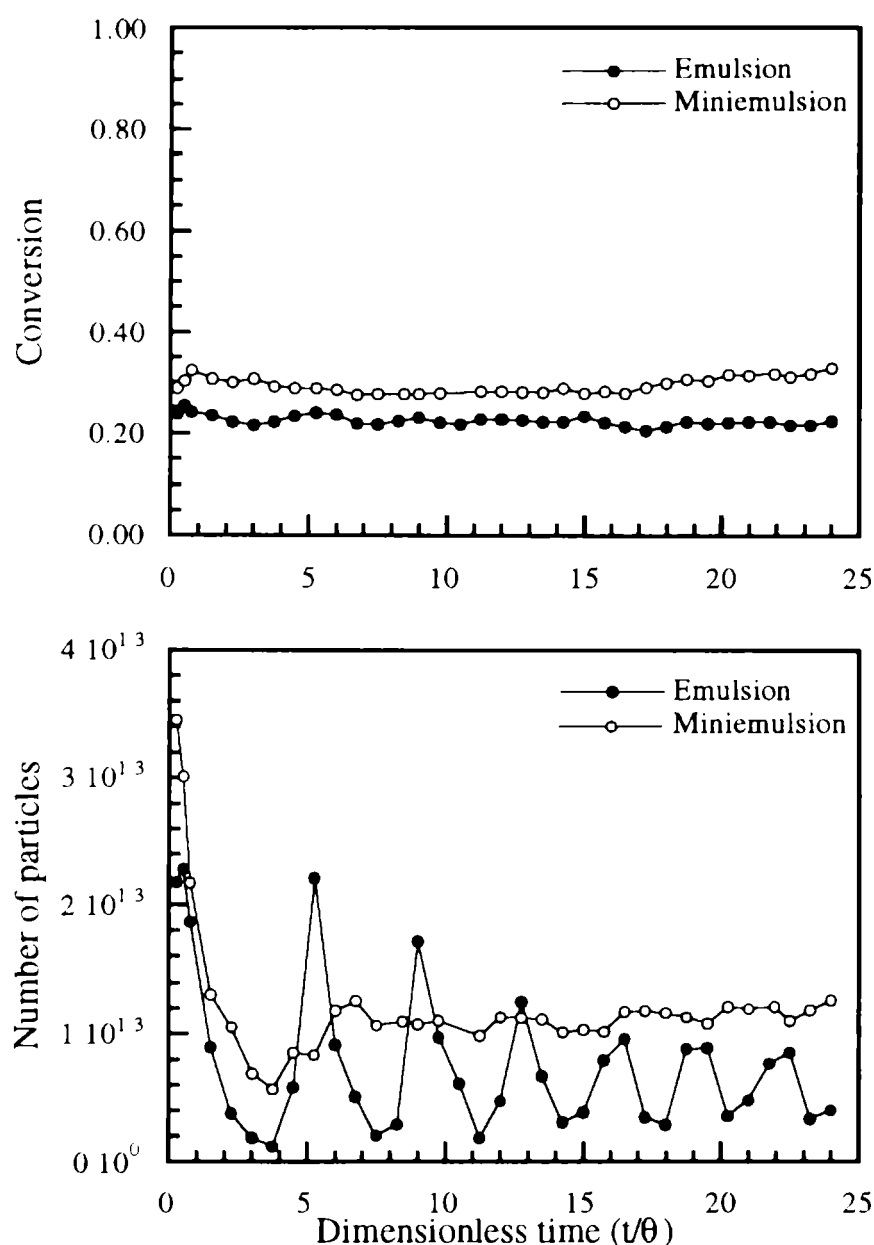


Fig. 5.- Evolution of conversion and number of particles for the miniemulsion and conventional emulsion polymerization of VAc in a CSTR with pVAc as the sole hydrophobe.

ACKNOWLEDGEMENTS

Financial support from *the Diputación Foral de Gipuzkoa* and *Universidad del País Vasco (UPV 221.215-TA202/95)* and the fellowships for I. Aizpurua by *the Basque Government* and for J. I Amalvy by *AECI-UPV* are gratefully appreciated.

REFERENCES

- [1] J. Ugelstad, M. S. El-Aasser, J. W. Vanderhoff.- **J. Polym. Sci., Polym. Lett.** **11**, 503 (1973).
- [2] F. K. Hansen, J. Ugelstad.- **J. Polym. Sci., Polym. Chem. Ed.** **17**, 3069 (1979).
- [3] Y. T. Choi, M. S. El-Aasser, E. D. Sudol, J. W. Vanderhoff.- **J. Polym. Sci., Polym. Chem. Ed.** **23**, 2973 (1985).
- [4] D. T. Barnett, F. J. Schork.- **Chem. Eng. Comm.** **80**, 113 (1989).
- [5] J. Delgado, M. S. El-Aasser, C. A. Silebi, J. W. Vanderhoff.- **J. Polym. Sci., Polym. Chem. Ed.** **28**, 777 (1990).
- [6] J. Delgado, M. S. El-Aasser.- **Makromol. Chem. Macromol. Symp.** **31**, 63 (1990).
- [7] J. M. Asua, V. S. Rodriguez, C. A. Silebi, M. S. El-Aasser.- **Makromol. Chem., Macromol. Symp.** **35/36**, 59 (1990).
- [8] P.L. Tang, E. D. Sudol, M. E. Adams, M. S. El-Aasser, J. M. Asua.- **J. Appl. Polym. Sci.** **42**, 2019 (1991).
- [9] J. A. Masa, L. López de Arbina, J. M. Asua.- **J. Appl. Polym. Sci.** **48**, 205 (1993).
- [10] M. J. Unzue, J. M. Asua.- **J. Appl. Polym Sci.** **49**, 81 (1993).
- [11] K. Fontenot, F. J. Schork.- **J. Appl. Polym. Sci.** **49**, 633 (1993).
- [12] J. A. Alduncin, J. Forcada, J. M. Asua.- **Macromolecules** **27**, 2256 (1994).
- [13] J. A. Alduncin, J. M. Asua.- **Polymer** **35**, 3758 (1994).
- [14] C. M. Miller, P. J. Blythe, E. D. Sudol, C. A. Silebi, M. S. El-Aasser.- **J. Polym. Sci.:Part A: Polym. Chem.** **32**, 2365 (1994).
- [15] C. M. Miller, E. D. Sudol, C. A. Silebi, M. S. El-Aasser.- **Macromolecules** **28**, 2754 (1995).
- [16] C. M. Miller, E. D. Sudol, C. A. Silebi, M. S. El-Aasser.- **Macromolecules** **28**, 2765 (1995).

- [17] C. M. Miller, E. D. Sudol, C. A. Silebi, M. S. El-Aasser.- **Macromolecules** **28**, 2772 (1995).
- [18] S. Wang, F. J. Schork.- **J. Appl. Polym. Sci.** **54**, 2157 (1994).
- [19] J. L. Reimers, F. J. Schork.- **J. Appl. Polym. Sci.** **60**, 251 (1996).
- [20] W. J. Smith, R. M. Ewart.- **J. Chem. Phys.** **16**, 592 (1948).

THERMODYNAMIC CONSIDERATION OF THE RETENTION MECHANISM IN A POLY(PERFLUOROALKYL ETHER) GAS CHROMATOGRAPHIC STATIONARY PHASE USED IN PACKED COLUMNS

*CONSIDERACIONES TERMODINAMICAS ACERCA DEL MECANISMO DE RETENCION
EN UN POLI(PERFLUOROALQUIL ETER) UTILIZADO COMO FASE ESTACIONARIA
EN COLUMNAS RELLENAS PARA CROMATOGRAFIA GASEOSA*

R. C. Castells¹, L. M. Romero and A. M. Nardillo¹

SUMMARY

Retention volumes of fifteen hydrocarbons were measured in columns containing several concentrations of a commercial poly(perfluoroalkyl ether), Fomblin Y HVAC 140/13, as the stationary phase. Two different type of packing were studied: one of them employed pre-silylated Chromosorb P AW DMCS as the solid support, and the other type was prepared by coating the stationary phase on Chromosorb P AW and silylating on-column. On-column silylated columns showed unequivocal symptoms of partial deactivation; retention volumes changed regularly with the content of stationary phase in pre-silylated columns. Analysis of retention in pre-silylated columns indicates that a mixed mechanism (partition and adsorption on the gas-liquid interface) is operative. Systems hydrocarbon + perfluorocompound show pronounced positive deviations from the ideal behaviour that can be attributed to repulsion between the hydrocarbon and the perfluorocompound segments.

Keywords: *Gas chromatography, Poly(perfluoroalkyl ether), hidrocarbons, adsorption on liquid surfaces, mixed retention*

INTRODUCTION

Perfluorinated substances have been sporadically employed as stationary phases in gas chromatography, and this mostly for the separation of substances of high chemical reactivity or

¹ Miembro de la Carrera del Investigador del CONICET, UNLP

perfluorocompounds and freons. Excellent review articles have been written by Pomaville and Poole [1] and by O'Mahony et al.[2].

Highly fluorinated fluids are characterized by their chemical inertia and by very weak molecular interactions, either at the pure state or in their mixtures with other substances. Cohesive energy densities of perfluoroalkanes and perfluorocycloalkanes are much less than those of the corresponding hydrocarbons [3], and although fluorocarbons and hydrocarbons are individually highly non polar, their mixtures show important deviations from Raoult's law [3-5]. These properties have two important consequences in relation with their use as gas chromatographic stationary phases. On one side, as pointed out by Poole and collaborators [1,6,7], retention times in highly fluorinated stationary phases shall be shorter than in conventional phases, thus enabling the separation of low volatility or thermally labile substances.

On the other side, weak interactions with the solid support or the capillary wall result in insufficient surface deactivation, uneven distribution and poor film stability, reflected in peak asymmetry, low efficiency and retention time variations; all of these deleterious symptoms are very markedly displayed in using perfluoroparaffins.

Drastic improvements in the chromatographic behaviour is obtained by incorporating polar groups in the stationary phase molecules. The poly(perfluoroalkyl ether) phase Fomblin YR, $[(OCFCF_3CF_2)_n - (OCF_2)_m]$, was introduced in 1983 by Dhanesar and Poole [6,7]; paraffinic and olefinic hydrocarbons, injected at temperatures markedly lower than their boiling points, elute from these columns in short retention times, with very good peak shapes, but asymmetric peaks are obtained for solutes of higher polarity. Furthermore, the authors found that packings prepared by coating previously silylated supports (Gas-Chrom Q) gave symmetrical peaks when tested at low temperatures, but after heating to above 100 °C and returning to low temperatures for re-testing, shorter retention times and asymmetric peaks were obtained, a behaviour that the authors attribute to film contraction, that results in bare surface exposition and liquid lenses. Columns stable at temperatures higher than 200 °C and with efficiencies similar to those obtained for conventional phases were obtained by coating Chromosorb P, packing the columns with coated support, and on-column silylating by injection of Silyl-8 or bis(trimethylsilyl)trifluoroacetamide (BSTFA) [6,7].

Mixtures of fluorocarbon compounds and aliphatic or alicyclic hydrocarbons are the only known example of systems with large positive excess functions where none of the components is polar; as such, they have been the subject of many studies since the 1950s [8,9]. Although these trends are qualitatively consistent with the large differences in cohesive energy density of fluorocarbons and hydrocarbons, the solubility parameter approach does not give a satisfactory quantitative explanation [3]. Plots of surface tension against composition also show pronounced deviations from the ideal behaviour [10,11]. The objective of the present paper is to obtain thermodynamic data for the processes of solution and adsorption on the gas-liquid interface for a group of hydrocarbons at infinite dilution in a highly fluorinated stationary phase in the neighbourhood of room temperature. A high molecular weight perfluoroalkane was supposed to be used as the solvent, according with the original plan; the poor performance of these substances as stationary phases compelled us to modify the project. Fomblin was then chosen because of its characteristics and to profit from the experience collected by Poole and his group on this stationary phase.

EXPERIMENTAL SECTION

Materials and columns. Fomblin Y HVAC 140/13 (weight average molecular weight 6500) and 1,1,2-trichlorotrifluoroethane (Freon 113) were purchased from Aldrich; BSTFA was obtained from Supelco. Hydrocarbon solutes of different origins, all of them more than 99% pure, were used as received. Column packings were prepared in a rotary evaporator, using Freon 113 as solvent. Coated supports were packed into 0.53 cm i.d. and 1.0 m in length stainless steel tubes with the aid of vacuum suction and gentle tapping. Two sets of columns were prepared:

a) On-column silylated columns: a packing containing 5.67% by weight of Fomblin on Chromosorb P AW 60/80 was prepared by the above mentioned method. A 1.80 m x 0.4 cm i.d. glass column containing this packing was installed in a Konik gas chromatograph (see later) with a glass lined injector; the injector and the column oven were set to 100 and 150° C, respectively, and on-column silylation was performed by slowly injecting 100 μ L of BSTFA with a nitrogen flow rate of 5 ml/min. The column was held at 150° C for several hours, and the silylating treatment was then repeated after reversing the column end connections. The column was carefully emptied and its content was used as starting material to prepare packings with higher stationary phase concentrations, by successively adding Fomblin by the above mentioned coating technique. By this method four columns containing 5.67, 8.30, 13.36 and 22.05 by weight percentage (w) of Fomblin on the same lot of solid support were prepared, with the objective of minimizing unpredictable effects associated with the silylating process.

b) Pre-silylated columns, containing 4.29, 5.56, 7.50, 10.89, 15.52 and 19.40% by weight of Fomblin were prepared using Chromosorb P AW DMCS 60/80 as the solid support.

Apparatus and procedure. The study of thermal stability of packings was performed in a Konik 3000 gas chromatograph, equipped with a FID and a Spectra Physics Datajet Integrator, using 1.50 x 2 mm i.d. glass columns.

A home assembled apparatus, in which column temperature was controlled to better than ± 0.05 °C by immersion in a water bath, was used for the remaining measurements. Nitrogen, successively passed through a molecular sieves trap (Davidson 5A), a Brooks 8606 pressure regulator, a Brooks 8743 flow controller and a 2 m x 1/8" o.d. coiled copper tube immersed in the column bath, was used as the carrier gas. Inlet pressures were measured by means of a mercury manometer at a point between the copper coil and a Swagelok 1/4" s.s. "T"; one branch of this last was provided with a septum, and the columns were connected to the remaining branch. Solute vapours were on-column injected by using Hamilton syringes. Eluates were detected with a Hewlett-Packard 5750 FID and electrometer signals were fed to a Hewlett-Packard 3396A integrator. Flow rates ranging between 15 and 30 ml/min were measured by means of a water jacketted soap film flow meter.

Sample sizes of the order of 10^{-2} μ mole resulted in symmetrical peaks for all the studied solutes, thus warranting Henry's law conditions for all the retention mechanisms. Aromatic hydrocarbons, whose peaks displayed a slight asymmetry that persisted at the smallest sample sizes compatible with instrumental noise, were excluded from this study. Solute vapours and a small methane sample were simultaneously injected; net retention times were measured to 10^{-3} min between the maxima of the solute and the methane peaks. Specific retention volumes (V_g°)

and net retention volumes per gram of packing (V_N) were calculated from values of the operating parameters in the usual form [12]. Values at each temperature were means of no less than four injections; retentions were measured for groups of 3-4 solutes at five temperatures equally spaced within the range 22 - 35 °C, and the measurements for the same group of solutes were repeated after 2 - 3 weeks.

Densities of Fomblin were measured at twelve temperatures between 19 and 41 °C with a 3 ml pycnometer that had been carefully calibrated through the same temperature interval, and least squares fitted to the following polynomial:

$$\rho_2(t/^{\circ}\text{C}) = 1.94429 - 1.2808 \times 10^{-3} t - 1.30 \times 10^{-5} t^2 + 10^{-7} t^3 \quad (1)$$

The thermal expansion coefficient, as calculated from eq. (1), is $\alpha_2 = 9.15 \times 10^{-4} \text{ K}^{-1}$.

RESULTS AND DISCUSSION

Comparing pre-silylated and on-column silylated packings. The pattern displayed in Fig. 1 for four representative cases is shared for all the solutes. V_N increases in a satisfactory linear fashion with percentage Fomblin in the pre-silylated Chromosorb P phases. A V_N fall of concern occurs, particularly with unsaturated solutes, when the Fomblin proportion rises from 5.7%.

A series of alternative suggestions could be advanced to explain the behaviour observed in on-column silylated packings. Identification of the retention mechanisms that operate in these columns and discriminating between their respective contributions to the total retention would be a difficult task, with dubious results. Pre-silylated packings represent a more attractive option when the objective is to isolate the effects of the liquid phase from those of the solid support.

Physical meaning of retention volumes measured in pre-silylated columns, on the other side, could be questioned in terms of the thermal instability of these packings. Therefore, and although retention volumes demonstrated excellent reproducibility in the 22 - 35 °C temperature range, a test addressed to check the stability of pre-silylated packings under conditions considerably more stringent than those prevailing during the thermodynamic measurements was performed. N-nonane and n-decane retention volumes were measured at six temperatures between 40 and 75 °C in columns containing 10.89 and 19.40 % packings; the columns were then slowly heated to 120 °C and kept for 1.5 h at this temperature, spontaneously cooled down to room temperature, and heated again to 120° C for 1.5 h; retention volumes were then re-measured in the 40 - 75 °C interval. The results of this experiment have been gathered in Table I, and show that not only the retention volumes measured before and after heating are coincident, but that also the slopes of the plots of $\ln V_g^{\circ}$ vs. $1/T$ remain constant. The efficiency of both columns is poor and heating seems to produce a drop in the number of theoretical plates of the column containing the 10.89 % packing. Summarizing, there are no counter-indications for the employment of these columns in the measurement of thermodynamic properties, where column efficiency is a desirable but not an essential parameter.

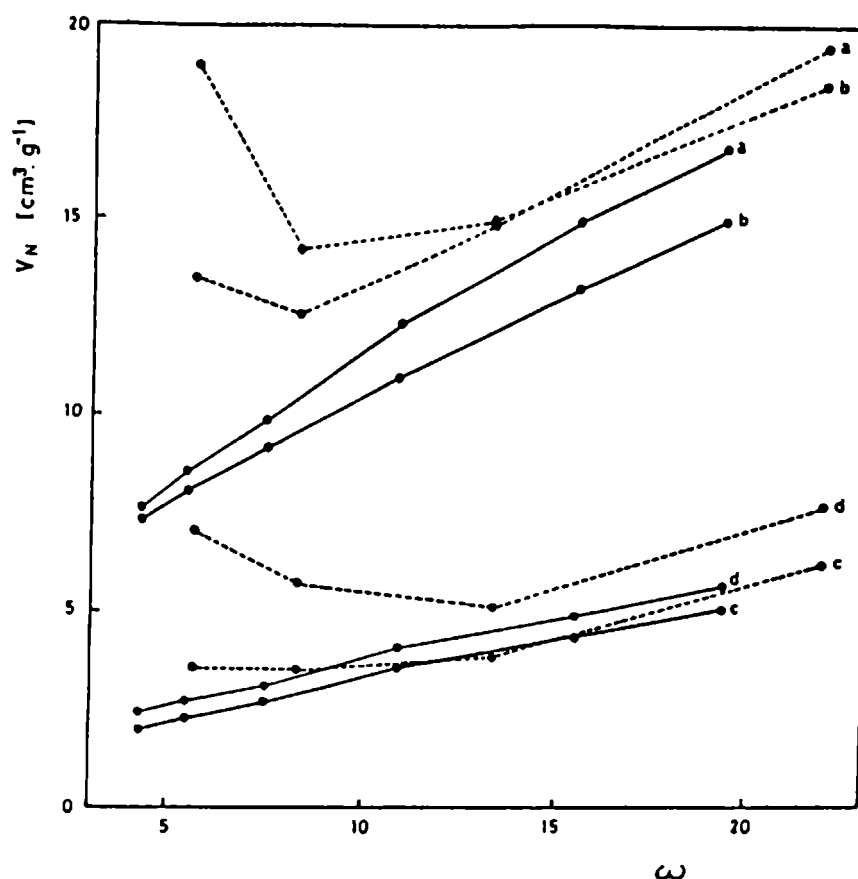


Fig. 1.- Retention volume per gram of packing at 25 °C (V_N) against percentage by weight of stationary phase (w).
Dotted lines: on-column silylated packings. Continuous lines: pre-silylated packings. Solutes: (a) n-octane;
(b) 1-octene; (c) cyclohexane; (d) cyclohexene.

Only results obtained using pre-silylated packings are referred to in the following sections.

Obtaining the thermodynamic results. Experimental results obtained on each column were fitted to the equation

$$\ln V_g^\circ = - \Delta H_s^\circ / RT + \text{constant} \quad (2)$$

where ΔH_s° , the heat of sorption, corresponds to the transfer of one mole of solute from an ideal vapour phase at a partial pressure of 1 atm to an stationary phase of yet undefined characteristics. Regression analysis of the results obtained in a given column showed that: a) values of percent standard deviation of the heats of sorption, $100 s(\Delta H_s^\circ) / \Delta H_s^\circ$, were smaller than 1.5 % for all the solutes; b) retention volumes obtained in a just conditioned column differed by less than 0.8 % from those obtained under identical conditions after two or more weeks of column use, and the differences between the corresponding heats of sorption was smaller than 4 %.

In Fig. 2 and 3 V_g° values at 25° C and heats of sorption, respectively, have been plotted against w for a group of representative solutes. The existence of a mixed retention mechanism is made evident by both plots, since straight lines parallel to the horizontal axis should be obtained for a purely partitioning process; furthermore, it can be advanced from Fig. 3 that the adsorptive component is markedly more exothermic than its solution counterpart [13].

TABLE I

Effect of thermal treatment on specific retention volumes, their temperature dependence and the efficiency of columns packed with Fomblin coated on Chromosorb P AW DMCS.

	n - Decane		n - Nonane	
	PRE	POST	PRE	POST
w = 10.89 %				
V_g° , 45° C	193.7	192.7	93.75	94.00
V_g° , 55° C	129.9	129.2	65.32	65.64
V_g° , 70° C	67.56	67.37	36.53	36.63
B	4626	4663	4149	4170
N, 50° C	1670	1450	1450	1200
N, 70° C	1400	990	875	810
w = 19.40 %				
V_g° , 50° C	115.5	113.42		
V_g° , 62° C	70.82	70.00		
V_g° , 74° C	44.64	44.82		
B	4506	4409		
N, 50° C	1260	1320		
N, 74° C	1300	1260		

PRE, POST: Results before and after the thermal treatment (details in the text).

B: least squares slopes for the fit to the equation $\ln V_g^\circ = B / T + \text{constant}$.

N: Number of theoretical plates.

Several years ago Conder et al. [14] proposed the following equation to express the retention volume per gram of packing when mixed mechanisms are operative:

$$V_N = K_L V_L + K_A A_L + K_S A_S \quad (3)$$

K_L is the liquid-gas partition coefficient, K_A and K_S are the adsorption coefficients at the gas-liquid and at the liquid-solid interfaces, respectively, and V_L , A_L and A_S represent the liquid volume, the gas-liquid interfacial area, and the liquid-solid interfacial area, all of them expressed per gram of packing; adsorption on bare portions of the support is not considered in eq. (3), what can be a reasonable attitude for packings containing more than 3-4 % by weight of stationary phase on Chromosorb P. Models endeavouring more detailed descriptions, involving equations with larger number of terms and, as such, of more difficult and dubious applicability to real data, have been more recently proposed [15].

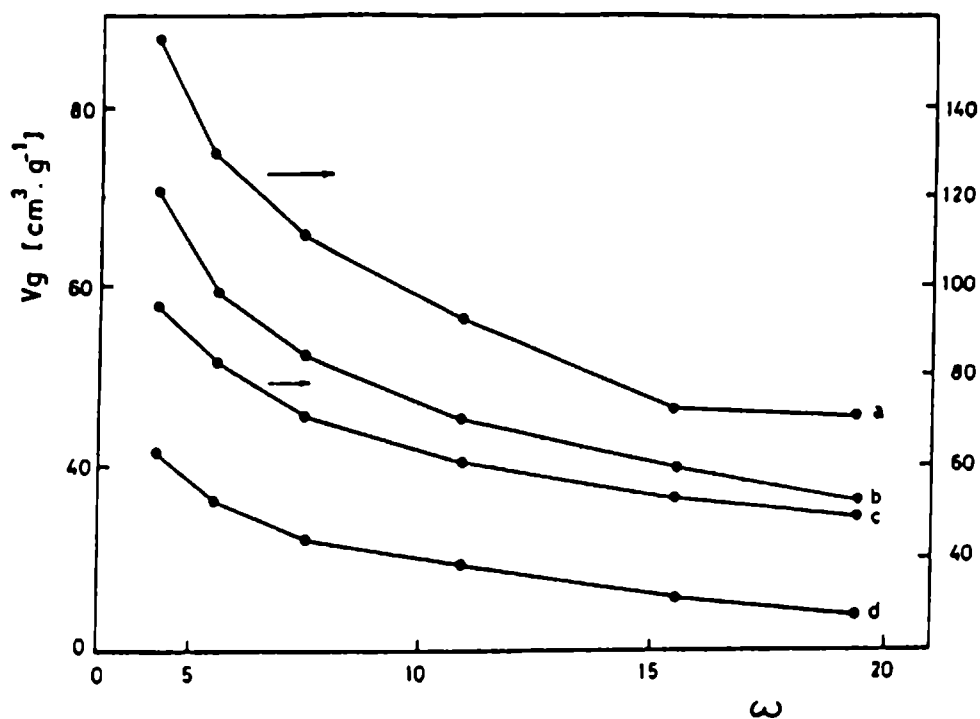


Fig. 2.- Specific retention volumes at 25° C (V_g°) against percentage by weight of stationary phase (w). Solutes: (a) 1-octene; (b) n-heptane; (c) 2,2-dimethylhexane; (d) cyclohexene.

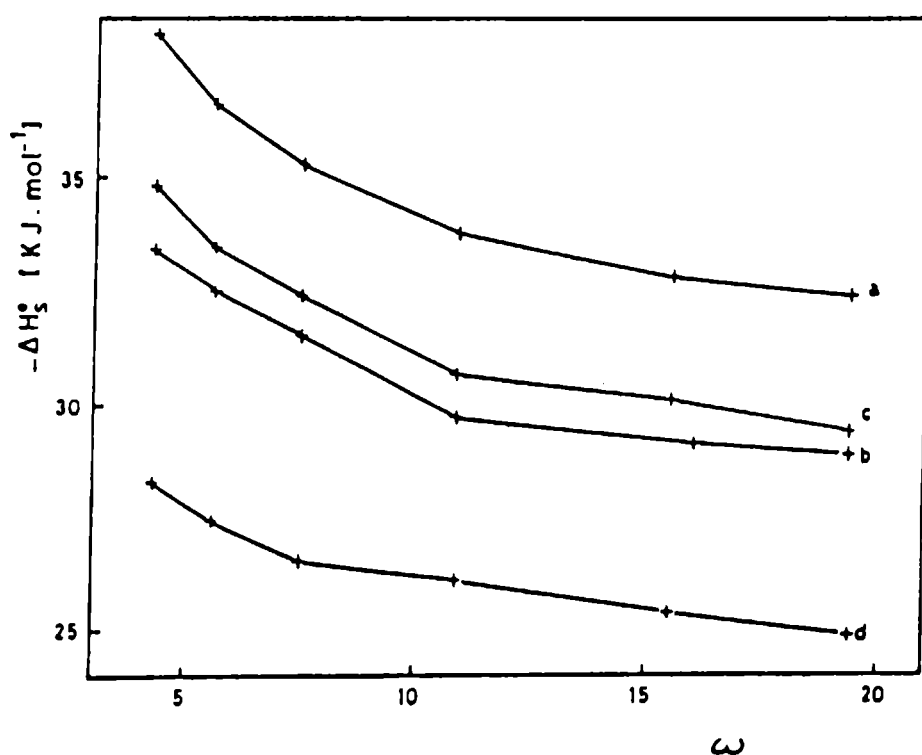


Fig. 3.- Heats of sorption (ΔH_s°) against percentage by weight of stationary phase (w). Solute symbols as in Fig. 2.

The values of A_L necessary to fit experimental results to eq. (3) were calculated by following the proposal of Martire et al. [16], taking into consideration the large difference between densities of β , β' -thiodipropionitrile and of Fomblin.

Multiple linear regression to eq. (3), assigning to A_s values calculated from the specific surface area of the support, was unsuccessfully attempted in the first place; the fit was insensible to very large changes in the values assigned to A_s , the coefficients had no statistical significance and, furthermore, it was found that eq. (3) was overparameterized, as evidenced by dependencies larger than 0.9999. On the other side there was a good linear relationship

between the variables V_N / V_L and A_L / V_L , as indicated by correlation coefficients higher than 0.997 and by the small coefficients of variation of both the intercepts and the slopes (see second and fifth columns in **Table II**, respectively). In terms of eq. (3), since V_L increases almost five times and A_L decreases by about 60 % between the lower and the higher stationary phase loading, it is reasonable to conclude that K_s is negligible under the present circumstances. In other words, that within the experimental errors of our measurements, the intercepts and the slopes obtained by means of the linear regression can be identified with the coefficients K_L and K_A , respectively.

These results indicate that hydrocarbons retention in columns containing Fomblin coated on Chromosorb P AW DMCS can be attributed to partition and adsorption on the gas-liquid interface. Depending on the solute, adsorption contribution to the total retention ranges between 50-60 % at the lower loading and 10-15 % in the column with higher concentration of stationary phase, as calculated by using the K_L and K_A results obtained as indicated in the former paragraph together with the V_L and A_L values characteristic of each column.

Standard enthalpies of solution, corresponding to the transfer of one mole of solute from an ideal vapour phase at a pressure of 1 atm to an hypothetical solution at unitary weight fraction, with behaviour extrapolated from infinite dilution, were calculated by means of the equation [18]

$$\Delta H_L^\circ = -R[\partial \ln K_L / \partial (1/T)] - RT(1 - \alpha_2 T) \quad (4)$$

The assumption of ideal vapour behaviour implied in eq. (4) is justified by a rapid calculation [12] which indicates that the nonideality correction in the case of the most volatile solute at the higher experimental temperature (n-hexane at 35° C) amounts to about 0.3 % of K_L , a value below our estimation of the experimental error.

Enthalpies of adsorption were computed from the expression

$$\Delta H_A^\circ = -R[\partial \ln K_A / \partial (1/T)] \quad (5)$$

and it can be shown [19] that correspond to the transfer of one mole of solute from an ideal vapour phase at 1 atm to an ideal adsorbed state in which the molecules of adsorbate interact with the surface only. Inasmuch as adsorbate-adsorbate interactions are absent, the value of the adsorption enthalpy does not depend on the definition of the adsorbed state; this statement obviously does not apply to the adsorption free energy and entropy.

Solution and adsorption properties have been gathered in **Table II**. As already mentioned, the uncertainties assigned to K_L and K_A values are the standard deviations for the intercept and the slope, respectively, obtained in the regression of V_N / V_L against A_L / V_L . The confidence ranges for ΔH_L° and ΔH_A° at the 95 % level were estimated by following a method proposed some years ago [13], that takes into consideration that two successive regressions are necessary to obtain the enthalpy values. The latent heats of condensation, ΔH_C° [20], were included in **Table II** with comparative purposes.

TABLE II. Thermodynamic Functions of Partition and Adsorption of Vapours at Infinite Dilution in Fomblin at 25° C

SOLUTE	$K_L \pm s(K_L)$	$-\Delta H_L^\circ$ [KJ/mol]	χ^* (int)	$[K_A \pm s(K_A)] \times 10^{-4}$ [cm]	$-\Delta H_A^\circ$ [KJ/mol]	$-\Delta H_C^\circ$ [KJ/mol]
n-Hexane	29.21±1.12	24.7±3.2	2.462	0.573±0.031	30.5±5.4	31.6
n-Heptane	65.33±1.64	28.1±2.8	2.761	1.239±0.042	36.4±4.4	36.6
2-Methylhexane	53.21±1.31	26.2±2.8	2.605	0.998±0.033	35.7±4.5	34.8
2,3-Dimethylpentane	60.12±1.71	26.1±2.7	2.472	0.949±0.044	35.4±5.5	34.2
n-Octane	145.1±6.95	31.1±4.9	3.058	2.970±0.177	42.7±8.2	41.5
2-Methylheptane	117.5±6.04	30.7±4.9	2.883	2.337±0.154	40.4±8.4	39.7
2,2-Dimethylhexane	88.90±2.28	28.4±2.8	2.646	1.681±0.058	38.7±4.7	37.3
2,2,4-Trimethylpentane	77.93±3.10	26.4±3.7	2.406	1.353±0.079	38.0±7.3	35.1
n-Nonane	325.5±15.7	36.0±5.6	3.340	6.906±0.400	45.8±8.6	46.4
1-Heptene	55.7±2.13	26.2±3.8	2.764	1.287±0.054	36.6±5.6	36.1
1-Octene	122.9±3.82	30.6±3.4	3.057	3.090±0.097	40.9±4.6	40.8
Cyclohexane	45.68±2.03	25.3±3.4	2.671	0.621±0.052	30.5±7.7	33.0
Cyclohexene	48.73±2.41	26.9±4.5	2.758	0.872±0.061	28.8±6.9	33.3
Methylcyclohexane	79.24±3.68	27.6±4.1	2.713	1.165±0.094	35.1±8.8	35.4
Ethylcyclohexane	191.1±9.16	31.0±4.6	3.020	2.808±0.233	40.5±10.2	40.5

Results in the table change very regularly with the molecular structure of the solutes. Thus the plots of $\ln K_L$ for n-alkanes against their carbon number, N , are straight lines with correlation coefficients $r = 0.99997$, and those of $\ln K_A$ against N result in $r = 0.9997$. Both K_L and K_A are smaller for branched than for normal alkanes with the same N , and (excepting the K_L result for 2,3-dimethylpentane) both values decreases as branching increases. The alkenes partition coefficients are smaller than those of the corresponding alkanes, while the opposite trend is observed for the adsorption coefficients. Partition coefficients of cycloalkanes are larger than those of the alkanes with the same carbon number, but the adsorption coefficients of both groups of substances are coincident within experimental error.

As could be expected, a lower regularity is detected when the enthalpies are compared: plots of ΔH_L° and of ΔH_A° against N for n-alkanes are well represented by straight lines, but their correlation coefficients drop to 0.994 and 0.991, respectively. In general terms, branched alkanes and alkenes show less negative ΔH_L° and ΔH_A° values than normal alkanes with the same N .

Figures 4 and 5 show that there is a strong correlation between K_A and K_L on one side, and between ΔH_A° and ΔH_L° on the other. It can be concluded from this behaviour that solution and adsorption are ruled by the same physical factors, either energetic or statistical. However, when the enthalpies of adsorption and of solution are compared with the latent heats of condensation it is found that :

a. the differences $\Delta H_A^\circ - \Delta H_C^\circ$ are zero within experimental error, indicating that the liquid-gas interface of Fomblin is a low energy surface on which the hydrocarbon molecules adsorb without experiencing the influence of large repulsion or attraction forces.

b. the differences $\Delta H_L^\circ - \Delta H_C^\circ$, rough estimators of infinite dilution excess enthalpies, range between 7 and 10 KJ/mol, indicating that the solute molecules are repelled from the bulk liquid and demand the absorption of important quantities of energy in order to penetrate it.

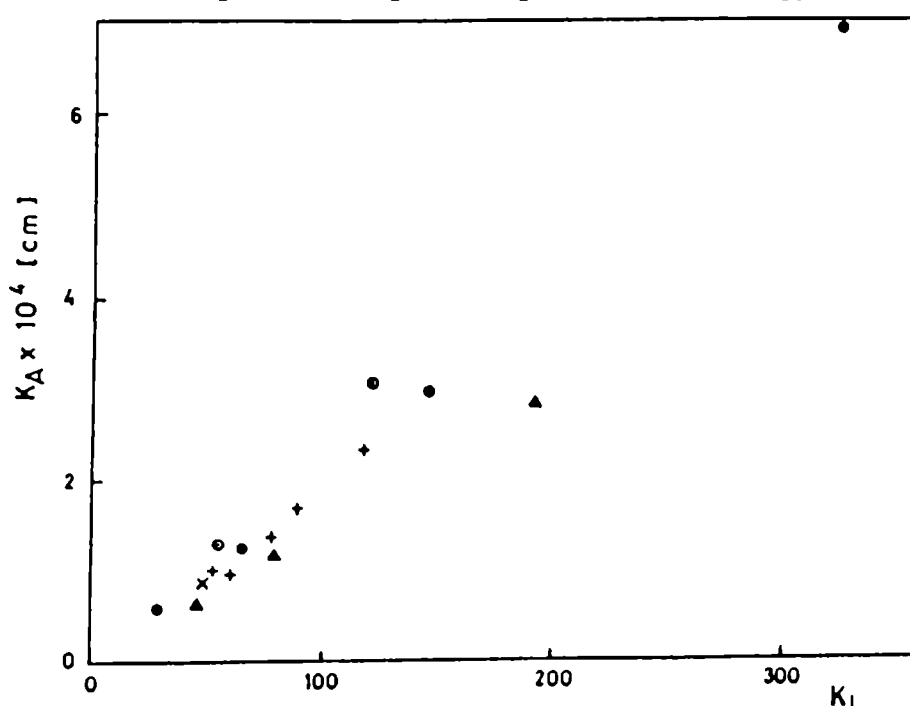


Fig. 4.- Adsorption coefficients (K_A) against partition coefficients (K_L) at 25° C. Solutes: (•) n-alkanes; (+) branched alkanes; (o) alkenes; (Δ) cycloalkanes; (x) cyclohexene.

Deviations from the ideal behaviour are more important in bulk mixtures than in surfaces, a fact already detected by Handa and Mukerjee [10], who attributed it to the lower number of nearest neighbours that a molecule has on the surface as compared to bulk solution. These authors semiquantitatively explained the surface properties of n-alkane + perfluoroalkane mixtures by assuming unitary surface activity coefficients and modeling the bulk activity coefficients by means of the regular solution or the Flory-Huggins approaches.

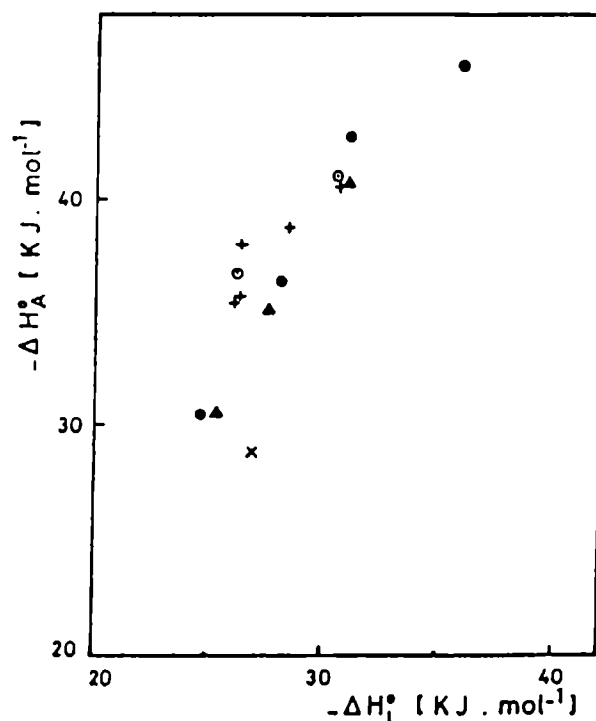


Fig. 5.- Enthalpy of adsorption (ΔH_A°) against enthalpy of solution (ΔH_L°). Symbols as in Fig. 4.

Flory-Huggins interaction parameters, χ^* , were calculated with the equation [21]

$$\chi^* = \ln (RTp_2 / K_L p_1^\circ M_1) - \ln (v_1^* / v_2^*) - 1 + (M_1 v_1^* / M_2 v_2^*) \quad (6)$$

where M_1 and p_1° represent the solute molecular weight and vapour pressure at the column temperature, respectively, M_2 is the polymer number average molecular weight and v_1^* and v_2^* are the solute and the polymer specific "hard core" volumes, calculated by means of Flory state equation [22] using experimental thermal expansion coefficients. The interaction parameter is an adimensional free energy term that includes all the non-combinatorial contributions to excess free energy; Flory and collaborators [22] express χ^* as a sum of two contributions:

$$\chi^* = \chi^*(fv) + \chi^*(int) \quad (7)$$

$\chi^*(fv)$ is the free volume contribution, and $\chi^*(int)$ results from contact interactions.

Unusually high χ^* values, ranging between 2.4 and 3.4, are obtained for the systems studied in the present paper. With the only exception of n-hexane, free volume effects contribute less than 2.5 % to the total interaction parameter. The highly positive nonideality of these mixtures results from very large differences between the force fields surrounding the hydrocarbon and the perfluorocarbon segments.

Values of χ^* (int) can be read on the fourth column of **Table II**; they were fitted by a non-linear regression method to the equation

$$\chi^* (\text{int}) = (V_1^* / RT)(\delta_1 - \delta_2)^2 \quad (8)$$

where $V_1^* = M_1 v_1^*$, δ_1 is the solute solubility parameter [23] and δ_2 , the polymer solubility parameter, was the fitting parameter. A value $\delta_2 = 7.65 \text{ J}^{1/2} \cdot \text{cm}^{-3/2}$ is thus obtained; the standard deviation obtained for δ_2 is only $0.084 \text{ J}^{1/2} \cdot \text{cm}^{-3/2}$, indicating that the experimental results fit nicely to eq.(8). However the value returned for δ_2 is unusually low and, from our point of view, its physical meaning is not clear. This is by no means a novelty in dealing with polymer solubility parameters.

ACKNOWLEDGEMENT

This work was sponsored by CONICET (Consejo Nacional de Investigaciones Científicas y Tecnológicas) through PID-BID 1121, and by CICPBA (Comisión de Investigaciones Científicas de la Provincia de Buenos Aires)

REFERENCES

- [1] Pomaville R.M. and Poole C.F.- **Anal. Chim. Acta**, **200**, 151 (1987).
- [2] O' Mahony T.K.P., Cox A.P. and Roberts D.J.- **J. Chromatogr.**, **637**, 1 (1993).
- [3] Hildebrand J.H., Prausnitz J.M. and Scott R.L.- **Regular and Related Solutions**, Van Nostrand-Reinhold, New York, 1970.
- [4] Bedford R.G. and Dunlap R.D.- **J. Am. Chem. Soc.**, **80**, 282 (1958).
- [5] Dunlap R.D., Bedford R.G., Woodbrey J.C. and Furrow S.D.- **J. Am. Chem. Soc.**, **81** 2927 (1959).
- [6] Dhanesar S.C. and Poole C.F.- **J. Chromatogr.**, **267**, 388 (1983).
- [7] Dhanesar S.C. and Poole C.F.- **Anal. Chem.**, **55**, 1462 (1983).
- [8] Scott R.L.- **J. Phys. Chem.**, **62**, 136 (1958).
- [9] Swinton F.L.- In M. L. McGlashan (Editor), **Chemical Thermodynamics, Specialist Periodical Reports**, Chemical Society, London, 1978, Vol. 2, 147.
- [10] Handa T. and Mukerjee P.- **J. Phys. Chem.**, **85**, 3916 (1981).
- [11] Mukerjee P.- **Colloid Surface A**, **84**, 1 (1994).

- [12] Conder J.R. and Young C.L.- *Physicochemical Measurements by Gas Chromatography*, Wiley, New York, 1979, Ch. 2.
- [13] Castells R.C.- *J. Chromatogr.*, **111**, 1 (1975).
- [14] Conder J.R., Locke D.C. and Purnell J.H.- *J. Phys. Chem.*, **73**, 700 (1969).
- [15] Nikolov R.- *J. Chromatogr.*, **241**, 237 (1982).
- [16] Martire D.E., Pecsok R.L. and Purnell J.H.- *Trans. Faraday Soc.*, **61**, 2496 (1965).
- [17] Martin R.L.- *Anal. Chem.*, **33**, 347 (1961).
- [18] Castells R.C.- *J. Chromatogr.*, **350**, 339 (1985).
- [19] Meyer E.F.- *J. Chem. Educ.*, **57**, 120 (1980).
- [20] Dreisbach R.R.- *Adv. Chem. Ser.* **15** (1955); **22** (1959).
- [21] Patterson D., Tewari Y.B., Schreiber H.P. and Guillet J.E.- *Macromolecules* **4**, 356 (1971).
- [22] Eichinger B.E. and Flory P.J.- *Trans. Faraday Soc.*, **64**, 2035 (1968).
- [23] Barton A.F.M.- *Handbook of Solubility Parameter*, CRC Press, Boca Raton, Florida, 1983.

ACTIVITY COEFFICIENTS OF HYDROCARBONS AT INFINITE DILUTION IN DI-N-OCTYLTIN DICHLORIDE. COMPARISON WITH RESULTS OBTAINED IN OTHER ALKYLTIN SOLVENTS

MEDICION POR CROMATOGRAFIA GASEOSA DE COEFICIENTES CON ACTIVIDAD DE HIDROCARBUROS A DILUCION INFINITA EN DICLORO DIOCTILESTAÑO. COMPARACION CON RESULTADOS OBTENIDOS EN OTROS SOLVENTES ALQUILESTANNICOS

A.M. Nardillo¹, D.B. Soria², C.B.M. Castells² and R.C. Castells¹

SUMMARY

The gas chromatographic method was employed to measure the infinite dilution activity coefficients of twenty-eight hydrocarbons of different types in di-n-octyltin dichloride between 323.15 and 353.15 K, and of seven branched alkanes in tri-n-octyltin chloride between 313.15 and 333.15 K. A comparison is made between the results obtained for all the solutes in both solvents and in tetra-n-octyltin.

Keywords: *Gas-liquid chromatography, di-n-octyltin dichloride, tri-n-octyltin chloride, tetra-n-octyltin, hydrocarbon solution, infinite dilution activity coefficients.*

INTRODUCTION

Gas chromatographically measured activity coefficients of fifteen hydrocarbons at infinite dilution in tetra-n-octyltin (TOT) [1] and in tri-n-octyltin chloride (TOTC) [2] at five temperatures between 313.15 and 333.15 K were reported and discussed in two recent publications. Data for seven branched alkanes in TOT were added in a more recent paper [3].

In the present paper the results obtained in the measurement of the infinite dilution activity coefficients of twenty-eight hydrocarbons in di-n-octyltin dichloride (DOTDC) at several temperatures between 323.15 and 353.15 K, and of seven branched alkanes in TOTC at five temperatures in the interval 313.15 - 333.15 K are reported. Non-idealities observed in the binary systems formed by this group of hydrocarbons and the three alkyltin solvents are compared and their possible causes are discussed.

¹ Miembro de la Carrera del Investigador del CONICET, UNLP

² División de Química Analítica, Facultad de Ciencias Exactas, UNLP

EXPERIMENTAL

DOTDC was prepared by reacting equimolar quantities of TOT and tin (IV) chloride [4]. The mixture was heated at 110° C for 1 h and at 220° C for 2 h, with continuous stirring, and then fraction-distilled under reduced pressure. A light yellow product, melting between 43 and 45° C, was collected at about 170° C/ 0.2 Torr (164 - 165°C/0.16 Torr in [4]). This was further purified by using a vacuum sublimator immersed in a silicone oil bath at 80° C, with its cold finger cooled by circulating tape water; pressure was not recorded in this instance. The product obtained after discarding head and tail portions was almost white, melted at 47.0 - 48.8°C (47.5 - 48.5°C in the literature [4]), and its tin content (determined as detailed in [1]) was 28.64% by weight (28.53% calculated). Densities, measured as described in the former papers [1-3] at nine temperatures between 48.5 and 82° C, were least squares fitted to the equation

$$d(t/^{\circ}\text{C}) = 1.21712 - 5.8313 \times 10^{-4} t - 8.472 \times 10^{-6} t^2 + 4.13 \times 10^{-8} t^3 \quad (1)$$

Chromosorb W AW DMCS 60/80 was coated with 8.28% w/w of DOTDC in a rotary evaporator, using benzene as the volatile solvent. The dry coated support was packed into 0.22 cm i.d. x 1.0 - 2.0 m in length stainless steel tubes; the columns were conditioned for 4 h at 80° C under nitrogen flow before use. A Hewlett-Packard 5880A gas chromatograph, equipped with a flame ionization detector, was employed for the chromatographic measurements; nitrogen at flow rates of about 20 mL.min⁻¹ was used as the carrier gas. The hydrocarbon solutes were of different origins, more than 99% pure, and were injected in the vapor form, either pure or in mixtures, by means of Hamilton microsyringes. Sample sizes of the order of 100 ng were simultaneously injected with a small methane sample; all the peaks were highly symmetric, and net retention times were measured to 0.001 min between the maxima of the solute and the methane peaks. Net retention time at each temperature was the mean of not less than four separate injections.

RESULTS AND DISCUSSION

Specific retention volumes were calculated from net retention times and from the values of operating parameters in the usual form [5]; from them hydrocarbons infinite dilution and zero pressure activity coefficients, $\gamma_1^{\infty}(0)$, were calculated as detailed in a former paper [3]. The results for twenty-eight hydrocarbons at several temperatures in DOTDC have been gathered in Table I, and those of seven branched alkanes in TOTC can be read in Table II. We estimate these results accurate to ± 0.003 from repeated measurements performed independently. Partial molar excess enthalpies, $H_1^{E,\infty}$, estimated from the linear regression of $\ln \gamma_1^{\infty}(0)$ against $1/T$, have been also included in the tables.

The solutes can be split into two groups, according with their behavior in the three solvents. The first group includes all the solutes, excepting the aromatic hydrocarbons; their activity coefficients increase noticeably in passing from TOT to TOTC, and suffer a further increase in passing from TOTC to DOTDC. Typical values for solutes of this group at 50° C are 0.58 - 0.70 in TOT, 0.80 - 1.00 in TOTC, and 1.40 - 1.70 in DOTDC; when the activity coefficients in DOTDC at 50° C are plotted against the corresponding values in TOT, the points corresponding to solutes of this group fall on a common line, with 0.985 as correlation

coefficient, and the same relationship is shown by the data in the solvents TOTC and TOT, the correlation coefficient being 0.982 in this case. The aromatic solutes constitute the second group of solutes; their activity coefficients suffer only minor increases in passing from TOT to one of the chlorinated solvents, and are smaller than unity in the three stationary phases.

TABLE I
Infinite Dilution Activity Coefficients and Partial Molar Excess Enthalpies of
Hydrocarbons in DOTDC

SOLUTE	t / ° C							H ₁ ^{E,∞} ± s ^{a,b}
	50	55	60	65	70	75	80	
n-Hexane	1.414	1.386	1.357		1.332			2740 ± 380
2-Methylpentane	1.451		1.415	1.401	1.396		1.375	1680 ± 160
3-Methylpentane	1.369		1.338	1.324	1.322		1.297	1660 ± 150
2,2-Dimethylbutane	1.400		1.353	1.340	1.323		1.306	2190 ± 240
n-Heptane	1.506		1.454	1.441	1.422	1.404		2590 ± 130
2-Methylhexane	1.554		1.508		1.479		1.454	2080 ± 110
3-Methylhexane	1.491		1.449		1.423		1.398	2000 ± 140
2,3-Dimethylpentane	1.382		1.334	1.315	1.300		1.279	2450 ± 230
2,4-Dimethylpentane	1.577	1.542	1.511		1.484			2770 ± 410
n-Octane	1.618		1.559	1.539	1.519	1.497	1.483	2750 ± 110
2-Methylheptane	1.663		1.613		1.579		1.551	2200 ± 150
4-Methylheptane	1.615	1.578	1.544		1.510			3080 ± 390
2,2-Dimethylhexane	1.666		1.604		1.568		1.536	2540 ± 230
2,5-Dimethylhexane	1.681	1.641	1.606		1.568			3170 ± 360
2,2,4-Trimethylpentane	1.616		1.570		1.523		1.495	2520 ± 140
2,3,4-Trimethylpentane			1.434	1.419	1.398	1.382	1.367	2400 ± 70
Cyclohexane	1.013		0.988		0.959		0.956	1950 ± 360
Methylcyclohexane	1.095		1.057	1.041	1.032		1.015	2400 ± 240
Ethylcyclohexane	1.226		1.191		1.168		1.149	2020 ± 160
1-Hexene	1.179		1.146	1.135	1.127		1.119	1650 ± 270
1-Heptene	1.273		1.234	1.218	1.209		1.193	2050 ± 250
1-Octene	1.372		1.344		1.310		1.293	1910 ± 140
Benzene	0.682		0.671		0.668		0.667	680 ± 220
Toluene			0.725	0.725	0.724	0.722	0.720	390 ± 70
Ethylbenzene	0.800		0.805		0.801		0.801	-50 ± 220
o-Xylene			0.775	0.773	0.772	0.770	0.769	380 ± 40
m-Xylene			0.797	0.796	0.795	0.793	0.794	230 ± 70
p-Xylene			0.788	0.788	0.788	0.786	0.785	210 ± 50

^a Units: J.mol⁻¹. ^b s: standard deviation.

In order to attempt an interpretation for this behavior the combinatorial and the free volume contributions to the infinite dilution activity coefficients, $\gamma_1^\infty(\text{comb})$ and $\gamma_1^\infty(\text{fv})$ respectively, were computed by means of the corresponding expressions [1] deduced from the model of Flory [6], using the reduction parameters listed in the former publications for the solutes, for TOT and for TOTC [1-3]; for DOTDC a molar volume reduction parameter $V_2^* = 282.8 \text{ cm}^3.\text{mol}^{-1}$ was computed from eq.(1). The activity coefficients were considered as resulting from the following contributions:

$$\ln \gamma_1^\infty(0) = \ln \gamma_1^\infty(\text{comb}) + \ln \gamma_1^\infty(\text{fv}) + \ln \gamma_1^\infty(\text{res}) \quad (2)$$

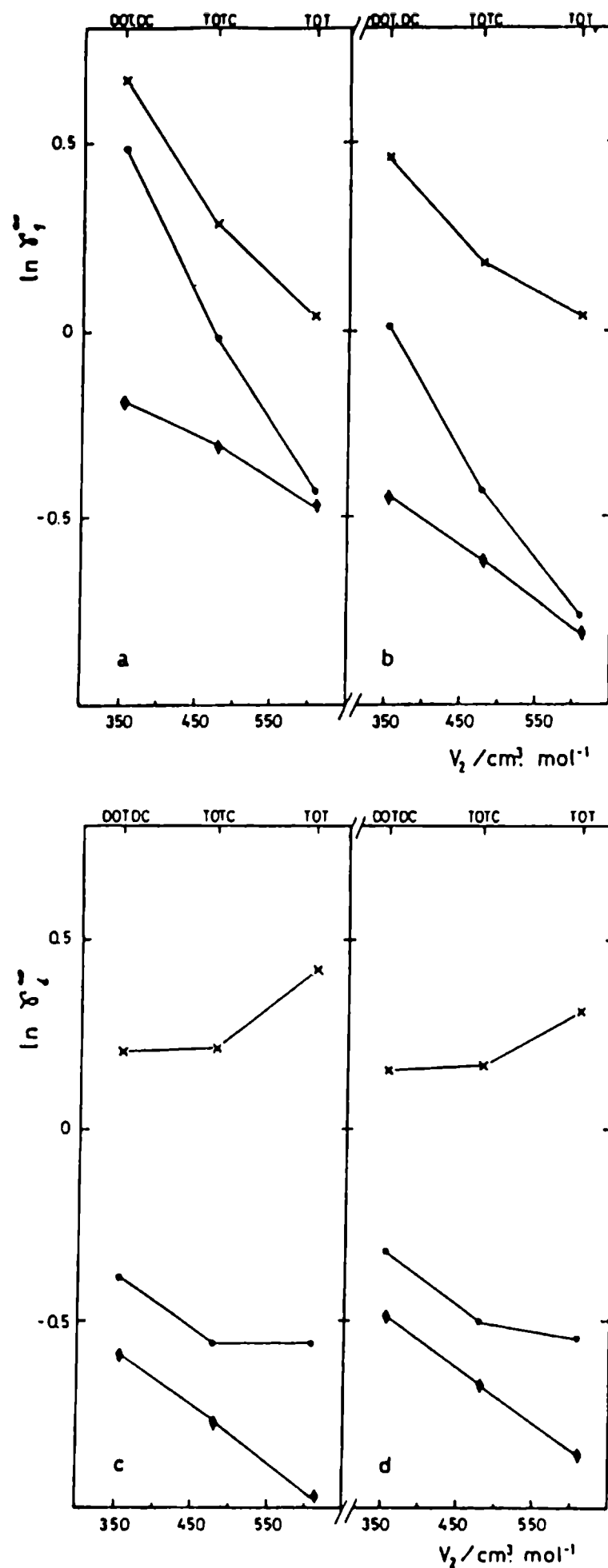


Fig. 1.- Plot of the infinite dilution activity coefficients against the solvent molar volume at 50° C, for four representative solutes. (a) n-Octane; (b) cyclohexane; (c) benzene; (d) toluene. (•) Experimental activity coefficients; (♦) combinatorial plus free volume contributions; (x) residual contributions.

where $\gamma_1^\infty(\text{res})$ is a residual value, obtained by subtracting both theoretical contributions from the experimental value, to which a physical interpretation has to be assigned. In **Figure 1** the values of $\ln \gamma_1^\infty(0)$, of the sum $\ln \gamma_1^\infty(\text{comb}) + \ln \gamma_1^\infty(\text{fv})$, and of $\ln \gamma_1^\infty(\text{res})$ have been plotted against the solvent molar volume for two solutes belonging to the first group and for two aromatic solutes, at 50° C.

TABLE II
Infinite Dilution Activity Coefficients and Partial Molar Excess Enthalpies of Hydrocarbons in TOTC

SOLUTE	t/° C					$H_1^{E,\infty} \pm s^{a,b}$
	40	45	50	55	60	
2-Methylpentane	0.903	0.895	0.884	0.880	0.878	1280 ± 180
3-Methylpentane	0.860	0.852	0.844	0.839	0.834	1360 ± 100
2-Methylhexane	0.956	0.946	0.935	0.928	0.922	1590 ± 90
2,4-Dimethylpentane	0.979	0.969	0.959	0.952	0.946	1490 ± 100
4-Methylheptane	0.987	0.976	0.966	0.958	0.952	1580 ± 90
2,2-Dimethylhexane	1.028	1.015	1.002	0.993	0.985	1850 ± 100
2,5-Dimethylhexane	1.030	1.019	1.007	0.998	0.991	1690 ± 80

^a Units: J.mol⁻¹. ^b s: standard deviation.

In discussing the results plotted in **Fig. 1** it has to be pointed out firstly that since reduced volumes of the three solvents differ very little, the free volume contributions for a given solute are almost equal in the three stationary phases. Therefore the drops observed for the plots of $\ln \gamma_1^\infty(\text{comb}) + \ln \gamma_1^\infty(\text{fv})$ against the solvent molar volume have to be attributed to decreasing values of the combinatorial contribution resulting from important increases in solvent molar volume in the direction DOTDC < TOTC < TOT. The residual contribution is very small for solutes of the first group in TOT, but increases markedly when one chlorine atom replaces an octyl group in the solvent molecule, and even more by the introduction of a second chlorine atom; in our opinion this effect is purely interactional, and reflects very large differences between the force fields in the vicinity of the hydrocarbonaceous solute chain and of the solvent halogen atoms. Benzene, on the other side, shows an important residual contribution in TOT that decreases by the introduction of halogen atoms in the solvent molecule; this trend can be explained in terms of interactional effects resulting from dipole induction into the aromatic nucleus by the highly polar chlorinated solvents.

Partial molar excess enthalpies for the same group of four solutes have been plotted against the solvent molar volume in **Fig. 2**. All the systems display endothermal mixing at infinite dilution; however the chlorination of the solvent molecules produces opposite effects in solutes of the two groups. These trends are coherent with those described in the previous paragraph.

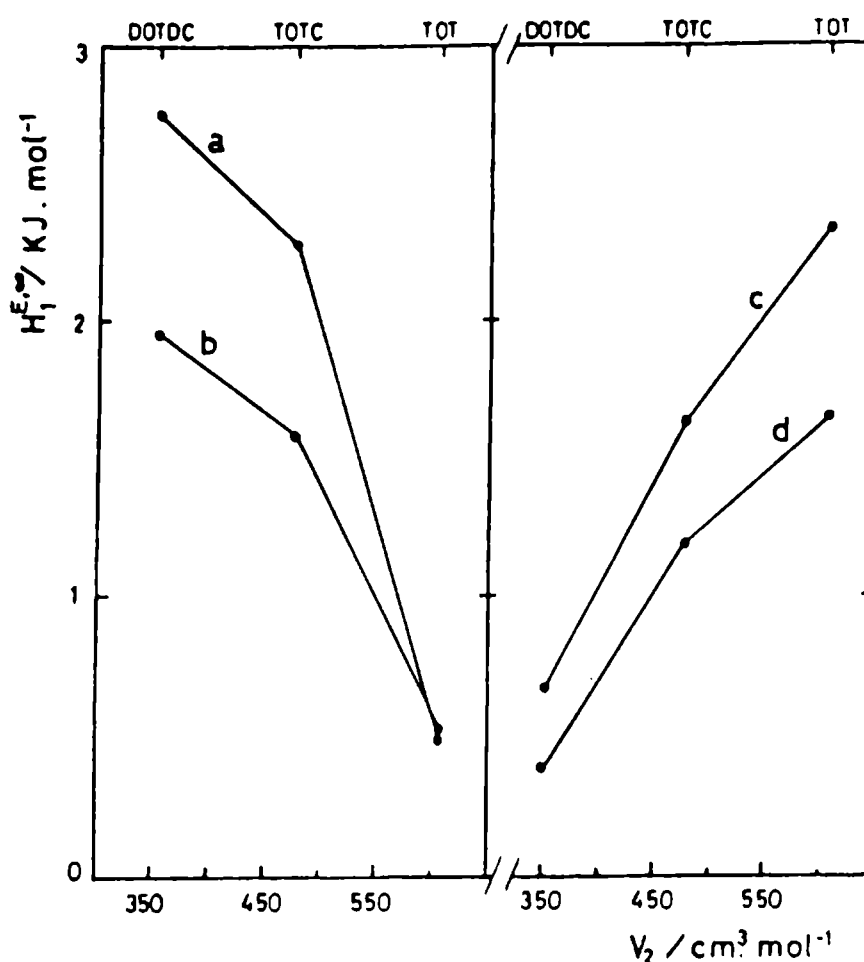


Fig. 2.- Infinite dilution partial molar excess enthalpy of four solutes against the solvent molar volume. Solute identification as in Fig. 1.

ACKNOWLEDGMENT

This work was sponsored by CONICET (Consejo Nacional de Investigaciones Científicas y Tecnológicas) and by CICPBA (Comisión de Investigaciones Científicas de la Provincia de Buenos Aires).

REFERENCES

- [1] Castells R.C. and Castells C.B.M.- *J. Solution Chem.* **21**, 129 (1992).
- [2] Castells R.C. and Castells C.B.M.- *J. Solution Chem.* **21**, 1081 (1992).
- [3] Castells R.C. and Castells C.B.M.- *J. Solution Chem.* **24**, 285 (1995).
- [4] van der Kerck G.J.M. and Luitjen J.G.A.- *J. Appl. Chem.* **7**, 369 (1957).
- [5] Conder J.R. and Young C.L.- *Physicochemical Measurements by Gas Liquid Chromatography*, Wiley, New York (1979).
- [6] Eichinger B.E. and Flory P.J.- *Trans. Faraday Soc.* **64**, 2035 (1968).

THERMODYNAMICS OF SOLUTIONS OF HYDROCARBONS IN LOW MOLECULAR WEIGHT POLY(ISOBUTYLENE). A GAS CHROMATOGRAPHIC STUDY

TERMODINAMICA DE SOLUCIONES DE HIDROCARBUROS EN POLI(ISOBUTILENO) DE BAJO PESO MOLECULAR. UN ESTUDIO POR CROMATOGRAFIA GASEOSA

R.C. Castells¹, L.M. Romero² and A.M. Nardillo¹

SUMMARY

The reduced chemical potentials (χ^) of twenty normal and branched alkanes, cyclohexane and three aromatic hydrocarbons at infinite dilution in polyisobutylene (PIB) were measured by gas-liquid chromatography at five temperatures between 35 and 65°C. Reduced partial molar residual enthalpies (κ^*) were calculated from the temperature dependence of χ^* ; they are positive for PIB+alkane systems, but smaller than those obtained in former chromatographic studies. Although uncertainties on κ^* are at least one order of magnitude larger than those on χ^* , binary X_{12} Flory parameters obtained from κ^* display a good correlation with the structural parameter θ_{av} , defined as the ratio of the number of hydrogen atoms on methyl groups to the total number of hydrogen atoms in the alkane molecule. Very poor or nil correlation exists between X_{12} values obtained from χ^* and θ_{av} . The evidence is by no means conclusive, but in principle the χ^* results obtained for PIB + alkane systems could be explained in terms of free volume contributions and of the antipathy between methyl groups on the alkanes molecules and the polymer side groups. Positive partial molar residual entropies were detected for the three aromatic hydrocarbons; their partial molar residual enthalpies are however highly positive, resulting in their poor solvent properties towards PIB.*

Keywords: *Poli(isobutileno), hidrocarburos, termodinámica, cromatografía gaseosa, soluciones de polímeros, Modelo de Flory.*

INTRODUCTION

Notwithstanding that many years have passed since its conception, Flory theory [1,2] is probably still the most useful interpretative framework for the discussion of the thermodynamic properties of non-electrolyte mixtures. The theory recognizes three contributions to the mixing

¹ Miembro de la Carrera del Investigador del CONICET, UNLP

² División Química Analítica, Facultad de Ciencias Exactas, UNLP

functions: combinatorial, free volume and interactional; they were reviewed in a recent paper [3].

The theory has been most usually checked against calorimetric results; the interactional contribution is obtained by deducting the free volume contribution (calculated from equation of state data of the pure components by means of Flory's equations) from the excess enthalpy, H^E . The interactional contribution is characterized by the X_{12} parameter, that denotes the energy change for formation of contacts between species 1 and 2 in exchange for contacts between like species; according with the theory X_{12} is temperature and concentration independent. Another way of approach has been the measurement of excess free energies, G^E , by osmometric methods, by vapor sorption, or by gas liquid chromatography (glc). After correction for the free volume and for the combinatorial contributions (this last usually calculated in terms of segment fractions using the Flory-Huggins equations [4,5]) the interactional contribution and the X_{12} parameter are obtained. Both experimental approaches, but more frequently the calorimetric one, have been profusely employed to study hydrocarbon mixtures [3,6].

It is not surprising that the behavior of real systems deviates from the predictions of Flory's semiempirical approach. Flory himself discovered that X_{12} parameters obtained by fitting to experimental H^E were larger than those obtained when fitting was made to G^E [2,7]. Patterson and collaborators advanced the idea that the discrepancies stem from theory's neglect of liquid structure; their arguments were supported on Rayleigh scattering measurements of Bothorel *et al* [8,9], and were latter reinforced with numerous calorimetric results on carefully selected systems [10-12]. Short range orientational order, that can be thought as a partial alignment of neighboring segments or even of whole molecules, would be present in liquids formed from long non-branched molecules; this order is destroyed or replaced by weaker correlations on mixing with molecules of more globular shape, giving rise to positive contributions both to H^E and S^E . Since H^E and $T S^E$ are almost equal an enthalpy-entropy compensation occurs during the process, that is characterized by small contributions to G^E . Furthermore, order would be expected to decrease as the temperature raises, and its contributions to all the excess properties should become smaller.

A new contribution related with liquid structure was detected when the number of available experimental results increased. Important differences were found among the mixing enthalpies of a given normal alkane with a group of isomeric branched alkanes for which Rayleigh scattering indicated the same decrease in order during mixing; differences in H^E correlated with differences in the branched alkanes molar volumes [13,14]. The same type of correlation was latter found between mixing entropies (corrected for combinatorial and free volume contributions) and molar volumes [15]. A lower molar volume is associated with a higher crowding of groups within the molecule, *i.e.* with steric hindrance to the free rotation of groups; negative enthalpy and entropy contributions occur on mixing rigid molecules with molecules freer in rotation, as normal alkanes, through mechanisms yet not known but that could be related to a coupling of the modes of both types of molecules that results in an increase of order in the solution.

Delmas *et al.* [16], using calorimetry, found that the enthalpy of mixing PIB with alkanes at low polymer concentration is negative. Flory and collaborators [17,18] suggested that this behavior could be accounted for a combination of a negative free volume contribution

and a small positive term that the authors attributed to interchange of neighbor species in contact; their prediction for the PIB+n-pentane system was a strong concentration dependence of the κ^* parameter (*i.e.*, the reduced excess enthalpy calculated on a segment fraction basis), which was negative through most of the range but reached + 0.2 at the glc condition of polymer segment fraction $\varphi_2 = 1$.

In contradiction with these predictions glc measurements by Hammers and de Ligny [19] resulted in negative κ^* 's for a group of PIB+alkane systems that included n-pentane. Negative values of κ^* at several concentrations were also obtained by Gaecklé *et al.* [20] for the system PIB+n-pentane using calorimetry; concentration dependence was negligible so that it would be negative at $\varphi_2 = 1$.

Leung and Eichinger [21,22] employed the glc method to study the mixing of PIB with hydrocarbons; their residual chemical potentials at 25°C, χ^* , were very near to those obtained by extrapolating vapor sorption results to infinite dilution of the hydrocarbon, and the X_{12} parameters calculated from χ^* differed by less than 1.2 J.cm⁻³ from those calculated by Flory from integral heats of mixing. The values of χ^* for normal alkanes fell markedly with increase of temperature; hence the κ^* parameters were large, between + 0.6 and + 0.8.

Hammers and de Ligny injected the solutes in the liquid form, and their sample sizes were large, about 1 μ mol, obtaining skewed peaks whose retention volumes decreased with mean flowrate; both deleterious effects disappeared above 100°C. Smaller sample sizes were used by Leung and Eichinger, about 0.05 μ mol in the vapor form, and no dependence of the fully corrected retention volumes from flow rate was detected; however their peaks were skewed, a fact that the authors attributed to instrumental causes. The polymers employed in both chromatographic studies had a viscosity average molecular weight of 4×10^4 ; results could be affected by poor equilibration in the column due to slow diffusion of the vapours in PIB. This by no means explains the reasons why κ^* parameters with opposite sign were obtained by both groups of workers.

The study of PIB + hydrocarbon mixtures by the glc method is taken up again in the present paper with the aim of settling some of the aforementioned discrepancies. A PIB specimen with a molecular weight markedly lower from those employed in former studies was used in order to minimize eventual diffusional effects; sample sizes were the smallest compatible with instrumental noise and dead volumes between column and detector were minimized. Results for twenty-four hydrocarbons, most of them normal and branched alkanes, were obtained at five temperatures within the interval 35 - 65°C. The choice of the solutes was dictated by our interest in studying the effects of branching on the excess properties; measurements were performed at several temperatures in the hope that, in spite of known restrictions of the glc method for the measurement of excess enthalpies, the most important tendencies could be detected.

EXPERIMENTAL SECTION

Materials and columns. PIB was a gift from Polibutenos Argentinos SA; GPC analysis resulted in $\overline{M}_n = 2300$, $\overline{M}_w / \overline{M}_n = 1.45$, and less than 1% by weight of molecules

with $M_n < 500$. The polymer was coated on Chromosorb P AW DMCS 60/80 from a solution in n-hexane (Mallinckrodt p.a.) in a rotary evaporator, under a slow nitrogen flow. Coated support contained 9.954 % by weight of PIB and was packed into 0.43 cm i.d. and 1-2 m in length stainless steel tubes; columns were kept overnight at 90°C with 5-10 ml/min of nitrogen flow rate before using. Hydrocarbons of several origins, more than 99% pure, were used without further purification

Apparatus and procedure. Measurements were performed with a home assembled apparatus, in which column temperature was controlled to better than $\pm 0.05^\circ\text{C}$ by immersion in a water bath. Nitrogen, successively passed through a molecular sieves trap (Davidson 5A), a Brooks 8606 pressure regulator, a Brooks 8743 flow controller and a 2 m x 1/8" o.d. copper tube immersed in the column bath, was used as the carrier gas. Inlet pressures were measured by means of a mercury manometer at a point between the copper coil and a Swagelok 1/4" s.s. "T"; one branch of this last was connected to the column and the remaining branch was provided with a septum through which solute vapors were injected by means of Hamilton microsyringes, applying the headspace sampling technique. Eluates were detected with a Hewlett-Packard 5750 FID and electrometer; signals were fed to a Hewlett-Packard 3396A integrator. Flow rates ranging between 20 and 50 ml/min were measured by means of a water jacketed soap film flowmeter.

Sample sizes were always smaller than 0.05 μmol ; highly symmetrical peaks were obtained, indicating that Henry's law conditions had been attained. Solute vapors and a small methane sample were simultaneously injected; net retention times (in no instance smaller than 2 min) were measured to ± 0.001 min between the times for the solute (t_R) and the methane (t_o) peaks maxima. Retention times for groups of 3-6 solutes were measured at five temperatures equally spaced between 35 and 65°C; measurements at each temperature were made at least in quadruplicate. Measurements for a given solute, repeated after an interval of several days, differed from the original ones in less than 0.5%.

Density of the PIB sample was measured at ten temperatures between 23 and 65°C, by means of a 25 ml pycnometer that had been carefully calibrated through the same temperature interval, and least squares fitted to the equation

$$\rho_2 = 0.9166 - 5.470 \times 10^{-4} t \quad (1)$$

where t is the temperature in degrees Centigrade. Eq. (1) is accurate to $\pm 1.7 \times 10^{-4}$ in the temperature range of the measurements; the fit does not improve by using a second degree polynomial. The thermal expansion coefficient derived from eq.(1) is (in deg^{-1})

$$\alpha_2 = 5.96 \times 10^{-4} + 3.74 \times 10^{-7} t \quad (2)$$

RESULTS

Specific retention volumes, V_g° , were calculated from the relation [23]

$$V_g^\circ = j(F_i / w)(273.15 / T_i)(t_R - t_o)(P_o - p_w) / P_o \quad (3)$$

where j is the James-Martin carrier gas compressibility correction factor, w is the mass of PIB within the column, F_t is the carrier flow rate measured at the temperature T_t and pressure P_o of the flowmeter, and p_w is the water vapor pressure at T_t . Measurements at 50°C for a selected group of solutes were performed at several flow rates between 17 and 55 ml/min; V_g° results, as calculated by eq(3), were coincident within experimental error.

Equation (4) was used to calculate the χ^* parameters [24]

$$\chi^* = \ln(273.15 R v_2^* / p_1^\circ V_g^\circ V_1^*) - 1 + V_1^* / \bar{M}_n v_2^* - p_1^\circ (B_{11} - V_1) / RT + (2B_{13} - \bar{V}_1^\infty) P_o J_3^4 / RT \quad (4)$$

where p_1° , V_1 and \bar{V}_1^∞ are the solute vapor pressure, liquid-state molar volume and partial molar volume at infinite dilution in the polymeric solvent (approximated by V_1 in the present paper), respectively; B_{11} and B_{13} are the second virial coefficients for the solute-solute and solute-nitrogen interactions in the vapor phase, and J_3^4 is a function of the columns inlet and outlet pressures [23].

The polymer characteristic specific volume, v_2^* , and the solute characteristic molar volume, V_1^* , are obtained from pure component volumetric data, as detailed by Flory and collaborators [1,2]. Vapor pressures were calculated by using the equation of Antoine with the coefficients compiled by Dreisbach [25]; for the molar volumes the density data of Orwoll and Flory [7] or those given by Timmermans [26] were used. Second virial coefficients were computed by means of the corresponding states equation of McGlashan and Potter [27], using critical constants given by Kudchadker *et al.* [28] and by Reid *et al.* [29]. The solutes characteristic parameters in terms of the Flory state equation theory (V_1^* , T_1^* and p_1^*), calculated from density, thermal expansion coefficient and thermal pressure coefficient at 25°C, have been tabulated in former publications [30,31]. The polymer characteristic parameters v_2^* and T_2^* were calculated by using equations (1) and (2); our results at two temperatures are compared in Table I with those obtained by Eichinger and Flory [32] for a higher molecular weight specimen. Differences in the properties of both polymers are in the sense that could be qualitatively predicted from their molecular weights; values of v_2^* , however, differ by less than 0.5%.

TABLE I

Equation of State Data and Characteristic Parameters for Two PIB Specimens of Different Molecular Weight

	$\bar{M}_v = 4 \times 10^4$ ^a		$\bar{M}_n = 2300$ ^b	
	25°C	50°C	25°C	50°C
ρ_2 / g.cm ⁻³	0.9169	0.9042	0.9029	0.8893
α_2 / deg ⁻¹	5.55	5.60	6.06	6.15
\tilde{v}_2	1.1488	1.1610	1.1609	1.1752
v_2^* / cm ³ .g ⁻¹	0.9493	0.9525	0.9540	0.9562
T_2^* / K	7577	7726	7134	7250

^a Viscosity average molecular weight, ref. 30.

^b Number average molecular weight, this work.

Values of χ^* at each of the five experimental temperatures were calculated using mean values for not less than two independent measurements of V_g^* . Our estimation of the uncertainty on χ^* is about ± 0.01 , resulting from the quoted dispersion in V_g^* plus contributions of the remaining terms in eq(4). Partial molar residual enthalpies were calculated by means of the equation

$$\bar{H}_1^R = R \{ \partial \chi^* / \partial (1/T) \} \quad (5)$$

assuming \bar{H}_1^R constant within the 35-65°C interval. No trend could be detected for the residuals, this indicating that the error of the model (*i.e.*, assuming a temperature independent excess enthalpy) is overcome by the experimental error. The uncertainties on \bar{H}_1^R , as estimated from the least squares fit, range between ± 100 and ± 250 J/mol. Therefore, only a semiquantitative significance can be assigned to the values of the reduced partial molar residual enthalpy and entropy, calculated by means of the relations $\kappa^* = \bar{H}_1^R / RT$ and $\bar{S}_1^R / R = \kappa^* - \chi^*$, respectively. Results for χ^* , κ^* and \bar{S}_1^R / R at 50°C have been gathered in Table II. All the alkanes' κ^* values are positive, in coincidence with the findings of Leug and Eichinger; our results, however, are considerably smaller than theirs.

DISCUSSION

According to the Flory state equation theory the solute residual chemical potential and partial molar enthalpy at infinite dilution in the polymer are given by the following equations:

$$\chi^* RT = p_1^* V_1^* \{ 3 \bar{T}_1 \ln[(\tilde{v}_1^{1/3} - 1) / (\tilde{v}_2^{1/3} - 1)] + \tilde{v}_1^{-1} - \tilde{v}_2^{-1} \} + X_{12} V_1^* / \tilde{v}_2 \quad (6)$$

$$\kappa^* RT = p_1^* V_1^* [(\alpha_2 T / \tilde{v}_2)(T_2^* / T_1^* - 1) + \tilde{v}_1^{-1} - \tilde{v}_2^{-1}] + X_{12} V_1^* (1 + \alpha_2 T) / \tilde{v}_2 \quad (7)$$

where reduced volumes and temperatures are defined by $\tilde{v}_i = v_i / v_i^*$ and $\bar{T}_i = T / T_i^*$, respectively. The first term in equations (6) and (7) represents the contribution from free volume effects. In Flory's original model the second term in each of these equations was identified with contact interaction contributions only, but in Patterson's scheme they could equally well represent contributions from order, or from steric hindrance, or eventually from a combination of the three effects. Furthermore, Patterson and collaborators have denied any importance to interactional contributions in alkane mixtures; as a matter of fact much of the work done in this area during the last twenty years was devoted to the identification of the origins of these contributions. Such an assignment is not a direct or simple matter in the present circumstances, as we pass to discuss.

TABLE II

Reduced Residual Chemical Potentials (χ^*), Reduced Partial Molar Residual Enthalpies (κ^*) and Reduced Partial Molar Residual Entropies (\bar{S}_1^R / R) for Hydrocarbons at Infinite Dilution in Polyisobutylene at 50°C.

SOLUTE	χ^*	κ^*	\bar{S}_1^R / R
n-Pentane	0.707	0.28	- 0.43
n-Hexane	0.623	0.17	- 0.50
2-Methylpentane	0.648	0.32	- 0.33
3-Methylpentane	0.605	0.32	- 0.29
2,2-Dimethylbutane	0.678	0.56	- 0.12
2,3-Dimethylbutane	0.606	0.49	- 0.12
n-Heptane	0.570	0.13	- 0.44
2-Methylhexane	0.589	0.28	- 0.31
3-Methylhexane	0.558	0.30	- 0.26
2,2-Dimethylpentane	0.625	0.57	- 0.05
2,3-Dimethylpentane	0.504	0.45	- 0.06
2,4-Dimethylpentane	0.629	0.38	- 0.25
n-Octane	0.518	0.11	- 0.41
2-Methylheptane	0.535	0.25	- 0.29
4-Methylheptane	0.510	0.26	- 0.25
2,2-Dimethylhexane	0.570	0.40	- 0.17
2,5-Dimethylhexane	0.572	0.35	- 0.22
2,2,4-Trimethylpentane	0.563	0.52	- 0.04
2,3,4-Trimethylpentane	0.451	0.49	- 0.04
n-Nonane	0.487	0.13	- 0.36
Cyclohexane	0.478	0.55	0.08
Benzene	0.818	0.95	0.14
Toluene	0.665	0.92	0.25
Ethylbenzene	0.641	0.87	0.23

In order to validate our results it is necessary to mention that our χ^* results are smaller than those obtained by Leung and Eichinger [21,22]; differences drop from 0.08-0.15 at 25°C (extrapolation of our data) to 0.04-0.10 at 65°C. These discrepancies have their origin in the different volumetric behavior displayed by the polymer employed by Leung and Eichinger and that used in the present paper; when the free volume contributions are deducted from the experimental χ^* by using eq(6) and the data in **Table I**, coincident residual contributions are obtained from both sets of results.

Values of X_{12} calculated from χ^* (eq(6)) decrease linearly with temperature (0.01-0.05 J.cm⁻³.K⁻¹ for alkanes and 0.02-0.08 J.cm⁻³.K⁻¹ for aromatics and cyclohexane). On the other side X_{12} parameters obtained from κ^* by means of eq(7) are between two and four times larger than those obtained from χ^* . These are very large differences, and are displayed by all the systems studied in the present work; therefore they cannot be attributed to the uncertainties inherent in the calculation of the excess enthalpies from experimental activity coefficients. This is the type of behavior that could be expected in case orientational order exists in PIB, an hypothesis difficult to sustain on account of the numerous methyl side groups in the polymer molecule. However similar behavior was detected in chromatographic studies involving hydrocarbons and stationary phases for which it would be rather bold to assume order, as tetra-n-amyltin [31]. It may be presumed that some degree of ordering could exist in almost any liquid suitable to be employed as stationary phase in glc, and that the effects of this order should be specially noticeable under the conditions of extremely low concentration prevailing in chromatographic measurements; the first molecules to get into solution shall find the stationary phase in its more ordered state, promoting the largest order perturbations. The solid support surface, on the other side, may well induce some type of ordering of the stationary phase molecules.

Flory *et al.* [18] found that a smooth curve was obtained when X_{12} values for PIB + normal alkane systems (calculated from enthalpies of mixing) were plotted against the reciprocal of the number of carbon atoms in the alkane chain. This was attributed by the authors to contact interactions and, since X_{12} increases with the proportion of methyl groups in the alkane molecule, important chemical differences have to be admitted between this last type of group and the highly crowded methyl groups that constitute, almost completely, the surface of the polymer molecule. Delmas [33] suggested that this effect could have its origin in an overestimation of the free volume term by the Flory theory for systems with large differences in expansion coefficient. The value of α_2 for our low molecular weight PIB is about 10% higher than those of polymers used by former authors, and it was seemingly interesting to check whether the effect persisted or not.

Following this line of argument X_{12} values calculated from κ^* have been plotted in **Figure 1a** against the fraction of methyl type surface in the alkane molecules, θ_{e1} , calculated as the ratio of the number of hydrogen atoms on methyl groups to the total number of hydrogens in the molecule. There is a strong correlation between both variables; a least squares analysis performed under the assumption of a first order linear relationship results in a correlation coefficient of 0.83 and an ordinate that does not differ significantly from zero. The mean of the residuals is 2.3 J.cm⁻³, in coincidence with our estimation of the uncertainty on X_{12} parameters calculated from κ^* . On the other side no correlation can be detected between values of X_{12} calculated from χ^* at 50°C and θ_{e1} , as shown in **Figure 1b**; individual points are scattered about a mean of 4.6 J.cm⁻³, with a mean deviation smaller than 1 J.cm⁻³. Flory [2,7] suggested that contact interaction contributions to the excess properties were not only of enthalpic nature; it may be expected that entropy shall also be affected. To account for this effect he substituted X_{12} in eq(6) for $X_{12}^H - Q_{12}T\bar{v}_2$, where X_{12}^H and Q_{12} are temperature and volume independent terms, associated with enthalpic and entropic effects of contact interactions; differentiation of so modified eq (6) results in eq (7), but with X_{12} replaced by X_{12}^H . The results displayed in **Figures 1a and 1b** suggest the existence of positive contributions from contact interaction, of similar importance both in H^E and in TSE , that

to leave only a small contribution to G^E . In our opinion ordering of the stationary phase by the solid support, although not totally rejectable, cannot be responsible of so notorious effects; a silanized solid support was employed and, according with its specific surface area (about $4 \text{ m}^2 \cdot \text{g}^{-1}$) and the stationary phase concentration, the mean thickness of the PIB film was about 300 Å.

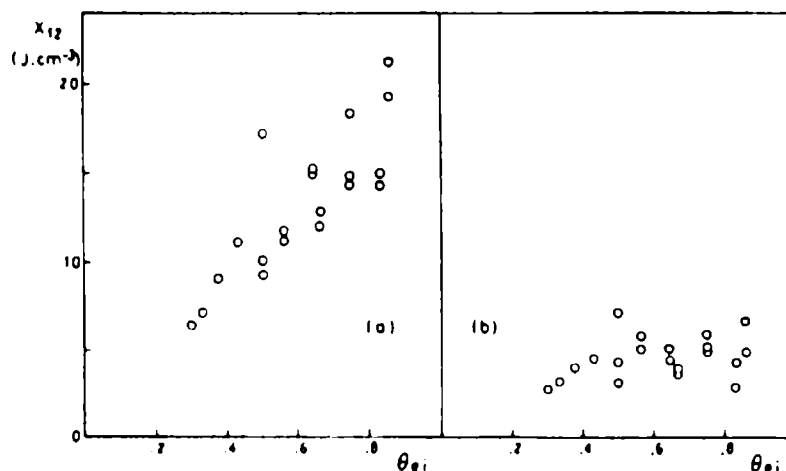


Fig. 1.- Binary Flory interaction parameters (X_{12} , $\text{J} \cdot \text{cm}^{-3}$) for PIB + alkane mixtures against the fraction of hydrogen atoms on methyl groups (θ_{e1}). (a) X_{12} calculated from κ^*
(b) X_{12} calculated from χ^*

χ^* values for alkanes at 50°C are plotted against molar volumes in **Figure 2**. First to be noted is the smooth downfall of the normal alkane points; second, straight lines can be drawn through points corresponding to isomeric solutes. The slopes of those drawn in the figure for hexanes, heptanes and octanes are coincident and the correlation coefficients are higher than 0.98 in the three cases. These trends could be associated with steric hindrance effects; however there are several reasons to disregard that possibility. First, κ^* values do not change regularly with molar volumes within a given isomers group. Second, since PIB segments are highly sterically hindered, the larger effects (negative contributions to H^E , S^E and G^E) should be observed on mixing with isomers of larger molar volume. Finally a plot of free volume contributions to χ^* against V_1 reproduces the principal characteristics of **Figure 2**, although a larger scatter of the points is observed; the quality of thermal pressure coefficient values of the branched alkanes, taken from different sources, can be the cause of this poorer correlation.

Solutions of aromatic hydrocarbons are markedly more endothermic than those of the alkanes; partial molar residual entropies, however, are positive for aromatics and negative for the alkanes. Since free volume contributions do not justify these differences, they must be attributed to their chemical dissimilarity. Interactional contributions to the reduced chemical potential, reduced partial molar enthalpy and entropy for n-hexane, cyclohexane and benzene have been gathered in **Table III**; they were calculated using X_{12} parameters obtained from residual enthalpies in eq (6) and (7). These results, that must be considered cautiously on account of their very indirect origin, indicate important differences between the three solutes. According with these numbers cyclohexane molecules are more strongly repelled by the PIB segments and are freer in their motions than those of n-hexane. PIB repulsion for benzene is yet stronger than that for cyclohexane, but no difference exists between the interactional partial molar entropy of both solutes.

TABLE III

Interactional Contributions to the Reduced Chemical Potential (χ_{int}^*), Reduced Partial Molar Residual Enthalpy (κ_{int}^*) and Reduced Partial Molar Residual Entropy (\bar{S}_1^R / R_{int}).

Solute	χ_{int}^*	κ_{int}^*	\bar{S}_1^R / R_{int}
n-Hexane	0.14	0.4	0.3
Cyclohexane	0.13	0.7	0.6
Benzene	0.47	1.1	0.7

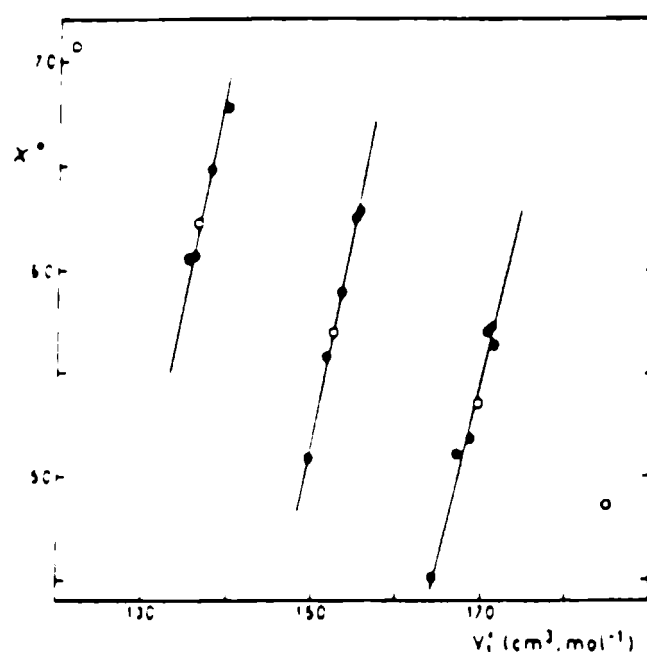


Fig. 2.- Infinite dilution residual chemical potentials of alkanes at 50°C (χ^*) against their molar volumes ($V_{1,}$). (o) Normal alkanes. (●) Branched alkanes.

ACKNOWLEDGEMENT

This work was sponsored by CONICET (Consejo Nacional de Investigaciones Científicas y Técnicas de la República Argentina) and by CICIPBA (Comisión de Investigaciones Científicas de la Provincia de Buenos Aires).

REFERENCES

- [1] Flory P. J., Orwoll R. A. and Vrij, A.- *J Am. Chem. Soc.*, **86**, 3507, 3515 (1964).
- [2] Eichinger B. E. and Flory P. J.- *Trans. Faraday. Soc.*, **64**, 2035 (1968).
- [3] Patterson D.- *J. Solution Chem*, **23**, 105 (1994).

- [4] Flory P. J.- **J. Chem. Phys.**, **10**, 51 (1942); *ibid*, **12**, 425 (1944).
- [5] Huggins M. L.- **Ann. N. Y. Acad. Sci**, **43**, 9 (1942).
- [6] Bhattacharyya S. N., Costas M. and Patterson D.- **Fluid Phase Equil**, **20**, 27 (1985).
- [7] Orwoll R. A. and Flory P. J.- **J. Am. Chem. Soc.**, **89**, 6814, 6822 (1967).
- [8] Bothorel P., Clement C. and Maraval P.- **Compt. Rend**, **264**, 658 (1967).
- [9] Quinones H. and Bothorel P.- **Compt. Rend.**, **277**, 133 (1973).
- [10] Lam V. T., Picker P., Patterson D. and Tancrede P.- **J. Chem. Soc. Faraday II**, **70**, 1465 (1974).
- [11] Tancrede P., Patterson D. and Lam V. T.- **J. Chem. Soc. Faraday II**, **71**, 985 (1975).
- [12] Barbe M. and Patterson D.- **J. Phys. Chem**, **82**, 40 (1978).
- [13] Tancrede P., Bothorel P., de St. Romain P. and Patterson D.- **J. Chem. Soc. Faraday II**, **73**, 15 (1977)
- [14] de St. Romain P., Van H. T. and Patterson D.- **J. Chem. Soc. Faraday I**, **75**, 1700 (1979).
- [15] Barbe M. and Patterson D.- **J. Solution Chem.**, **9**, 753 (1980).
- [16] Delmas G., Patterson D. and Somcynsky T.- **J. Polym. Sci.**, **57**, 79 (1962).
- [17] Eichinger B. E. and Flory P. J.- **Trans. Faraday Soc.**, **64**, 2053, 2061, 2066 (1968).
- [18] Flory P. J., Ellenson J. L. and Eichinger, B. E.- **Macromolecules**, **1**, 279 (1968).
- [19] Hammers W. E. and de Ligny, C. L.- **Rec. Trav. Chim.**, **90**, 912 (1971).
- [20] Gaecklé D., Kao W. P., Patterson D. and Rinfret M.- **J. Chem. Soc. Faraday I**, **69**, 1849 (1973).
- [21] Leung Y. K. and Eichinger B. E.- **J. Phys. Chem.**, **78**, 60 (1974).
- [22] Leung Y. K. and Eichinger B. E.- **Macromolecules**, **7**, 685 (1974).
- [23] Conder J.R. and Young C.L.- *Physicochemical Measurements by Gas-Liquid Chromatography*, Wiley, New York (1979).
- [24] Patterson D., Tewari Y. B., Schreiber H. P. and Guillet.- **Macromolecules**, **4**, 356 (1971).

- [25] Dreisbach R. R.- *Physical Properties of Chemical Compounds. Advances in Chemistry Series*, 15 (1955); 22 (1959); 29 (1961), American Chemical Society, Washington, DC.
- [26] Timmermans J.- *Physical Constants of Pure Organic Compounds*; Vol. I (1950); Vol. II (1965), Elsevier, New York.
- [27] McGlashan M. L. and Potter J. B.- *Proc. Roy. Soc. A*, 267, 478 (1967).
- [28] Kudchadker A. P., Alani G. H. and Zwolinski J. B.- *Chem. Rev.*, 68, 659 (1968).
- [29] Reid R. C., Prausnitz J. M. and Poling, B. E.- *The Properties of Gases and Liquids*; McGraw-Hill, Singapore, (1988).
- [30] Castells R. C. and Castells C.B.- *J. Solution Chem.*, 21, 129 (1992).
- [31] Castells R. C. and Castells C. B.- *J. Solution Chem.*, 24, 285 (1995).
- [32] Eichinger B. E. and Flory P. J.- *Macromolecules*, 1, 285 (1968).
- [33] Phuong-Nguyen H. and Delmas G.- *Macromolecules*, 12, 740, 746 (1979).

REVISIÓN SOBRE LOS ASPECTOS BIOLÓGICOS DEL "FOULING"

BIOFOULING: AN OVERVIEW

M.C. Pérez y M.E. Stupak

SUMMARY

The development of fouling communities is object of world-wide research since the last half of the century. Biological fouling of vessels has been known since the beginning of man's maritime activities. Biological corrosion became a problem of concern when steel replaced wood as the primary ship construction material.

The purpose of the present paper is to present a guide about biological aspects of fouling for the non-specialist (the non-biologist). The scope of this guide is to give some historical references, development sequences of the fouling community, abiotic factors influence, fouling problems, study methodology and enough elements to recognize the most important taxa with some pictures. Also, in relation to freshwater fouling, a basic approach and comments about exotic species introduction by ships are presented. A glossary and a broad bibliography on this subject are included.

Keywords: biofouling, microfouling, macrofouling, raft trials, laboratory trials

INTRODUCCION

El presente trabajo ofrece una síntesis sobre la temática del "fouling", enfocada desde el punto de vista biológico, con la finalidad de que pueda servir como guía para quienes se inician en el tema o para quienes dirigen sus investigaciones exclusivamente hacia la aplicación de sistemas de control.

El origen de la vida, claramente explicado por Darwin, fue un complejo desarrollo que comenzó con organismos unicelulares. Los océanos fueron una parte intrínseca de esta evolución, y están ahora habitados por formas que van desde pequeñas bacterias hasta enormes ballenas. Algunas de las numerosas especies que pueblan los océanos nadan o son llevadas por las corrientes, pero muchas tienen que encontrar una superficie dura para fijarse con el fin de cumplir sus ciclos de vida. La escasez de sustratos duros naturales en el medio marino trae como consecuencia que cada espacio disponible sea disputado y cubierto por una variedad de cirripedios, algas, bacterias, etc. Los cascos de los barcos así como otras estructuras sumergidas, están también expuestos a esta fijación potencial de plantas y animales, comunmente llamada "fouling" [1].

El término "**fouling**" puede ser usado en un sentido amplio incluyendo la fijación y crecimiento de micro y macroorganismos sobre cualquier sustrato sumergido natural o construido por el hombre [2].

El eje del presente trabajo se basa fundamentalmente en los aspectos biológicos del "fouling" marino, presentándose algunas referencias históricas, las secuencias de su formación, la influencia de los factores abióticos, los problemas que acarrea, la metodología de estudio y las características generales de los principales organismos incrustantes, incluyendo figuras para facilitar la lectura y reconocimiento del material. También se hace una breve referencia sobre el "fouling" de agua dulce a fin de obtener una noción sobre los problemas que ocasiona principalmente por la introducción de especies exóticas. Por último se presenta un glosario y la bibliografía consultada que permitirá, a quien lo desee, ahondar sobre los temas tratados.

BREVE RESEÑA HISTORICA [3-11]

"...Viendo Dios que la tierra estaba corrompida, dijo a Noé: ...Haz para tí un arca de madera de gopher bien acepillada; en el arca dispondrás de celditas y la calafatearás por dentro y por fuera..." (Cap. VI del Génesis).

Desde tiempos muy remotos el hombre construyó embarcaciones y siempre tuvo la necesidad de proteger fundamentalmente la parte sumergida.

A través de los poemas de Homero se tiene noticia de las "navis lunga" (galeras primitivas) de los micenos (1300-1100 a.C.), quienes con el fin de conferir estanqueidad al casco y protegerlo de las "bromas" (moluscos perforadores de madera) aplicaban una pintura a base de pez (naves negras) o de minio (naves rojas).

Aristóteles (siglo IV a.C.) hizo referencia sobre el efecto "frenador de barcos" causado por las rémoras, peces del género *Echeneis* que tienen la aleta dorsal modificada en forma de ventosa por medio de la cual se adhieren.

Hacia el año 412 a.C. se comenzaron a usar mezclas con alquitrán, azufre y arsénico para proteger los barcos de madera del ataque de gusanos tubícolas. En virtud de los descubrimientos realizados al comienzo de este siglo, pudo establecerse que hacia el 480 a.C. se utilizaban bronce y láminas de plomo para proteger los cascos de los barcos de guerra.

A fines del siglo I Plutarco mencionó, además de las rémoras, la presencia de otros organismos, enfatizando sobre las ventajas de raspar las algas y el limo adherido a los cascos de los barcos para que pudieran avanzar más fácilmente en el agua.

Las evidencias arqueológicas indican que los normandos y los vikingos (siglos VII y VIII) no protegían sus embarcaciones; sus barcos eran livianos y se retiraban del agua cuando no se los utilizaban.

En la Edad Antigua los griegos y romanos utilizaron con éxito placas metálicas, mientras que en la Edad Media era poco frecuente el uso de metales para recubrir barcos.

Los cascos de madera de las carabelas utilizadas por Colón estaban protegidos con sebo y alquitrán y las embarcaciones de Vasco da Gama con carbón; siglos después, en Inglaterra se siguió utilizando este método.

En 1559 Laevinus Lemnius hizo también referencia al efecto frenador producido por las rémoras y los moluscos y a la necesidad de eliminarlos por medio de cepillos, debiendo cubrirse los barcos con sebo para que navegaran más rápidamente.

La primera patente “antifouling” fue concedida a William Beale en 1625 en Inglaterra; la pintura para evitar la fijación de los gusanos tubícolas, estaba basada en polvo de hierro, cemento y probablemente compuestos de cobre.

En el siglo XVIII se otorgaron licencias para implementar métodos de protección con recubrimientos metálicos. Comenzó a utilizarse estaño, al principio en forma de polvo; simultáneamente, se obtuvieron resultados exitosos con recubrimientos de cobre en gran cantidad de embarcaciones inglesas y americanas. Una de las primeras embarcaciones con el casco recubierto con lámina de cobre fue la corbeta inglesa Dolphin que, capitaneada por John Byron, recorrió las costas argentinas a fines del siglo XVIII.

Los primeros antecedentes sobre barcos de metal están referidos a un buque de pasajeros construido en 1777 en Yorkshire (Inglaterra) y al Aaron Manby, barco a vapor para el transporte de pasajeros entre Inglaterra y Francia, botado en 1820.

Es muy importante destacar el viaje del capitán FitzRoy a bordo del Beagle que, cumpliendo una misión del Almirantazgo Británico (1831-1835), llegó a la parte más austral de América del Sur con el fin de perfeccionar la cartografía de dicha zona. En Islas Malvinas, con el fin de llevar a cabo su objetivo, compró una goleta ballenera que fue enviada al Río de la Plata donde se aplicó al casco una lámina de cobre. El fondo revestido de cobre no permitía la fijación de lapas y un velero equipado de ese modo podía navegar con mucha rapidez; ese fue el secreto del éxito de la Marina Real durante muchos años. Este viaje fue trascendental para las ciencias naturales, ya que el naturalista que se encontraba a bordo del Beagle era nada menos que Charles Darwin, quien a través de sus continuas observaciones y descripciones de nuevas especies planteó la teoría de la evolución que revolucionó la biología. En 1851 y 1854 Darwin publicó sus monografías sobre cirripedios en donde detalla los sustratos naturales y/o artificiales sobre los cuales se fijan. Por ej. cita a *Balanus improvisus* adheridos a la lámina de cobre del casco del Beagle varado en las costas de Santa Cruz (sur de la Patagonia); *Balanus amphitrite* sobre cañas, maderas flotantes, guijarros, valvas de moluscos. Menciona además que las especies más ampliamente distribuidas son aquéllas que se adhieren con mayor facilidad a los cascos de los barcos.

Paralelamente, en Europa, las reservas de madera se iban agotando por lo que surgió la necesidad de buscar nuevos materiales para la construcción de barcos; es así que comienza a utilizarse el hierro que podía obtenerse a través de la industria y que resultaba más resistente que la madera. En 1849 causó sensación la presencia en el Riachuelo del barco La Merced, primer buque a vapor con casco de hierro de la Armada Argentina, de fabricación inglesa.

En 1851, en Alemania, los barcos de hierro comenzaron a protegerse con barnices oleosos, pero el método resultaba muy caro debido a los largos períodos de secado en dique. Posteriormente, el uso de sistemas de pinturas solubles en benceno posibilitó una combinación

más efectiva y barata de resinas, cuya principal ventaja fue su fácil aplicación tanto en climas cálidos como templados, manteniéndose su utilización hasta el presente.

En 1860 fue construido el Warrior (del Almirantazgo Británico), primer buque de guerra del mundo realizado totalmente en hierro. En el mismo año el capitán Rahtjen desarrolló una pintura “antifouling” basada en una solución de goma laca alcohólica cuyas sustancias activas eran arsénico y óxido de mercurio. La formulación dio excelentes resultados pero acarreó muchos problemas económicos y técnicos.

Entre 1870 y 1880 comenzó a sustituirse el hierro por el acero por ser de producción más fácil, económica y por sus elevadas características de resistencia, que a su vez permitió aligerar la estructura de los cascos.

A fines del siglo pasado (1898) fue construida la fragata Sarmiento en Birkenhead (Inglaterra), con el casco de acero Siemens recubierto, hasta la línea de flotación, con madera y ésta a su vez con lámina de cobre.

Alrededor de 1920 las investigaciones sobre pinturas “antifouling” comenzaron a complementarse con investigaciones biológicas; los avances en zoología y botánica proveyeron descripciones de la forma, ciclos de vida y comportamiento de muchos grupos del “fouling”.

Investigadores del CIDEPINT a partir del año 1964 y hasta la actualidad han realizado estudios de las comunidades incrustantes y de los sistemas de control, en el área portuaria de Mar del Plata y de Puerto Belgrano. Con el transcurso del tiempo se obtuvieron resultados satisfactorios de control del “fouling” con pinturas formuladas empleando óxido cuproso como tóxico principal. También han sido utilizados óxido de cinc, arseniatos, compuestos de tributil y trifenil estaño y diferentes extendedores [12]. Algunas de estas sustancias están hoy excluidas desde el punto de vista ecológico.

Las pinturas "antifouling" han sido por muchos años la mejor vía de protección de los barcos, habiéndose logrado hasta el presente un caudal de información considerable sobre su comportamiento a escala de planta piloto, en balsas experimentales y en servicio. Hay además otros métodos alternativos para controlar las incrustaciones, como por ejemplo ondas de sonido de baja frecuencia, sonidos de alta intensidad y superficies de baja energía [13-16]. Cabe mencionar también la posibilidad del control biológico; por ejemplo en experiencias llevadas a cabo en Israel, fueron utilizadas lapas para controlar el “biofouling” marino dominado por *Balanus amphitrite* [17-19].

SECUENCIAS DE EVENTOS EN LA FORMACION DEL “BIOFOULING” [1, 20-21]

El proceso del "fouling" biológico comienza en el instante en que un sustrato duro se sumerge en un medio líquido con organismos. La secuencia de eventos continúa hasta un nivel de desarrollo de la comunidad incrustante que eventualmente puede impedir el movimiento de los barcos, desestabilizar estructuras oceánicas sumergidas, aminorar el intercambio de calor en torres de enfriamiento, restringir el pasaje de sangre en circuitos naturales o artificiales y promover caries dentales. Esta importante secuencia sigue un orden universal, inmediatamente

del contacto inicial, una superficie es modificada por adsorción de biopolímeros y luego ocurre la fijación y proliferación de células pioneras. En el caso de las incrustaciones biológicas sobre sustratos sumergidos en el mar esa fijación inicial es seguida por algas e invertebrados. Lo expresado se indica en la **figura 1**.

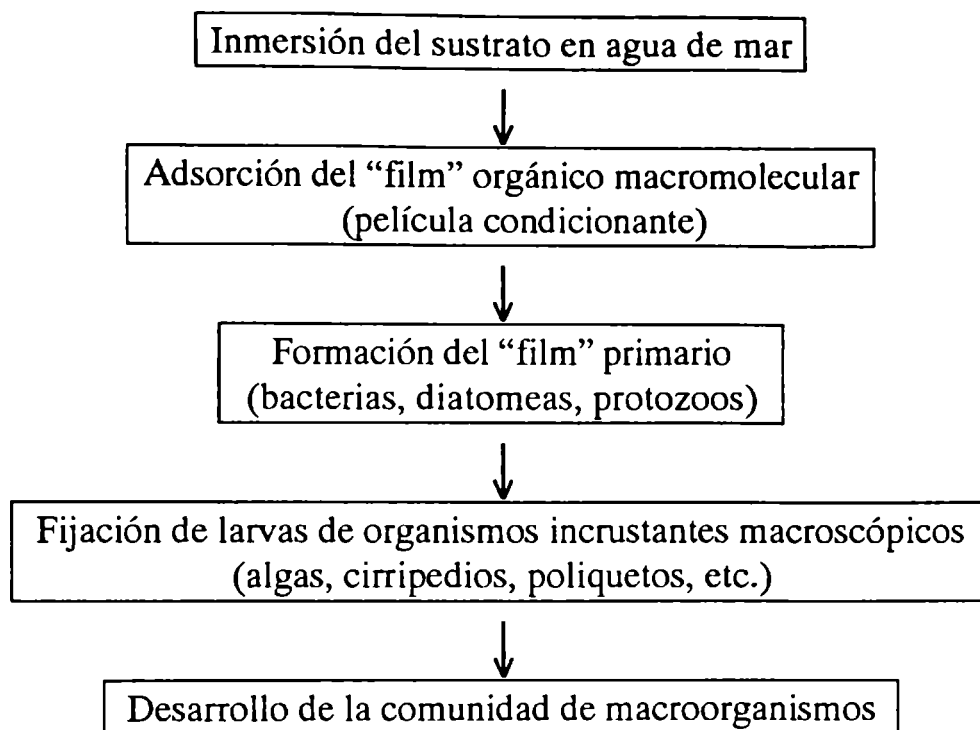


Fig. 1.- Secuencia de la fijación de las incrustaciones biológicas en un sustrato sumergido en el mar.

El carácter de la comunidad resultante es determinado por la naturaleza del sustrato, la disponibilidad y diversidad de los colonizadores, la eficiencia de su fijación al sustrato y los eventos bióticos/abióticos (a menudo directamente el hombre) que ocurren durante y después de la fijación.

El problema del "biofouling" varía de localidad en localidad, por eso es necesario el conocimiento de la biología de sus organismos para aplicar medidas más efectivas de prevención y control. La estructura y composición del "fouling" muestra amplias variaciones temporales y regionales, las que son en general gobernadas por las condiciones hidrológicas y geográficas.

INFLUENCIA DE LOS FACTORES ABIOTICOS [22-24]

Es importante hacer una mención de la influencia de los factores abióticos sobre los organismos. Parámetros tales como temperatura, salinidad, pH, oxígeno disuelto, luz y tipo de sustrato juegan un importante rol en la determinación de la composición, desarrollo y sucesión de la comunidad. Estos factores también tienen efecto sobre el funcionamiento de las pinturas "antifouling".

La **temperatura** del agua ejerce un gran control sobre la distribución y funciones vitales de los organismos (maduración sexual, crecimiento, desarrollo). Con respecto a las

pinturas antiincrustantes un aumento de temperatura disminuye la vida útil de las mismas por el incremento de la disolución del tóxico y del ligante.

La **salinidad** afecta los fenómenos de ósmosis de los organismos. La mayor parte de los especies marinas han desarrollado estrategias adaptativas para mantenerse en equilibrio osmótico con el medio que los rodea. Además, los cambios en la salinidad varían la densidad específica del agua influyendo en la flotabilidad de los organismos. En general, la salinidad del agua de mar oscila entre 34-36 ‰, aunque en las zonas costeras pueden ocurrir variaciones debidas a los aportes de agua dulce, desagües pluviales, evaporación, etc. En lo referente a las pinturas “antifouling” la concentración de cloruro de sodio afecta la solubilidad de la colofonia (al aumentar la salinidad aumenta su solubilidad) y por consiguiente la lixiviación del tóxico.

El **pH** normal del agua de mar es de alrededor de 8,2. Las variaciones influyen sobre la actividad enzimática y las reacciones fisiológicas de los organismos. El pH afecta la solubilidad de la resina colofonia de las pinturas antiincrustantes; a mayores valores de pH mayor solubilidad de la colofonia y menor del óxido cuproso.

El **oxígeno** es un elemento de vital importancia para los organismos ya que es fundamental para llevar a cabo los procesos de intercambio gaseoso, a excepción de las bacterias anaeróbicas. Los aportes principales de oxígeno al agua son debidos a la actividad fotosintética de las algas y al intercambio con el medio aéreo por agitación y turbulencia. La cantidad de oxígeno disuelto puede variar cuando hay polución en áreas relativamente cerradas (disminuyendo la concentración) o en zonas litorales con gran abundancia de algas (aumentando la concentración). En cuanto a las pinturas “antifouling”, el oxígeno no afecta la disolución de la colofonia luego de la inmersión del sustrato pintado.

La **luz** es uno de los factores más importantes que determina la distribución vertical de los organismos. Las algas están confinadas a la zona eufótica para disponer de energía y gran parte de los animales se localizan en esta zona o cercanos a ella dado que obtienen su alimento directa o indirectamente de los vegetales. La variaciones lumínicas tanto diarias como estacionales provocan migraciones del fito y zooplancton, movilizándolo a su vez a los organismos que los secundan en la trama trófica. La luz no causa efectos directos sobre el funcionamiento de las pinturas antiincrustantes.

El **sustrato** es un factor primordial para tener en cuenta dado que los organismos incrustantes necesitan una superficie donde desarrollarse; las características de dureza, textura, composición química, color e inclinación condicionan el asentamiento de las distintas especies. Es necesario reiterar la importancia de las implicancias económicas que trae aparejado el biodeterioro sobre los sustratos artificiales sumergidos. En lo referente a las formulaciones “antifouling”, se debe tener en cuenta la preparación del sustrato a proteger (acero, aluminio, madera, fibra de vidrio, etc.) a fin de lograr una adecuada adhesión del sistema de pinturas.

Los factores abióticos mencionados no actúan en forma independiente, sino que están estrechamente interrelacionados, por ej. la fotosíntesis producida por una densa vegetación algal actúa sobre los niveles de oxígeno así como los de dióxido de carbono, afectando al pH del agua; cuando disminuye el oxígeno, aumenta el dióxido de carbono y desciende el pH, lo que provoca una rápida descomposición bacteriana. La temperatura afecta la solubilidad del oxígeno siendo su concentración mayor en aguas más frías; por otra parte altas temperaturas favorecen la evaporación modificando en consecuencia la salinidad del agua.

ACCION DEL "FOULING" SOBRE LOS OBJETOS SUMERGIDOS [25-30]

Actividad de los organismos	Efectos de la fijación
* Fijación en cascos de embarcaciones, particularmente en estadias en puertos	<ul style="list-style-type: none"> * Reducción de la velocidad de desplazamiento debido a la rugosidad que se genera * Incremento en el consumo de combustible * Deterioro de la película protectora * Inicio de procesos de corrosión * Mayor frecuencia de entradas a dique seco con consecuencias económicas: lucro cesante, alquiler de dique, limpieza del caso, reparación y/o reposición de partes deterioradas, pintura y mano de obra
* Fijación en equipos de sonar	<ul style="list-style-type: none"> * Reducción de la sensibilidad y transmisión del sonido * Disminución de la efectividad del sonar al aumentar los ruidos por cavitación. Las medidas de emisión y recepción de señales con transductores sumergidos "incrustados" muestran una reducción de sensibilidad axial entre 0 y 10 dB en el intervalo de frecuencias de 1 a 20 KHz
* Fijación en sistemas de cañerías en plantas desalinizadoras; sistemas de refrigeración en plantas de energía eléctrica, etc.	<ul style="list-style-type: none"> * Reducción del diámetro interior de cañerías y por ende del flujo de agua; los organismos que se despegan (caparazones de mejillones) bloquean el flujo de agua en válvulas y en sectores donde la cañería se estrecha
* Fijación externa y/o en sistemas de filtrado en estructuras "off-shore" y en sistemas OTEC (Ocean Thermal Energy Conversion)	<ul style="list-style-type: none"> * El peso de los organismos del "fouling" puede afectar la flotabilidad y estabilidad de las estructuras, acelerar los procesos de corrosión, etc. * Obstrucción de los sistemas de enfriamiento y/o filtrado con la consecuente interrupción del funcionamiento de los equipos
* Superficies metálicas	<ul style="list-style-type: none"> * Debajo de caparazones de cirripedios muertos se produce corrosión por picado debido a la formación de celdas de concentración de oxígeno. Otras condiciones favorables para la corrosión son las generadas por productos metabólicos, particularmente óxidos y sulfuros. Las bacterias sulfato reductoras promueven la corrosión anaeróbica.
* Recubrimientos protectores	<ul style="list-style-type: none"> * El "fouling" daña los recubrimientos en varias formas; por ej. cuando por cualquier razón, el caparazón de un cirripedio pierde su adherencia al recubrimiento, la pintura base también puede reducir su adherencia al sustrato debilitada por la acción de los productos metabólicos en el lugar de fijación; los filosos bordes de los caparazones penetran en el recubrimiento a medida que los animales crecen exponiendo, eventualmente, la superficie metálica base (ver pág. 125). Las pinturas son deterioradas también por las bacterias del agua de mar que atacan a componentes del ligante.
* Superficies plásticas y de vidrio	<ul style="list-style-type: none"> * Ventanas de estructuras sumergidas y lentes de cámaras comienzan a bloquearse y requieren frecuente limpieza.

METODOLOGIA PARA EL ESTUDIO DEL “FOULING”

Ensayos en balsa experimental

Para realizar los estudios del “fouling” tanto desde el punto de vista biológico como de su control, es necesario contar con sustratos artificiales adecuadamente preparados (superficies inertes y con rugosidad suficiente para facilitar la fijación, superficies pintadas con formulaciones conocidas, etc.), realizar una adecuada programación para el desarrollo de las tareas y posibilidades de realizar inspecciones periódicas. Las balsas experimentales han sido diseñadas fundamentalmente con el fin de llevar a cabo las tareas de investigación en puertos o en aquellos lugares donde el “biofouling” es muy abundante (**Fig. 2**). Los períodos de estudio no deben ser inferiores a un año para poder tener un registro lo más completo posible de la comunidad incrustante y de las secuencias estacionales que puedan ocurrir. También son necesarios los ensayos a largo plazo (de dos o más años de muestreos) pues representan una herramienta eficaz para interpretar los resultados de los ensayos a corto plazo, ubicarlos dentro de un contexto y comprender la dinámica y estructura de la comunidad [31-33].

Los paneles inertes se colocan en bastidores y los mismos se disponen en las balsas experimentales en series de cuatro, se sumergen a distintas profundidades, en general desde la superficie hasta dos metros. Se llaman paneles de “línea de flotación” a los más superficiales. Esta denominación no es la más correcta dado que la balsa acompaña los movimientos de las mareas y no queda una franja que, periódicamente, se sumerge y expone al aire, tal como ocurre en los barcos durante sus operaciones de carga y descarga. Por otra parte, los tres paneles más profundos se denominan “paneles de carena”.

En general se utilizan paneles de acrílico arenados que se emplean como testigos no tóxicos para la recolección de las especies incrustantes. Se estiman la abundancia y la distribución de los organismos en función de la profundidad. Una serie de paneles se reemplaza todos los meses (paneles mensuales o de reclutamiento), con los datos obtenidos mes a mes se determinan los ciclos de fijación y tendencias de reclutamiento.

Para realizar el estudio del desarrollo de la comunidad se sumergen simultáneamente tantas series de paneles como meses dure el ensayo (por ej. para un estudio anual se sumergen doce series de paneles). Todos los meses se retira una serie de estos paneles llamados acumulativos y con los datos registrados de abundancia y distribución se establecen las etapas sucesionales de la comunidad. Si en el laboratorio se quieren observar los organismos vivos, una vez retirados los paneles inertes con los respectivos organismos adheridos se los acondiciona en cajas o en bolsas plásticas con agua de mar del lugar de muestreo y se colocan dentro de recipientes herméticos con hielo. Otro procedimiento es fijar el material en una solución de formol al 4%. Esta metodología de muestreo se diferencia de la técnica no destructiva en que en esta última, los paneles con sus organismos fijados son observados “in situ” y se vuelven a sumergir.

Paralelamente en otros bastidores de las mismas balsas experimentales, se estudia el comportamiento de distintas formulaciones antiincrustantes aplicadas sobre otros paneles. Los datos obtenidos de los paneles inertes y los pintados se comparan para determinar la eficiencia de las pinturas ensayadas.



Fig. 2.- Aspecto de la balsa experimental del CIDEPINT fondeada en la Base Naval de Puerto Belgrano.



Fig. 3.- Aspecto de una marina del Club de Motonáutica de Mar del Plata con series de paneles experimentales.

El CIDEPINT en sus balsas experimentales fondeadas en puerto Mar del Plata y en Puerto Belgrano, realizó estudios del “fouling” desde el punto de vista biológico [34-50] y de los sistemas de control por medio de pinturas. Estos últimos se complementaron con otras experiencias en servicio, tal como se realizó en Puerto Belgrano empleando para ello diversas embarcaciones de la Armada [12, 22, 24, 51-56].

Las balsas experimentales pueden ser sustituidas por otro tipo de construcciones desde las cuales puedan ser suspendidas las series de paneles, como es el caso de las marinas utilizadas para amarrar embarcaciones. El Area de Incrustaciones Biológicas del CIDEPINT utilizó para tal fin las marinas del Club de Motonáutica de Mar del Plata (Fig. 3) para realizar estudios de reclutamiento y desarrollo de la comunidad sobre series de paneles inertes, utilizando para ello cerámicos no vítreos [49]. Se comprobó que no existen diferencias significativas en la fijación ocurrida entre los paneles de acrílico arenados y los cerámicos no vítreos [50, 57].

Estudios en laboratorio

En el laboratorio cada panel se observa macro y microscópicamente, se determinan las especies, sus abundancias y distribución espacial. Con los datos de los paneles mensuales se grafican los ciclos de fijación, determinándose si son anuales o estacionales (Fig. 4). A su vez con la información obtenida de los paneles acumulativos se estudia el desarrollo de los organismos a lo largo del tiempo, el condicionamiento del sustrato para la fijación y/o alimentación de otras especies, fenómenos de epibiosis y de competencia, etc.

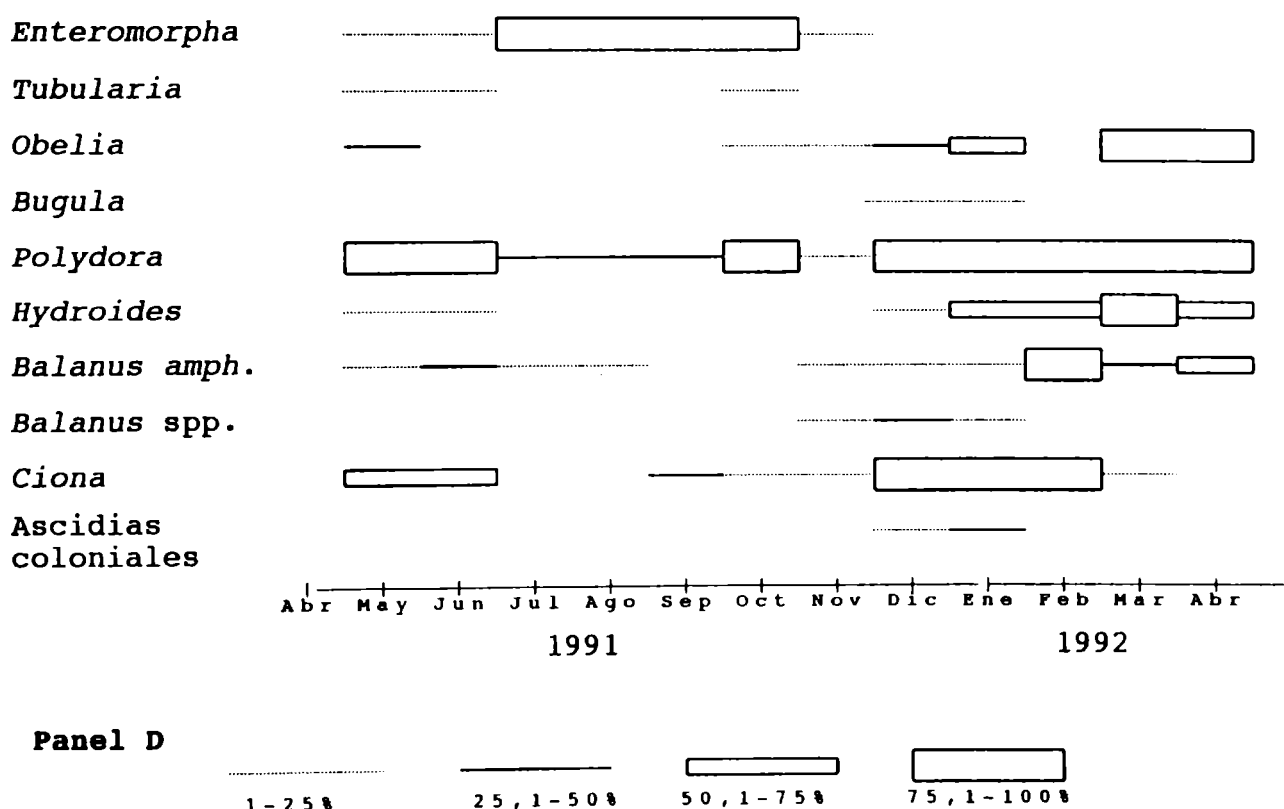


Fig. 4.- Ciclos de fijación de organismos registrados durante el período 1991-92 sobre los paneles D mensuales (puerto Mar del Plata). *Polydora* es el único que presenta un ciclo de fijación anual, los restantes con distintos períodos estacionales.

Además, con los datos registrados se pueden aplicar distintos programas de computación para hacer estudios de agrupamiento de taxones a través de análisis estadísticos en función de abundancias, profundidades, épocas del año, etc. [49, 58-71].

Los estudios de fijación sobre paneles inertes se complementan con otras experiencias en laboratorio. Se crían organismos a partir de larvas obtenidas del plancton recolectado en el lugar de muestreo. Estos cultivos se pueden realizar en agua de mar natural o artificial adecuándose la temperatura, el fotoperíodo y el alimento de acuerdo a las especies; se realizan ensayos con los distintos estadios larvales para observar los efectos que ejercen la luz, la rugosidad y naturaleza del sustrato sobre la fijación de organismos [72-89].

También se pueden realizar experiencias para observar la acción directa de distintas concentraciones de sustancias “antifouling” y evaluar a lo largo del tiempo el efecto de pinturas antiincrustantes sobre los organismos, se puede determinar paralelamente la velocidad de lixiviación del tóxico [90-95]. Asimismo se pueden realizar ensayos con sustancias antiincrustantes no tóxicas, de acuerdo con las propuestas mundiales de preservación del medio ambiente [96-106].

PRINCIPALES ORGANISMOS INCRUSTANTES

El “fouling” puede ser clasificado en dos grandes grupos, de acuerdo al tamaño de los organismos:

- “**microfouling**”, que incluye bacterias, protozoos y diatomeas.
- “**macrofouling**”, que incluye animales (cirripedios, serpulidos o gusanos con tubo, hidroides, moluscos, etc.) y vegetales (algas verdes, marrones, etc.).

Se presenta una lista sistemática simplificada con los principales taxones del “fouling”. La sistemática es el estudio científico de la clasificación, incluye sus bases, principios, procedimientos y reglas. Tiene por finalidad agrupar aquellos organismos que poseen atributos en común en cuanto a nivel de organización, cavidades del cuerpo, caracteres anatómo-fisiológicos, etc. Las categorías sistemáticas básicas son: Reino, Phylum (=División, para la nomenclatura botánica), Clase, Orden, Familia, Género y Especie, pudiendo a su vez realizarse agrupamientos por encima y por debajo de cada uno de los niveles, por ej. Superorden y Suborden, Superfamilia y Subfamilia, etc.

Pueden considerarse tres tipos de componentes vivos: los **productores**, **fagótrofos** y **saprótrofos** como los tres reinos funcionales de la naturaleza, ya que se basan en el tipo de nutrición y en la fuente de energía utilizados. Estas categorías ecológicas no deben confundirse con los reinos taxonómicos, pese a que existen entre ellos ciertos paralelismos. Algunas especies de organismos ocupan posiciones intermedias ya que son capaces de modificar su modo de nutrición de acuerdo con las circunstancias ambientales, existiendo controversias acerca de la ubicación sistemática de los mismos.

Sistemática

Reino Monera

División Cyanobacteria

Clase Cyanophyta

División Bacteria

Reino Protista

Rama Protophyta

División Chrysophyta

Clase Bacillariophyceae (diatomeas: *Achnanthes*, *Skeletonema*)

Rama Protozoa (*Euplotes*, *Vorticella*)

Reino Plantae

División Chlorophyta (algas verdes: *Enteromorpha*, *Ulva lactuca*, *Bryopsis*)

División Phaeophyta (algas pardas: *Ectocarpus*)

División Rhodophyta (algas rojas: *Bangia*, *Ceramium*, *Polysiphonia*, *Porphyra*)

Reino Animalia

Phylum Porifera (esponjas)

Clase Demospongiae (*Haliclona*)

Phylum Cnidaria

Clase Hydrozoa (pólipos y medusas)

Suborden Athecata

Familia Tubulariidae (*Tubularia crocea*)

Suborden Thecata

Familia Campanulidae (*Obelia dichotoma*, *O. longissima*)

Clase Anthozoa (anémonas, corales)

Phylum Platyhelmintha (gusanos planos)

Phylum Nematoda (gusanos cilíndricos)

Phylum Annelida (gusanos segmentados)

Clase Polychaeta

Familia Spionidae (gusanos formadores de tubos arenosos: *Polydora ligni*)

Familia Cirratulidae (*Cirratulus cirratus*)

Familia Capitellidae (*Capitella capitata*)

Familia Polynoidae (*Halosydna australis*)

Familia Syllidae (*Syllis*, *Typosyllis*)

Familia Serpulidae (gusanos formadores de tubos calcáreos:

Hydroides elegans, *Ficopomatus enigmaticus*)

Familia Spirorbidae (gusanos formadores de tubos calcáreos: *Spirorbis*)

Phylum Mollusca

Clase Bivalvia

Familia Mytilidae (mejillón: *Mytilus edulis*, *Limnoperna fortunei*)

Familia Ostreidae (ostra: *Ostrea*)

Familia Corbiculidae (peste de agua: *Corbicula fluminea*)

Familia Dreissenidae (mejillón cebra: *Dreissena polymorpha*)

Clase Gastropoda

Orden Nudibranchia (*Tenellia pallida*)

Phylum Arthropoda

Clase Crustacea

Subclase Copepoda (*Tisbe*, *Parathea minuta*)

Subclase Cirripedia

Familia Balanidae (cirripedios no pedunculados: *Balanus*)

Familia Lepadidae (cirripedios pedunculados: *Lepas*)

Subclase Malacostraca

Superorden Peracarida

Orden Isopoda (bicho bolita de mar: *Sphaeroma*)

Orden Amphipoda (*Corophium*)

Superorden Eucarida

Orden Decapoda (cangrejos: *Cyrtograpsus*)

Phylum Bryozoa (colonias arborescentes o incrustantes: *Bugula*, *Conopeum*)

Phylum Chordata

Subphylum Tunicata

Clase Ascidiacea (papas de mar: *Ciona intestinalis*)

En la actualidad se tiende a clasificar los organismos bajo un sistema multi-reino, pero no existe unificación de criterios, por lo que la sistemática varía de acuerdo a los autores. Debido a que la finalidad del presente trabajo no es realizar una revisión sistemática, se optó por presentar una clasificación en la forma más sencilla que permita al lector ubicarse rápidamente en la escala zoológica o botánica (ver pág. 107).

En esta revisión se detallan algunas de las características biológicas de los organismos sedentarios citados, haciéndose referencia a la presencia en el puerto Mar del Plata [34-37, 39, 42-43, 45-49] y en Puerto Belgrano [38-41, 44, 48]. También se hacen comentarios sobre grupos de hábitos errantes cuya importancia radica en el rol que cumplen en el flujo de materia y energía dentro de las comunidades incrustantes.

“Film” primario

El desarrollo de una comunidad de organismos incrustantes sobre una superficie sumergida, es un proceso secuencial iniciado con la adsorción de material disuelto que da origen a la formación de la **película condicionante** que modifica las propiedades originales del sustrato [21, 107-110]. Continúa con la formación de un **“film” primario**, llamado también **“film” inicial**, **biopelícula** o **“microfouling”** [111-112]. Este “film” está compuesto por una intrincada asociación de microorganismos, sus productos de secreción, partículas de materia orgánica e inorgánica, detritos, areniscas y limo. Entre los organismos predominantes están las bacterias y las diatomeas, que producen abundante material mucilaginoso [6, 113], protozoos, dinoflagelados, hongos y esporas de algas [114-116].

La colonización es un proceso selectivo. La primera colonización bacteriana en medio marino, produce grandes cantidades de ácidos polisacáridos y puede proporcionar una superficie aprovechable para la subsiguiente colonización microbiana [117-118]. Los primeros organismos que llegan al sustrato son pequeñas bacterias en forma de bastón de menos de 0,8 μm de longitud, que se asientan durante las primeras horas de inmersión. En las siguientes 6-8 horas lo hacen formas de mayor tamaño (cocoidales, espiraladas), pertenecientes a los géneros *Pseudomonas*, *Achromobacter*, *Flavobacterium*. Al cabo de 24 horas de exposición se encuentran bacterias pediceladas y en forma de capullo, tales como *Caulobacter* e *Hyphomicrobium*, así como las primeras diatomeas y protozoos [111, 119].

La capacidad de colonización de los organismos del “fouling” fue claramente demostrada por Zobell [120], quien sumergió en el mar una placa no tóxica de una pulgada cuadrada y contó el número de organismos adheridos después de 24, 48 y 96 horas. Después de 24 horas, la población de bacterias fue de alrededor de 2.000.000, alcanzando alrededor de 78.000.000 después de 96 horas. Las diatomeas contadas incrementaron de 940 a más de 8.000 en el mismo período. Para los protozoos, larvas de cirripedios y otros organismos notó un incremento similar [1].

Las **diatomeas** son organismos unicelulares microscópicos de filiación vegetal que pueden vivir aisladas o en colonias, suspendidas en el agua (diatomeas planctónicas: *Skeletonema costatum*) o fijadas a sustratos sumergidos (diatomeas bentónicas: *Achnanthes longipes*), aunque por procesos de sedimentación es factible encontrar especies del plancton formando parte de las comunidades incrustantes (Fig. 5). En el caso de las diatomeas sésiles los sistemas adhesivos tienen morfologías variadas compuestos por polisacáridos ácidos

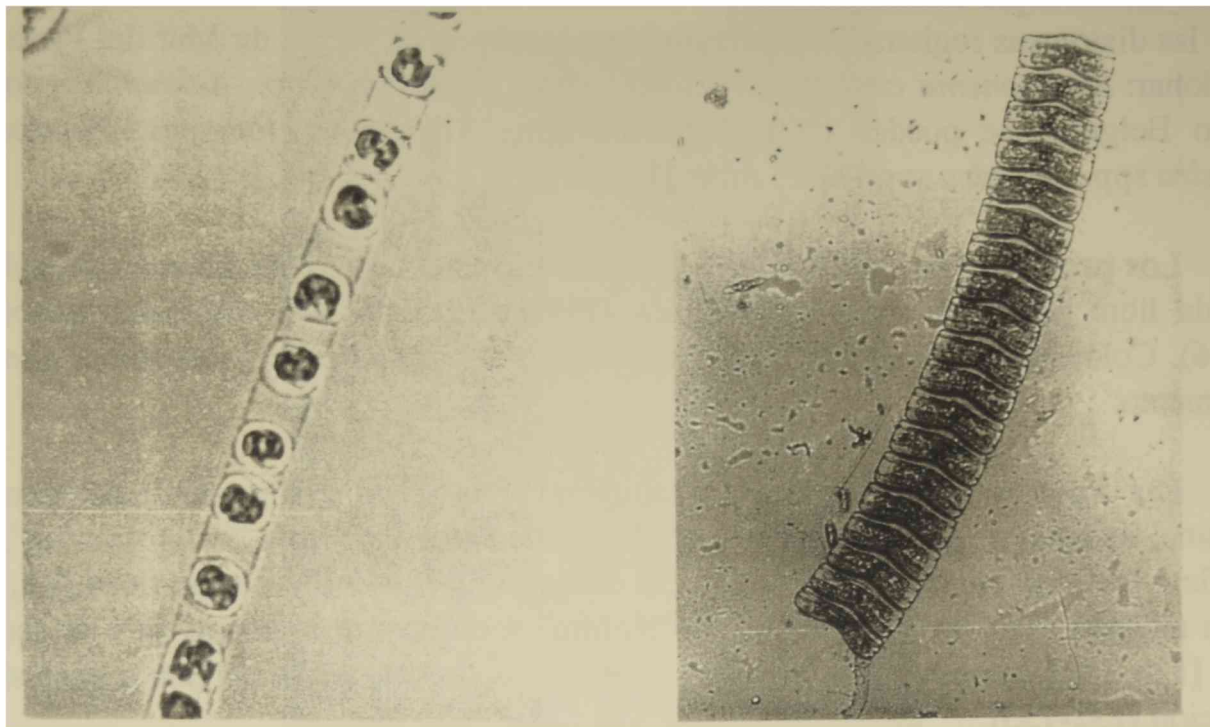


Fig. 5.- a) *Skeletonema costatum* (400 x), diatomea plactónica, células unidas por apéndices filiformes, formando cadenas largas y rectas; b) *Achnanthes longipes* (250 x), diatomea bentónica, células dispuestas en cadenas acintadas, adheridas a un sustrato por un pedicelo mucilaginoso.

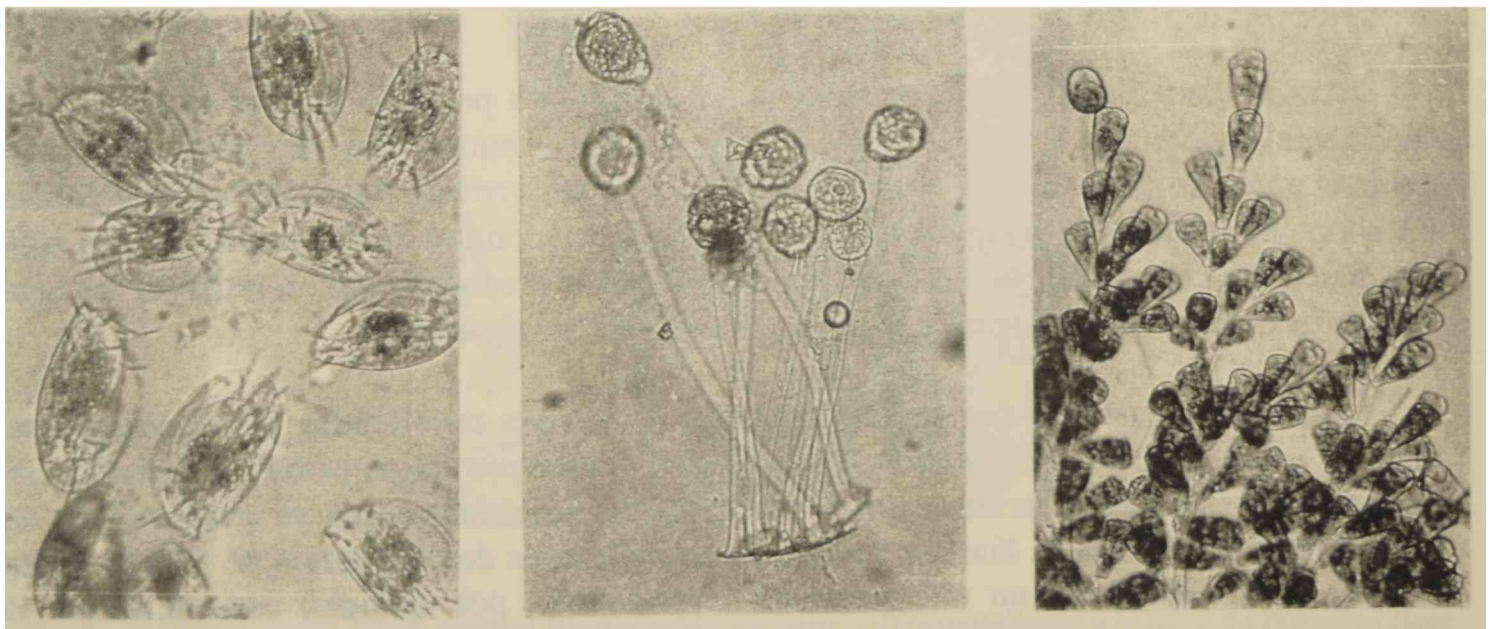


Fig. 6.- Protozoos ciliados. a) *Euplotes* (250 x), protozoos solitarios de vida libre; b) *Vorticella* (120 x), protozoos solitarios sésiles; c) *Zoothamnium* (100 x), protozoos coloniales sésiles.

mucilaginosos. Cada diatomea es una célula encerrada en un frústulo silíceo formado por dos partes o tecas que encajan perfectamente entre sí (similar a una caja de Petri), de estructuras simples u ornamentadas. En general, los estudios taxonómicos se basan en la observación, a nivel de microscopía electrónica, de las ornamentaciones y relieves característicos de las tecas. Entre las diatomeas registradas en mayor abundancia en el puerto de Mar del Plata se pueden mencionar: *Skeletonema costatum*, *Melosira* spp., *Licmophora* sp., *Achnanthes longipes*, en Puerto Belgrano se pueden citar: *Nitzschia* spp., *Achnanthes longipes*, *Pleurosigma* sp., *Melosira* spp., *Synedra* spp., entre otras [121].

Los **protozoos** son organismos unicelulares microscópicos de filiación animal, solitarios de vida libre (*Euplotes*), sésiles solitarios (*Vorticella*) o sésiles coloniales (*Zoothamnium*) (Fig. 6). Colonizan los sustratos sumergidos luego de las bacterias y diatomeas que les sirven de alimento.

Las especies de bacterias que constituyen la biopelícula y el grado de envejecimiento de la misma, influyen en la fijación y desarrollo de los organismos del “macrofouling”, pudiendo modificar las condiciones físicas y químicas del sustrato y la tensión superficial [15, 122-127]. Según algunos autores la presencia del “biofilm” sería un prerequisite para el asentamiento larval [128-131], mientras que otros sostienen que no es condición necesaria pero sí facilitaría la fijación [132-135].

Debido a la gran diversidad de organismos involucrados, es más difícil alcanzar un control completo del “film” primario que el de cualquier otra forma del “fouling”.

Algas [136]

Las algas marinas juegan un rol importante en el “fouling”, particularmente sobre sustratos artificiales sumergidos en aguas someras donde la luz es suficiente para que lleven a cabo sus funciones fotosintéticas, por ello es común encontrar distintas especies de algas en la parte superior de sustratos fijos y flotantes.

Aunque hay diversos phyla de algas marinas, sólo un pequeño número de especies se consideran importantes desde el punto de vista del biodeterioro. Los tres phyla principales desde el punto de vista económico son: Chlorophyta (algas verdes), Phaeophyta (algas pardas) y Rhodophyta (algas rojas) (Fig. 7). Los nombres vulgares con que se denominan a estas algas responden a la coloración que les confieren los pigmentos predominantes: clorofila en las algas verdes, fucoxantina en las algas pardas y ficoeritrinas en las algas rojas.

Las algas en general forman característicos cinturones constituidos principalmente por distintas especies de *Enteromorpha* (algas verdes) y *Ectocarpus* (algas pardas), de distribución cosmopolita. Son particularmente tolerantes al estrés ambiental como se evidencia en sus abundancias en la inestable línea de flotación y sobre la zona de salpicadura de las estructuras flotantes. Además tienen un alto potencial reproductivo, por ejemplo, cada filamento de *Enteromorpha* es capaz de producir cien millones de células reproductoras. Como consecuencia del carácter intermareal de su ambiente natural, tienen la capacidad de soportar condiciones extremas de temperatura, salinidad y desecación, también tienen otras características que contribuyen a su éxito dentro del “fouling”, tales como la capacidad para adherirse y crecer rápidamente sobre las superficies.

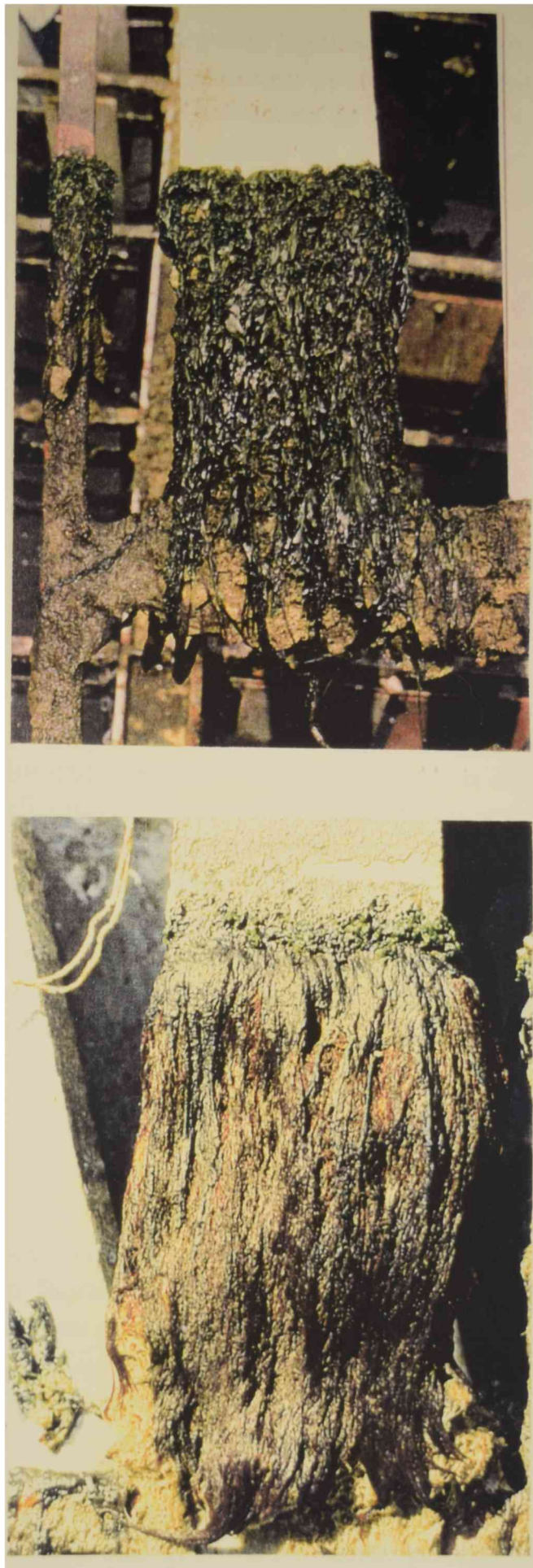


Fig. 7.- a) Chlorophyta (algas verdes) fijadas sobre un panel correspondiente a la línea de flotación (tres meses de inmersión); b) Rodophyta (algas rojas) fijadas sobre un panel correspondiente a la línea de flotación (ocho meses de inmersión).

Aunque la propagación vegetativa puede jugar un rol exitoso en la dispersión de muchas algas marinas, indudablemente el mecanismo predominante por el cual se alcanza la colonización de nuevos sustratos es a través de la liberación y asentamiento de estadios reproductivos por esporas móviles (flageladas). En la mayoría de las algas, el asentamiento inicial es seguido rápidamente por un proceso de adhesión activo que involucra la secreción de un material adhesivo entre la membrana que reviste la espora y el sustrato. Estudios de microscopía electrónica de varias esporas algales han demostrado que este material adhesivo se produce por pequeñas vesículas subcelulares del aparato de Golgi durante los últimos estadios de diferenciación de las esporas. En el caso de la clorofita *Enteromorpha*, la sustancia producida es un mucopolisacárido consistente en proteínas y carbohidratos [137-138]. Las esporas recientemente adheridas son muy vulnerables al ataque de predadores tales como bacterias o a la acción tóxica de compuestos “antifouling” dado que están rodeadas sólo por una membrana simple y delgada. Sin embargo, luego de unos minutos la pared comienza a desarrollarse alrededor de las células y luego de 4 horas alcanza un grosor sustancial. De este modo, en un corto período se logra una considerable protección física y química, que impide remover con facilidad la zoospora una vez que se ha adherido a una superficie. Aunque es extremadamente difícil medir cuantitativamente la fuerza de la adhesión entre las zoosporas y el sustrato, ha sido posible obtener información a diferentes tiempos luego del asentamiento usando chorros de agua estandarizados, este método demuestra que la adhesión de las esporas al vidrio mejora rápidamente durante las primeras horas luego del asentamiento, presumiblemente debido a los cambios físicos que ocurren por la descarga del adhesivo [139]. Luego que las esporas se adhieren a la superficie, comienza un período de rápido crecimiento que generalmente comprende la producción inicial de una capa protectora externa de idéntica composición que la pared celular. El proceso de germinación continúa con la formación de un sistema de anclaje eficiente que asegura el futuro desarrollo del talo. Esto es realizado por células rizoidales especializadas, incolores, que otorgan fuerzas de adhesión. Estos rizoides se producen en forma continua para soportar el incremento de tamaño del sistema erecto. A medida que emergen de la base, toman un aspecto compacto para formar la característica estructura de sostén (“holdfast”). Juntamente con el proceso de establecer un sistema de anclaje eficiente, ocurre el crecimiento y desarrollo de la porción macroscópica superior del cuerpo del talo. Los procesos de erección del talo se llevan a cabo por división de células meristemáticas.

Se ha comprobado por distintas experiencias que esporas de *Enteromorpha* pueden asentarse sobre sustratos en flujos de agua con velocidades superiores a 10 nudos, lo cual permitiría la fijación de estas algas mientras los barcos están en movimiento [140-141].

Puerto Mar del Plata. *Enteromorpha intestinalis* es la especie de clorofita que siempre ha estado presente en los paneles experimentales, variando su abundancia y distribución batimétrica de acuerdo a la transparencia del agua, pero en general prefieren las zonas más iluminadas o sea las superficiales. Existen otras clorofitas como *Bryopsis plumosa*, *Chaetomorpha* sp., *Ulva lactuca*, etc. que, cuando están presentes, se encuentran en bajas densidades.

Ectocarpus sp. (feofita: alga parda), *Bangia* sp., *Porphyra* sp., *Polysiphonia* sp. y *Ceramium* sp. (rodofitas: algas rojas), se presentan en general en bajas abundancias y con ciclos de fijación estacionales.

Puerto Belgrano. *Enteromorpha* sp. tiene, como en Mar del Plata, un ciclo de fijación anual, colonizando los distintos niveles con picos de mayor reclutamiento en los meses más cálidos. Otras clorofitas que aparecen en muy bajas densidades son: *Bryopsis plumosa*, *Chaetomorpha* sp. y *Ulothrix* sp.

Ectocarpus es la única feofita representada en bajas densidades durante todo el año.

Las rodofitas *Bangia* sp., *Ceramium* sp., *Griffithsia* sp., *Polysiphonia* sp. y *Porphyra* sp. se encuentran en bajas abundancias y con períodos de colonización breves.

Poríferos (esponjas) [142]

Las esponjas forman un importante grupo de animales bentónicos que se hallan distribuidos en todas las profundidades y latitudes. Su nivel de organización corresponde al celular dependiente o integrado dado que aún no constituyen verdaderos tejidos.

La superficie de una esponja está perforada por gran número de pequeñas aberturas llamadas ostíolos o poros incurrentes (**Fig. 8**); éstos comunican con canales que se abren a una cavidad interior denominada espongíocel (más o menos desarrollada según el grado estructural de la esponja), con una abertura superior u ósculo. El agua penetra por los ostíolos y pasa al interior del espongíocel; esta cavidad está tapizada por una capa de células denominadas coanocitos provistas de un flagelo y un collar gelatinoso en su parte basal. La agitación del flagelo atrae las corrientes de agua y de esta manera atrapa las pequeñas algas y células del plancton así como el oxígeno necesario para el intercambio gaseoso. El agua termina su recorrido desde el espongíocel al exterior por medio del ósculo. Como estructuras de sostén presentan espículas que pueden ser calcáreas, silíceas o de fibras de espongina. Las formas larvales son planctónicas (anfibrástulas o parenquímulas según sean calcáreas o demospongias respectivamente). Son de difícil identificación a simple vista, siendo necesaria la observación de las espículas bajo microscopio debido a la diversidad y estructura de las mismas [143].

Puerto Mar del Plata. No se registraron esponjas en los paneles experimentales ni en sustratos naturales.

Puerto Belgrano. Se registraron especies del género *Haliclona* y *Halichondria* (Demospongiae) en bajas densidades.

Cnidarios

***Hidrozoos* [144]**

Los hidrozoos son cnidarios polimórficos, es decir que en una parte de su ciclo de vida pueden presentarse como pólipos coloniales y en otra como medusas (aguas vivas). El nivel de organización es tisular (forman verdaderos tejidos). Muchas especies presentan la particularidad de alternar una fase de reproducción asexual (representada por la forma pólipo) y una fase de reproducción sexual (representada por la forma medusa); esta alternancia de generaciones se conoce como metagénesis. Desde el punto de vista del “fouling” interesan los pólipos debido a que son los que se fijan sobre los sustratos duros, generalmente forman



Fig. 8.- Aspecto general de *Haliclona* (Demospongiae) (10 x).

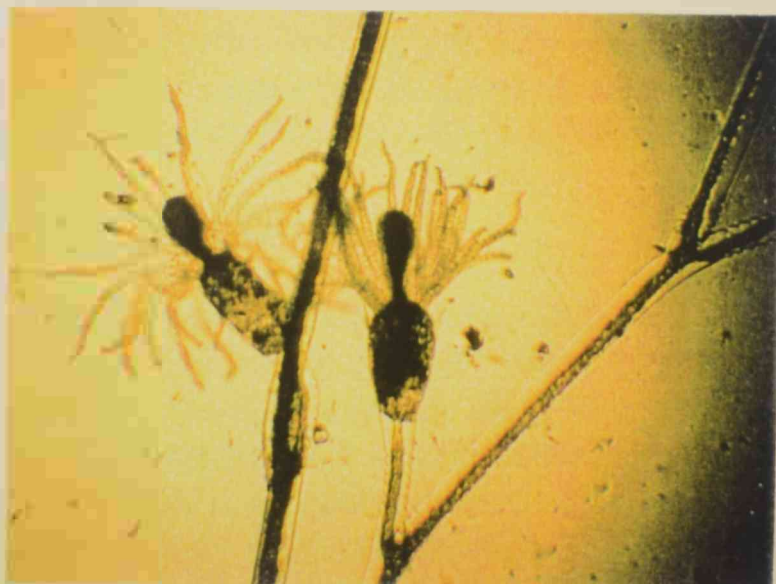


Fig. 9.- Detalle de una colonia de *Obelia* criada en laboratorio (40 x).

colonias constituidas por numerosos individuos que se especializan en distintas funciones. Por ejemplo, los gastrozoides cumplen funciones alimenticias, tienen una boca bien desarrollada y tentáculos, por otra parte, los gonozoides, tienen funciones reproductivas y pueden producir medusas por gemación. Las colonias tienen diversas formas de acuerdo a las familias o géneros, en general son filamentosas o arborescentes, se originan por un pólipo primario que se adhiere al sustrato por una hidrorriza filiforme y desarrolla nuevos pólipos (sésiles o pedicelados) por medio de reproducción asexual. Especies de las familias Tubulariidae (*Tubularia crocea*) y Campanulariidae (*Obelia dichotoma*, *O. longissima*, Fig. 9) son frecuentes en la comunidad del “fouling”, siendo en general las primeras colonizadoras sobre sustratos sumergidos.

Antozoos

Los antozoos son cnidarios polipoides en los que no se observa la forma medusa. Los pólipos pueden ser solitarios (anémonas de mar) o bien agruparse en colonias (corales).

Puerto Mar del Plata. Los cnidarios registrados sobre paneles experimentales pertenecen a la Clase Hidrozoa. En general presentan ciclos de fijación estacionales con ciertas diferencias entre los distintos períodos estudiados. En 1991-92, *Obelia longissima*, *O. dichotoma* y *Tubularia crocea* se registraron en períodos más breves que en ensayos anteriores. Con respecto a representantes de la Clase Anthozoa, puede mencionarse que fueron observadas anémonas sobre pilotes del Club de Motonáutica y sobre piedras en pozas de marea expuestas durante la bajamar.

Puerto Belgrano. Entre diciembre de 1993 y marzo de 1995, *Obelia* sp. fue la única especie de hidrozoos representada principalmente en los paneles acumulativos. En estudios previos fueron registradas *Plumularia setacea* y campanuláridos no determinados.

Anélidos

En el Phylum Annelida se considerarán principalmente aquellas especies que resultan relevantes desde el punto de vista del “fouling”, es decir aquellos poliquetos que construyen tubos arenosos o calcáreos. También se hace una breve mención de las especies que utilizan el sustrato en forma ocasional buscando alimento, refugio y/o soporte.

Poliquetos que forman tubos arenosos [145-148]

Dentro del grupo de gusanos que forman tubos arenosos, *Polydora ligni* es la especie más abundante registrada en el puerto de Mar del Plata. El primer estadio larval es libre, planctónico (trocófora), luego se alarga y segmenta hasta llegar al estadio de 15-16 segmentos (setígeros) en que la larva es bentónica y busca un sustrato donde adherirse para formar su habitáculo (Fig. 10). Por medio de la secreción de mucus y ayudado por sus palpos captura los granos de arena para construir tubos sinuosos y ramificados, en general de mayor tamaño que la longitud del gusano que lo habita, favoreciendo los fenómenos de epibiosis. En la mayor parte de los ensayos realizados en balsa se ha comprobado que se encuentran entre los primeros colonizadores de los sustratos inertes limpios. En etapas más avanzadas de desarrollo de la comunidad ofrecen sustrato secundario para el asentamiento de individuos de su misma u otras especies.

Polydora ligni además de ser una especie muy abundante dentro de la comunidad del “fouling”, cumple un rol muy importante en la sucesión. Se debe considerar su estudio en particular ya que es resistente a los distintos sistemas de control [93].

Puerto Mar del Plata. Los ciclos de fijación de *Polydora ligni* generalmente fueron anuales, siendo en determinados momentos la especie dominante de la comunidad incrustante.

Puerto Belgrano. A diferencia de lo que ocurre en Mar del Plata, *Polydora ligni* fue registrada en muy bajas densidades en forma ocasional.

Poliquetos que forman tubos calcáreos [145-146, 149]

Los poliquetos *Hydroides elegans*, *Ficopomatus enigmaticus* (Serpulidae) y *Spirorbis* spp. (Spirorbidae), son gusanos que forman tubos calcáreos que se encuentran distribuidos en la mayoría de los puertos del mundo.

Los serpúlidos secretan largos tubos sinuosos al comienzo y luego se extienden casi en línea recta ya sea sobre el sustrato o en forma perpendicular al mismo (Fig. 11). Además, pueden formar verdaderos macizos que obstruyen cañerías e impiden la rotación de las hélices de las embarcaciones.

Los tubos de los spirórbidos son más pequeños enrollados en una espiral plana (Fig. 12).

Los serpúlidos y spirórbidos se alimentan de organismos microscópicos y de partículas presentes en las corrientes de agua, el filtrado se efectúa por una corona branquial formada por largos tentáculos plumosos que a su vez tienen función respiratoria. Cuando el cuerpo del animal se retrae dentro del tubo, un opérculo de naturaleza córnea o calcárea obtura el habitáculo. En la mayoría de los casos los sexos son separados y las gametas son liberadas directamente al mar donde los huevos se fecundan y se desarrollan en larvas trocóforas; a medida que crece, la larva se alarga y elige un lugar para fijarse, etapa en la cual influyen la luz, la gravedad y la naturaleza del sustrato. Una vez que se ha fijado en un sitio adecuado se metamorfosea y comienza a secretar un delicado tubo calcáreo, no pudiendo moverse del lugar seleccionado. Dos grandes glándulas ubicadas en la región anterior del animal son las encargadas de secretar carbonato de calcio.

Poliquetos que no forman tubos

Se encuentran ocasionalmente especies pertenecientes a las familias Syllidae (*Syllis*, *Typosyllis*), Polynoidae (*Halosydnella australis*), Capitellidae (*Capitella capitata*) y Cirratulidae (*Cirratulus cirratus*). Con respecto a *Capitella capitata* cabe mencionar que es un buen indicador de zonas poluidas siendo capaz de colonizar áreas donde la fauna ha sido depredada en forma natural o por el hombre [145].

Puerto Mar del Plata. *Hydroides elegans* es el serpúlido dominante fundamentalmente en los meses de verano. En el ensayo realizado en 1976-77, esta especie no fue registrada, habiendo sido reemplazada por *Mytilus platensis* (mejillón).



Fig. 10.- *Polydora ligni*. a) larva de 15-16 setígeros (250 x); b) adulto (40 x); c) adulto dentro de su tubo arenoso (40 x).



Fig. 11.- Tubos de serpulidos adheridos a paneles de ensayo, a) vista frontal; b) vista lateral; c) Detalle (10 x).

Puerto Belgrano. Los poliquetos más abundantes son los spirórbidos, siendo dominantes en determinadas etapas de la comunidad. Los serpulidos en cambio están presentes en muy bajas densidades.

Moluscos

Los moluscos incluyen una gran variedad de formas marinas, terrestres y de agua dulce, provistas generalmente de valvas de carbonato de calcio y conchiolina, con un cuerpo dividido en cabeza, pie y masa visceral [6]. Sólo los bivalvos con biso (*Mytilus platensis*: mejillón, *Brachydontes rodriguezi*: mejillín) y los que se adhieren al sustrato por cementado directo de una de sus valvas (*Ostrea*: ostra) son importantes dentro de la comunidad del “fouling”.

En su mayoría, los bivalvos son de sexos separados y liberan gametas al mar donde se fecundan y desarrollan primero en larvas trocóforas y luego en larvas velíger; pasada la etapa juvenil buscan un sustrato donde adherirse. Sólo unas pocas especies de ostras son hermafroditas e incuban sus huevos.

Existen familias de bivalvos sésiles con pie reducido, que se adhieren al sustrato por medio de fuertes filamentos córneos llamados bisales o del biso secretados por una glándula del pie, como por ejemplo en los mejillones. Para la formación del filamento del biso, el pie ejerce presión contra el sustrato duro, fluye una secreción glandular a lo largo del mismo y sale por su extremo endureciéndose en contacto con el agua de mar; al retirarse el pie queda por detrás un filamento completamente formado. A continuación el pie secreta otro filamento en una nueva localización, y por último el molusco queda amarrado por una masa de filamentos. La mayoría de las especies pueden desprenderse y readherirse permitiendo al individuo moverse de un lugar a otro.

Según DeVore *et al.* [150] el cemento secretado es de naturaleza proteica y la formación del adhesivo incluye la interacción de por lo menos tres secreciones exocrinas: una proteína polifenólica, una sustancia mucosa y quizás colágeno. Nanishi *et al.* [151] consideran que el cemento está compuesto principalmente por tirosina y su mecanismo de entrecruzamiento sería similar al de las quinonas.

La mayor parte de los bivalvos son alimentadores de filtro, en los cuales las branquias, además de la función respiratoria, han asumido la de atrapar partículas alimenticias.

Por lo general, este grupo para concretar su colonización necesita que la comunidad incrustante se encuentre bastante desarrollada (Fig. 13). Es por ello que sobre los paneles mensuales suelen estar poco representados, pues las condiciones que les brindan los mismos no son las óptimas requeridas por las distintas especies.

Dentro de los moluscos, además de los mencionados, existen otros representantes importantes desde el punto de vista del biodeterioro por las perforaciones o excavaciones que hacen sobre distintos sustratos. Por ejemplo, *Teredo* produce grandes daños en pilotes y cascos de barcos de madera, la galería que excava se va agrandando a medida que el animal aumenta de longitud; los adultos pueden alcanzar hasta 30 cm (Fig. 14). La actividad perforante de muchas especies como *Petricola* queda restringida a bancos de arcilla y roca blanda, otras como *Pholas* y *Barnea* son capaces de perforar cemento armado y roca

relativamente dura. *Hiatella arctica* puede destruir diques y muelles de cemento, tiene 2,5 cm de longitud y excava agujeros de unos 15 cm de profundidad. El bivalvo *Litophaga* taladra piedras calizas por medio de un proceso químico; secreta un mucus ácido que ablanda la roca a nivel del punto a excavar.

Puerto Mar del Plata. Sólo en el ensayo realizado en 1976/77 se registró la presencia de *Mytilus platensis*; esta especie colonizó los cuatro niveles de profundidad estudiados aunque con una mayor preferencia por los niveles inferiores. En determinados momentos del desarrollo de la comunidad fue una de las especies dominantes de la misma. También se suele encontrar al nudibranquio *Tenellia pallida* (molusco sin valva) sobre colonias de campanuláridos.

Puerto Belgrano. En este puerto los moluscos no han estado representados en forma significativa, sólo unos pocos ejemplares de *Brachydontes rodriguezi* fueron mencionados para los períodos 1967 y 1971-72 en los paneles acumulativos.

Artrópodos

Crustáceos

Si bien este grupo está representado por numerosas especies pertenecientes a distintas subclases, órdenes y familias, cabe mencionar que desde el punto de vista del “fouling”, los **cirripedios** [4, 6, 77, 152] y los **anfípodos** tubícolas son considerados los más relevantes.

Entre los organismos más comunes e importantes del “fouling” se encuentran los **cirripedios** que producen un deterioro importante en la película de pintura (**Fig. 15**). Es el único grupo sésil de crustáceos y en consecuencia uno de los más atípicos de la clase Crustacea. Los cirripedios tienen forma de cono truncado; el cuerpo del animal está rodeado por placas calcáreas (generalmente 6: rostro, carina, 2 paredes carinales y 2 paredes rostrales) apoyadas sobre una base que puede ser calcárea (**Figs. 16 y 17**) o membranosa. Las placas que forman la pared se superponen unas a otras, y pueden conservarse unidas por tejido vivo, por extensiones de las paredes (alas y radios) que se encastran interiormente, o por fusión parcial de las mismas. La parte superior está cubierta por un opérculo, generalmente formado por dos tergos y dos escudos sumamente movibles, unidos a las paredes laterales por medio de una membrana resistente. El cierre hermético de los tergos y escudos permite aislar el cuerpo del animal del medio ambiente, por lo que pueden resistir períodos prolongados de desecación como los producidos durante las mareas bajas. La disposición y número de las placas, así como las características de la base y del opérculo, son importantes para la identificación de las especies. La cutícula o exoesqueleto, que reviste el interior de la cavidad del manto y que cubre los apéndices, experimenta mudas periódicas como en otros artrópodos. Las placas calcáreas son secretadas por el manto subyacente y no se desprenden al producirse la ecdisis. El crecimiento de las placas depende de la adición continua de materiales a sus bordes y superficies interiores, aumentando así su espesor y diámetro. El cuerpo dentro del caparazón está flexionado hacia atrás y los apéndices están dirigidos hacia arriba; existen en forma típica seis pares de apéndices alimenticios torácicos (cirros), de los cuales deriva el nombre de Cirripedia con el que se designa esta subclase. Durante la alimentación, se abren los tergos y escudos apareados, y los cirros se desenrollan y extienden a través de la abertura. El

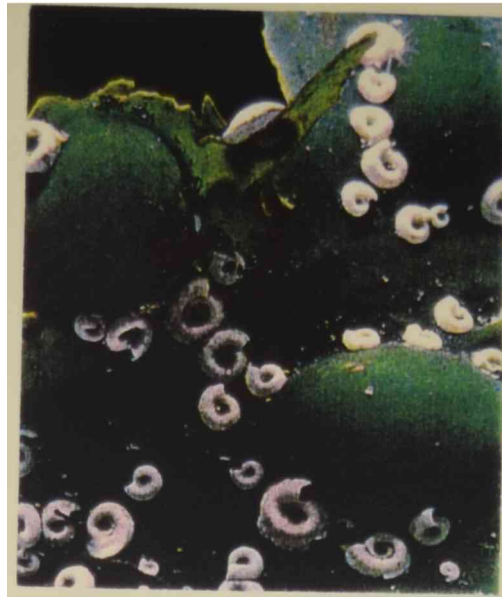


Fig. 12.- Tubos de spirórbidos (100 x).



Fig. 13.- *Mytilus platensis* (mejillones).



Fig. 14.- a) Aspecto externo de un pilote de madera perforado por *Teredo*; b) aspecto interno del mismo pilote; c) esquema del molusco dentro de su habitáculo.



Fig. 15.- Aspecto de la fijación de cirripedios sobre una placa pintada: la coloración de las paredes de los caparazones evidencia el crecimiento de los organismos por debajo de la película de pintura. Se observan ascidias fijadas sobre cirripedios (epibiosis).

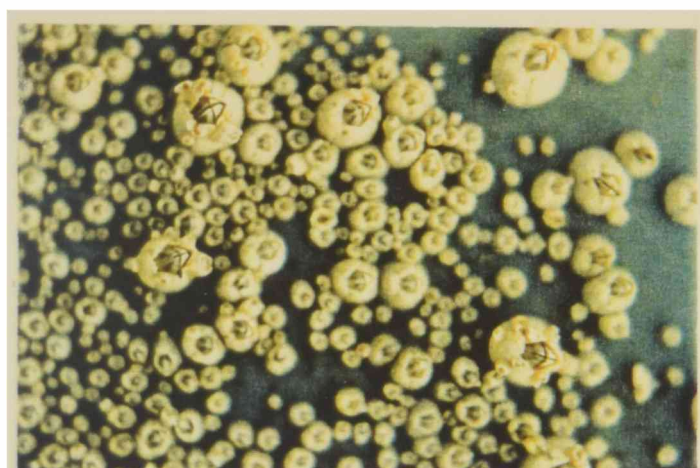


Fig. 16.- Cirripedios fijados sobre un panel testigo (1 mes de inmersión).

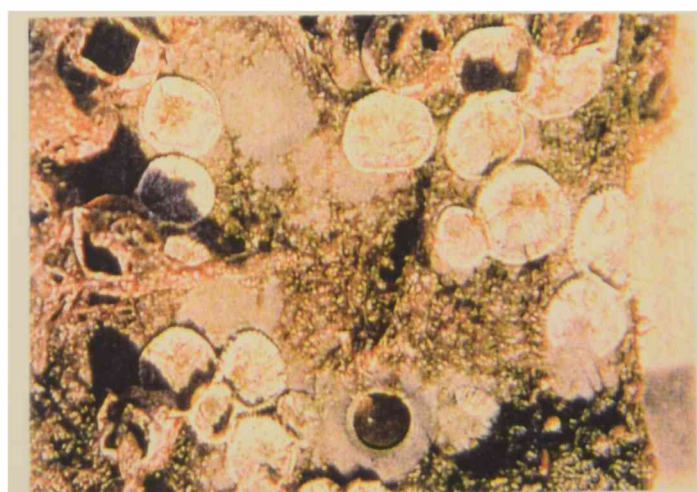


Fig. 17.- Bases calcáreas de cirripedios adheridas a un sustrato una vez desprendidas las paredes del caparazón.

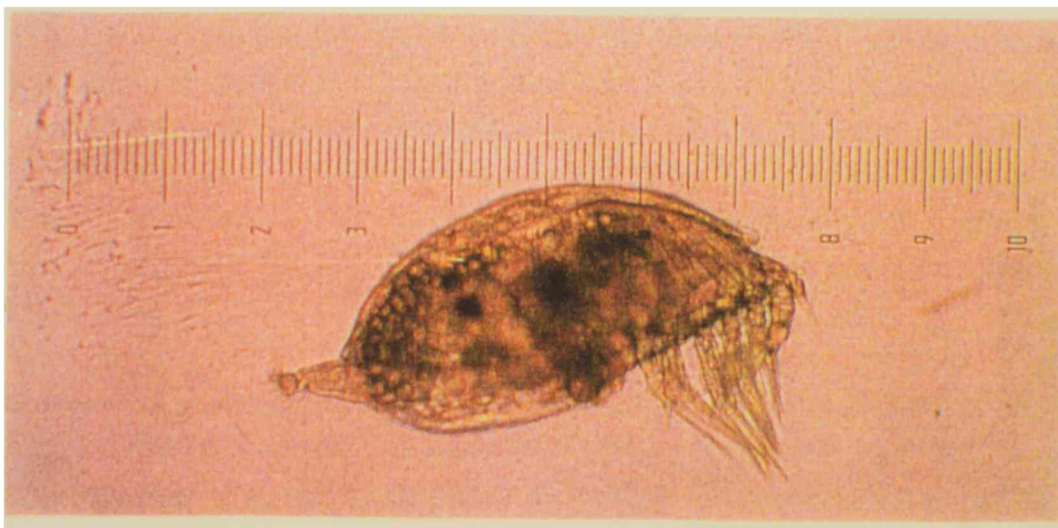
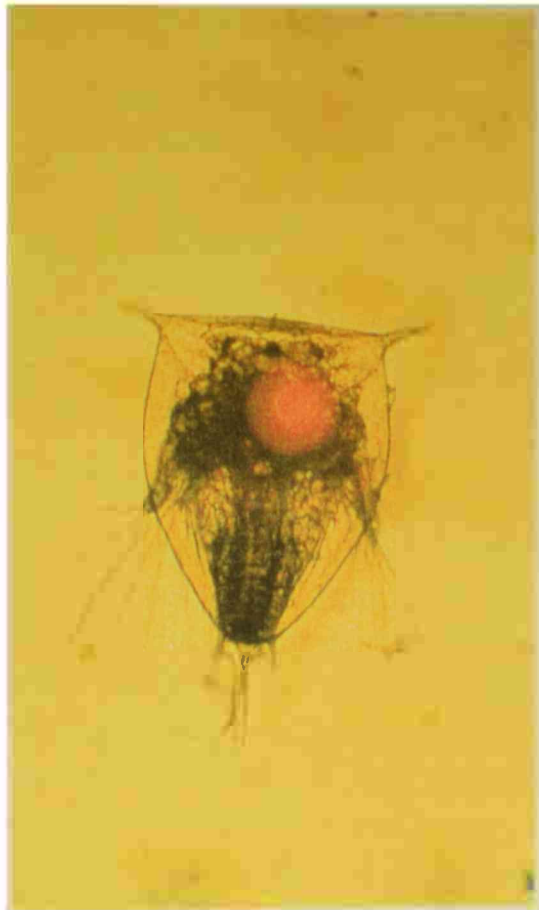


Fig. 18.- Larvas de cirripedios; a) nauplii VI (60 x); b) cipris (100 x).

movimiento que realizan es similar al de abrir y cerrar los dos puños de las manos simultáneamente estando en contacto las bases de las palmas; la velocidad del movimiento (un ciclo de apertura y cierre) es en promedio de unas 140 veces por minuto. La mayoría de los cirripedios se alimentan de microplancton.

Los cirripedios son hermafroditas y de fertilización cruzada. Las larvas nauplii recién eclosionadas del huevo pasan por seis estadios metamórficos precedidos cada uno por una muda o ecdisis. Luego del sexto estadio naupliar se transforma en cipris (**Fig. 18**), que en principio es una larva nadadora y luego se adhiere por medio de las ventosas de succión de las anténulas y por el cemento segregado por las mismas. El primer estadio naupliar se prolonga sólo por unos pocos minutos (15-30 minutos) y el tiempo para completar el desarrollo metamórfico varía de acuerdo a las especies [153-157]. Las cipris están protegidas por dos valvas quitinosas transparentes, no se alimentan y por lo tanto son menos susceptibles a tóxicos [158].

El asentamiento inicial de los cirripedios es sólo una adhesión mecánica producida por la succión hidráulica de las copas ubicadas en el extremo de las anténulas de las cipris ($7,5 \text{ dyn/cm}^2$). Esta adhesión inicial soporta una corriente de agua de $186,4 \text{ cm/seg}$ ($=3,6$ nudos); luego se refuerza por un cemento adhesivo que no es esencial para alcanzar la adhesión permanente [158-159]. Según Walker [160] la adhesión temporaria de las anténulas, cuando las cipris están buscando el lugar de asentamiento, es de 4 kg/cm^2 ; posteriormente este valor se incrementa. El cemento primero es líquido, luego se polimeriza y endurece. Yule *et al.* [161] encontraron una secreción antenular de naturaleza proteica durante la actividad exploratoria de la larva, lo que induciría el asentamiento de otras larvas.

Una vez que la cipris se fija, comienza la metamorfosis hacia la forma adulta, se despoja de su cutícula quitinosa y secreta un caparazón de placas calcáreas, frágiles y transparentes al principio, que se ajustan unas con otras formando un cono truncado.

En los adultos, el aparato del cemento está bien desarrollado, ubicado en ambos bordes del manto, constituido por glándulas permanentes que funcionan en forma periódica, con una red de túbulos que van creciendo con el animal, llenando el espacio entre el sustrato y la base; las glándulas del cemento se mantienen en el adulto [159]. La base se cementa firmemente al sustrato por la sustancia adhesiva, aunque se estima que la resistencia a la tracción del adhesivo de un cirripedio es alrededor de $1/10$ de la que proporcionan algunos productos epoxídicos comerciales [162].

Sobre la suposición de que las glándulas del cemento serían similares a las de la cutícula [163-164], muchos investigadores plantearon como hipótesis que el mecanismo de endurecimiento se debería al entrecruzamiento aromático [16, 165-168] y que el adhesivo de los cirripedios estaría compuesto por un enlace proteína-quinona-proteína. La caracterización química de la secreción del adhesivo de los cirripedios fue objeto de estudio de los últimos 20 años. Recientemente Naldrett [169] propuso que las quinonas no están presentes en el cemento y éste sería una mezcla de proteínas altamente hidrofóbicas que se unirían a través de residuos de cisteína, otorgándole resistencia a la degradación química y bacteriana.

Las investigaciones sobre el cemento no sólo se focalizan hacia el control del “fouling”, sino también hacia el desarrollo de cementos similares en dureza y resistencia al agua para uso odontológico o soldadura de huesos fracturados.

Los **anfípodos** tubícolas están representados principalmente por especies del gén. *Corophium* [6]. Los habitáculos que construyen son cortos y están constituidos fundamentalmente por limo y arena.

Entre los artrópodos también están incluidos los copépodos (*Tisbe*, *Paraltheuta minuta*), anfípodos (*Caprella* spp.), cangrejos (*Cyrtograpsus*), isópodos (*Sphaeroma*), etc. que, si bien son vágiles, juegan un rol importante en las relaciones tróficas de la comunidad incrustante.

Puerto Mar del Plata. *Balanus amphitrite* es la especie que siempre ha sido registrada. Tiene patrones de fijación estacionales, con altos picos de reclutamiento en el verano, pudiendo llegar a ser la especie dominante de la comunidad. Otra especie de cirripedio que se observa en la zona es *Balanus trigonus*; aparece fundamentalmente en verano sobre los paneles acumulativos, una vez que la comunidad ha comenzado a desarrollarse. Cuando está presente en los paneles de reclutamiento lo hace en bajas densidades y tiene ciclos de fijación muy cortos en los meses más cálidos.

En lo que respecta al anfípodo *Corophium* se ha notado, en los últimos ensayos, una disminución en la densidad de colonización.

Puerto Belgrano. *Balanus amphitrite* fue la única especie de cirripedio registrada en esta zona, tendiendo a colonizar los paneles de carena, probablemente por no tener en ellos problemas de competencia espacial con otras especies. El ciclo es marcadamente estacional durante los períodos de mayor temperatura.

En los primeros ensayos realizados en Puerto Belgrano el anfípodo *Corophium* sp. fue mencionado como epibionte de otros organismos, mientras que durante el último período ensayado los tubos estaban adheridos directamente a los paneles de acrílico.

Briozoos [170-171]

Los briozoos son animales coloniales sedentarios, arborescentes o rastreros. Las colonias exhiben una gran variedad de formas y hábitats, las cuales a simple vista pueden ser confundidas con otros organismos sedentarios tales como hidrozoos, ascidias coloniales o a menudo con algas. Pueden formar delicadas matas en las cuales los individuos están en series formando numerosas ramas. También pueden extenderse sobre el sustrato formando capas blandas o calcáreas en forma de encaje (**Fig. 19**).

Cada colonia libera larvas nadadoras planctónicas, denominadas cifonautas, las cuales seleccionan un lugar donde adherirse; posteriormente sufren una rápida transformación en zooide primario o ancéstrula. Cada individuo de la colonia, o zooide, mide aproximadamente 0,5 mm de longitud y se encuentra ubicado en un receptáculo llamado zoecio.

Algunas especies son resistentes a los tóxicos de las pinturas “antifouling” y sus colonias incrustantes pueden formar núcleos para el asentamiento de otros organismos.



Fig. 19.- a) Colonia de briozoo arborescente; b) colonia de briozoo calcáreo con forma de encaje.



Fig. 20.- a) Aspecto general de la fijación de *Ciona intestinalis* (ascidia solitaria) sobre un panel acumulativo en el puerto de Mar del Plata (4 meses de inmersión); b) detalle (10 x).

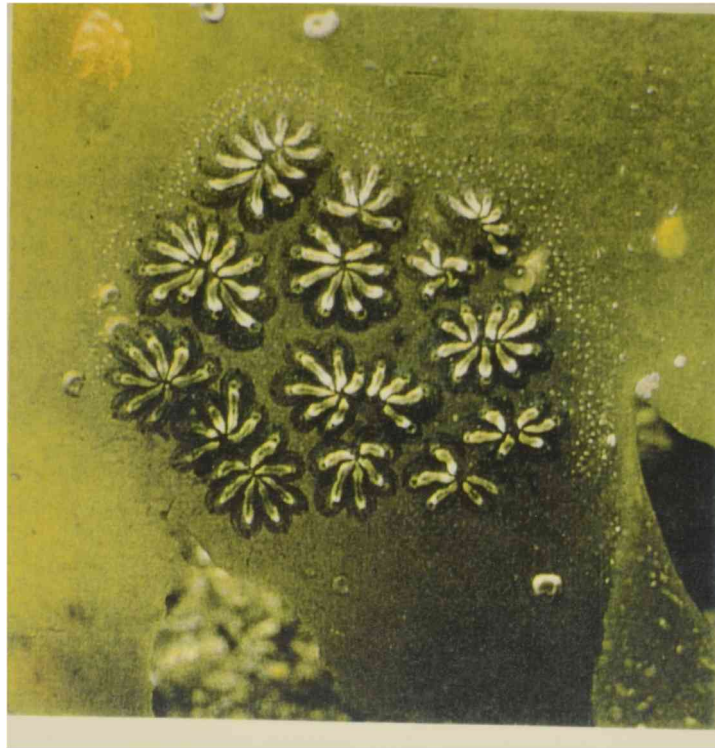


Fig. 21.- *Botryllus*: ascidia colonial (100 x).



Fig. 22.- *Dreissena polymorpha*: mejillón cebra.

Puerto Mar del Plata. El briozoo arborescente *Bugula stolonifera* es el más representativo del grupo, llegando a ser uno de los organismos dominantes durante ciertas etapas sucesionales de la misma.

Las colonias rastreras de *Bowerbankia gracilis*, en los estudios realizados en 1991-92, sólo fueron registradas sobre los paneles acumulativos. A lo largo de los años han presentado variaciones tanto en los períodos como en la densidad de colonización.

Las colonias calcáreas de *Conopeum* sp. han sido registradas siempre en muy bajas densidades por lo cual no son componentes importantes de la comunidad incrustante de la zona.

Puerto Belgrano. Los briozoos correspondientes a esta zona han sufrido cambios en los ciclos de fijación y en su densidad. *Bugula neritina* constituía uno de los organismos más representativos del “fouling” del Puerto Belgrano; su ciclo de fijación era anual con períodos de abundante fijación en los meses más cálidos. *Bugula stolonifera* se presentaba en menor densidad y con un ciclo más restringido que la especie anterior. En el último período de ensayo *B. neritina* decreció notoriamente en abundancia mostrando un ciclo similar al de *B. stolonifera*.

Las colonias incrustantes de *Conopeum* sp. y *Cryptosula pallasiana* también disminuyeron sus abundancias y acortaron sus ciclos de fijación. A pesar de ello, en el período 1993-95, estuvieron más representados que los briozoos arborescentes, formando un delicado tapiz sobre los paneles mensuales. En las etapas más avanzadas del desarrollo de la comunidad pueden competir por el espacio con otras especies, por consiguiente, las colonias pueden separarse del sustrato adoptando distintas formas erguidas o adhiriéndose sobre otros organismos (cirripedios, ascidias, spirórbidos).

Cordados

Ascidias [172]

Las ascidias son animales marinos sésiles, de hábitos filtradores, que pueden vivir en forma solitaria o colonial. Una de sus principales características es la presencia de una túnica de naturaleza química semejante a la celulosa. Habitan desde aguas costeras hasta grandes profundidades, siempre adheridas a sustratos duros.

La estructura esencial de una ascidia solitaria, como *Ciona intestinalis*, está constituida por un cuerpo adherido por su base, con un sifón inhalante y otro exhalante en el extremo opuesto libre (Fig. 20). Son hermafroditas y sus huevos son liberados al mar donde se fertilizan y desarrollan en larvas “renacuajo” de menos de 1 mm de longitud, nadan durante unas horas, pierden su extremo caudal, se fijan y metamorfosean en adultos [173].

En el caso de las ascidias coloniales los zooides están embebidos en una túnica común (Fig. 21) o bien permanecen como individuos unidos por estolones basales. Poseen un sifón inhalante individual y comparten el sifón exhalante. Los huevos fertilizados permanecen retenidos en la colonia y liberan las larvas en el momento que las mismas pueden nadar.

Puerto Mar del Plata. *Ciona intestinalis*, vulgarmente llamada ‘papa de mar’, ha presentado variaciones en su ciclo de fijación, pero siempre ha sido una de las especies dominantes, jugando un rol muy importante en el desarrollo de la comunidad. Se registraron además pocas ascidias coloniales (no determinadas) sobre los paneles de reclutamiento.

Puerto Belgrano. Durante el período 1993-95, las ascidias solitarias *Ciona intestinalis* y *Molgula* sp. presentaron ciclos de fijación breves y en bajas densidades, en ensayos anteriores sólo fue registrada *C. intestinalis*. En los paneles acumulativos *C. intestinalis* fue la especie dominante de la comunidad en desarrollo a partir del noveno mes de inmersión. *Botryllus* spp. y otras ascidias coloniales no determinadas fueron observadas en los paneles de reclutamiento, pero fueron más conspicuas en estados avanzados del desarrollo de la comunidad.

Otros grupos

Aunque es común encontrar dentro del “fouling” gusanos planos (Phylum Platyhelmintha) o cilíndricos (Phylum Nematoda) de vida libre, no se han encontrado registros bibliográficos sobre los mismos. Cabe señalar que los estudios sistemáticos de estos grupos están referidos a aquellas formas de vida parásita.

“FOULING” DULCEACUÍCOLA

Aunque en la mayoría de los casos el “biofouling” dulceacuícola no presenta las características de agresividad del medio marino, el aumento de la navegación en los ríos por buques de ultramar y los efectos de las construcciones realizadas por el hombre (diques, represas, embalses, etc.) imponen la necesidad de continuar efectuando relevamientos de las comunidades incrustantes en puntos económicamente importantes [174] a fin de verificar si es necesario emplear sistemas de control.

Existen en particular dos especies, *Corbicula fluminea* (Bivalvia, Corbiculidae) y *Dreissena polymorpha* (Bivalvia, Dreissenidae), que ocasionan graves problemas en distintos ambientes lóticos y lénticos del mundo [175]. Luego de la última glaciación del Cuaternario en que *Dreissena polymorpha* (Fig. 22) había quedado confinada a los mares Negro y Caspio, comienza su propagación hacia Inglaterra y Suecia. A través del curso de los ríos Volga, Dnieper y afluentes, pero fundamentalmente por el Danubio, *Dreissena* llegó al centro de Europa y, en la primera mitad del siglo pasado, ya se habían encontrado ejemplares en los ríos de Bélgica, Alemania, Dinamarca, y Holanda; en la segunda mitad, en Francia y más tarde en Suiza. En Italia se registró por primera vez en el lago de Garda, adherida al casco de una embarcación; su expansión fue tan rápida que actualmente “tapiza” los sustratos rocosos y detríticos. El éxito de su invasión se debe fundamentalmente a que mantuvo dos características típicas de los moluscos marinos: la larva velíger y la presencia de un biso. La presencia de una larva de tipo planctónico, es decir, capaz de ser transportada decenas de kilómetros por las corrientes, favorece la dispersión de *Dreissena* que, de este modo, puede fijarse en sitios alejados de su lugar de origen. Desde el lago de Garda se expandió hacia el sistema fluvial del río Po y colonizó los diques artificiales de la región. El éxito de su invasión se debió también a que pasó a ocupar un nicho ecológico prácticamente vacío ya que, excepto una pocas esponjas, no existen otros filtradores sobre sustratos duros en las aguas dulces.

La magnitud de los inconvenientes generados por la rápida colonización de estos moluscos en América del Norte, llevó a la organización de congresos y simposios dedicados exclusivamente a la actualización de los avances de las investigaciones en el campo de la biología, ecología, impacto sobre los ecosistemas, técnicas de monitoreo y alternativas de control [176-183].

La introducción de *Dreissena* y *Corbicula* se debió fundamentalmente al traslado de sus larvas en los lastres de los buques cargueros que, procedentes de Europa y Asia, llegaron a América (antropocoria inadvertida). La rápida maduración sexual, alta tasa reproductiva y adaptabilidad de estos organismos, permite su dispersión a través de los cursos de agua dulce y la colonización de distintos sustratos duros. Esta situación acarrea graves inconvenientes desde el punto de vista mecánico, porque pueden dificultar la apertura y cierre de compuertas de diques, obstruir cañerías en las tomas de agua de plantas potabilizadoras y canales de riego, y también en sistemas de enfriamiento industriales, plantas nucleares y usinas termoeléctricas. Además deben ser considerados desde el punto de vista sanitario, ya que afectan la calidad del agua de consumo por alteración de su sabor. En el aspecto comercial pueden afectar la industria de la extracción de arena y grava (por ejemplo, *Corbicula* causó el cierre de doce compañías areneras ubicadas sobre los ríos Cumberland y Tennessee [184] y, en el caso de los buques, es necesario el retiro de servicio para su limpieza en dique seco. Por otra parte, debido a sus hábitos filtradores, reducen el alimento disponible de larvas y adultos de peces de importancia económica. Desde el punto de vista biológico, la presencia de estos bivalvos también es altamente desfavorable ya que compiten por el alimento y espacio con las especies autóctonas desplazándolas y ocupando su nicho ecológico.

En virtud del incremento de los intercambios comerciales, han ocurrido fenómenos parecidos en Estados Unidos con el bivalvo *Corbula manilensis* (Bivalvia, Sphaerioidae), de origen chino, en Calcuta con *Modiolus striatulus* (Bivalvia, Mytilidae) y en Hong Kong con *Limnoperna fortunei* (Bivalvia, Mytilidae). Esta última especie ha sido registrada también en el litoral argentino del Río de la Plata en septiembre de 1991 en el Balneario Bagliardi (34° 55'S- 55° 49'W), dispersándose rápidamente hasta el arroyo Miguelín y Boca Cerrada (34° 48'S- 57° 59'W). *L. fortunei* junto con *Corbicula fluminea* y *C. largillierti* (también de origen asiático, citadas por primera vez en 1979) son las tres especies invasoras en aguas del Río de la Plata. *C. fluminea* ha sido registrada también hasta la desembocadura del brazo del Paraná de las Palmas (34° 19'S- 58° 30'W) y zonas de influencia del río Uruguay) [185-189].

Resulta fundamental estar alerta acerca de la necesidad de realizar muestreos periódicos, a fin de conocer la distribución de especies invasoras perjudiciales que puedan ingresar con los barcos que traen productos de importación.

CONSIDERACIONES FINALES

La gran diversidad de organismos que integran las comunidades incrustantes de los distintos mares y ríos del mundo impone la necesidad de realizar estudios teniendo en cuenta la mayor cantidad de variables posibles a fin de lograr un conocimiento global del problema. Los factores que influyen en el asentamiento y fijación de los organismos son, fundamentalmente, el grado de penetración de la luz, las variaciones del pH y la temperatura, la naturaleza química del sustrato, la tensión superficial y la competencia intra e interespecífica. Un aspecto sumamente importante es también el grado de urbanización que provoca un progresivo

incremento de la concentración de contaminantes que, no pudiendo incorporarse a los ciclos biogeoquímicos en forma natural, terminan deteriorando la calidad de las aguas ya sea por alteración de su transparencia, por elevación del tenor de iones tóxicos o, como en el caso de los detergentes, por disminución del intercambio de oxígeno con el medio aéreo.

Los factores anteriormente mencionados pueden producir variaciones anuales e inclusive entre las diferentes estaciones las cuales son observables a nivel de las poblaciones vegetales y animales. Todo esto justifica la necesidad de realizar estudios a corto plazo y continuar con las investigaciones sobre este tema, a fin de obtener información detallada de las tendencias de reclutamiento que, con el tiempo, permiten lograr un conocimiento más acabado del desarrollo de la comunidad. Este tipo de estudios integrados con ensayos a largo plazo ayudan a comprender la dinámica y estructura de las comunidades.

El conocimiento de la biología larval a través de muestreos de plancton *in situ* o bien por cultivo en laboratorio a partir de formas adultas, permite comprobar las preferencias de asentamiento en la etapa de fijación; de este modo es factible determinar predilecciones por sustratos limpios, o sustratos con organismos ya adheridos o bien por sustratos “impregnados” con extractos de los mismos. El comportamiento de las larvas y adultos del “fouling” en el medio marino es motivo de estudio en distintas latitudes, ya que es necesario contar con un patrón de referencia que permita estimar el efecto de los tóxicos incorporados a las pinturas utilizadas para su control. En general, se ha recurrido a los metales pesados para proteger las distintas estructuras sumergidas en el mar, pero la creciente preocupación por los efectos perjudiciales sobre la salud humana y el medio ambiente llevaron a restringir e incluso, en algunos casos, a prohibir su utilización. En la actualidad, la tendencia a nivel mundial es controlar las incrustaciones biológicas por medio de métodos alternativos; el desarrollo de esquemas “antifouling” novedosos por utilización de sustancias naturales o artificiales no tóxicas comprende muchos pasos, desde la etapa experimental a nivel de laboratorio hasta su potencial impacto en el medio ambiente.

Es un objetivo a nivel mundial integrar los resultados de la investigación científica y tecnológica al sistema de producción, con el fin de contribuir al desarrollo económico y social para obtener una mejor calidad de vida. Para ello, es necesario fortalecer la transferencia de tecnología entre el sector de la investigación, el sector de la producción y el de los usuarios. En lo que respecta al “fouling”, para lograr un efectivo control preservando a la vez el medio ambiente, es imprescindible realizar un trabajo interdisciplinario con la participación de biólogos, bioquímicos, ecotoxicólogos, químicos e ingenieros conjuntamente con la industria.

GLOSARIO

Algas. Plantas acuáticas, marinas o de agua dulce, fotosintetizantes. El cuerpo de la planta puede ser uni o multicelular. La clasificación sistemática se basa en la estructura, pigmentos, composición química de la pared celular, etc.

Ancéstrula. Primer zooide de una colonia de briozoos. Surge a partir de una larva producida sexualmente que luego se fija y metamorfosea; de ella se origina el resto de la colonia por reproducción asexual y su aspecto es, por lo general, diferente al de un zooide adulto siendo característico de cada especie.

Animales coloniales. Tipo de animales organizados en una asociación (*colonia) de individuos.

Bentónicos. Organismos que viven en o sobre el fondo.

Biso. Conjunto de filamentos córneos secretados por una glándula del pie por los cuales los Mytilidae (mejillones) se fijan a los sustratos duros.

Branquia. Estructura respiratoria característica de animales acuáticos.

Colonia. Grupo de individuos interconectados anatómica y funcionalmente.

Cutícula. Capa no celular que recubre a un animal o a una planta, segregada por la epidermis. La presentan la mayor parte de los invertebrados y está constituida principalmente por una proteína similar al colágeno o por *quitina. En los artrópodos tiene bastante consistencia para actuar como exoesqueleto. En los crustáceos está impregnada por sales cálcicas.

Ecdisis. Muda. En los artrópodos, cambio periódico de la *cutícula.

Epibiosis. Fenómeno por medio del cual un organismo utiliza a otro organismo como sustrato.

Espículas. Estructuras en forma de aguja u otras formas, de carbonato de calcio, material silíceo o córneo, que le brindan sostén al cuerpo de la mayoría de las esponjas.

Espongina. Material córneo fibroso flexible, similar al colágeno, que forma el esqueleto de varias demosponjas.

Eufótica. Zona de los estratos más superiores del agua que recibe luz suficiente para realizarse la fotosíntesis.

Fagótrofos. Organismos que se alimentan a expensas de materia orgánica ya formada. Consumidores primarios o herbívoros, consumidores secundarios o carnívoros.

Frústulo. Membrana silificada que constituye el caparazón de una diatomea y se compone de dos tecas, las cuales encajan una en otra por sus bordes, como una caja y su respectiva tapa.

Gemación. Reproducción asexual en la que una pequeña parte de un organismo desarrolla otros individuos u otras partes equivalentes de una colonia.

Hermafroditas. Organismos que producen gametas femeninas y masculinas.

Hidrorriza. Parte reptante de una colonia de hidrozooos, adherida al sustrato.

Larva. Forma preadulta en que salen del huevo algunos animales, capaz de alimentarse por sí misma aunque en general de una manera diferente a la del adulto. Se convierte en adulto mediante un proceso de metamorfosis.

Medusas. Cnidarios pelágicos con forma de sombrilla, vulgarmente denominados “aguas vivas”.

Metagénesis. Ciclo reproductivo con alternancia de generaciones sexual y asexual, como en muchos hidrozooos.

Metamorfosis. Sucesión de etapas, generalmente muy distintas, que componen el desarrollo de un animal, especialmente en lo que se refiere a invertebrados y vertebrados inferiores. Período de transformación del estado de *larva a la forma adulta.

Pez. Sustancia resinosa, sólida, de color pardo amarillento, lustrosa y quebradiza, que se obtiene vertiendo en agua fría el residuo que deja la trementina después de extraer el aguarrás.

Planctónicos. Organismos acuáticos flotantes; algunos pueden poseer movilidad pero su traslado se debe al movimiento del agua. En general son de tamaño pequeño.

Pólipos. Individuos bentónicos, solitarios o coloniales, representan la fase asexual del ciclo de vida muchos cnidarios. En los antozoos, que sólo tienen la forma pólipo, presentan las fases sexual y asexual.

Productores. Organismos que sintetizan materia orgánica a partir de sustratos inorgánicos: autótrofos (por ej. plantas).

Quitina. Polímero de la glucosamina sintetizada por muchos animales; forma una sustancia estable como una cubierta externa en artrópodos, impregnada de sales calcáreas, puede constituir un esqueleto firme y rígido.

Reclutamiento. Conjunto de organismos recién asentados sobre un sustrato.

Sésiles. Dícese de los organismos fijados sobre un sustrato: sedentarios.

Saprótrofos. Organismos que obtienen materia orgánica en disolución de los tejidos muertos o en descomposición de las plantas o animales (saprofíticos o saprozoicos, respectivamente), por ej. bacterias y hongos.

Sistemática. Término que con frecuencia se usa como sinónimo de *taxonomía, otras veces se interpreta en un sentido más amplio y abarca también la identificación, clasificación y nomenclatura de los organismos.

Taxón. Término general para un grupo taxonómico de cualquier categoría.

Taxonomía. Estudio de la clasificación de los organismos según sus semejanzas y diferencias.

Teca. Cada una de las dos piezas silíceas que forman la cubierta de la célula de una diatomea, comparables a la tapa y al fondo de una caja de Petri.

BIBLIOGRAFÍA

- [1] Sghibartz, C. M. "Antifouling paints - Today and tomorrow". Proc. 6th Int. Congr. Mar. Corr. Foul., Marine Biology, Athens, Greece, 399-413 (1984).
- [2] Evans, L. V., Hoagland, K. D. (eds.) "Algal biofouling". Studies in Environmental Science 28, Elsevier, VII-IX (1986).
- [3] Darwin, Ch. "A monograph on the sub-class Cirripedia, with figures of all the species. The Lepadidae; or, Pedunculated Cirripedes". Ray Society, London, 410 pp. (1851).
- [4] Darwin, Ch. "A monograph on the sub-class Cirripedia, with figures of all the species. The Balanidae, (or Sessile Cirripedes); The Verrucidae, etc.". Ray Society, London, 712 pp. (1854).
- [5] Caillet-Bois, T. "Historia Naval Argentina". Escuela Naval Militar, Río Santiago, 552 pp. (1944).
- [6] Woods Hole Oceanographic Institution. "Marine fouling and its prevention". United States Naval Institute, Annapolis, Maryland, 368 pp. (1952).
- [7] Destefani, L. H. "Famosos veleros argentinos". Centro Naval, Instituto de Publicaciones Navales, 213 pp. (1967).
- [8] Dick, R. J. "Antifouling coatings. Man versus marine fouling". Paint and Varnish Production, 35-40 (1970).
- [9] Pischky, H. "To the history of antifouling protection and the development of antifouling paint until now". Antifouling-Symposium, CIBA-GEIGY Marienberg GMBH, 1-7 (1971).
- [10] "El mar". Gran Enciclopedia Salvat, Salvat S.A. de Ediciones, Pamplona, 10 tomos (1975).
- [11] Marks, R. L. "Tres hombres a bordo del Beagle". J. Vergara (de.), Buenos Aires, 217 pp. (1994).
- [12] Rascio, V. "Antifouling protection by paints". Proc. Argentine-USA Workshop on Biodeterioration (CONICET-NSF). Published by AQUATEC Química S.A., Sao Paulo, Brasil, 259-278 (1985).
- [13] Murpphy, P. V., Michel, P., Guelorget, O., Latour, M. "Piezoelectric polymer hull vibrators for fouling prevention". Proc. 5th Int. Congr. Mar. Corr. Foul., Biología Marina, Barcelona, España, 293- 298 (1980).
- [14] Branscomb, E. S., Rittschof, D.E. "An investigation of low frequency sound waves as a means of inhibiting barnacle settlement." J. Exp. Mar. Biol. Ecol., 79(2), 149-154 (1984).

- [15] Fletcher, R. L., Baier, R. E., Fornalik, M. S. "The influence of surface energy on spore development in some common marine fouling algae". Proc. 6th Int. Congr. Mar. Corr. Foul., Marine Biology, Athens, Greece, 129-144 (1984).
- [16] Lindner, E., Dooley, C., Doeff, M. "Adhesion of barnacles and development of non-toxic antifoulants". Preprint 7th Int. Congr. Mar. Corr. Foul., Biología Marina, Valencia, España, 16 pp. (1988).
- [17] Safriel, U., Erez, N. "Effect of limpets on the fouling of ships in the Mediterranean". Mar. Biol., 95, 531-537 (1991).
- [18] Safriel, U., Erez, N., Keasar, T. "How do limpets maintain barnacle-free submerged artificial surfaces?". Bull. Mar. Sci., 54 (1), 17-23 (1994).
- [19] Shkedy, Y., Safriel, U., Keasar, T. "Life-history of *Balanus amphitrite* and *Chthamalus stellatus* recruited to settlement panels in the Mediterranean coast of Israel". Israel Journal of Zoology, 41, 147-161 (1995).
- [20] Goupil, D. W., DePalma, V. A., Baier, R. E. "Physical/chemical characteristics of the macromolecular condition film in biological fouling". Proc. 5th Int. Congr. Mar. Corr. Foul., Biología Marina, Barcelona, España, 401-410 (1980).
- [21] Stupak, M. E., Pérez, M. C., Di Sarli, A. "Relación entre la fijación de micro y macro 'fouling' y los procesos de corrosión de estructuras metálicas". Rev. Iberoam. Corr. Prot. XXI (6), 219-225 (1990).
- [22] Rascio, V., Bruzzoni, W. O., Bastida, R., Rozados, E. "Protección de superficies metálicas". Serie III - Manuales Científicos, Nº 1, LEMIT, 454 pp. (1977).
- [23] Kinne, O.(ed.) "Marine ecology. A comprehensive, integrated treatise on life in oceans and coastal waters. Vol I. Environmental factors". Part 1, John Wiley & Sons, 681 pp. (1978).
- [24] Rascio, V., Giúdice, C. A., del Amo, B. "Research and development on soluble matrix antifouling paints to be use on ships, offshore platforms and power stations. A review". Corrosion Reviews, VIII (1-2), 89-153 (1988).
- [25] Muraoka, J. S. "Effects of marine organisms". Machine Design, January 18, 184-187 (1968).
- [26] Pipe, A. "The fouling of fixed structures". Marine fouling, OYEZ International Business Communications, London, 7 pp. (1979).
- [27] Thorhaug, A., Marcus, J. "Macrofouling problems associated with Ocean Thermal Energy Conversion (OTEC) units". Proc. 5th Int. Congr. Mar. Corr. Foul., Biología Marina, Barcelona, España, 225-230 (1980).

- [28] Edyvean, R. G., Terry, L. A., Picken, G. B. "Marine fouling and its effects on offshore structures in the North Sea. A review". *International Biodeterioration*, 21 (4), 277-284 (1985).
- [29] Terry, L. A., Picken, G. B. "Algal fouling in the North Sea". En: 'Algal biofouling' (Evans, L V, Hoagland, K. D., eds.). *Studies in Environmental Science* 28, Elsevier, 179-192 (1986).
- [30] Santhakumaran, L. N. "The problems of marine fouling. A partial overview". *Proc. of the Specialists' Meetings on Marine Biodeterioration with reference to Power Plant Cooling Systems*, IGCAR, Kalpakkam, 26-28 April 1989, (Nair, K. V. K., Venugopalan, V. P., eds.), 19-34 (1990).
- [31] Ardisson, P. L., Bourget, E. "Large-scale ecological patterns: discontinuous distribution of marine benthic epifauna". *Mar. Ecol. Prog. Ser.*, 83, 15-34 (1992).
- [32] Lively, C. M., Raimondi, P. T., Delph, L. F. "Intertidal community structure: space-time interactions in the northern Gulf of California". *Ecology*, 74 (1), 162-173 (1993).
- [33] Southward, A. J. "The importance of long time-series in understanding the variability of natural systems". *Helg. wiss. Meer.*, 49, 329-333 (1995).
- [34] Bastida, R. "Preliminary notes of the marine fouling at the port of Mar del Plata (Argentina)". *Proc. 2nd Int. Congr. Mar. Corr. Foul.*, Athens, Greece, 557-562 (1968).
- [35] Bastida, R. "Las incrustaciones biológicas en el puerto de Mar del Plata, período 1966/67 (primera parte). Estudio sobre paneles mensuales". *LEMIT Serie II*, 1-68 (1968).
- [36] Bastida, R. "Las incrustaciones biológicas en el puerto de Mar del Plata, período 1966/67 (segunda parte). Estudio sobre paneles acumulativos". *LEMIT-Anales*, (4), 1-60 (1969).
- [37] Bastida, R. "Las incrustaciones biológicas de las costas argentinas. La fijación anual en el puerto de Mar del Plata durante tres años consecutivos". *Corrosión y Protección*, 2 (1), 21-37 (1971).
- [38] Bastida, R., Torti, M. R. "Estudio preliminar de las incrustaciones biológicas de Puerto Belgrano". *LEMIT-Anales*, (3), 45-75 (1971).
- [39] Bastida R. "Studies of the fouling communities along argentine coasts". *Proc. 3rd Int. Congr. Mar. Corr. Foul.*, National Bureau of Standards, Gaithersburg, Maryland, USA, 847-864 (1972).
- [40] Bastida, R., Spivak, E., L'Hoste, S., Adabbo, H. "Las incrustaciones biológicas de Puerto Belgrano. I. Estudio de la fijación sobre paneles mensuales, período 1971/72". *LEMIT-Anales* (3), 97-165 (1974).

- [41] Bastida, R., Spivak, E., L'Hoste, S., Adabbo, H. "Las incrustaciones biológicas de Puerto Belgrano. II. Estudio de los procesos de epibiosis registrados sobre paneles mensuales". LEMIT-Anales (3), 167-195 (1974).
- [42] Bastida, R., L'Hoste, S. "Trophic relations of the fouling communities at the port of Mar del Plata". LEMIT-Anales, 159-203 (1976).
- [43] Bastida, R., Adabbo, H. "Fijación de "fouling" en el puerto de Mar del Plata, período 1969/70". Corrosión y Protección, 8 (5), 1-14 (1977).
- [44] Bastida, R., Bastida, V. L. de, "Las incrustaciones biológicas de Puerto Belgrano. III. Estudio de los procesos de epibiosis registrados sobre paneles acumulativos". CIDEPINT-Anales, 54-97 (1978).
- [45] Bastida, R., Mandri, M. T. de, Bastida, V. L. de, Stupak, M. "Ecological aspects of the marine fouling at the Port of Mar del Plata, Argentina, during the period 1973/74". Proc. 5th Int. Congr. Mar. Corr. Foul., Biología Marina, Barcelona, España, 299-320 (1980).
- [46] Stupak, M. E., Bastida, R., Arias, P. J. "Las incrustaciones biológicas del puerto de Mar del Plata (Argentina). Período 1976/77". CIDEPINT-Anales, 173-231 (1980).
- [47] Stupak, M. E. "Acción de pinturas tipo matriz soluble sobre los componentes vegetales y animales del fouling". CIDEPINT-Anales, 261-309 (1982).
- [48] Stupak, M. E. "Studies of fouling of Argentine coasts". Proc. Argentine-USA Workshop on Biodeterioration (CONICET-NSF). Published by AQUATEC Química S.A., Sao Paulo, Brasil, 239-258 (1985).
- [49] Pezzani, S., Pérez, M., Stupak, M. "Macrofouling community at Mar del Plata harbor during a one-year period (1991-1992)". Corrosion Reviews, Special Issue on Industrial Paints for Corrosion Control, 14 (1-2), 73-86 (1996).
- [50] Pérez, M. C., García, M. T., Stupak, M. E. "Estudio del 'fouling' sobre balsa experimental en Puerto Belgrano. Diciembre 1993 a marzo 1995". Inédito.
- [51] Rascio, V., Giúdice, C. A., Benítez, J. C., Presta, M. A. "Comportamiento de pinturas antiincrustantes en servicio y balsa experimental". Rev. Iberoam. de Corrosión y Protección, 11 (2), 23-52 (1980).
- [52] Rascio, V. "Pinturas antiincrustantes". Manual ECOMAR de corrosión y protección, SENID, 93-101 (1981).
- [53] Rascio, V., Giúdice, C. A., Benítez, J. C., Presta, M. A. "Preliminary ships' trials of chlorinated rubber antifouling paints". CIDEPINT-Anales, 58-73 (1981).
- [54] Giúdice, C. A., Benítez, J. C., Rascio, V. "Influence of the use of chlorinated rubber on the anticorrosive properties of paints for ships' hulls". J. Oil Col. Chem. Assoc., 65(4), 148-165 (1982).

- [55] Giúdice, C. A., Benítez, J. C., Rascio, V. "Prevención del 'fouling' en carenas de embarcaciones con pinturas antiincrustantes a base de colofonia y caucho clorado". *Rev. Iberoam. de Corrosión y Protección*, 15 (1), 16-20 (1984).
- [56] Rascio, V., Giúdice, C. A., del Amo, B. "High build soluble matrix antifouling paints tested on raft and on ship bottom". *Progress in Organic Coatings*, 18 (4), 389-398 (1990).
- [57] Capitoli, R. R. "Sequência temporal de colonização e desenvolvimento da comunidade incrustante na região mixohalina da lagoa dos Patos; RS, Brasil". Tesis, Universidade do Rio Grande, 99 pp.(1983).
- [58] Sutherland, J. P., Karlson, R. H. "Succession and seasonal progression in the fouling community at Beaufort, North Carolina". *Proc. 3rd Int. Congr. Mar. Corr. Foul.*, National Bureau of Standards, Gaithersburg, Maryland, USA, 906-929 (1972).
- [59] Levin, S. A., Paine, R. T. "Disturbance, patch formation, and community structure". *Proc. Nat. Acad. Sci. (USA)*, 71, 2744-2747 (1974).
- [60] Menge, B. A., Sutherland, J. P. "Species diversity gradients: synthesis of the roles of predation, competition and temporal heterogeneity". *Am. Nat.*, 110, 351-369 (1976).
- [61] Karlson, R. "Predation and space utilization patterns in a marine epifaunal community". *J. Exp. Mar. Biol. Ecol.*, 31, 225-239 (1978).
- [62] Menge, B. A. "Predation intensity in a rocky intertidal community. Relation between predator foraging activity and environmental harshness". *Oecologia (Berlin)*, 34, 1-16 (1978).
- [63] Sousa, W. P. "The responses of the community to disturbance: the importance of successional age and species' life histories". *Oecologia (Berlin)*, 45, 72-81 (1980).
- [64] Ayling, A. M. "The role of biological disturbance in temperate subtidal encrusting communities". *Ecology*, 62 (3), 830-847 (1981).
- [65] Sutherland, J. P. "The fouling community at Beaufort, North Carolina: a study in stability". *Am. Nat.*, 118 (4), 499-519 (1981).
- [66] Chalmer, P. N. "Settlement patterns of species in a marine fouling community and some mechanisms of succession". *J. Exp. Mar. Biol. Ecol.*, 58 (1), 73-85 (1982).
- [67] Field, B. "Structural analysis of fouling community development in the Damariscotta river estuary, Maine". *J. Exp. Mar. Biol. Ecol.*, 57 (1), 25-33 (1982).
- [68] Greene, C. H., Schoener, A. "Succession on marine hard substrata: a fixed lottery". *Oecologia (Berlin)*, 55, 289-297 (1982).

- [69] Otsuka, C. M., Dauer, D. M. "Fouling community dynamics in Lynnhaven Bay, Virginia". *Estuaries*, 5 (1), 10-22 (1982).
- [70] Greene, C. H., Schoener, A. "Multivariate analysis of three-dimensional data in the study of succession in marine fouling communities". *Proc. 6th Int. Congr. Mar. Corr. Foul., Marine Biology*, Athens, Greece, 221-235 (1984).
- [71] Possingham, H. P., Roughgarden, J. "Spatial population dynamics of a marine organism with a complex life cycle". *Ecology*, 71 (3), 973-985 (1990).
- [72] Costlow, J. D. Jr., Bookhout, C. "Larval development of *Balanus amphitrite* var. *denticulata* Broch reared in the laboratory". *Biol. Bull. Mar. Biol. Lab.*, 114 (3), 284-295 (1958).
- [73] Barnes, H., Barnes, M. "In vitro development of cirripede eggs". *Vidensk. Medd. fra Dansk naturh. Foren.*, bd. 125, 93-100 (1963).
- [74] Freiburger, A., Cologer, C. "Rearing barnacles in the laboratory." *Naval Research Reviews*, 18 (10), 8-13 (1965).
- [75] Edwards, P., Baalen, Ch. "An apparatus for the culture of benthic marine algae under varying regimes of temperature and light-intensity". *Bot. Mar.*, XII, 42-43 (1970).
- [76] Jebram, D. "Preliminary experiments with Bryozoa in a simple apparatus for producing continuous water currents". *Helg. wiss. Meer.*, 20, 278-292 (1970).
- [77] Forbes, L., Seward, M., Crisp, D. J. "Orientation to light and the shading response in barnacles". 4th European Marine Biol. Symposium. (Crisp, D. J., ed.), Cambridge, 539-558 (1971).
- [78] Guillard, R. "Culture of phytoplankton for feeding marine invertebrates". *Coll. Rep. Woods Hole Ocean. Inst.*, 1 (3233), 29-60 (1975).
- [79] Denley, E. J., Underwood, A. J. "Experiments on factors influencing settlement, survival, and growth of two species of barnacles in New South Wales". *J. Exp. Mar. Biol. Ecol.*, 36, 269-293 (1978).
- [80] Hanisak, M. "Growth patterns of *Codium fragile* ssp. *tomentosoides* in response to temperature, irradiance, salinity, and nitrogen source". *Mar. Biol.*, 50, 319-332 (1979).
- [81] Jereos-Aujero, E. "Growth phases of culture algae used as larval food". *Quarterly Research Report, SEAFDE, Filipinas*, 4 (1), 15-16 (1980).
- [82] Seeliger, U., Cordazzo, C. V. "Critérios para la construção de uma sala de cultivos." *Atlântica*, Rio Grande, 4, 73-78 (1980).
- [83] Seeliger, U., Cordazzo, C. V. "Métodos de cultivo de algas marinhas bentônicas em laboratório". *Atlântica, Doc. Téc.*, (1980).

- [84] Rittschof, D. E., Branscomb, E., Costlow, D. J. "Settlement and behavior in relation to flow and surface in larval barnacles, *Balanus amphitrite* Darwin". J. Exp. Mar. Biol. Ecol., 82 (2-3) 131-146 (1984).
- [85] Stupak, M. E. "Método de concentración y conservación de *Skeletonema costatum* para la alimentación de larvas de cirripedios". CIDEPINT-Anales, 135-144 (1986).
- [86] D'Abramo, L. R., Reed, L., Heinzen, J. M. "A culture system for nutritional studies of crustaceans". Aquaculture, 72, 379-389 (1988).
- [87] Pérez, M. C., Stupak, M. E. "Influencia de luz de distintas longitudes de onda sobre la supervivencia de nauplii de *Balanus amphitrite* Darwin criadas en laboratorio". CIDEPINT-Anales, 93-105 (1988).
- [88] Stone, C. J. "A comparison of algal diets for cirripede nauplii". J. Exp. Mar. Biol. Ecol., 132, 17-40 (1989).
- [89] Stupak, M. E., Pérez, M. C. "Experiencias de cría en laboratorio de *Balanus amphitrite*". CIDEPINT-Anales, 105-118 (1990).
- [90] Kallas, D. H., Freiburger, A., Cologer, C. P. "A fundamental approach to marine fouling studies using laboratory reared organisms". Proc. 2nd Int. Congr. Mar. Corr. Foul., Athens, Greece, 609-623 (1968).
- [91] Tighe-Ford, D. J., Power, M. J. D., Vaile, D. C. "Laboratory rearing of barnacle larvae for antifouling research". Helg. wiss. Meer., 20, 393-405 (1970).
- [92] Phipps, G., Holcombe, G., Fiandt, J. "Saturator system for generating toxic water solutions for aquatic bioassays". Prog. Fish-Cult., 44 (2), 115-116 (1982).
- [93] Pérez, M. C., Stupak, M. E. "Pinturas antiincrustantes tipo matriz soluble; influencia de la relación tóxico principal/tóxico de refuerzo sobre larvas de *Balanus amphitrite* y *Polydora ligni*". CIDEPINT-Anales, 195-211 (1992).
- [94] Vetere, V. F., Pérez, M. C., Romagnoli, R., Stupak, M. E. "Chemical and biocidal properties of the cuprous thiocyanate used as antifouling pigment". CIDEPINT-Anales, 161-172 (1993).
- [95] Vetere, V. F., Pérez, M. C., Romagnoli, R., Stupak, M. E. "Solubility and toxic effects of the cuprous thiocyanate antifouling pigment on barnacle larvae" (Aceptado para su publicación en: J. C. T:).
- [96] Sieburth, J., Conover, J. T. "*Sargassum* tannin, an antibiotic which retards fouling". Nature, 208 (5005), 52-53 (1965).
- [97] Kirchman, D., Graham, S., Reisch, D., Mitchell, R. "Lectins may mediate on the settlement and metamorphosis of *Janua (Dexiospira) brasiliensis* Grube (Polychaeta: Spirorbidae)". Mar. Biol. Letters, 3, 131-142 (1982).

- [98] Mohamed, S., Ayoub, H. "TAN: a new molluscicide and algicide from the fruits of *Acacia nilotica*". J. Chem. Tech. Biotech., 32 (7), 728-734 (1982).
- [99] Standing, J. D., Hooper, I. R., Costlow, J. D. "Inhibition and induction of barnacle settlement by natural products present in octocorales". J. Chem. Ecol., 10, 823-834 (1984).
- [100] Maki, J. S., Mitchell, R. "Involvement of lectins in the settlement and metamorphosis of marine invertebrate larvae". Bull. Mar. Sci., 37 (2), 675-683 (1985).
- [101] Rittschof, D. E., Hooper, I. R., Branscomb, E., Costlow, J. D. "Inhibition of barnacle settlement and behavior by natural products from whip corals, *Leptogorgia virgulata* (Lamarck, 1815)". J. Chem. Ecology, 11 (5), 551-563 (1985).
- [102] Keifer, P. A., Reinhart, K. L., Hooper, I. R. "Renilla-foulings, antifouling diterpenes from the Sea Pansy *Renilla reniformis* (Octocorallia)". J. Org. Chem., 51 (23), 4450-4454 (1986).
- [103] Brady, R. F., Griffith, J. R., Love, K. S., Field, D. E. "Non toxic alternatives to antifouling paints". J. Coatings Technology, 59 (755), 113-119 (1987).
- [104] Goto, R., Kado, R., Muramoto, K., Kamiya, H. "Fatty acids as antifoulants in a marine sponge". Biofouling, 6, 61-68 (1992).
- [105] Willemsem, P. R., Ferrari, G. M. "The use of antifouling compounds from sponges in antifouling paints". Surface Coatings Intern., 10, 423-427 (1993).
- [106] Pérez, M., Gervasi, C., Armas, R., Stupak, M., Di Sarli, A. "The influence of cathodic currents on biofouling attachment to painted metals". Biofouling, 8, 27-34 (1994).
- [107] Zobell, C. "The effect of solid surfaces upon bacterial activity". J. Bacteriol., 46, 39-59 (1943).
- [108] Crisp, D. J. "The role of the biologist in antifouling research". Proc. 3rd Int. Congr. Mar. Corr. Foul., National Bureau of Standards, Gaithersburg, Maryland, USA, 88-93 (1972).
- [109] Neihof, R. A., Loeb, G. I. "Molecular fouling of surfaces in sea water" Proc. 3rd Int. Congr. Mar. Corr. Foul., National Bureau of Standards, Gaithersburg, Maryland, USA, 710-715 (1972).
- [110] Loeb, G. I., Neihof, R. A. "Applied chemistry to protein interfaces". (Baier, R. E., ed.), Adv. in Chem. Series 145, Amer. Chem. Soc., Washington, DC, 1-25 (1975).
- [111] Corpe, W. A. "Effect of the Ocean Environment on Microbial Activities". (Colwell, R. R. and Morita, R. Y., eds.), University Park Press, Baltimore, MD, 397-417 (1974).

- [112] Eashwar, M., Iyer, S. V. K. "Microfouling on cathodically protected mild steel in sea water". Bull. Electrochem., 2 (4), 341-343 (1986).
- [113] Christie, A. D, Evans, L. V., Callow, M. "A new look at marine fouling". Part 4. Shipping World and Shipbuilder, 121-124 (1976).
- [114] Sechler, G. E., Gundersen, K. "Role of surface chemical composition on the microbial contribution to primary films". Proc. 3rd Int. Congr. Mar. Corr. Foul., National Bureau of Standards, Gaithersburg, Maryland, USA, 610-616 (1972).
- [115] Gerchakov, M. S., Marszalek, D. S., Roth, F. J., Udey, L. R. "Succession of periphytic microorganisms on metal and glass: surfaces in natural sea water". Proc. 4th Int. Congr. Mar. Corr. Foul., Antibes, Juan-Les Pins, Francia, 203-211 (1976).
- [116] Marszalek, D. S., Gerchakov, M. S., Udey, L. R. "Influence of substrate composition on marine microfouling". Appl. Environ. Microbiol., 38 (5), 987-995 (1979).
- [117] Zobell, C., Allen, E. "The significance of marine bacteria in the fouling of submerged surfaces". J. Bacteriol., 29, 239-251 (1935).
- [118] Marshall, K. C. "Water Pollution Microbiology". (Mitchell, R., ed.), John Willey & Sons, V. 2, 51-70 (1978).
- [119] Corpe, W. A. "Microfouling: the role of primary film forming marine bacteria". Proc. 3rd Int. Congr. Mar. Corr. Foul., National Bureau of Standards, Gaithersburg, Maryland, USA, 598-609 (1972).
- [120] Zobell, C. "Marine microbiology". Chronica Botanica Co., Waltham, Mass., 194-230 (1946).
- [121] Bastida, R., Stupak, M. E. "Las diatomeas de las comunidades incrustantes del puerto de Mar del Plata. Clave para su reconocimiento". CIDEPINT-Anales, 91-167 (1979).
- [122] Crisp, D. J., Meadows, P. S. "The chemical basis of gregariousness in cirripedes". Proc. Roy. Soc. London, B 156, 500-520 (1962).
- [123] Crisp, D. J., Meadows, P. S. "Absorbed layer: the stimulus to settlement in barnacles". Proc. Roy. Soc. London, B 158, 364-387 (1963).
- [124] Terry, L. A., Edyvean, R. "Influences of microalgae on the corrosion of structural steel". (Lewis, J. R. and Mercer, A. D., eds.) Corrosion and Marine Growth on Offshore Structures. Ellis Horwood Ltd. Chichester, 38-45 (1984).
- [125] Maki, J. S., Rittschof, D., Costlow, J. D., Mitchell, R. "Inhibition of attachment of larval barnacles, *Balanus amphitrite*, by bacterial surface films". Mar. Biol., 97, 199-206 (1988).

- [126] Maki, J. S., Rittschof, D., Samuelsson, M. O., Szewzyk, U., Yule, A. B., Kjelleberg, S., Costlow, J. D., Mitchell, R. "Effect of marine bacteria and their exopolymers on the attachment of barnacle cypris larvae". *Bull. Mar. Sci.*, 46 (2), 499-511 (1990).
- [127] Maki, J. S., Yule, A. B., Rittschof, D., Mitchell, R. "The effect of bacterial films on the temporary adhesion and permanent fixation of cypris larvae, *Balanus amphitrite* Darwin". *Biofouling*, 8, 121-131 (1994).
- [128] Miller, B. T. "The development of marine fouling communities". *Biol. Bull.*, 89, 103-112 (1945).
- [129] Meadows, P. S., Williams, G. B. "Settlement of *Spirorbis borealis* Daudin larvae on surfaces bearing films of micro-organisms". *Nature*, 198 (4880), 610-611 (1963).
- [130] Young, L. Y., Mitchell, R. "The role of microorganisms in marine fouling". *Int. Biodetn. Bull.*, 9 (4), 105-109 (1973).
- [131] Cook, P. A., Henschel, J. R. "The importance of a primary film of microorganisms on the subsequent establishment of a macrofouling community". *Proc. 6th Int. Congr. Mar. Corr. Foul., Marine Biology, Athens, Greece*, 211-20 (1984).
- [132] Miller, M. A., Rapean, J. C., Whedon, W. "The role of slime film in the attachment of fouling organisms". *Biol. Bull.*, 94 (2), 143-57 (1948).
- [133] Crisp, D. J., Ryland, J. S. "The influence of filming and surface texture on the settlement of marine organisms". *Nature*, 188 (4706), 119 (1960).
- [134] Barnes, H. "Adhesion in biological systems". (Mainly, R. S., ed.), Academic Press, 89-111 (1970).
- [135] Dexter, S. C., Wood, R. W. , Mihm, J. "Factors influencing microbial attachment and adhesion". *Proc. Argentine-USA Workshop on Biodeterioration (CONICET-NSF)*. Published by AQUATEC Química S.A., Sao Paulo, Brasil, 145-180 (1985).
- [136] Fletcher, R. L. "Marine fouling algae". *Catalogue of main marine fouling organisms, Algae, Vol. VI, ODEMA*, 62 pp. (1980).
- [137] Evans, L. V., Christie, A. D. "Studies on the ship-fouling alga *Enteromorpha*. I. Aspects of the fine-structure and biochemistry of swimming and newly settled zoospores". *Ann. Bot.*, 34 (135), 451-456 (1970).
- [138] Chamberlain, A. H. L. "Algal settlement and secretion of adhesives materials". *3rd Int. Biodegradation Symposium (Sharpley, J. M., Kaplan, A. M., eds.)*, 417-432 (1976).
- [139] Christie, A. D., Evans, L. V., Callow, M. "A new look at marine fouling". Part 2. *Shipping World and Shipbuilder*, 1043-1045 (1975).

- [140] Houghton, D., Pearman, I., Tierney, D. "The effect of water velocity on the settlement of swarmers of *Enteromorpha* spp.". Proc. 3rd Int. Congr. Mar. Corr. Foul., National Bureau of Standards, Gaithersburg, Maryland, USA, 682-690 (1972).
- [141] Christie, A. D, Evans, L. V. "A new look at marine fouling". Part 1. Shipping World and Shipbuilder, 953-955 (1975).
- [142] Sarà, M. "Marine sponges". Catalogue of main marine fouling organisms, Vol. V, CREO, 42 pp. (1974).
- [143] Cuartas, E. "Algunas Demospongiae (Porifera) de Mar del Plata, Argentina con descripción de *Axociella marplatensis*, sp.n.". Iheringia, Sér. Zool., Porto Alegre (73), 3-12 (1992).
- [144] Morri, C., Boero, F. "Marine fouling hydroids". Catalogue of main marine fouling organisms, Vol. VII, ODEMA, 88 pp. (1986).
- [145] Fauchald, K. "The polychaete worms. Definitions and keys to the orders, families and genera". Natural History Museum County, Science Series 28, 188 pp. (1977).
- [146] Fauvel, P. "Faune de France. 16. Polychètes sédentaires. Addenda aux Errantes, Archiannélides, Myzostomaires". Office Central de Faunistique, Kraus Reprint, Nendeln/Liechtenstein, 494 pp. (1977).
- [147] Kinne, O. "Cultivation of animals: Annelida". Marine ecology. A comprehensive, integrated treatise on life in oceans and coastal waters (Kinne, O., ed.), Vol. III: Cultivation, Part 2, John Wiley & Sons, 720-742 (1977).
- [148] Amaral, A. C., Nonato, E. F. "Anelídeos poliquetos da costa brasileira. Características e chave para famílias. Glossário". CNPq, Série Manuais de Identificação da Fauna Brasileira, Vol. 1/2, 47 pp. (1981).
- [149] "Serpules tubicoles". Catalogue des principales salissures marines, Vol. III, OCDE, 79 pp. (1967).
- [150] DeVore, D. P., Engebretson, G. H., Schachtele, C. F., Sauk, J. J. "Isolation and characterization of adhesive proteins secreted by the sea mussel, *Mytilus edulis*". Proc. 6th Int. Congr. Mar. Corr. Foul., Marine Biology, Athens, Greece, 245-258 (1984).
- [151] Nanishi, K., Murase, M., Yonehara, Y., Kishihara, M., Hiramata, T. "Surface properties of non-toxic antifouling paint film". Preprint 7th Int. Congr. Mar. Corr. Foul., Valencia, España, sección II, 10 pp. (1988).
- [152] Southward, A. J., Crisp, D. J. "Barnacles of european waters". Catalogue of main marine fouling organisms, Vol. I, OECD, 46 pp. (1963).
- [153] Pilsbry, H. A. "The sessile barnacles (Cirripedia) contained in the collections of the U. S. National Museum; including a monograph of the american species". Bull. 93, United States National Museum, 442 pp. (1916).

- [154] Bassindale, R. "The development stages of three English barnacles *Balanus balanoides* (Linn.), *Chtamalus stellatus* (Poli), and *Verruca stroemia* (O. F. Müller)". Proc. Zool. Soc. London, 106, 57-74 (1936).
- [155] Barnes, H., Barnes, M. "Egg size, nauplius size, and their variation with local, geographical, and specific factors in some common cirripedes". J. Anim. Ecol., 34, 391-402 (1965).
- [156] Freiburger, A., Cologer, C. "Rearing acorn barnacle cyprids in the laboratory for marine fouling studies". Naval Engineers Journal, 881-890 (1966).
- [157] Lacombe, D. "Criação de balanídeos em laboratório". Trab. V Congr. Latinoam. Zool., 1, 168-174 (1973).
- [158] Saroyan, J. R. "Countdown for antifouling paints". Proc. 2nd Int. Congr. Mar. Corr. Foul., Athens, Greece, 469-494 (1968).
- [159] Saroyan, J. R., Lindner, E., Dooley, C. A. "Attachment mechanism of barnacles". Proc. 2nd Int. Congr. Mar. Corr. Foul., Athens, Greece, 495-512 (1968).
- [160] Walker, G. "The adhesion of barnacles". J. Adhesion, 12, 51-58 (1981).
- [161] Yule, A. B., Walker, G. "Settlement of *Balanus balanoides*: the effect of cyprid antennular secretion". J. Mar. Biol. Ass. UK, 65, 707-712 (1985).
- [162] Walker, G., Yule, A. B. "Temporary adhesion of the barnacle cyprid: the existence of an antennular adhesive secretion". J. Mar. Biol. Ass. UK, 64, 679-686 (1984).
- [163] Yonge, C. "On the nature and permeability of chitins. I. The chitin lining the foregut of decapod crustacea and the function of the tegumental glands". Proc. Roy. Soc. London, B 111, 298-329 (1932).
- [164] Thomas, H. "Tegumental glands in the Cirripedia Thoracica". Quart. J. Micr. Sci., 84, 257-282 (1954).
- [165] Harris, J. "Report on antifouling research, 1942-1944". J. Iron Steel Inst., 154, 297-333 (1946).
- [166] Pyefinch, K. "Notes on the biology of cirripedes". J. Mar. Biol. Assoc. UK, 27, 464-503 (1948).
- [167] Crisp, D. J. "Mechanisms of adhesion of fouling organisms". Proc. 3rd Int. Congr. Mar. Corr. Foul., National Bureau of Standards, Gaithersburg, Maryland, USA, 691-709 (1972).
- [168] Lindner, E. "Experiments in synthesis of barnacle adhesive". Proc. 5th Int. Congr. Mar. Corr. Foul., Biología Marina, Barcelona, España, 189-212 (1980).

- [169] Naldrett, M. J. "The importance of sulphur cross-links and hydrophobic interactions in the polymerization of barnacle cement". J. Mar. Biol. Ass. UK, 73, 689-702 (1993).
- [170] Ryland, J. S. "Catalogue of main marine fouling organisms, 2, Polyzoa". Organization for Economic Co-operation and Development, París, 82 pp. (1965).
- [171] Bastida, V. L. de, Bastida, R. "Los briozoos de las comunidades incrustantes de puertos argentinos". Proc. 5th Int. Congr. Mar. Corr. Foul., Biología Marina, Barcelona, España, 371-390 (1980).
- [172] Millar, R. H. "Ascidians of european waters". Catalogue of main marine fouling organisms, Vol. IV, OECD, 34 pp. (1969).
- [173] Stoner, D. G. "Recruitment of a tropical colonial ascidian: relative importance of pre-settlement vs. post-settlement processes". Ecology, 71(5), 1682-1690 (1990).
- [174] García Solá, E., Mendivil, A., Leiva, A., Díaz, E. de, Báez, L., Niveyro, G. "Fluvial corrosion in the Plata River drainage basin". Corrosion Reviews, XII (1-2), 61-70 (1994).
- [175] Carlton, J., Geller, J. "Ecological roulette: the global transport of nonindigenous marine organisms". Science, 261, 78-82 (1993).
- [176] 2nd International *Corbicula* Symposium, Little Rock, AR (USA), 21-24 June 1983.
- [177] International Zebra Mussel Conference '90, Columbus, Ohio (USA), 5-7 December 1990.
- [178] 2nd International Zebra Mussel Research Conference, Rochester, NY (USA), 19-22 November 1991.
- [179] Neumann, D., Jenner, H. A. "The zebra mussel *Dreissena polymorpha*". Limnol. Akt. Stuttgart Gustav. Fischer-Verlag, 4, 262 pp. (1992).
- [180] 3rd International Zebra Mussel Conference '93, Toronto, ON (Canada), 23-26 February 1993.
- [181] 36th Conference of the Int. Association for Great Lakes Research, De Pere, WI (USA), 4-10 June 1993.
- [182] Nalepa, T. F., Schloesser, D. W. (eds.). "Zebra mussels biology, impacts and control". Boca Raton, FL USA, CRC Press (1993).
- [183] Stupak, M., Pérez, M., García, M., García Solá, E., Azuaga, A., Mendivil, A., Niveyro, G. "Preliminary study of the biofouling of the Paraná River (Argentina)". Corrosion Reviews, Special Issue on Industrial Paints for Corrosion Control, 14 (1-2), 145-155 (1996).

- [184] Sinclair, R. M., Isom, B. "Further studies on the introduced asiatic clam (*Corbicula*) in Tennessee". Tennessee Stream Pollution Control Board, Tennessee Dept. Publ. Health, 79 pp. (1963).
- [185] Ituarte C. "Primera noticia acerca de la introducción de pelecípodos en el área rioplatense (Mollusca, Corbiculidae)". Neotrópica, 27 (77), 79-82 (1981).
- [186] Darrigran, G. "Moluscos del área rioplatense. I. Aspectos biológicos. Importancia económica y sanitaria". Anales de la Sociedad Científica Argentina, 219, 15-35 (1989).
- [187] Darrigran, G. "Variación temporal y espacial de la distribución de las especies de *Corbicula* Megerle, 1811 (Bivalvia, Corbiculidae), en el estuario del Río de la Plata, República Argentina". Neotrópica, 38 (99), 59-63 (1992).
- [188] Darrigran, G., Pastorino, G., Martín, S., Lunaschi, L. "Reciente introducción de otro bivalvo invasor en aguas del Río de la Plata". Resúmenes XVI Reunión Argentina de Ecología, Pto. Madryn, Chubut, Argentina, 328 (1993).
- [189] Pastorino, G., Darrigran, G., Martín, S., Lunaschi, L. "*Limnoperna fortunei* (Dunker, 1857) (Mytilidae), nuevo bivalvo invasor en aguas del Río de la Plata". Neotrópica, 39 (101-102), 34 (1993).

AGRADECIMIENTOS

Las autoras agradecen al Consejo Nacional de Investigaciones Científicas y Técnicas (CONICET) y a la Comisión de Investigaciones Científicas de la Provincia de Buenos Aires (CIC) por el apoyo financiero brindado para llevar a cabo el presente trabajo. Asimismo expresan su agradecimiento a la Srta. Mónica García y al Dr. Vicente Rascio por la lectura crítica del manuscrito.

NEW TRENDS IN INDUSTRIAL PAINTING

NUEVAS TENDENCIAS EN PINTURAS INDUSTRIALES

Vicente J.D. Rascio¹

SUMMARY

Technics for the corrosion control of structures or industrial equipment are very diversified. Materials selection, use of inhibitors, cathodic protection and paint systems are the methods usually employed.

Many metals as iron (steel), aluminium and zinc owe their importance to the fact that their tendency to corrode can be controlled by organic coatings. The satisfactory performance of an organic coating, in turn, depends on the composition of the products employed.

Paint makers, raw materials producers and users of paints are affected by the ecological restrictions in force worldwide. In particular, volatile organic compounds (VOC's) and some pigments and additives included in the formulations are objected.

Legislation regulates, directly or indirectly, the supply, formulation and conditions of use of paints and related products and covers not only toxicity affecting humans but also flora, fauna and danger of the ozone layer disrupting.

New inhibitive pigments are introduced to replace chrome and lead ones. Formulations of low VOC-content are used, and powder, polyurethane, water-borne, high-solids, and radiation cure coatings replace, in many cases, products with binders formulated with alkyds, chlorinated rubber, and vinyl resins containing a high level of solvent.

Keywords: *Corrosion protection, ecological regulations, new anticorrosive pigments, volatile organic compounds.*

INTRODUCTION

In order to establish the adequate protective paint system for a specific use, particularly in the case of industrial painting, both the characteristics of the substrate and the environmental conditions must be taken into account.

¹ Investigador Emérito de la CIC, Director del CIDEPINT

The quality control of coatings and application processes is important to determine the probability of problems arising from the use of these materials.

The aspects to be considered are:

- Employment of solvents for removing films (stripping) applied previously in the case of the presence of failures as blistering, chalking, checking or cracking.
- Surface preparation with free silicon mineral compounds or grit blasting or by chemical treatments.
- Characteristics of the aggressive medium (air, water, chemicals, ground).
- Design of an adequate paint system (primer, sealer and top coat).

The principal problem to be considered is the corrosion protection of structures or equipment. The annual cost of metallic corrosion is estimated in 4.2 % of the gross national product of each country. Coatings usually employed until 1960 were formulated with binders based on vegetable oils, alkyd or phenolic resins and bitumen. Between 1960-70 the formulations included resins as chlorinated rubber, vinyls and epoxy. After 1970, polyurethanes, silicones, water-borne, powder, radiation curing and high-solid coatings give the best protection in different media and are adequate to the environmental new regulations actually in force.

Metal composition (steel, aluminium, zinc or different kind of alloys) owes its importance to the fact that the tendency to corrode can be controlled by paint systems. The satisfactory performance of an organic coating, in turn, depends on the properties of the formulations employed. The technics applied for quality control are established in ISO Series, ASTM, DIN, BS or SSPC specifications.

Despite the widespread evolution of the paints and coatings industry and the generalized use of these products (**Table I**) there have been no significant technological advances in the following areas:

- Chemical resistant coatings or coating systems to be applied over poorly prepared steel surfaces.
- Universal and easily applied coatings that can resist a wide variety of service environments and temperature conditions.
- Practical procedures of chemical cleaning of metallic surfaces for field painting replacing sandblasting and gritblasting.

On the other hand the coatings industry expends considerable time and effort in the research and development of new products. Primers are formulated with non pollutant pigments as zinc dust, zinc phosphate, zinc basic phosphate, zinc molybdophosphates, ion-exchanged silica gel, to replace zinc chromates (particularly zinc yellow and zinc tetroxychromate) and lead pigments as red lead. Epoxy coaltar, epoxy, polyurethanes, vinyl, and chlorinated rubber (of low carbon tetrachloride contents) are employed for binders formulations.

TABLE I
Evolution of coatings technology

Before 1960	1960-70	1970-80	From 1980 →	1990
Oils Alkyds Phenolics Bitumen	Chlorinated rubber Vinyls Epoxies Epoxycoaltar	Polyurethanes Silicones Water-borne	Water-borne (new developments) Powder Radiation curing (UV & EB curable) High-solids Others: Solvents of reduced toxicity	Revision of the procedures for certifying quantity of VOC's emitted by paints, inks and other coatings
	↑ Increase of environmental control of the emission of pollutants to air, to water and to soils			

THE CORROSION PROBLEM

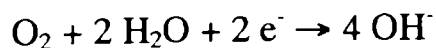
In the particular case of metallic corrosion, the most important fact, from an industrial point of view, is that the anodic reaction involves metal dissolution; metal ions remain in solution and react with cathodic products.

Different possibilities may be considered:

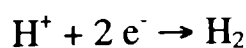
a) Dissolution of the metal at the anode forming metallic ions:



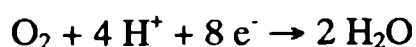
b) Reaction in neutral or basic solutions:



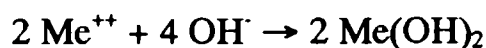
c) Reaction in acid solution, without the presence of oxygen:



d) Reaction in acid solution, in presence of oxygen:



e) Formation of the corrosion product:



In the presence of a medium containing dissolved inorganic salts (case of chlorides) the rate of the corrosion process increases, but other ions (as chromates) can inhibit the corrosion reaction. It is very important to remark this fact in order to explain the anticorrosive properties of some paints.

Variables influencing the corrosion process are: humidity (dew point), salts (identity and concentration), UV exposition, temperature (cycles and ranges), bacterial action, pH, standing water and contact with chemicals.

PROTECTION BY ORGANIC COATINGS

Paints and linings with organic binders are the usual products employed for the corrosion protection of metals. The different paint types, application processes and the possibility of combining paints with metallic coatings or cathodic protection lead to the importance of this type of protection.

Control of the corrosion process normally involves interference with the electrochemical corrosion mechanisms previously indicated, and it is the key to corrosion control by protective coatings. Restricting the access of water and oxygen to the metal it is possible to reduce the chances of attack. Unfortunately, no coating at normal thicknesses (50-75 μm) provides sufficient barrier protection.

Properly designed coating systems can be used, therefore, to filter ionic components of the electrolyte from corrosive salt solutions of the environment when the coated metal comes into contact with the medium.

Another approach used in coatings technology is the selection of materials as pigments or binders.

ANTICORROSIVE PIGMENTS

Inhibitive pigments must be divided into traditionally employed **lead** and **chromate products**, and the modern ecological **lead** and **chromate free** ones, as borates, phosphates or molybdates or ion-exchanged silica compounds (**Table II**).

TABLE II
List of inhibitive pigments

Traditional lead and chromate inhibitors

Lead pigments	Red lead Lead suboxide Basic lead silico chromate Dibasic lead phosphite Tribasic lead phosphosilicate Calcium plumbate Lead nitrophthalate
Chromate pigments	Zinc potassium chromate (zinc yellow) Basic zinc chromate (zinc tetroxychromate) Strontium chromate Calcium chromate Barium chromate

Lead- and chromate-free inhibitor pigments

Metallic pigments	Zinc (spherical or lamellar particles)
Phosphates	Zinc phosphate (dihydrate) Zinc phosphate (tetrahydrate) Basic zinc phosphate Basic aluminium zinc phosphate Basic zinc molybdate phosphate Zinc hydroxy phosphite Zinc phosphosilicate Calcium barium phosphosilicate Calcium phosphosilicate Calcium strontium phosphosilicate Zinc barium phosphate Zinc magnesium phosphate
Molybdates	Basic zinc molybdate Basic zinc calcium molybdate
Borate pigments	Calcium borosilicate Barium metaborate Zinc borate
Others	Zinc ferrite Calcium ferrite Zinc nitrophthalate Tungstates 2-Benzothiazolythio succinic acid Calcium oxide Calcium ion-exchanged silica gel
Auxiliary pigments	Zinc oxide Modified calcium silicate Manganese tetroxide

Some pigments **dissolved in water**, passing through the film and the solution react with the metallic substrate to form monomolecular films. In the **particular case of chromates** their action is based on the fact that paint films are permeable to water, particularly in the case of anticorrosive formulations with a pigment volume concentration (PVC) near to the critical pigment volume concentration (CPVC).

The solubility of chromate pigments varies widely from 17 g CrO₃/liter in the case of calcium chromate to 0.00005 g CrO₃/liter for lead chromate (**Table III**)

TABLE III
Solubility of different chromate pigments

Calcium chromate	CaCrO ₄	17 g/l CrO ₃
Zinc yellow	4 ZnO.K ₂ O.4CrO ₃ .3H ₂ O	1.1 g/l CrO ₃
Strontium chromate	SrCrO ₄	0.6 g/l CrO ₃
Zinc tetroxychromate	4.5 ZnO.CrO ₄ .4H ₂ O	0.02 g/l CrO ₃
Barium chromate	BaCrO ₄	0.001 g/l CrO ₃
Lead chromate	PbCrO ₄	0.00005 g/l CrO ₃

Zinc yellow is employed in the case of classic anticorrosive paint systems for atmospheric corrosion control and **zinc tetroxychromate** for marine formulations. The solubility of the pigment is a very important parameter. Theoretically, at least, while the reserve of chromate ions and the rate of water transport remain constant, the primer film maintains its protective properties. The nature of the binder establishes the necessary quantity of chromate ions in contact with steel to provide passivation of the metal. The employment of other pigments as ferric oxide and extenders or a coat of a sealer contribute to regulate chromate ions release, maintaining the passivation over a longer time.

Chromate ions are produced as water passes through the paint film, dissolving small quantities of pigment. When salts (i.e. chlorides) are present in the liquid in contact with the painted substrate, this fact tends to restrict the access of chromate ions to the steel.

In the case of **lead pigments**, the most important is **red lead** which is now questionable from an ecological point of view. It is very effective as corrosion inhibitor of iron and steel when employed in alkyd and oleoresinous primers. Basic lead pigments (and other basic inhibitors such as zinc oxide) provide protection by reacting with mono and dicarboxylic acid breakdown products of oxidizing vehicle systems, such as the mentioned binders. The reaction produces lead soaps, which act as inhibitors, forming an oxide layer on the metal surface, not only in new steel but also on rusted surfaces adequately cleaned to eliminate not adherent corrosion products.

NEW INHIBITIVE PIGMENTS

Sacrificial pigments, as **metallic zinc** (spherical or lamellar) give good cathodic protection to a steel substrate. Different **organic binders** are employed in this type of anticorrosive formulations. In this case it is important to employ a low level of binder to assure both electrical contact between pigment particles and good physical properties of the film as cohesion and adhesion. A low quantity of zinc causes the binder to encapsulate the pigment, improving adhesive and cohesive strength of the film, but reducing the contact between zinc particles. The film is too low to permit galvanic conductivity. With an excessive quantity of zinc the contact between pigment particles is assured, but as the film has a low quantity of binder it will show poor adhesion and low values for the physical properties associated to cohesive strength, film continuity, flexibility and resistance to cracking. Thus, the manufacturer should provide the adequate PVC/CPVC ratio and the applicator should be careful to maintain an adequate homogeneity by agitating the paint during application. This aspect is very important as zinc is a heavy pigment and tends to settle during paint storage and even during paint application. A lack of homogeneity in the coat may lead to failures in corrosion protection.

It is possible to formulate **zinc rich primers** with **inorganic binders**. They have a different mechanism of action: the binder reacts with zinc particles instead of encapsulating them as in the case of organic binders. Lower levels of zinc are employed in the formulation, but the increase of zinc always improves coat performance.

Other new inhibiting pigments satisfying ecological regulations are **micronized** or **not micronized zinc phosphate** and **molybdophosphates**. These pigments are very insoluble in water at pH = 7. Accelerated laboratory tests performed with these formulations have been extremely disappointing but long term field studies have been more encouraging. The mechanism of protection seems to be connected with the reaction of tribasic iron phosphate or molybdophosphate films with the metallic substrate. Another theory includes the hydrolysis of the salt to form secondary phosphate ions which produce adherent and inhibiting complexes. Researches performed at CIDEPINT have demonstrated that micronized molybdates and molybdophosphates are effective as inhibitors, in particular in their basic form. In the case of oleoresinous binders this could result from the formation of soaps.

Ion-exchanged silica gel is also employed as anticorrosive inhibitor. In this case, when the aggressive ion enters in the film, it contacts the silica and an ion-exchange occurs; the aggressive ion is locked onto silica and a corresponding calcium ion is released to the metal surface.

IMPORTANCE OF THE BINDER

The binder tends to control the access of water, oxygen and ions to take contact with the metal, but paint films cannot effectively exclude this process and thereby suppress the cathodic reaction.

For these reasons different resins have been studied and a classification of coatings is particularly referred to the nature of the resin employed in binder formulation. Some binders dry by solvent evaporation (as vinyl and chlorinated rubber ones); epoxy and polyurethanes

have a curing mechanism involving in some cases more than one component; latex paints are emulsions in which the resin is suspended in water as microscopic particles and the coat cures by coalescence, which means that after paint application the water starts to evaporate and the contact among particles results in the formation of a film (in this case some additives are necessary to improve the properties of the obtained coat).

It is important to establish briefly the most important differences between the previously mentioned binders.

- a) **Alkyds.** The coatings obtained cure by oxidation in contact with air. The formulation includes an oil (i.e. linseed, tung, soja) and it is possible to obtain products acting as primers, as intermediate coats or as top coats. Coating systems based on oils and alkyd resins have moderate water vapor transport rates and, as a consequence, they have only limited barrier protection properties; so, anticorrosive pigments are included in primer formulations in the case of steel protection. They have good exterior durability in non aggressive media, can be formulated in different colours and are the less expensive of the resins existing in the market.
- b) **Chlorinated rubber and vinyl resins.** As alkyds, they are organic resins and they cure by solvent evaporation with no changes in the resins composition; therefore the dry film is soluble in the solvents employed in the formulation. They show very low water vapor transport rates, forming very good barrier coats, with high chemical resistance. They are also characterized by a good exterior resistance, particularly in contaminated atmospheric conditions. Due to a high volatile organic content (approximately 40 or 50 per cent in the formulation), they are ecologically objected. The high gloss retention permits their use as topcoats.
- c) **Bituminous.** The organic resin included in a bituminous coating is derived totally or partially from crude oil or coal distillation. They are relatively inexpensive and have a high water resistance. The colour, black, is a limitation variable for the obtained formulations. They are used directly or in a modified form (epoxybituminous or epoxycoaltar) for protecting buried structures as pipelines (exterior protection) in contact with aggressive soils. They are not recommended for exterior use due to the poor resistance to sunlight which acts producing the cracking of the film.
- d) **Epoxies.** They cure by a chemical reaction when the resin is mixed with a hardener; amines or polyamides are usually used as curing agents. Generally epoxy paints are packed in two containers, one for the resinous component and the other for the hardener. They are mixed prior to application and the curing time varies according to the formulation. These paints give a film of excellent adhesion, durable and very resistant to solvents, water and chemical agents. The film is hard and abrasion resistant. The outdoors use is not advised due to chalking produced by the sunlight action. Another problem is the recoating of the surface; an abrasive treatment of the old film is necessary before painting in order to obtain an adequate roughness for good adhesion.
- e) **Silicones.** Silicone resins contain silicon in the polymer and they have good gloss retention and heat resistance. Added to alkyds, the resulting formulations are better in colour and gloss retention.

- f) **Phenolic.** Phenolic formulations are based on a phenol-formaldehyde resin. Pure phenolic resins cure by heat, and the film obtained has good resistance to water, solvents and chemicals. Air drying phenolic paints are obtained by reaction of the resin with some vegetable oils, in particular with tung oil. This type of coats is used in the formulation of anticorrosive paints to be employed in marine medium.
- g) **Polyester and vinyl esters.** These coatings are based on an organic unsaturated polyester dissolved in an unsaturated monomer. They cure by a free radical reaction which is initiated by a peroxide radical. The most important characteristics is their acid and chemical resistance; so they are used as linings including reinforcing materials (composite materials).
- h) **Alkyd, acrylic, epoxy and poliurethane water-borne resins.** They are employed as latex. In the formulations the resin is dispersed in water to form a latex emulsion. These resins are used for architectural or industrial protective coatings in the form of primers, intermediate coats or topcoats. The paints cure by solvent evaporation followed by the coalescence of the resin particles. They are used to protect concrete and also in anticorrosive paints for steel using different pigments.
- i) **Polyurethanes.** It is possible to establish two groups according with the curing mechanism: chemical curing chemically or moisture curing. The first group (**chemical cure**) characterized by the presence of an isocyanate functional group ($-N=C=O$), which reacts crosslinking the resin. Other resins as epoxies, vinyls and polyesters can be used to copolymerize urethanes. Two containers are necessary for package to be mixed before application. They have a limited pot life after mixing. The final product has good water and chemical resistance. In some cases it is possible to obtain films of good gloss and colour retention. In the urethanes **curing in the presence of water** the isocyanate group is attached to a polymer; firstly, after application, some of the isocyanate groups react with moisture to form an amine which reacts with other isocyanate polymers to form the film. This type of urethane is packed in one container and the moisture needed for curing is obtained from the air. The film is characterized by a strong resistance to chemicals and to exterior exposure (sunlight and water).

A guide for selection of industrial painting in relation with properties of different coatings types is presented in **Table IV**.

SOLVENTS

Solvents are used in paint formulations to obtain an adequate viscosity, a very important parameter which affects paint application, flow and final uniformity of the film. As a complement the solvent must be compatible with the resins employed and no harmful for humans.

The most commonly used solvents are:

- Halogenated (i.e. methylene chloride)
- Aliphatic hydrocarbons (i.e. white spirit)
- Aromatic hydrocarbons (i.e. toluene and xylene)
- Oxygenated (i.e. alcohols, esters, ethers and ketones).

TABLE IV**Properties of different coatings types****A guide for selection in industrial painting**

Type	Strength	Weakness
Alkyd-oil Alkyd-vynil Alkyd-silicone	Weathering Weathering, acids Weathering, heat	Chemicals Caustics Caustics
Vynils Chlorinated rubber Water-borne acrylics Water-borne epoxy and polyurethane Coal tar	Weathering, water, chemicals Weathering, water, chemicals Weathering, gloss, colour Weathering, water, gloss, colour Water, acids, salts	Application, solvents, heat Application, solvents, heat Solvents, heat Solvents, heat Heat, only 1 colour (black), hardness
Epoxy polyamide Epoxy-amine Epoxy-coaltar	Water, alkali, hardness Water, chemicals, solvents Water, salts	Recoating Recoating Recoating, only 1 colour (black)
Urethane moisture cure Urethane two components Polyesters	Hardness, abrasion, impact Abrasion, impact Acids, oxidizing agents	Low humidity cure Recoating Alkalis
Epoxy powder Vynil powder	Water, alkali, solvents Chemicals, salts, hardness	Application, recoating Application
Organic zinc epoxy polyamide Inorganic zinc silicates Water-borne Solvent-borne	Application, weathering Weathering, solvents, heat, impact, abrasion, moisture Weathering, solvents, heat, impact, abrasion, moisture	Chemicals, solvents Acids, alkalis Acids, alkalis

According to regulations existing in the developed countries about the volatile organic compounds (VOC's), it is very important the adequate selection of solvents in paint formulations.

Normal paraffins, isoparaffins, dearomatized aliphatics, mono-esters or heavy aromatics are used to reduce the proportion of more aggressive or toxic solvents. They are miscible with other hydrocarbons. These solvents show low solvency properties for most resins commercially used; an adequate solvent mixture must be selected in each case to avoid this problem.

ADDITIVES

These components are incorporated to the formulations to regulate some properties. The most important are:

- Antisettling agents
- Antiskinning agents
- Antifoams
- Dispersing and emulsifying agents
- Driers
- Fungicides
- Ultraviolet absorbers
- Coalescent agents
- Surfactants
- Thixotropic agents

The proper selection of the most adequate additives and their level (generally low) in the formulation involve a considerable amount of time in research and development and it is very difficult their determination in the chemical analysis of the paint.

SOME PAINTS USED AT PRESENT IN INDUSTRIAL PAINTING

Powder coatings

They are the lowest VOC-content coatings, because **they are 100 % solids and VOC's emission during application is negligible**. The only exception is the case of powder coatings employing blocked isocyanates, in which the blocking agent evolves prior to the curing process.

The major developments in powder coatings started in 1980. More recent formulations have centered in the use of new blocking agents and the cross-linking employing different polymers. Research and development have been focused now in the application of these paints to protect substrates, other than metals, as plastics or wood.

There are **two types** of powder coatings.

a) The **thermoplastic powder coatings**, including polyolefins, vinyl resins and polyamides. They melt and flow when heat is applied without change of chemical composition after cooling. High molecular weight solid resins are employed giving a film with good abrasion, wear and impact resistance.

b) The **thermosetting powder coatings**, which are based on lower molecular weight solid resins, melting, flowing and curing by heating. A chemical crosslinking determines the high resistance properties of the coat as mechanical behaviour and impact resistance. These coatings include epoxy, polyester, hybrid epoxy-polyester, acrylic and polyurethane resins.

In the two previously mentioned cases, the resin to be used is selected according with the use of the object to be coated, and particularly with the environmental conditions of the medium in contact with the painted surface, specially when exterior durability is required. It is very important to establish the difference between decorative and protective characteristics; in the first case it is possible to obtain a good performance with a film thickness lesser than 100 microns, but for good protective performance in industrial protection more than 100 microns are necessary.

Powder coatings technology provides the following **advantages**:

a) For industrial finishing, thermoplastic coatings are applied using conventional and electrostatic fluidized bed; spray methods are more common in the case of thermosetting powders. For spraying the powder particles are electrostatically charged; the powder is attracted to the metallic surface and a coat of particles is deposited. An efficiency of 80-90 % is considered as good from the economic point of view and the residual powder (not adhered) is recovered and recycled.

b) The choice of the powder coating polymer depends on the conditions of use (i.e. cleanliness of the substrate, surface preparation and roughness or environmental exposition). Epoxy powders are adequate in the case of the protection to aggressive chemicals, but not for exterior exposition due to the tendence to chalking in only a few months. Polyester, polyurethane and polyester resins show adequate durability in both cases.

c) Powder coatings require no primer or topcoat (only pretreatment of the surface to be painted).

d) They melt at 75-80 °C but it is important to reach 140-200 °C to obtain an adequate hardness after curing. The powder not adhered to the surface is recirculated and no solvent contamination is produced.

Some of the **disadvantages** are pointed below:

a) It is not convenient to obtain lower thickness films (under 50 µm); pinholes can be formed if coalescence of the powder particles is not completed. A film of 100 µm obtained by electrostatic spray gives adequate protection.

b) The film obtained is not very flexible.

c) Colour changes (during application) are a serious problem; it is necessary good cleaning of the equipment before another colour can be used.

In the case of powder coatings it is necessary to follow an adequate control of raw materials (color, softening point, equivalent weight and reactivity with the hardener), testing during production and of the finished powder, and, from the laboratory point of view, the appearance of the film (colour, gloss), adhesion to the substrate, flexibility, impact resistance, hardness and abrasion resistance, water and solvents resistance, resistance to accelerated weathering and salt spray.

Many other tests exist which are specific to certain applications or customers, particularly to establish correlations between service life and laboratory results.

It is possible that powder coatings continue to enjoy higher growth rates than other products of the industry since antipollution legislation will continue to become more exigent and more heavily enforced.

Polyurethane coatings

Two-components polyurethanes are used not only in the case of industrial maintenance coatings but also as architectural coatings. A high performance was obtained applying them over metal, concrete, wood or plastics. It is possible to formulate products of different qualities, from hard and rigid to soft and flexible ones. They resist wide environmental conditions and the action of aggressive solvents and chemicals.

Manufacturers of polyurethane coatings have been focusing research and development on reducing VOC content of the formulations but maintaining or improving the performance properties of the coatings.

The two components of the polyurethanic paint must be thoroughly mixed in the moment of use and they maintain workability properties between 4 to 6 hours. Depending on the formulation, the product can be applied using spray, brush, roller or trowell methods, according to the requirements of the user or the coat thickness established in the specification.

The polymeric film is formed by the polyaddition of the resin and the hardener, both oligomeric, with the formation of a polyurethane network on the substrate. The hardener is a polyisocyanate having active hydrogen atoms, such as alcohols and amines, to form polyurethanes and polyureas. The polyisocyanates dry by solvent evaporation and by a chemical curing reaction.

As curing starts immediately after mixing, the two components are packed separately. One package of the system contains the solution of the polyisocyanate and the other includes the co-reactants, pigments, additives and solvents.

The co-reactants are polyalcohols or polyamines specifically chosen to produce coatings with determined performance properties. Pigments for these products are incorporated to obtain some properties as colour and hiding power, but in particular to

complement some resin properties, as impact resistance or mechanical strength. The additives influence flow properties after application or are incorporated to increase the resistance of the film to the destructive effect of sunlight.

Solvents are selected for their properties to reduce the mixture viscosity or for obtaining a good levelling in the application. The environmental pollution affects the choice of solvents.

These paints give good performance to different chemicals, in particular salts, acids or seawater, including corrosion protection or abrasion resistance.

From the point of view of the applicator, an overexposure to polyisocyanates can irritate eyes, nose, throat, skin and lungs.

A new generation of polyisocyanates reduces the viscosity and a lesser quantity of solvent is required in the formulation.

Water-borne coatings

An important effort is put at present in the development of water-borne coatings, not only for architectural use but also for anticorrosive protection of steel. Research was performed to obtain gloss top coats for interior and exterior use. The use of water replacing volatile organic compounds give a number of advantages. Water has a low viscosity, allowing formulation of coatings with convenient application viscosity. Water is used as diluent and the paints are not toxic.

Two water-borne technologies are developed: one for decorative emulsion paints and the other for electrodeposition coatings.

In the case of decorative paints (for architectural use) the low solvent level is an advantage, and it is possible to formulate paints of different colour and gloss. In some cases it is necessary to employ a primer to obtain good application properties. These paints are widely accepted in this field.

Electrodeposition coatings may be either dispersions or water soluble polymers and are used particularly in the case of the application of anticorrosive coatings, as it is explained below.

Some problems are related with the use of water-borne in industrial and architectural painting. Water has a slow evaporation rate and a high heat of vaporisation. As a consequence, more energy is necessary to evaporate water than that necessary in the case of organic solvent based products. The easiness of water evaporation is very dependent on the ambient humidity. In indoor applications the relative humidity is low and temperature is high. Consequently water-borne coatings dry fast giving a film with good adhesion. Water-borne paints applied outdoors in a cold or damp medium dry very slowly and an unexpected rain may remove partially or completely the coat. In industrial painting, drying time depends on the humidity of the surrounding air.

Water-borne paints applied to ferrous substrates show “flash rusting”, that is the rapid corrosion of the substrate during application and drying. A longer contact with water favours the attack; as a result, corrosion products appear on the surface of the coat, modifying colour or physical properties of the film. To avoid this problem coatings are formulated with “flush rusting” inhibitors or a previous pretreatment is necessary to avoid this problem. The application of thin films is convenient to obtain a rapid drying time.

Microbial degradation is other of the problems related to the use of water-borne coatings and this makes necessary the incorporation of biocides and fungicides. As these materials are toxic, small quantities are added to obtain good protection in the can or in the applied film. An important line of research on this topic is performed actually at CIDEPINT.

Other problem is connected with the use of some volatile organic compounds used as cosolvent or coalescing agent in the formulations. Coalescing agents based on ethylene glycols are replaced now by less toxic propylene glycol based derivatives. It is important in actual and future research the reduction or the complete elimination of organic solvents in water-borne coatings without affecting the product performance.

High-solid coatings

Different types were considered, according to the amount of solvent in the formulation. In general it is accepted to define high-solid coatings as paints with higher than 80 % of non-volatiles by volume.

The high solids content leads to different advantages:

- To obtain a specific film thickness with less number of coats.
- Reducing solvent content which reduces the total volume of paint and the transport and storage costs.
- Lesser insurance costs (due to the reduction of solvent content), minimizing risks of fire or explosion .

A disadvantage is the possibility of solvent retention in high thickness films, reducing the performance of the paint. To avoid this problem it is necessary to employ adequate equipment and qualified operators.

Radiation cure coatings

Radiation curing is the case of a polymerization started by ultraviolet (UV) irradiation or by means of high energy electrons (EB). Two forms of polymerization are in use: free radical and cationic polymerization.

These coatings consist of resins dissolved or dispersed in non-reactive volatile liquids. The liquid is removed rapidly after application; this process requires thermal energy and often leads to undesirable emissions. The key of UV/EB curing is that reactive (monomeric) liquids eliminate the need of volatile solvents.

When the coating is irradiated after application, copolymerization of free radicals is instantaneous. The transformation of the liquid film in a solid coating takes place in a fraction of second after exposure to the radiation. The speed to obtain the protective coating allows the immediate package of painted object with a reduction of the production rates.

In radiation curing technology no heating is necessary to remove volatile solvents. Radiation curing equipment is small in comparison with electrical ovens installed in some production lines. The energetic cost is 70 % of that of conventional heat drying.

A typical UV formulation comprises a photoinitiator (a dye or a pigment) and a combination of monomers and oligomers. In some cases, to obtain particular properties, it is necessary to use more specialized and more expensive photoinitiators. The monomers and oligomers are typically conventional monomers and resins modified by the addition of acrylate functionality.

The cost of UV curing equipment is relatively low compared to that of electron beam, infrared, electric or gas-fired ovens.

This type of protection is applied in wood furniture (beds, chairs), in printing (book and magazine covers, credit cards), electronics (printed circuits) and sport packaging.

THE ECOLOGICAL PROBLEM

As it was explained previously, paint makers, raw materials producers and users of paints are affected by the restrictions in force worldwide. In particular volatile organic compounds (VOC's) and some pigments and additives are objected (**Table V**).

The scope of the environmental legislation includes:

- Chemical and dangerous substances employed in the paint industry (solvents, pigments and biocides).
- Pollution control (air, water, marine environment, ground contamination, waste disposition).
- Health and safety (equipment employed and operators exposure).
- Products packaging and transport conditions.
- Consumers protection during and after paint application.

As a consequence, legislation regulates, directly or indirectly, the supply, formulation and conditions of use of paints or related products and covers not only toxicity affecting humans but also flora, fauna and the danger of the ozone layer disrupting.

The challenge has been accepted. New trends, objectives and targets are in progress.

TABLE V
Scope of environmental legislation

Health & Safety

- Workplace and equipment
- Occupational exposure
- Work conditions: hours, holiday, maternity, young people
- Physical/chemical/biological agents
- Major accident hazards

Chemicals:

Dangerous substances/preparations

- Notification
- Classification, labelling, packaging
- Safety data sheets
- Risk assessment
- Marketing and the restrictions
- Biocidal products

Pollution control

- Air
- Water
- Marine environment
- Ground contamination
- Waste
- Packaging waste

Transport

- Classification, packaging, labelling
- Export/import of dangerous goods
- Physical integrity of packaging (testing)

Consumer protection

- Toy safety
- Food safety
- Construction products
- Product safety

BIBLIOGRAPHY

- Anderson, D.G. "Coatings". *Anal.Chem.*, **67**, 12 (1995): pp. 33R-46R.
- Berry J.C. "Environmental Protection Agency (EPA) and the Industry; a History of Success, a Future Challenge". *ASTM Standardization News*, Oct. (1995): pp. 32-39.
- Bodnar E. "Powder coatings, a technology on the future". *Eur. Coat. J.*, 10 (1993): pp. 714-731.
- Brandau A. "Introduction to coatings technology." In *Federation Series on Coatings Technology*, Blue Bell, USA: 1990.
- Brezinsky J.J. "Regulation of volatile organic compounds emission from paints and coatings". In *Paint and Coatings Testing Manual*, Chapter 1, 14th Edition: 1995.
- Bud Jenknis V.C., Reilly J.C., Sypowicz B., Wills M.T. "VOC testing comparison: EPA Method 24 versus the Cal Poly Method". *J.Coat.Tech.*, **67**, 841 (1995): 53-59.
- Chapman M. "Water-based anticorrosive systems". *Surface Coatings Int. (JOCCA)*, **77**, 7 (1994): 297-302.
- Corbitt R.A. *Standard Handbook of Environmental Engineering*. McGraw Publ. Co., N.Y.: 1989.
- Costanza J.R., Silveri A.P., Vona J.A. "Radiation cured coatings". In *Federation Series on Coatings Technology*, Blue Bell, USA: 1986.
- Cunningham G.P. "Using ASTM Standards in attaining ISO 9000 Registration". *ASTM Standardization News*, Oct. (1995): 28-31.
- Ebbrecht T., Lersch P., Wewers D. "Silicone acrylate systems". *Eur.Coat.J.*, 10 (1994): 498.
- Hare, C.- *Protective coatings; fundamentals of chemistry and composition*. Technology Publishing Co., Pittsburgh, Pennsylvania: 1994.
- Hiroshi Fujimoto K.- "Partnering to develop ASTM Standards for hazardous air pollutants". *ASTM Standardization News*, Oct. (1995): 62-67.
- ISO (International Organization for Standardization).- *ISO 9000, Quality Management*. 5th Edition, Switzerland: 1994.
- Jilek J.H.- "Powder Coatings". In *Federation Series on Coatings Technology*, Blue Bell, USA: 1991.
- Jotischky H.- "Coatings under the legislative spectra". *Eur.Coat.J.*, 1-2 (1996): 21-26.
- Kennedy R.- "Compilance coatings: pros and cons". *Eur.Coat.J.*, 10 (1994): 670.
- Kettley J.- "New developments in powder". *Eur.Coat.J.*, 1-2 (1993): 24-30.

Koleske J.V.- "25 Years of Paint and Technology. From past to present". *ASTM Standardization News*, Oct. (1995): 73-77.

Koleske J.V.- "Cationic radiation curing". In *Federation Series on Coatings Technology*, Blue Bell, USA: 1991.

Mirgel V., Sonntag M.- "High performance polyurethane coatings". *Eur.Coat.J.*, 10 (1994): 690-700.

Nadkarni R.A.- "The quest for quality in the laboratory". *An.Chemistry*, 63, 13 (1991): 672A-675A.

Reck E., Marron J.J., Balfour J., Moulton D.V.- "Parameters affecting the performance of powder coatings". *Eur.Coat.J.*, 6 (1994): 373-381.

Reisch M.S.- "Paints and Coatings, Government Mandates". *Chem. & Eng. News*, Oct., 3 (1994): 44-66.

Smith Lloyd M., General Editor.- *Generic Coating Types*. Technology Publ. Co., Pittsburgh, USA: 1996.

Visciglio G.- "Quality and Certification". *Pitture e Vernici*, 66 , 10 (1990): 9-17.

COMPARATIVE CORROSION BEHAVIOUR OF 55ALUMINIUM-ZINC ALLOY AND ZINC HOT-DIP COATINGS DEPOSITED ON LOW CARBON STEEL SUBSTRATES

COMPORTAMIENTO FRENTE A LA CORROSION DE ACERO RECUBIERTO CON CINC
O ALUMINIO-CINC APLICADOS POR INMERSION

P.R. Seré¹, M. Zapponi², C.I. Elsner³, A.R. Di Sarli⁴

SUMMARY

A comparative study related with the anticorrosive behaviour of 55Aluminium-Zinc-alloy and Zinc coatings, both applied by hot-dip process on steel, was performed using salt spray and humidity cabinet tests as well as immersion ones. Electrochemical tests including polarization curves and cathodic protection efficiency were also carried out. The surface degradation of the coated steel was studied by SEM and EDS, whilst the corrosion products were characterized using XRD. Preliminary results showed that the corrosion resistance of the 55Al-Zn alloy coating was higher than that of Zn alone particularly in presence of chloride ions. The morphological characteristics of the corrosion products formed also differed.

Keywords: *Galvanized steel, cincalum coatings, accelerated weathering tests, electrochemical tests.*

INTRODUCTION

Exposed to specific aggressive media, the metal or alloy stability depends upon the protective properties of the surface film formed on it, because its chemical composition, conductivity, adherence, solubility, hygroscopicity and morphological characteristics determine the film capacity to work like a controlling barrier of the corrosion type and/or rate [1]. In such a sense, the steel galvanic protection by means of zinc is a common example due not only to the fact that being the Zn electrochemically more active than the steel corrodes preferentially, but also to the barrier effect of the corrosion products precipitated on the metallic surface. Particularly, the coatings based on Zn are widely used in order to protect steel structures against atmospheric corrosion [2], because of the protective properties afforded by an insoluble film of basic zinc carbonate. However, if the exposure conditions are such that there

¹ Becario de la CIC, UNLP

² Investigador del CINI, SIDERAR Planta Ensenada

³ Miembro de la Carrera del Investigador del CONICET, UNLP

⁴ Miembro de la Carrera del Investigador de la CIC

is either depletion of air but high humidity or else a medium containing strongly aggressive species like chloride or sulphate ions, the Zn dissolves forming soluble, less dense and scarcely protective corrosion products, which sometimes lead to the localized corrosion phenomenon [2-4]. This condition can be reached during the storage and transportation of galvanized steel sheets or when they are exposed to marine and/or industrial environments

On the other hand, aluminium coatings have overcome these two factors. Nevertheless, as they cannot provide cathodic protection to exposed steel in most environments, early rusting occurs at coating defects and cut edges; besides, these coatings are also subjected to crevice corrosion in marine environments [5].

For years, many attempts to improve the corrosion resistance of zinc and aluminium coatings through alloying were carried out. Although the protective effect of combinations of these two elements was known, they were not used until the discovery that silicon inhibits the rapid alloying reaction with steel [6]; thus, the alloy commercially known as Galvalum or Cinalum arose, and its composition: 55% Al, 1.6% Si, the rest Zn, was selected from a systematic study, providing an excellent combination of galvanic protection and low corrosion rate. Currently, the steel sheet coated with this alloy has gained an important portion of the market to the galvanized steel, mainly in the building, electrodomestic and automotive industries.

In order to be used under specific service conditions, the choice of the best coating should be done taking into account that the longest useful life obtained at the lowest cost is the paramount market parameters. Due to the reactive nature of these coatings, the corrosion products play an important role in the protection mechanism, turning still more complicated the selection procedure. When cost or time reasons make not possible that natural ageing tests can take place, the so called laboratory accelerated tests such as the salt spray cabinet, according to the ASTM Standard B-117/85, is the world-wide used procedure to study anticorrosive performances in marine environments.

The aim of this paper is to present the results of an experimental investigation about both the Zn and 55Al-Zn alloy hot dip coated steel behaviour under either standardized salt spray (ASTM B-117/85) and humidity (ASTM D-2247/94) cabinets tests or not normalized ones such as immersion in 3% NaCl solution. Besides, electrochemical studies about the corrosion behaviour of Zn, 55Al-Zn alloy and Al hot-dip coated steel sheets by using both polarization curves as well as tests under free corrosion conditions, in order to determine the cathodic protection afforded by the coatings to the substrate, were also performed. The surface degradation of the coated steel was studied by scanning electron microscopy (SEM) and energy-dispersive X-ray spectrometry (EDS), while the corrosion products were characterized using X-ray diffraction (XRD) at different immersion times to give a tentative explanation of the protection mechanism in each steel/metallic coating system.

EXPERIMENTAL DETAILS

Surface characterization

The studies were carried out with commercially available steel sheets of 15x8x0.1 cm hot-dip coated with Zn or 55Al-Zn alloy. **Table I** gives the chemical composition of the

substrates, while the thickness, microhardness and average roughness of the studied coatings measured with standard equipment are presented in Table II. All the samples were degreased with alkaline detergent and toluene; then, they were kept in a dessicator until the tests start. The coatings microstructure was analyzed using a scanning electron microscope (Philips SEM 505) equipped with an energy-dispersive X ray spectrometer (EDAX 9100).

Table I

Chemical composition of the tested coatings (wt %)

	Zn	Al	Si	Sb	Cd	Pb	Fe
Galvanized	99.72	0.10	----	0.09	0.004	0.05	0.03
55Al-Zn alloy	43.33	55	1.6	----	----	0.03	0.04

Table II

Coatings Thickness, Microhardness and Roughness

	Thickness / μm (*)	Microhardness / HV (**)	Roughness / μm (***)
Galvanized	15.2	157.12	0.31
55Al-Zn alloy	22.5	221.14	0.80

(*) Elcometer mod 300

(**) Microhardmeter Shimadzu type M.I.

(***) Hommel Tester mod T 1000

Salt spray cabinet, humidity cabinet and immersion tests

After the coating characterization, the salt spray and humidity cabinet tests were performed under the criteria established by ASTM B-117/85 and ASTM D-2247/94 standards, respectively. During the tests, the specimen position within the cabinet was changed after each inspection so as to neglect the possibility that the position might affect the results. The cathodic protection afforded by each coating was also assessed utilizing some of the exposed samples; in these, a cross scribe through the coating was made with a sharp instrument so that a small area of the underlying steel be in contact with the environment. Simultaneously, and with the same objective, immersion tests using samples of 15x3x0.1 cm were arranged with an inclination 30° angle from the vertical, in a glass vessel filled out with 3% NaCl solution kept at 25°C. Corrosion progresses were monitored by means of periodical visual inspections, while the degree of attack was estimated from the corroded area percentage determined with the help of an optical microscope. Corrosion products morphology and coating degradation were further studied using a SEM equipped with EDS; the identification of corrosion products or their powders was made by means of XRD directly applied on the tested samples or the

powders, respectively. The X-ray diffraction was carried out using a Philips diffractometer with a copper tube anode (1.54 Å) operated at 50 kV/30 mA. The samples were step-scanned between 5 and 80° with a step size of 0.02° and a time step of 1 s.

Polarization curves

In the electrochemical cell, the working electrode was a coated steel sheet of 13.9 cm² of geometric area with edges isolated by an epoxy resin. A graphite cylinder of great area and a saturated calomel electrode (SCE) were used as counter and reference electrodes, respectively. The polarization curves were performed in a potentiostatic mode with a PAR 273A potentiostat. They were built-up polarising the sample first in the cathodic sense and then in the anodic one. The potential rate sweep was 0.1 mVs⁻¹ (sufficiently low to guarantee an almost steady state).

Cathodic protection level

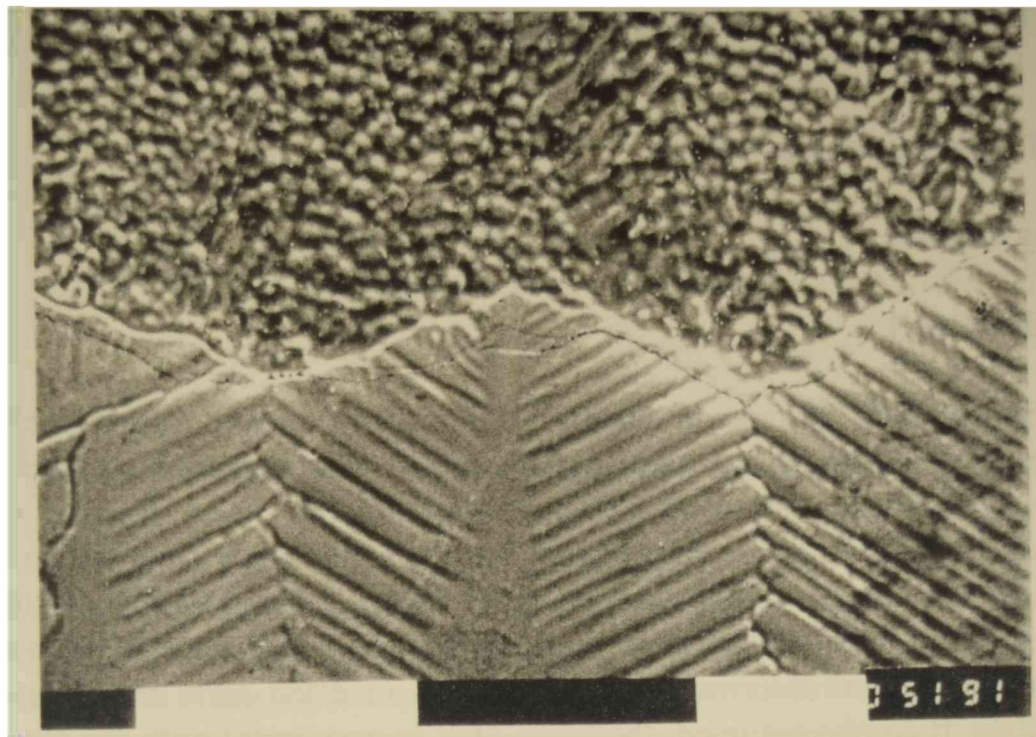
The ability of Zinc, 55Al-Zn alloy and Aluminium hot-dip coatings to cathodically protect steel was evaluated. The approach adopted was to determine the potential distribution along steel strips partly coated with the different metallic coatings. The tested electrodes were prepared from steel sheets partially hot-dip coated with one of the metallic coatings assessed. An insulated copper wire was spot-welded to a corner of each coated sample. The wire was encapsulated and isolated from the electrolytic medium by an epoxy resin. The bare steel-to-coating area ratio was of 4/1.

The partly coated steel strips were positioned either horizontally or vertically in the electrolyte. A series of 6 Luggin capillaries were positioned above or before the steel strip from a rigid frame, respectively. Each Luggin capillary was in solution contact with a separated saturated calomel electrode (SCE). The first Luggin capillary was placed either directly over or at the level of the coating and the others were placed along the steel at distances of 2; 4.1; 6.1; 8.1 and 11.4 cm for the horizontal arrangement and of 2; 4.1; 6.1; 8.1 and 10 cm for the vertical one, in both cases measured from the edge of the coating. The gap between the steel strip and the tip of each Luggin capillary was set at 2mm. The experimental arrangement was like that presented by Baldwin et al. elsewhere [7]. The steel strip and each reference electrode were connected to a high impedance voltmeter. The potential at each position along the steel strip was measured as a functions of the immersion time. The experiments were halted when the potential along the entire length of the steel strip reached the open circuit potential of steel alone.

In all the electrochemical tests, the electrolyte was a quiescent 3% NaCl solution, pH = 8.2, neither air sparged nor deaerated.

RESULTS AND DISCUSSION

Fig.1a-b exhibits the characteristics “flowers” of the Zn and the two-phase structure of the 55Al-Zn alloy coatings, respectively. The latter was formed by an Al rich phase occupying



a) galvanized steel



b) 55Al-Zn alloy/steel

**Fig. 1.- SEM micrograph of the steel hot-dip coated samples before the ageing tests.
Magnification = 350X.**

dendritic places and other rich in Zn filling the interdendritic ones. It is important to remark that these results were confirmed by EDS studies and are in accordance with publications of other authors [5, 8, 9].

1. Analysis of the corrosion products

1.1. Salt spray cabinet

1.1.1. Galvanized steel

After 5h exposure, hexagonal plane crystals called platelets having preferential facing (normal to the substrate plane) can be observed, **Fig.2a**. These crystals grow forming islands which spread all over the surface as the exposure time increases, **Fig.2b**; many of them nucleate heterogeneously on the surface defects but the majority do it on NaCl crystals that, in turn, precipitate on the metallic surface [10]. XRD analysis (**Fig.3**) indicated that $\text{Zn}_6(\text{OH})_8\text{Cl}_2 \cdot \text{H}_2\text{O}$ (Simonkolleite) was the major component of the corrosion products, whilst EDS results confirmed that chlorine, zinc and oxygen were the main elements present in the hexagonal crystals. It can be assumed, therefore, that in agreement with the proposal of other authors [10,11], the hexagonal crystals observed by means of SEM are of Simonkolleite. Traces of zinc oxide (ZnO) and zinc hydroxycarbonate (Hydrozincite) $[\text{Zn}_5(\text{CO}_3)_2(\text{OH})_6]$ were also detected.

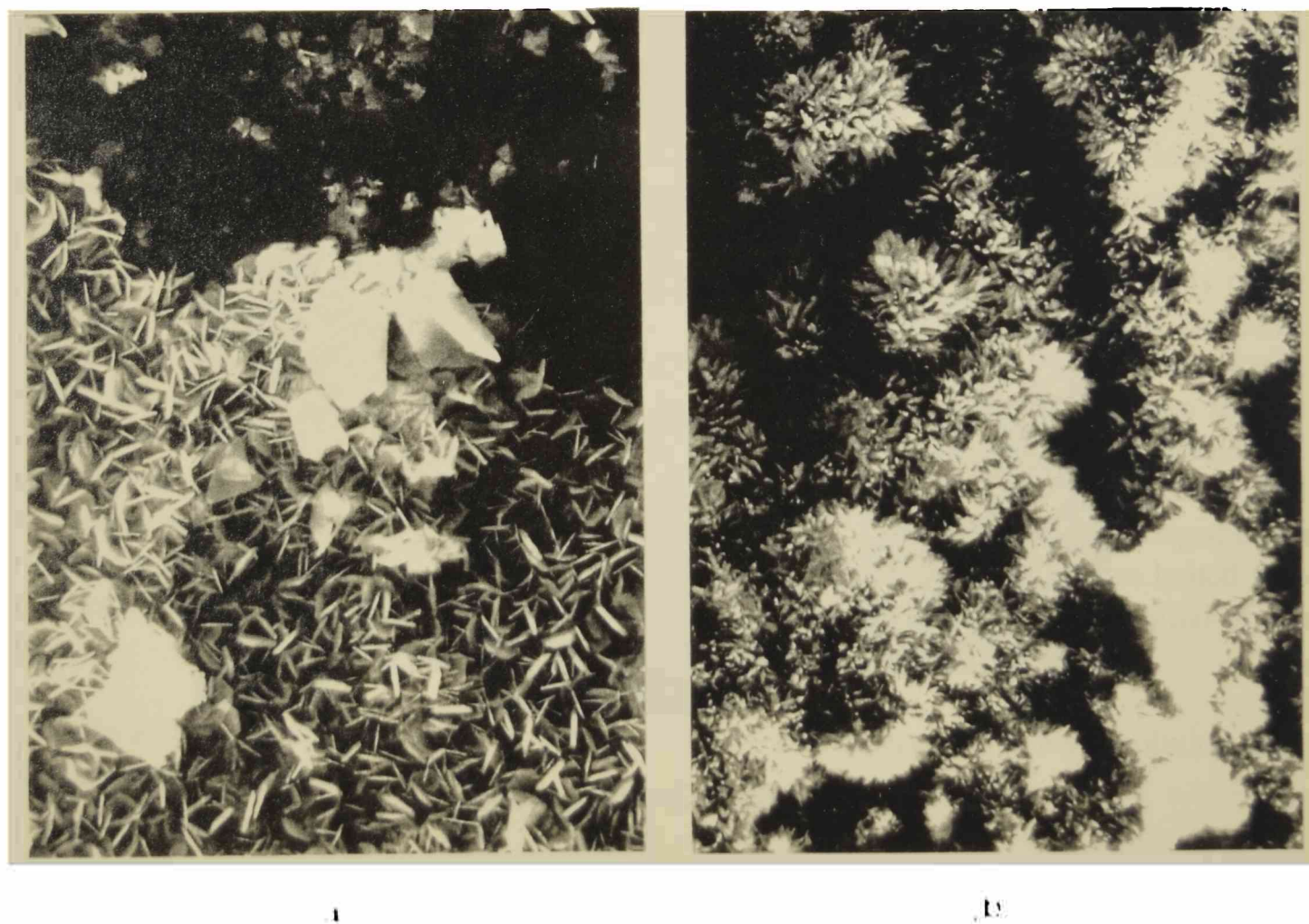


Fig. 2.- SEM micrographs of a galvanized steel sample after a) 5h and b) 72h exposure in salt spray cabinet. Magnifications = 1600X and 140X, respectively.

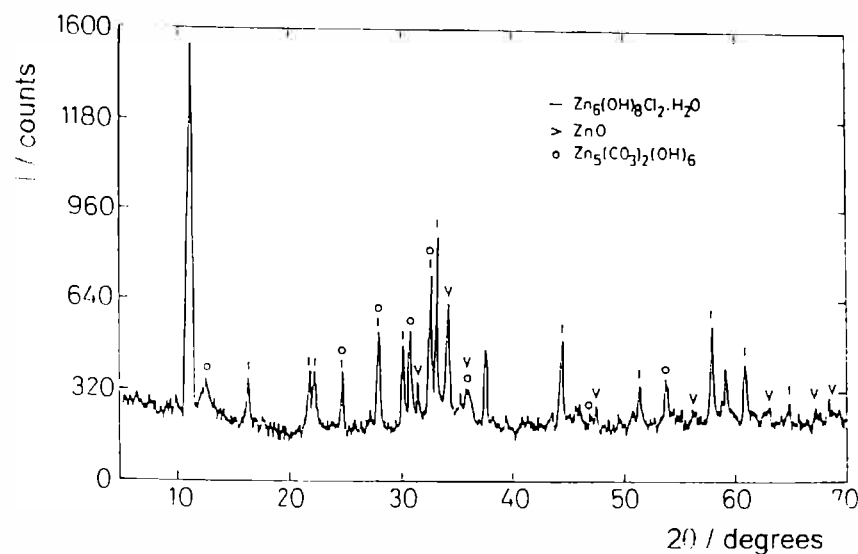


Fig.3.- XRD spectrum of a galvanized steel sample after exposure in salt spray cabinet.

1.1.2. Steel/55Al-Zn alloy

Fig.4a showed that after 24h exposure, the two-phase structure of the 55Al-Zn coating displayed no evidence of attack; however, when the same zone was seen with 1500X (**Fig.4b**), the formation of small acicular crystals into the interdendritic places (Zn rich phase) could be observed. These acicular crystals may be of Hydrozincite [11] and it would demonstrate a preferential interdendritic dissolution of the zinc rich phase as the first step of the system corrosion with a kinetics lower than that in the galvanized steel sheet [9]. After 360h, the XRD analysis identified the basic zinc aluminium carbonate [$\text{Zn}_6\text{Al}_2(\text{OH})_{16}\text{CO}_3 \cdot 4\text{H}_2\text{O}$] (**Fig. 5**) as the main corrosion product; this compound has also been found in Galfan (5%Al, Zn the rest) in marine environments accompanied, in less quantity, by $\text{Al}(\text{OH})_3$ [12].

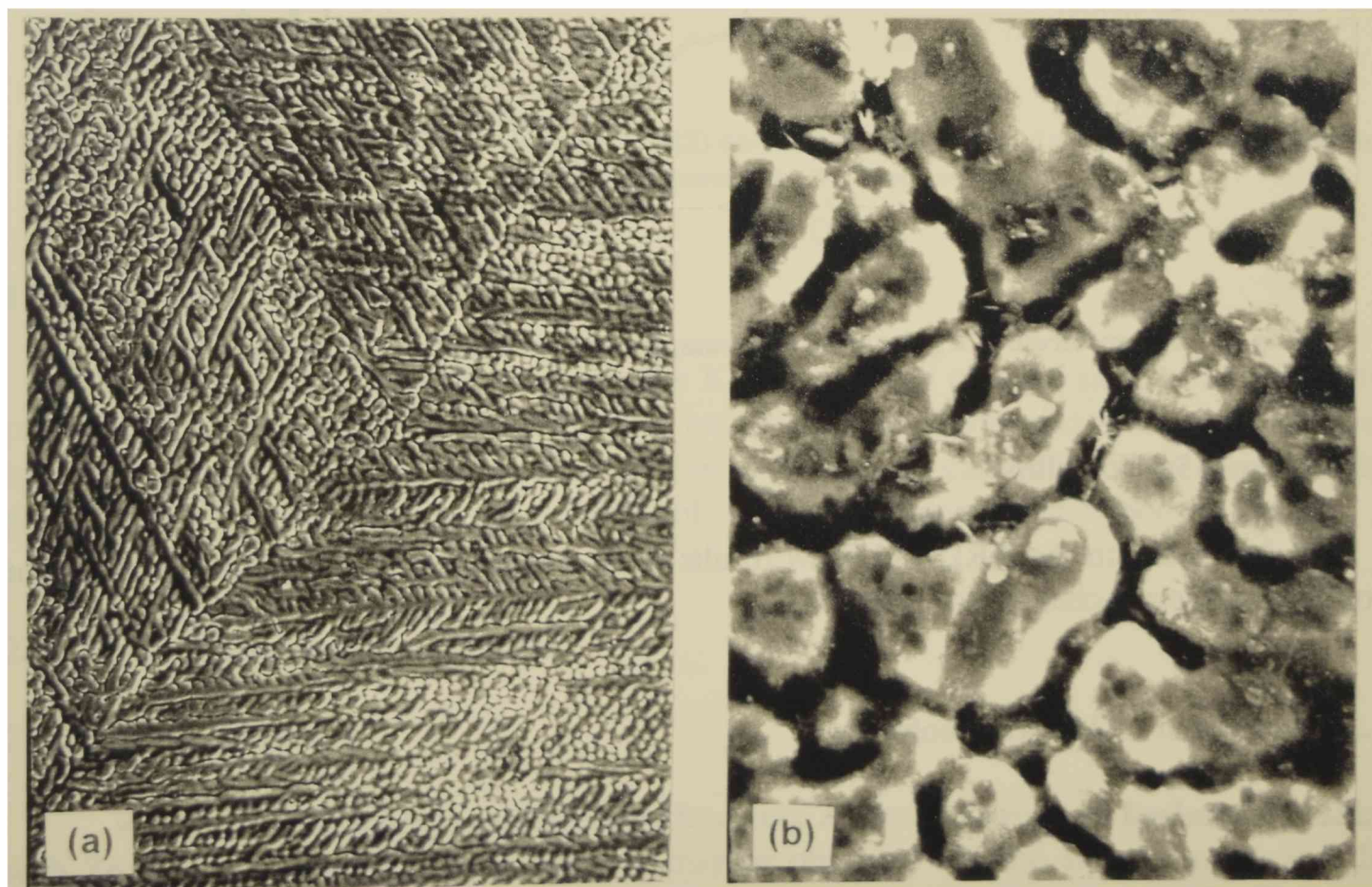


Fig.4.- SEM micrographs of a steel/55Al-Zn alloy coating sample after 24h exposure in salt spray cabinet.
a) Magnification = 200X and b) Magnification = 1500X.

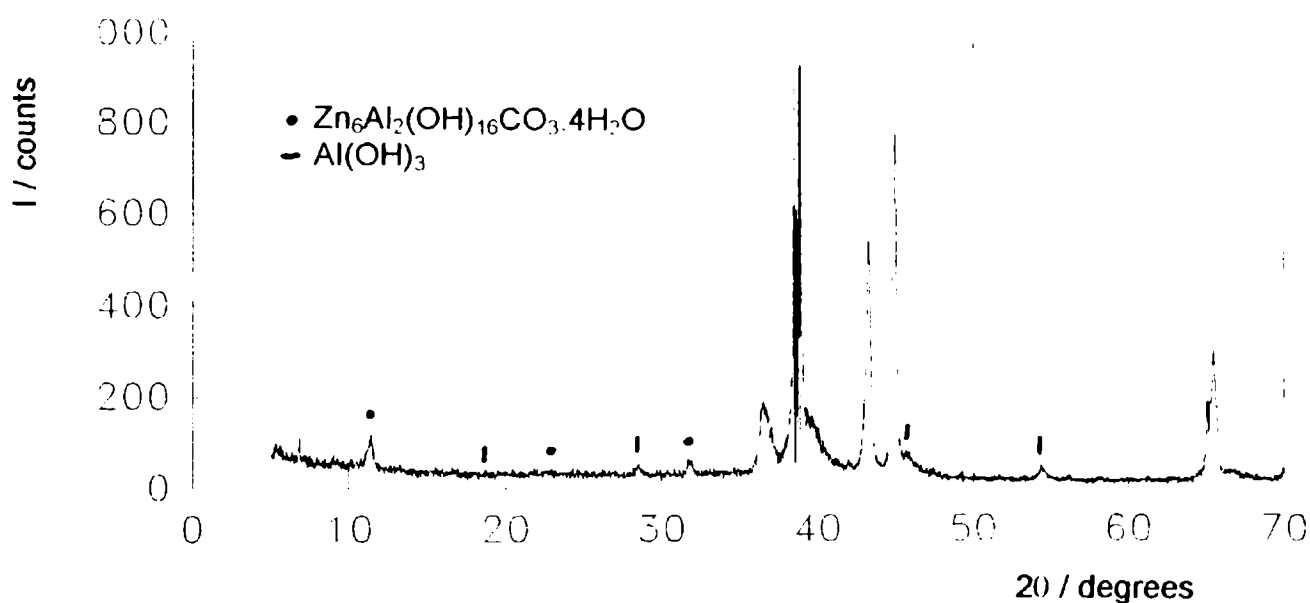


Fig.5.- XRD spectrum of a steel/55Al-Zn alloy coating sample after 360h exposure in salt spray cabinet.

1.2. Humidity cabinet (360h exposure)

1.2.1. Galvanized steel

XRD studies showed that basic zinc carbonate was the only constituent of the corrosion products, **Fig.6**.

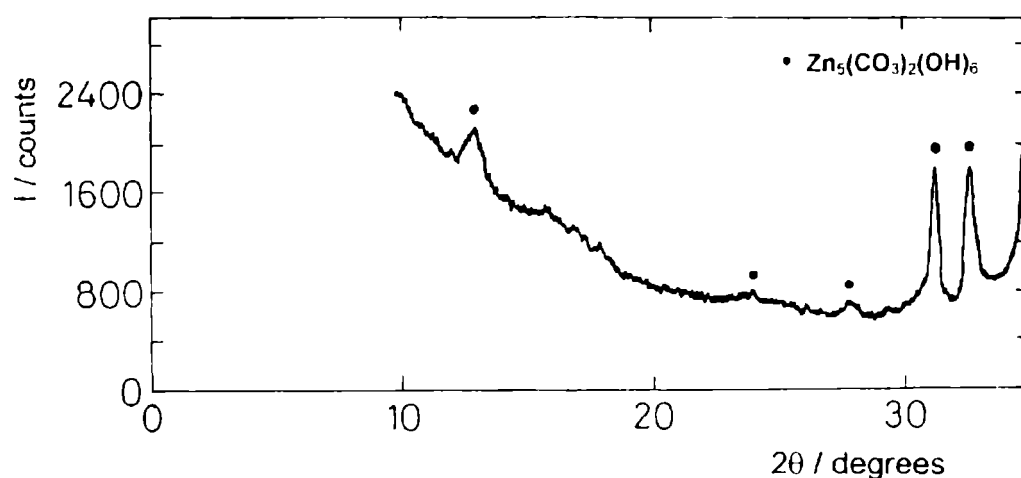


Fig.6.- XRD spectrum of a galvanized steel sample after 360h exposure in humidity cabinet.

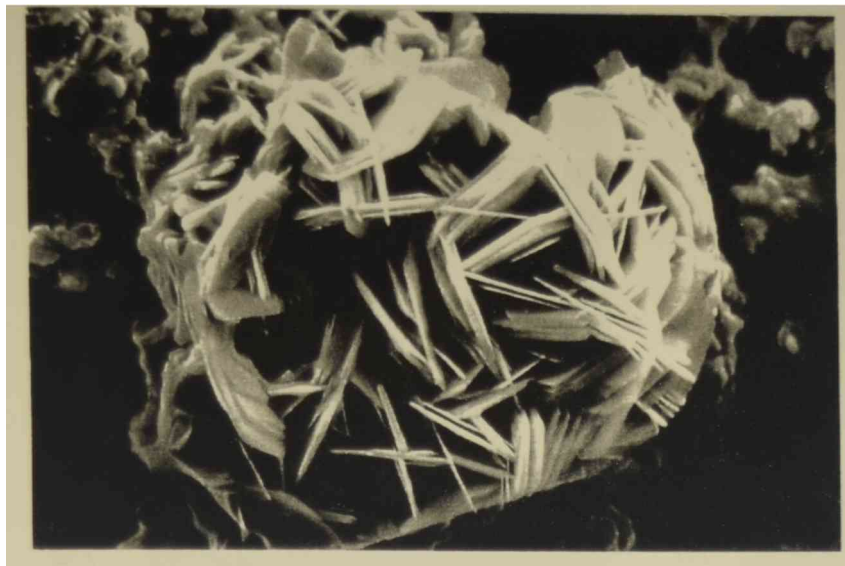
1.2.2. Steel/55Al-Zn alloy

According to the XRD and SEM results there was neither corrosion products on the coating surface nor changes in its structure.

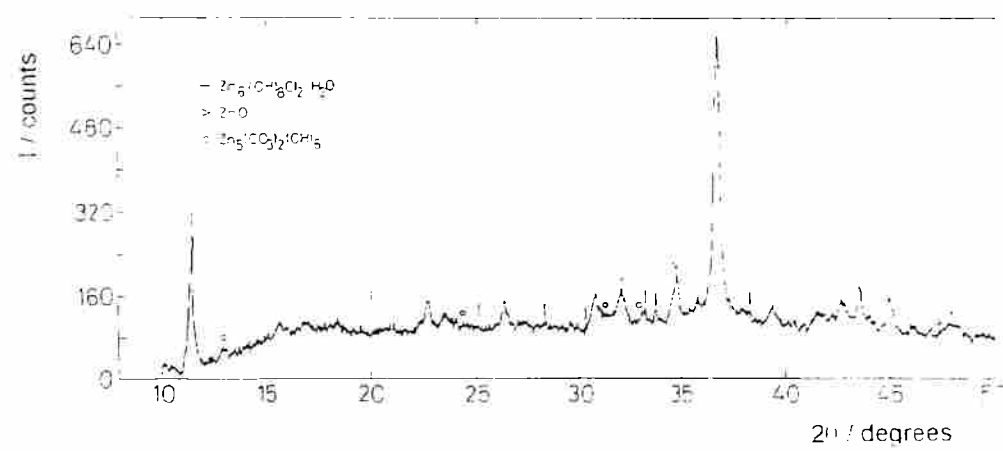
1.3. Immersion in 3% NaCl solution

1.3.1. Galvanized steel

The XRD spectra and SEM observations indicated that the corrosion products were the same obtained at the salt spray cabinet ones, **Fig.7a-b**.



(a)



(b)

Fig.7.- a) SEM micrograph (Magnification = 1500X) and b) XRD spectrum of a galvanized steel sample after 720h immersion in 3% NaCl solution.

1.3.2. Steel/55Al-Zn alloy

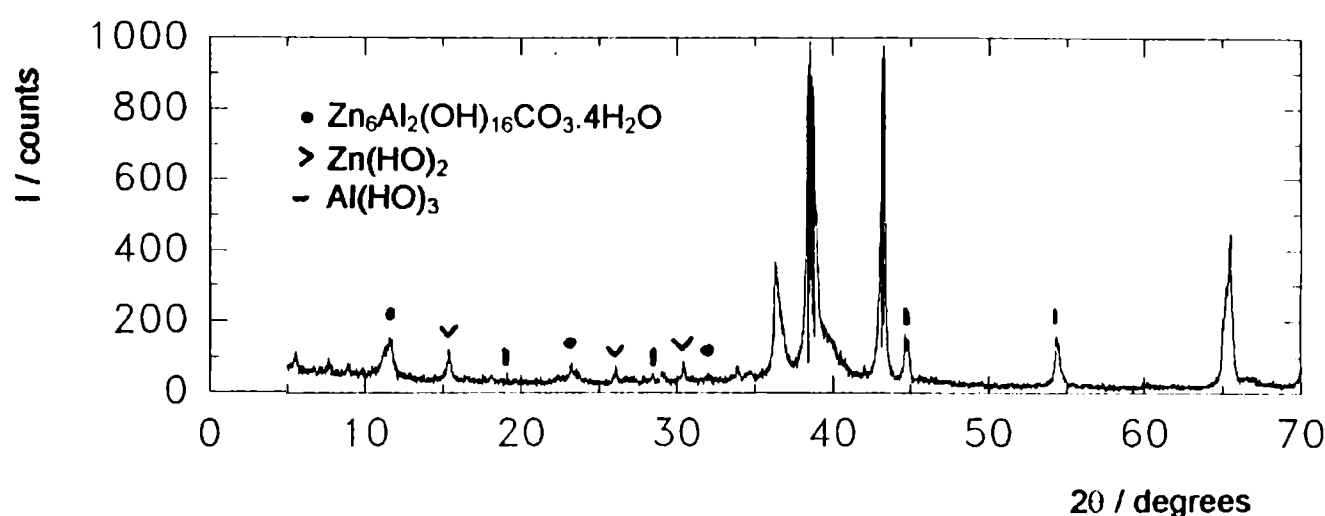
Likewise that at the salt spray test, the XRD performed on aged samples identified the presence of basic zinc-aluminium hydroxide, but in this case it was also found traces of zinc hydroxide (**Fig.8a**). On the other hand, similar investigations carried out on powders of the precipitated corrosion products led to detect solely basic zinc-aluminium carbonate, **Fig.8b**.

2. Analysis of the corrosion process

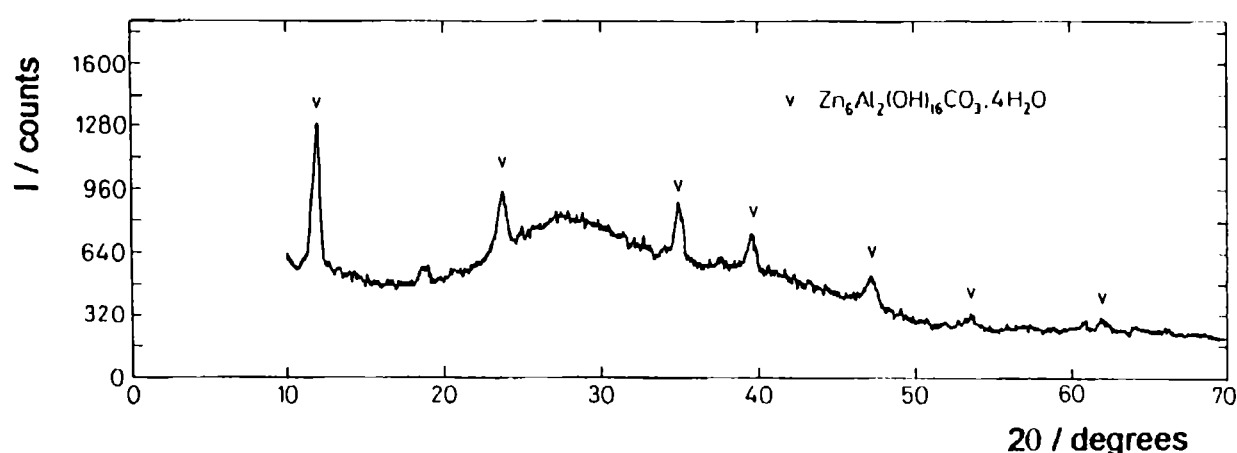
2.1. Salt spray cabinet

Fig.9a-b summarizes the different performance against corrosion of steel sheets coated with Zn or 55Al-Zn alloy. In this figure it may be observed the end state (**Fig.9a**) and the progress of the corrosive attack (**Fig.9b**), the latter estimated from the corroded area percentage. All the steel/55Al-Zn alloy coating systems showed an attack limited to the

unmasked cut edges, while in the galvanized steel it was not only more intense but also extended to the major part of the surface, **Fig.9a**.



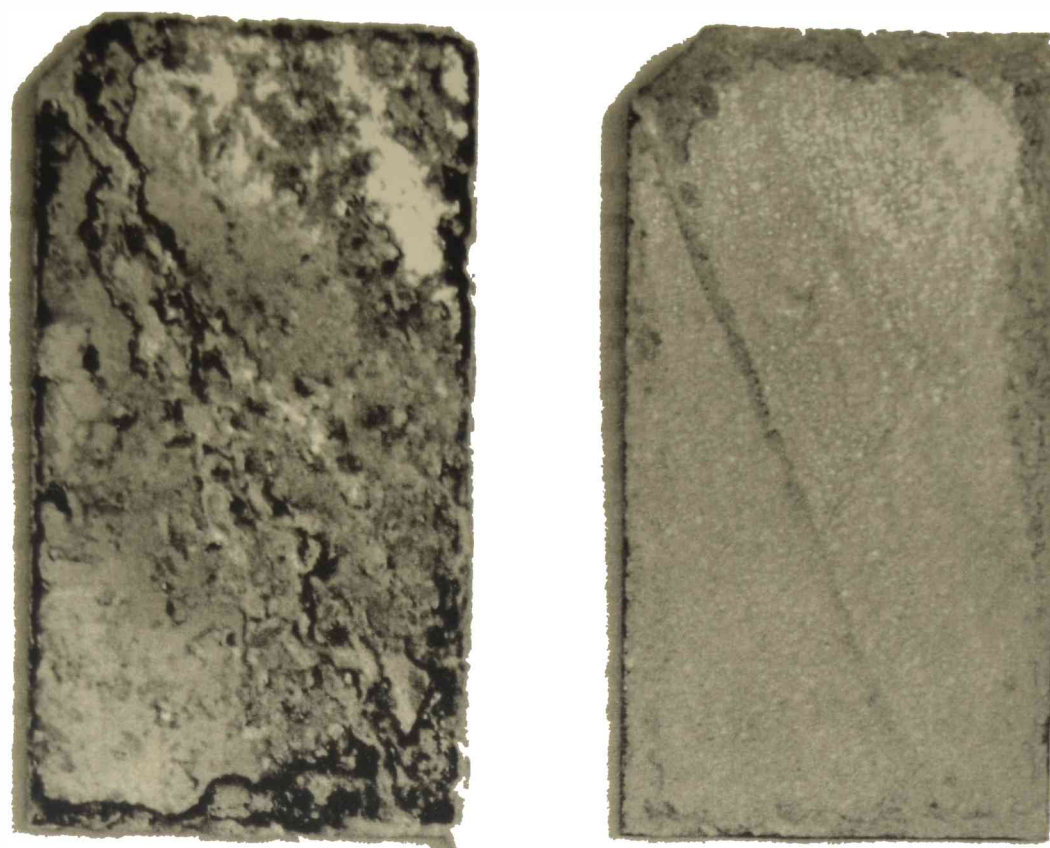
(a)



(b)

Fig.8.- XRD spectra corresponding to a) a steel/55Al-Zn alloy coating sample and b) its corrosion products, after 720h immersion in 3% NaCl solution.

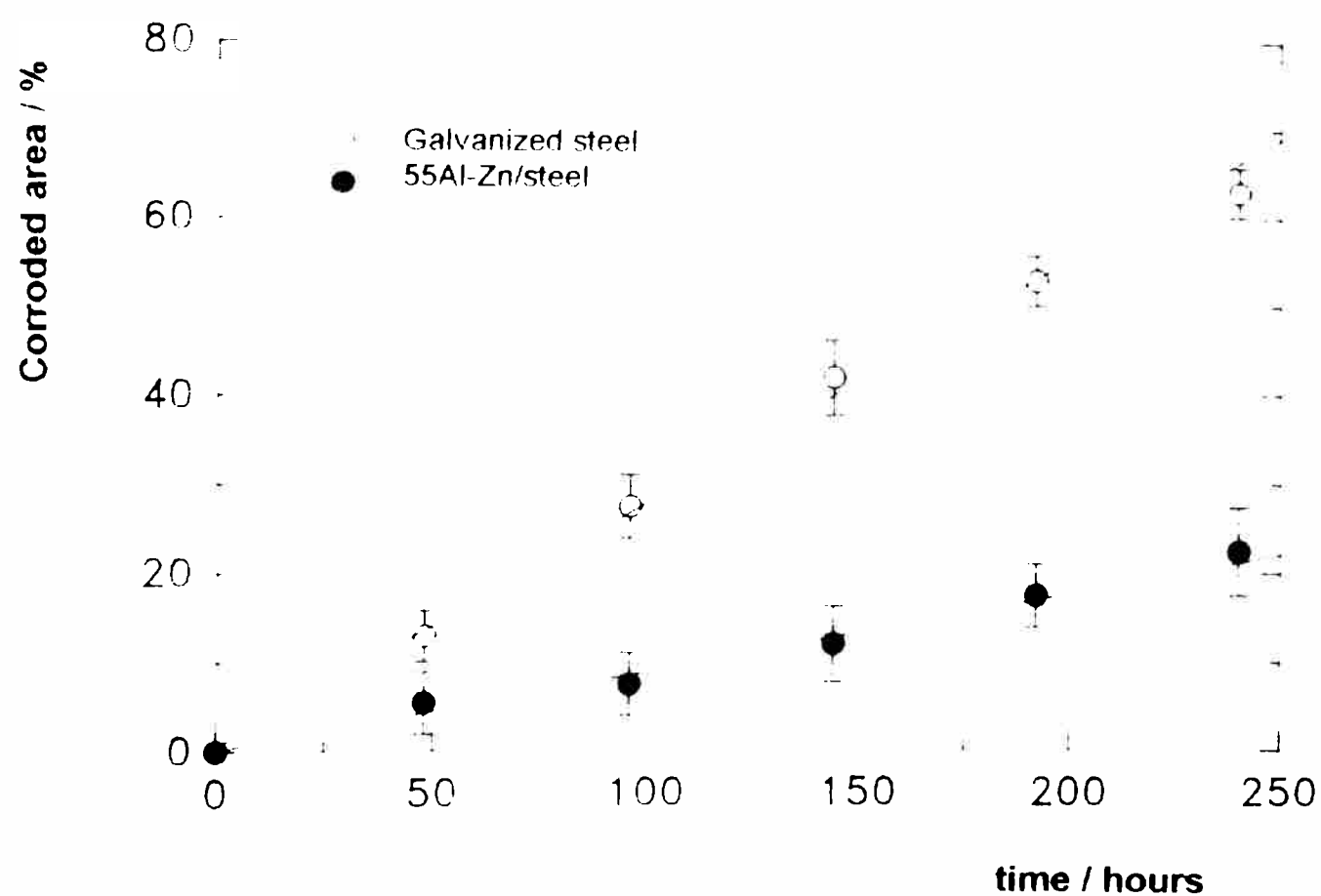
Fig.10 allows to observe the state of both cross scribed coating surfaces after 200h of exposure. Thus, it can be seen that the galvanized samples exhibited intense low carbon steel corrosion and the Zn nearby the cross was totally consumed. Instead, for the steel/55Al-Zn systems a high protective capacity and absence of both steel corrosion products and significant coating attack near the cross was found, but dense and dark corrosion products adhered to the exposed substrate could be observed. This compound was mostly $\text{Al}(\text{OH})_3$, a product commonly found on 55Al-Zn coating surface in contact with highly moist environments [5] and also on aluminium substrates in salty media [13]. After 360h of exposure, the substantial differences (**Fig.11**) showed that in media highly polluted with Cl^- ions, the 55Al-Zn coating provides not only cathodic protection but also barrier protection to the steel substrate, the latter due to the alloy coating further enhanced by the formation of a layer of the coating corrosion products precipitated on the surface active sites, which may help to account for its improved performance against corrosion, when it is compared with the Zn coating under the current experimental conditions.



galvanized steel

55Al-Zn/steel

(a)



(b)

**Fig.9.- a) Appearance of the samples after 260h exposure in salt spray cabinet and
b) Corroded area percentage vs. Exposure time.**

These results suggest that the first step in galvanized steel surface degradation may be zinc oxidation followed by hydration and fast carbonation, mechanism also outlined by several other authors [10-12, 14, 15], being the last the formation of Simonkolleite because of the NaCl crystallization on some surface points. In such circumstances, a localized concentration of Cl^- ions in combination with humidity may promote the coated substrate corrosion by substitution of the carbonate ions of the dense, slightly soluble, thin and partially insulating (from the medium) Hydrozincite layer, thereby weakening its protective capacity. This process has a fast kinetics [10], and it agrees with SEM results since, after only 5h of exposure in salt spray, a great amount of Simonkolleite on the Zn surface could be observed, **Fig.2a**; furthermore, the Simonkolleite being slightly dense and highly soluble provides a low barrier effect because the condensed solution is continuously washing the surface and, consequently, leaving bare zinc exposed. In this way, a dynamic and quick Zn consumer process leads to catastrophic results after short exposure periods, at least, from the anticorrosive point of view.

In the 55Al-Zn coating the first stage of the corrosion process would be the formation of aluminium hydroxide from the reaction between Al^{3+} ions with H_2O [16] within the dendrites (Al rich phase), which creates a thin film adhered to the metallic surface [13]. After 360h of exposure in the salt spray test, the **Fig.12** shows that on the 55Al-Zn coating surface there was a layer with the basic zinc-aluminium carbonate, formed presumably from the reaction between aluminium hydroxide and Hydrozincite, as the main component. Although being cracked, this layer covers homogeneously all the surface, and is denser and orderer than the film deposited on the zinc coating, which grows forming aislands and is highly voluminous. In addition, the absence of Cl^- ions in the layer of 55Al-Zn corrosion products turns it slightly soluble and, therefore, provides barrier protection limiting both the exposed area and the corrosion rate; however, as the steel is not completely isolated from the medium, the coating also works like a sacrificial anode supplying cathodic protection to the substrate.

2.2. Humidity cabinet test

The performance of both coatings against corrosion showed differences less significant than in salt spray, **Fig.13**. Thus, the corresponding to the 55Al-Zn coating was excellent since no steel corrosion product was found after 360h of exposure. On the other hand, the Hydrozincite identified by XRD accounts for why this metallic system behaves better in humidity cabinet than in atmospheres containing Cl^- ions; being the Hydrozincite denser and less soluble than the Simonkolleite, the surface became completely covered with a thin and continuous film providing barrier protection after certain exposure period. According to Odnevall [10], the film initially deposited on the zinc coating surface would be constituted by the ZnO coming from the reaction between the Zn and the atmospheric oxygen; given the atmospheric conditions, this oxide transforms in $\text{Zn}(\text{OH})_2$ which, in absence of other pollutants, reacts instantly with the CO_2 in the atmosphere forming carbonates, preferentially basic salts such as $\text{Zn}_5(\text{CO}_3)(\text{OH})_6$.

2.3. Immersion test

In spite that a less corrosive attack has been observed, the response of the steel sheets coated with either 55Al-Zn alloy or Zn alone was very similar to the salt spray one, particularly in the galvanized samples. It is emphasised that in order to understand better the complex

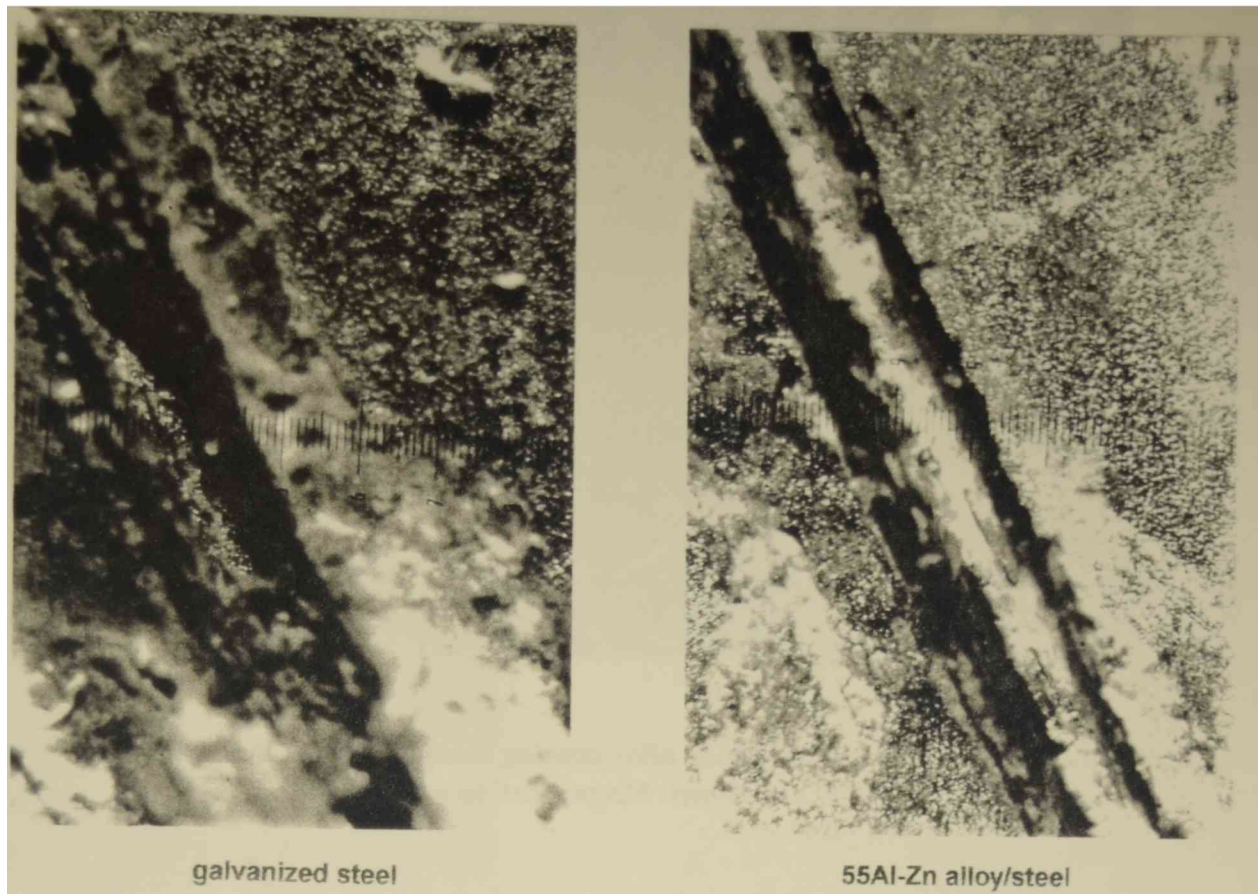


Fig.10.- Appearance of the samples after 260h exposure in salt spray cabinet. Magnification = 40X.

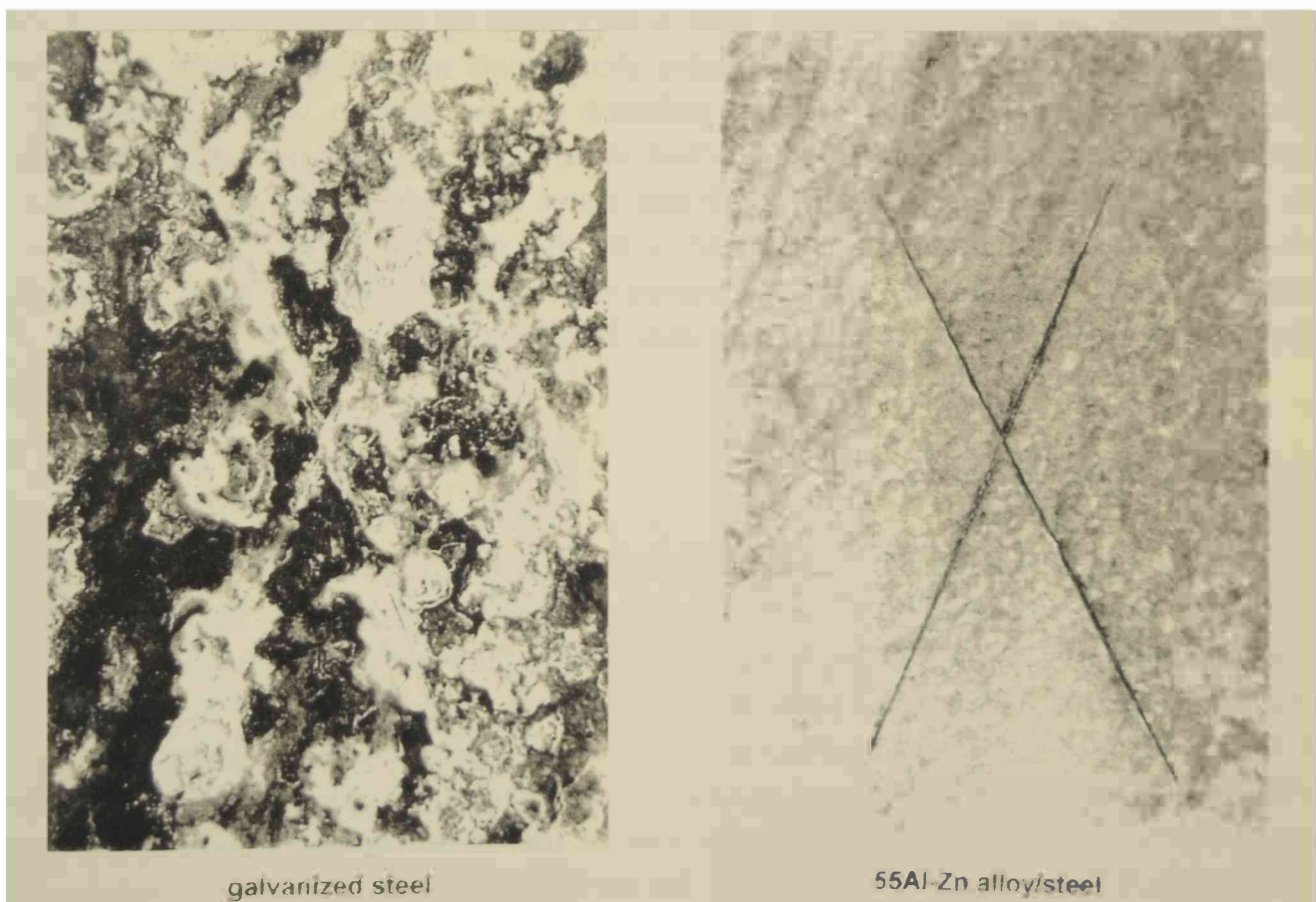


Fig.11.- Appearance of the samples after 360h exposure in salt spray cabinet.

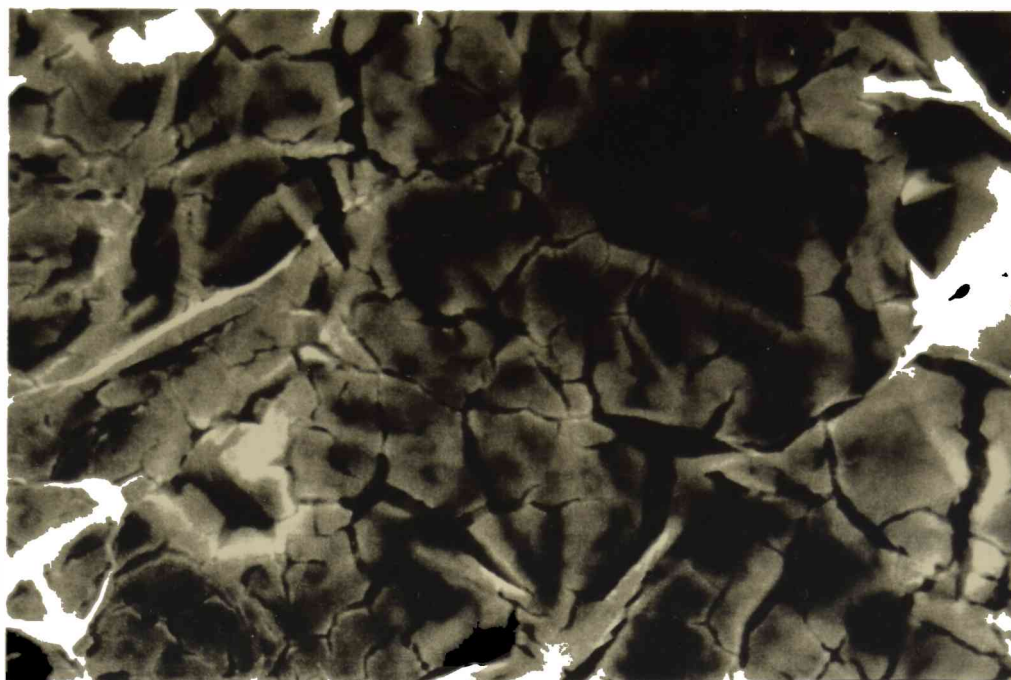


Fig.12.- SEM micrograph of a steel/55Al-Zn alloy coating sample after 360h exposure in salt spray cabinet. Magnification = 2200X.

processes involved in all the above mentioned environments new studies are in progress, however, a first approach to explain the changes observed in the coatings behaviour when are submitted to immersion or salt spray tests assumes that differences in the oxygen availability may be a variable to take into account. This is supported by the fact that the attack intensity decreased as the submerged part of the coated steel sheets moved away from the air/solution interface; furthermore, the Simonkolleite gathered on the surface would provide a barrier protection enhanced with regard to that reached in salt spray because no surface washing takes place. This may be confirmed from the different states showed by the two faces of the tested panels after being submerged (inclined 30° from the vertical) in the NaCl solution since, presumably due to the thicker layer of corrosion products deposited on it, the upper face displayed much less attacked than the down one, **Fig.14**.

3. Electrochemical measurements

Polarization curves obtained for the different coated steel samples are shown in **Fig.15**. None of the samples showed an important cathodic contribution within the 0.5V of cathodic polarization and there was no meaningful differences in their anodic behaviour; all the samples dissolved at a similar rate and no passivation effect was observed. As the anodic polarization went by the electrolyte became opalescent due to a corrosion products suspension; thus, after polarizing 0.5V the dissolution current gradually decreased in the galvanized and 55Al-Zn alloy coatings, but not in the aluminized ones, because of the barrier protection provided by a layer of such products which completely covered the surface. In addition, on the aluminized as well as on the 55Al-Zn alloy coatings a gas bubble evolution was noted. Since at the reached potential level neither hydrogen nor oxygen can evolve electrolytically, the bubbles would probably be a consequence of the water hydrolysis in presence of active aluminium.

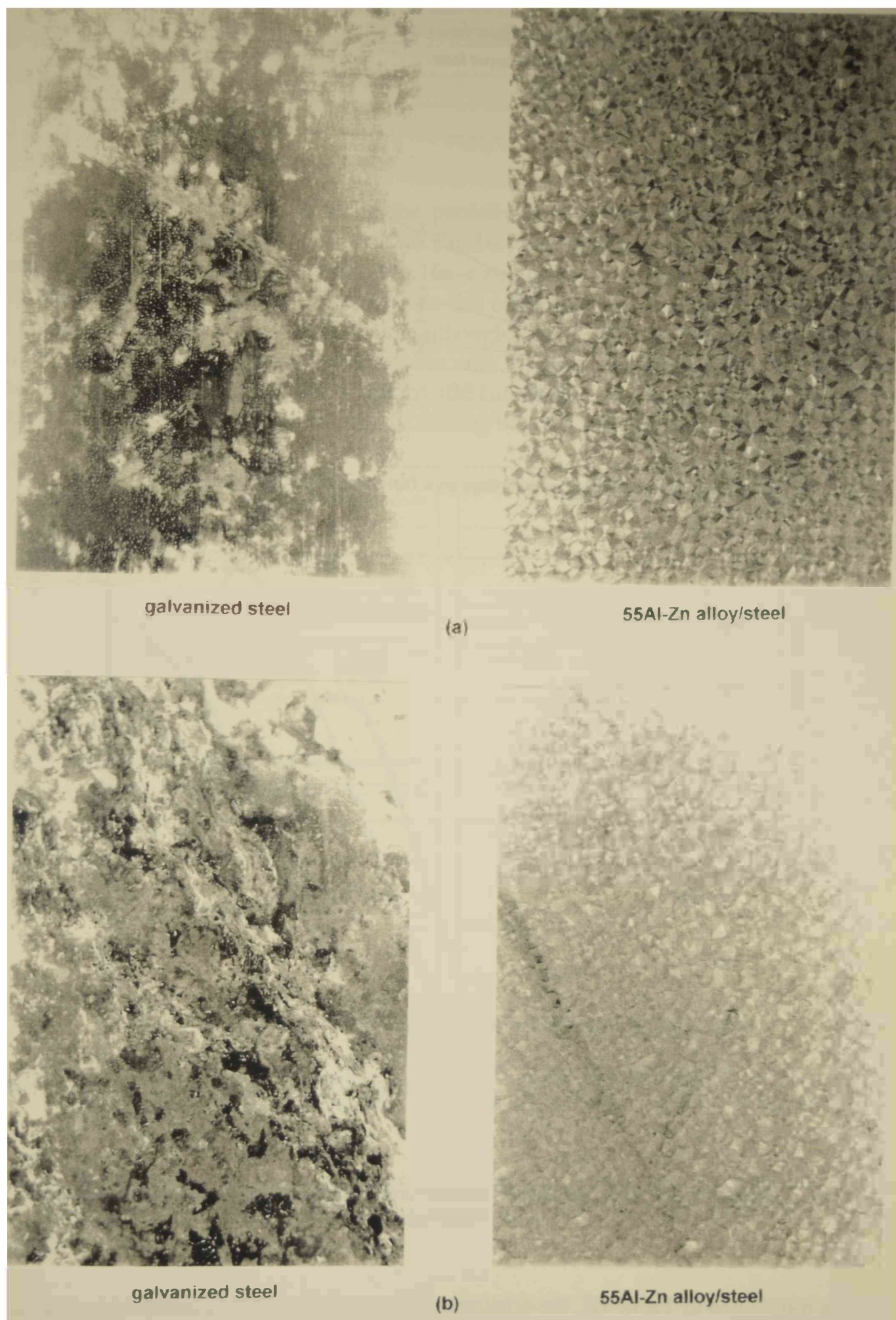


Fig.13.- Appearance of the samples after the ageing test. a) Humidity cabinet for 360h and b) Salt spray cabinet for 264h.

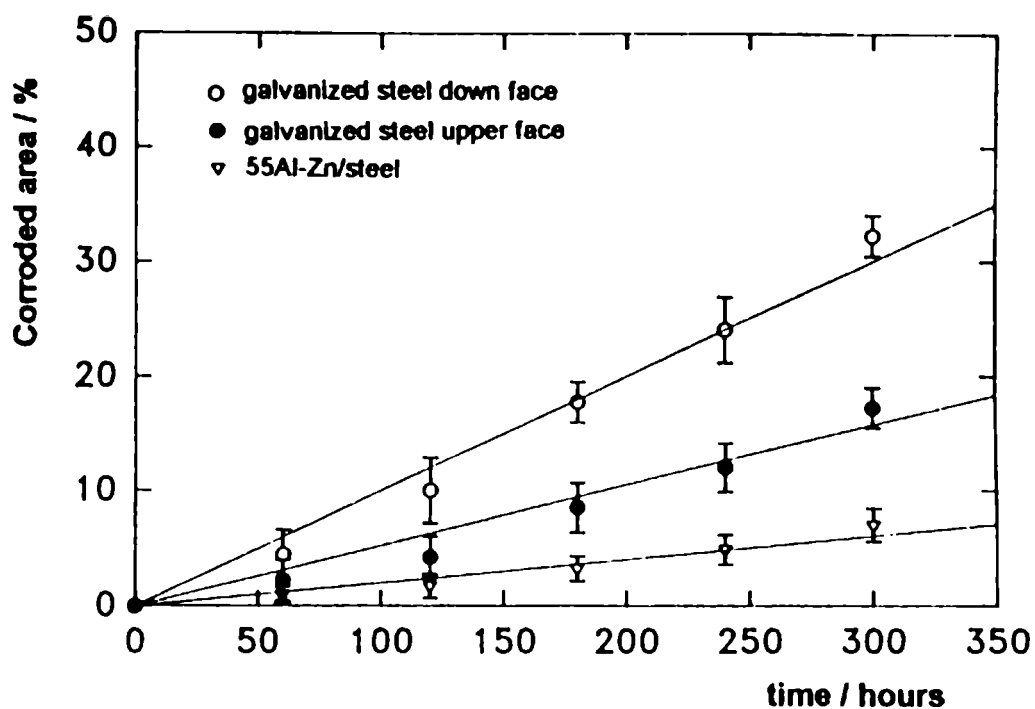


Fig.14.- Corroded area percentage as a function of the exposure time.

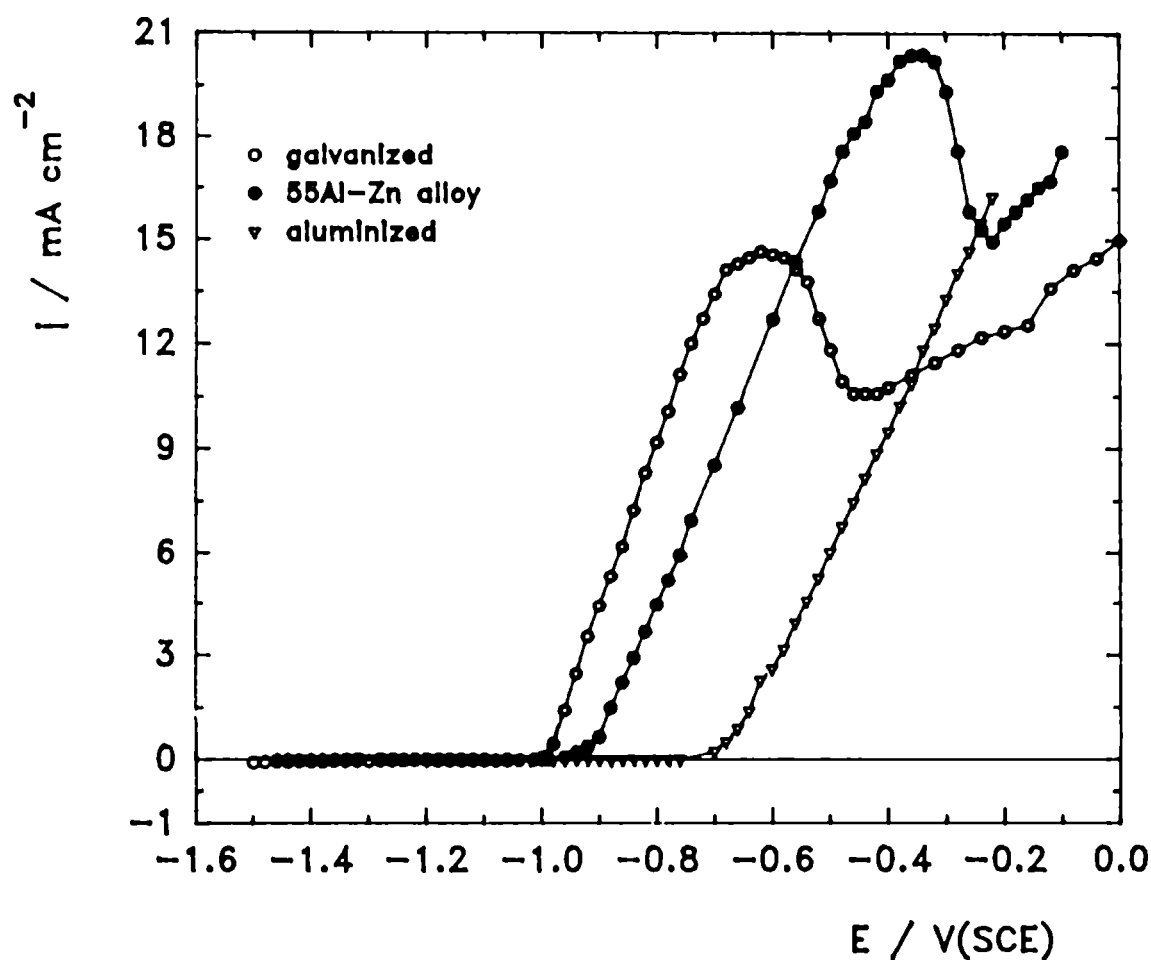


Fig.15.- Polarization curves of galvanized, aluminized and 55Al-Zn alloy coated steel samples in 3% NaCl solution.

As it is shown in **Table III**, the coatings became less electrochemically active as the Al-content increased. Nevertheless, as the steel corrosion potential in this medium is around -0.7 V(SCE), all of them may provide cathodic protection to the substrate.

Table III

Sample	Open circuit potential / V(SCE)
Galvanized	-1.020
55Al-Zn alloy	-0.980
Aluminized	-0.780

The variation of potential along the partially coated steel strip during immersion in quiescent 3% NaCl solution is shown in Fig.16. Experimental results obtained for the horizontal arrangement are displayed in Fig.16a-c and those corresponding to the vertical one in Fig.16d-f. In general, as the distance from the coating steel boundary was increased, the steel potential moved in a positive direction although, due to the high electrolyte conductivity, no more than 0.020 V. A potential dependence with the immersion time was also found; thus, as the immersion time went by the shape of the curves did not change but the open circuit potential shifted to more positive values, decreasing the cathodic protection level.

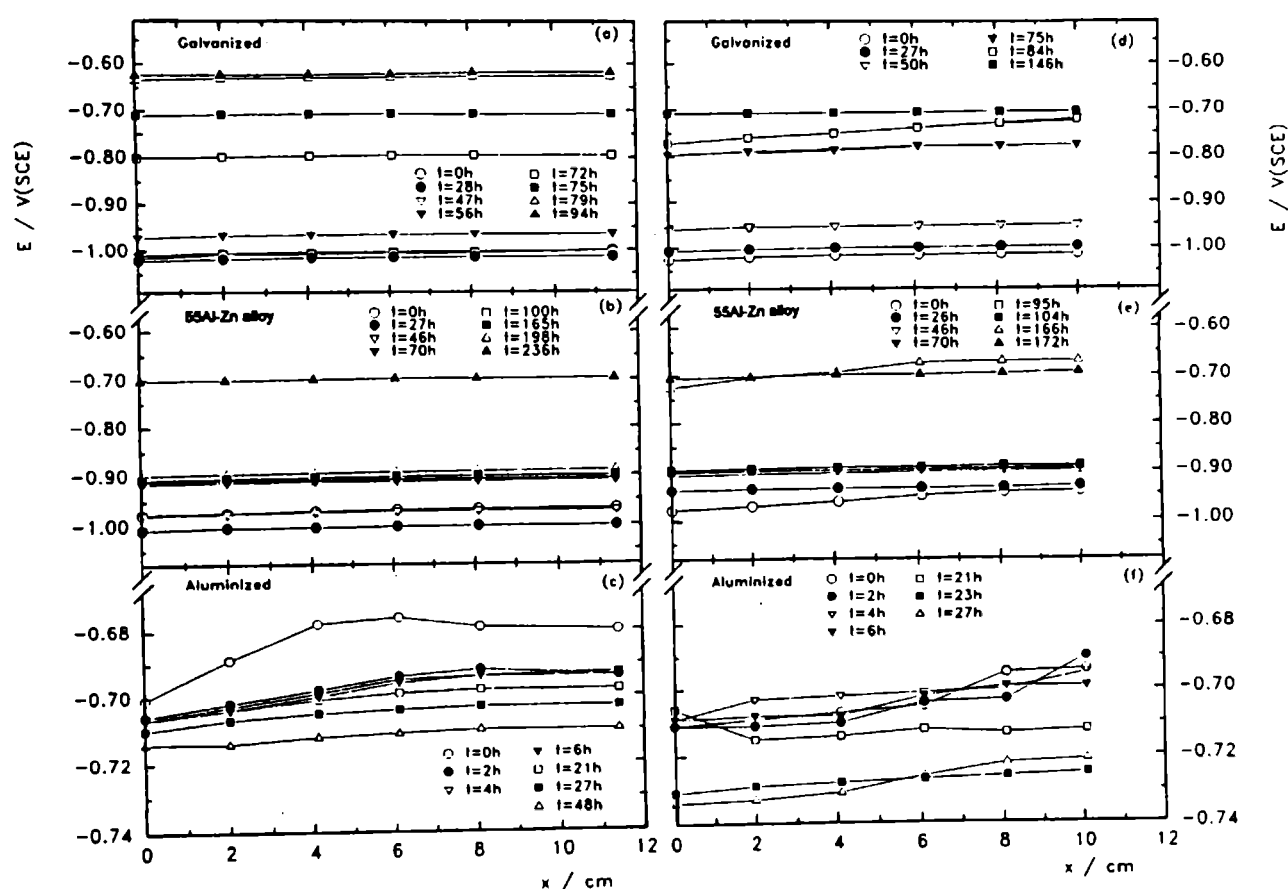


Fig.16.- Open circuit potential distribution vs. distance from the edge of the partly coated steel area, using the exposure time as parameter. a-c: horizontal arrangement; d-f: vertical one.

At the beginning of the experiments, partially galvanized steel samples had the most active potential value, -1.020 V(SCE), and aluminized ones the least, which was around -0.7 V(SCE).

Galvanized and 55Al-Zn alloy samples, placed in the horizontal arrangement showed a similar behaviour, since potential vs. distance curves shifted to more negative potentials over the first 27 hours immersion and then increased. This was an interesting observation because it suggested that the coatings ability to cathodically protect steel was not static. It initially

increases with time, and later the cathodic protection level gradually decreases as the immersion elapsed (**Fig.16a-c**). Galvanized samples showed a potential value near -1.0 V(SCE) up to 56 h immersion and then suddenly increased up to -0.8 V(SCE) after 72 h; the total loss of cathodic protection was observed at 94 h. The 55Al-Zn alloy coating performance was better than the previous one. A satisfactory protection level was maintained until 196 h immersion and the total loss occurred after 236 h, when the potential distribution was around -0.7 V(SCE). Aluminized samples (**Fig.16c**) showed an entirely different behaviour; the cathodic protection level increased as the immersion time elapsed but, this increase was no greater than 0.015 V. The potential distribution was always near to the steel corrosion potential and, therefore, the protection efficiency was lesser.

For the vertical arrangement, the potential distribution vs. distance was of the same order of magnitude than in the previous case but no initial shift to more negative potentials was observed for galvanized and 55Al-Zn alloy samples. An acceptable cathodic protective level (\approx -0.9 V(SCE)) was kept up to 50 h and 104 h by the Zn and 55Al-Zn alloy coatings, respectively; however, at 146 h and 172 h such a protection had completely been lost. The less cathodic protection period (27 h) was again given by the partially aluminized samples and the potential distribution vs. distance curves exhibited a random relationship with the immersion time.

For both, horizontal and vertical arrangements, the solution became opalescent because of the great amount of white corrosion products formed. In general, the horizontal arrangement gave the longest cathodic protection period, probably due to the barrier protection of the corrosion products deposited on the surface of the whole strip. Galvanized and 55Al-Zn alloy coatings were completely consumed along the exposure time, which account for the eventual loss of cathodic protection.

The samples visual inspections accomplished throughout the experiments showed that galvanized coating dissolution was complete and uniform (**Fig.17a**), whilst the morphology of the corroded 55Al-Zn alloy coating surfaces indicated a selective interdendritic dissolution of the Zn-rich phase (**Fig.17b-c**), being in accordance with that reported by other authors [9]; on the contrary, partially aluminized steel areas were found to be quite intact at the end of the coupling experiment even after the steel strips had rusted (**Fig.17d**)

CONCLUSIONS

- All the coatings were more active than steel and none of them showed passivation under the current experimental conditions. Therefore, all of them provide cathodic protection to steel substrates, although with a level which is variable along the immersion time. Thus, the Zn and 55Al-Zn alloy coatings showed better protection level than the aluminized ones for long immersion periods.
- The 55Al-Zn alloy coated steel shown to have a synergistic effect since its corrosion performance was superior to the each one of the metals used individually. Furthermore, a comparative analysis of the electrochemical potential data proved that 55Al-Zn alloy was the most effective coating since provided both good cathodic protection level (for at least 172 h or 236 h in vertical and horizontal arrangement, respectively) and barrier protection (supplied by the basic zinc-aluminium carbonate layer) to the substrate.

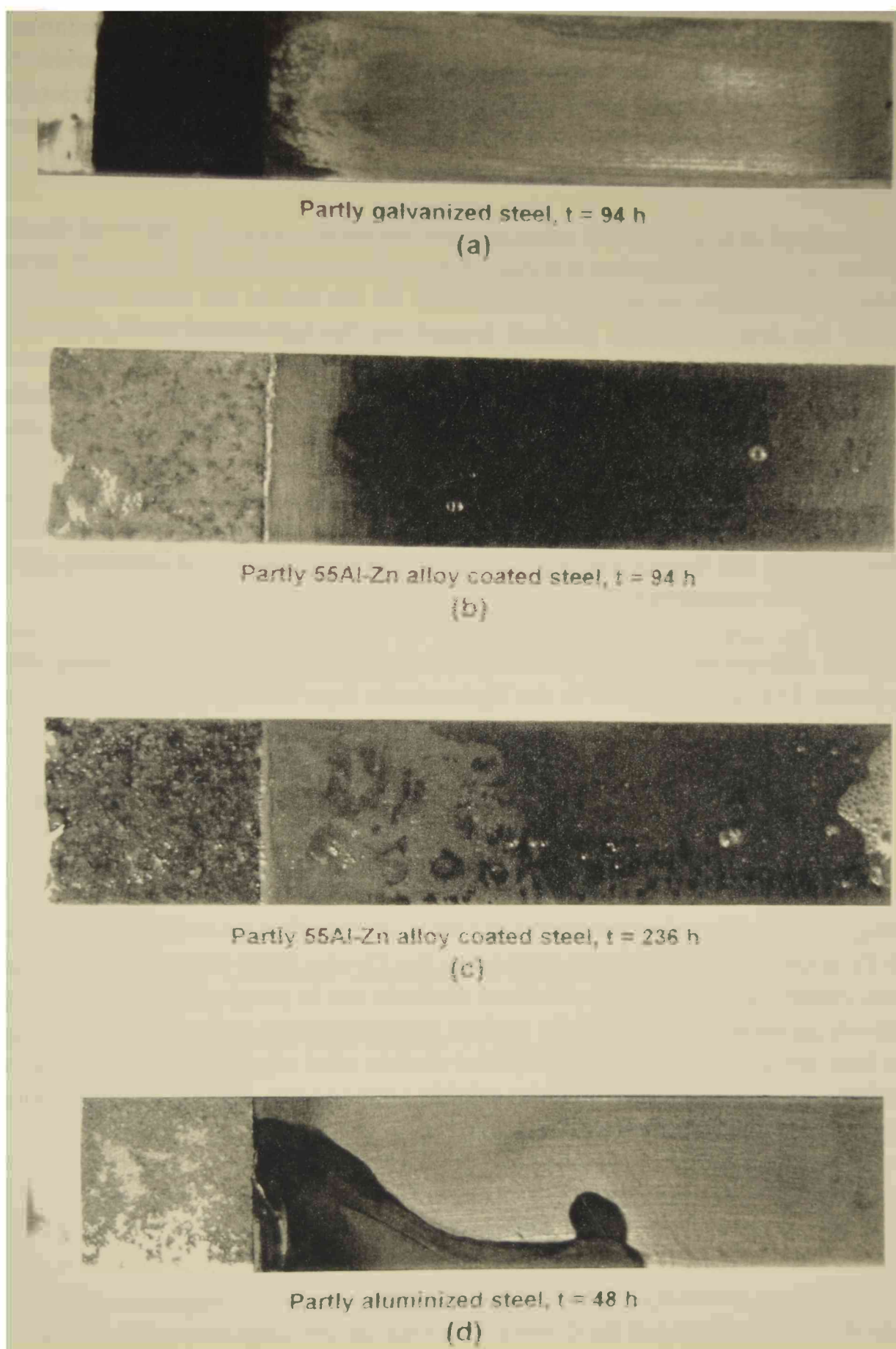


Fig.17.- Photographs of the steel coated appearance after the cathodic protection tests. a) Galvanized, for 94h; b) 55Al-Zn alloy, 94h; c) 55Al-Zn alloy, 236h and d) Aluminized, 48h.

- Due to the high crystallinity degree of the corrosion products formed from the Zn and 55Al-Zn coatings dissolution, the X-ray diffraction resulted to be a very useful technique for their characterization. The nature and composition of such products have allowed to explain some of the differences found in the tested samples behaviour. Thus, in accordance with the electrochemical results, the superior performance against corrosion provided by the steel/55Al-Zn coating system was accounted for in terms of an efficient barrier protection (ascribed basically to the basic zinc-aluminium carbonate layer) and cathodic protection to the substrate.
- The normalized salt spray tests were also an interesting tool for assessing the corrosion resistance properties of the hot dip coated steel sheets, essentially due to its advantage in providing reproducible experimental conditions. At the end of the tests, Simonkolleite was found as the final corrosion product formed on the galvanized steel. This compound growing in preferential places was, therefore, unable to develop a barrier protection and there was always bare zinc in contact with the environment; besides, the high rate of Simonkolleite formation made the process highly dynamic and leading to bad results from the corrosion resistance viewpoint. Instead, on the 55Al-Zn coating, the final corrosion product was basic zinc-aluminium carbonate which, being less soluble than the Simonkolleite because of the absence of Cl⁻ ions in its structure, formed a protective layer limiting not only the transport of aggressive species towards the steel/medium interface but also the metallic corrosion rate.
- Only small differences between the both coatings performance in the humidity cabinet test were found. This was attributed to the Hydrozincite layer formed on the Zn coatings, which provided high corrosion protection and, therefore, longer useful life.
- It was assumed that the galvanized steel behaved better in immersion tests than in the salt spray one because of the lower oxygen availability for the cathodic reaction caused by the Simonkolleite layer precipitated on the Zn surface.
- Although all the gathered experimental evidence showed that the corrosion behaviour of the 55Al-Zn alloy coating was always better than the Zn one, more investigations including new optical, electrochemical and standardized methods are in progress. Their main objective is to provide an insight concerning the surface characterization and protection mechanisms of these two hot-dip applied coatings on low carbon steel sheets in order to optimize their paintability as well as to develop more suitable anticorrosive organic coatings to be used in highly aggressive environments.

Acknowledgments

The authors gratefully acknowledged the Comisión de Investigaciones Científicas de la Provincia de Buenos Aires and the Consejo Nacional de Investigaciones Científicas y Técnicas (CONICET) by the financial support to this investigation work.

REFERENCES

- [1] M. Stratman, K. Bohnenkamp & W.J. Engell, *Corros. Sci.*, **23**, 969 (1983).

- [2] A.R. Cook, *Anti-Corr. Methods Mater.*, **23**(3), 5, (1976).
- [3] C.E. Bird & F.J. Strauss, *Mater. Perform.*, **15**(11), 27 (1976).
- [4] F.E. Goodwin, *Zinc-Based Steel Coatings Systems: Metallurgy and Performance*, Ed. by G. Krauss, The Minerals, Metals & Materials Society (1990).
- [5] ASMs Handbook, vol.13, *Corrosion*, ASM International ed., 1992.
- [6] J.C. Zoccola, et. al., *Atmospheric Factors Affecting the Corrosion of Engineering Metals*, STP 646, American Society for Testing and Materials, 165-184 (1978).
- [7] K.R. Baldwin, C.J.E. Smith & M.J. Robinson, *Corrosion*, **51**(12), 932 (1995).
- [8] A.J. Stavros, "Galvalume Wire" presented at 51st Wire Association Intl Conference, Atlanta, GA, oct. 12-16, 1981, pag. 8.
- [9] E. Dalledone, M.A. Barbosa & S. Wolyneć, *Materials Performance*, july, 24 (1995).
- [10] A.M. Beccaria, *Corros. Prev. and Control*, June, 53 (1994).
- [11] I. Odnevall, Doctoral Thesis, Depart. of Materials Sci. and Eng., Div. of Corros. Sci., Royal Institute of Technology, Stockholm, 1994.
- [12] E. Almeida & D. Pereira, *Prog. Org. Coatings*, **17**, 175 (1989).
- [13] J.A. Gonzalez & J. M. Bastidas, *Rev. Iber. de Corr. y Prot.*, **13**, 7 (1982).
- [14] J.F.A. van Eijnbergen, *The Zinc Patina*, Stichting Doelmatig Verzinken, Holland, 1972.
- [15] T. Aoki, Y. Miyoshi & T. Kittaka, *Galvatech '95 Conference Proceedings*, p 463.
- [16] K. Capoum & A. Cepero, *Rev. Iber. Corros. y Prot.*, Vol **XVII**(3), 212 (1986).

Reactive Surfactants in Heterophase Polymerization of High Performance Polymers. VIII.¹

Emulsion polymerization of alkyl sulfopropyl maleate polymerizable surfactants (surfmers) with styrene

SURFACTANTES REACTIVOS EN POLIMERIZACION HETEROFASICA DE POLIMEROS DE ALTAS PRESTACIONES. VIII. POLIMERIZACION EN EMULSION DE SURFACTANTES POLIMERIZABLES (SURFMERS) DEL TIPO SULFOPROPIL ALQUIL MALEATOS

Harold A.S. Schoonbrood², María J. Unzué³, Javier I. Amalvy⁴, José M. Asua³

SUMMARY

The copolymerization of styrene with two polymerizable surfactants (surfmers) based on maleic acid (dodecyl sodium sulfopropyl maleate and tetradecyl sodium sulfopropyl maleate) was studied in batch emulsion polymerizations. The surfmer conversion was obtained by serum replacement with water and subsequent analysis of the recovered, unreacted surfmers with two-phase titration. It was found that both surfmers copolymerized well with styrene, and their partial conversion was higher than that of styrene. These results are contradictory to what was found before in literature using ultrafiltration with methanol, and the differences are explained on the basis of oligomer formation: the oligomers formed are detected if the latices are washed with methanol. It was found that at the end of the polymerization (almost complete conversion of both styrene and surfmer) only 45% of the surfmer groups were present on the particle surface, which is in agreement with a high conversion of the surfmer at the beginning of the reaction.

Keywords: *emulsion polymerization, surfmers, copolymerization of styrene*

INTRODUCTION

In two publications by the present authors [1a,b] several anionic polymerizable surfactants (surfmers) with varying copolymerization reactivities were studied in the semi-continuous emulsion terpolymerization of styrene (S), butyl acrylate (BA) and acrylic acid (AA). It was found that surfmers with low to intermediate reactivity with the main monomers (S and BA) were most useful: a surfmer derived from maleic acid (tetradecyl sodium sulfopropyl maleate, M14) seemed to function better than the reactive methacrylate derivative and the unreactive crotonate derivative [1a]. The methacrylate surfmer led to very unstable latices, and the crotonate surfmer was not incorporated to an extent that makes its use interesting [1b]. Although M14 functioned the most favourably of the three surfmers, its

¹ Esta publicación es parte de una serie de publicaciones del European Union Programme "Human Capital and Mobility"

² Present address: Rhône-Poulenc. Centre de Recherches d'Aubervilliers, Francia

³ Grupo de Ingeniería Química, Departamento de Química Aplicada, Facultad de Ciencias Químicas, Universidad del País Vasco, España

⁴ Miembro de la Carrera del Investigador de la CIC

straightforward use in the semi-continuous emulsion terpolymerization of S, BA and AA (with constant addition rate of all monomers including the surfmer) results in very high instantaneous conversions of the surfmer (for particle sizes below 100 nm), and only a fraction (35%) of the surfmer groups could be retraced at the particle surface at the end of the process. In the ideal case 100% should be situated at the surface. It was suggested that this be a consequence of the high conversion of the M14 throughout the reaction, as determined by serum replacement with water. This high conversion was also observed for the dodecyl derivative (M12) [1c] in similar reactions, and also for the M14 in aqueous phase reactions [1b]. However, Goebel *et al.* [2] and Stähler [3] reported that the conversion of these surfmers (measured with ultrafiltration in methanol) in the batch emulsion polymerization of styrene remained very low up to conversions of styrene of 80%, and that at higher conversions of the styrene (between 80% and 95%) a rapid polymerization of the maleates to completion was observed. This was ascribed to the fact that upon the system becoming glassy at high styrene conversion, the reaction locus was shifted from the whole particle volume to the particle surface. At first sight, this may not seem contradictory to the results obtained during the semi-continuous emulsion terpolymerization of S, BA and AA because a relatively high conversion was achieved during the process (although the polymerization proceeded by no means under strictly starved conditions) [1]. However, this system is always above its glass transition temperature ($T_g \approx 2^\circ\text{C}$, $T_{\text{reaction}} = 80^\circ\text{C}$). This prompted us to study the batch emulsion polymerization of styrene and these maleate surfmers.

In the following we will present results of batch emulsion polymerizations of styrene (S) with M14 and M12, where the conversions of S and surfmer were determined as function of time. A mechanism is proposed that can account for the experimental observations.

EXPERIMENTAL

The following chemicals were used: styrene (S) was distilled and stored at -18°C . Potassium persulfate (KPS, Fluka, 99%), α,α' -azobisisobutyronitril (AIBN, Fluka), and sodium bicarbonate (Merck, 99.5%), were used as received. The surfmers M12 and M14 were synthesized according to methods described in literature [2]. The purity of M12 was approx. 92%, and that of M14 approx. 76% [1a]. M12 was obtained from K. Stähler, Max Planck Institut für Kolloid- und Grenzflächenforschung. The reactions are carried out in glass reactors (500 ml) with a water jacket for temperature control. A heat exchanger connected with tap water was placed between the reactor and the water bath to control any sudden heat production and to keep the reactor at the set temperature (80°C). Styrene conversion was determined by gravimetry. Particle size was determined with light scattering (LS) with a Malvern System 4700c. This technique gives a z-average particle size ($d_z = \Sigma(n_i d_i^5) / \Sigma(n_i d_i^4)$).

Apart from samples for gravimetry, also samples for determination of the conversion of the surfmers were taken. Two techniques were used to separate the serum from the latex particles to determine the free surfmer content. In most cases serum replacement was used, but in some cases (additional) results with successive centrifugation/redispersion stages were obtained. Note that a large part of the unreacted surfmer can be adsorbed on the surface of the latex particles. Therefore one cannot apply coagulation or a one-step filtration/centrifugation, because then only the unreacted surfmer in the aqueous phase will be determined. Serum replacement (SR) was performed with a UHP-76 of MicroFiltration Systems, flushing distilled water through in discontinuous mode and the affluent was collected for later analysis of the

surfmmer concentration. Ultracentrifugation (UC) was carried out with a Centrikon H-401 (Kontron), at 22,000 rpm for 30 min - 2 h. The method of two-phase titration to determine surfmer concentration and the conductrimetric titration for the determination of the surface charge density have been described before [1b].

A summary of the reactions carried out for the present work is given in **Table I**.

Table I

Recipes of batch emulsion polymerizations of S with maleate surfmers carried out at 80°C.

components (g)	A ^{b)}	B ^{c)}	C	D	E	F
S	100	70	100	100	149.5	149.5
M14	3.21	2	2	1.77	1.59	-
M12	-	-	-	-	-	1.49
AIBN	0.875	-	-	-	-	-
KPS	-	0.15	0.15	0.136	0.037	0.037
NaHCO ₃	-	0.15	0.15	0.136	0.039	0.039
H ₂ O	500	232	232	75.8	349	349
cyclohexane	-	30	-	-	-	-
latex C	-	-	-	263.3	-	-
solid content (%)	17.7	30	30	40	30	30
final particle size (nm)	87		78	92	103	104
surfmmer recovery method ^{a)}	UC-MeOH	UC-MeOH	UC-MeOH SR-H ₂ O	SR-H ₂ O	SR-H ₂ O	SR-H ₂ O

^{a)} UC-MeOH = ultracentrifugation in methanol; SR-H₂O = serum replacement with water.

^{b)} reaction A is a repetition of the reaction of Goebel *et al.* [2]

^{c)} reaction B was carried out at 68°C.

RESULTS AND DISCUSSION

Goebel *et al.* [2] copolymerized maleate surfmers with S in low solid content (17%) batch emulsion polymerizations. As initiator they used α,α' -azobisisobutyronitrile (AIBN), which is oil-soluble. The surfmer conversion was determined by ultrafiltration with methanol. They found very similar conversion results for the tetradecyl and octadecyl maleates. In **Fig. 1** the results of the reaction with the tetradecyl maleate are presented. As can be seen, the conversion of the maleate surfmer remained very low during most of the reaction, and when the S reached a conversion of about 80%, the partial conversion of the maleate started to increase rapidly, and reached a conversion higher than that of S. It was concluded that the maleate must be a good surfmer for the S emulsion polymerization, as most of it reacts at the end, ensuring a 100% incorporation at the particle surface [2]. Unfortunately, the surface charge density of the particles was not determined. The sudden increase of the partial conversion of the maleate was explained by a shift of the locus of polymerization from the

whole particle volume to the particle surface due to the transition into the glassy regime at high S conversion. The transition slows down the rate of diffusion of both monomers and radicals, and this would then force the reaction to take place solely at the particle surface.

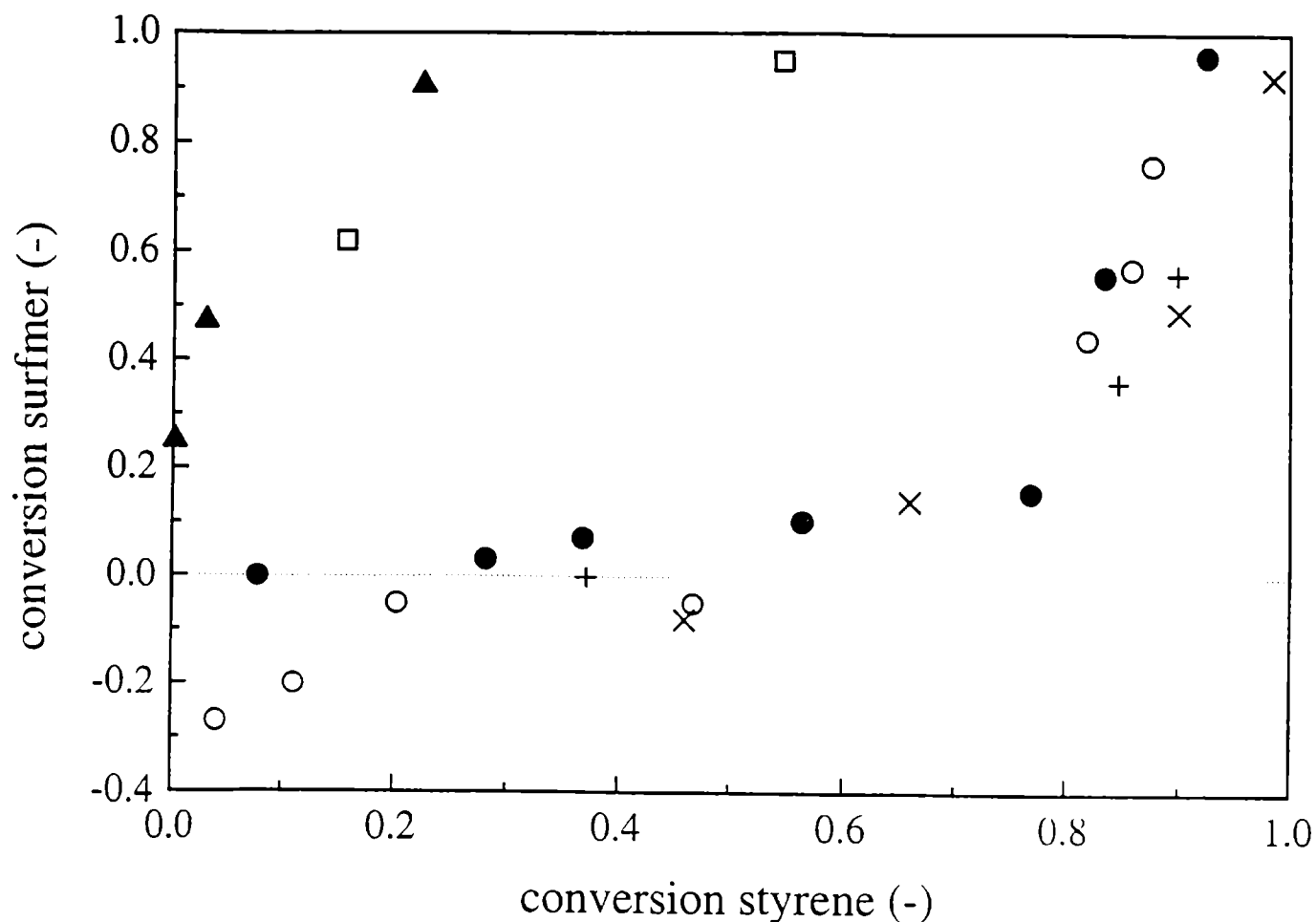


Fig. 1.- Conversion of surfmer (M14) versus conversion of S in batch emulsion polymerizations: (●), data obtained from ref. 2); (○), reaction A; (X), reaction B; (▲), reaction C analysed with SR-H₂O; (+), reaction C analysed with UC-MeOH; (□), reaction D.

We repeated the reaction carried out by Goebel *et al.* [2] with AIBN and the tetradecyl maleate (M14) (recipe (A) in Table I), analysing the surfmer conversion with ultracentrifugation in methanol and subsequent two-phase titration. The results of reaction A are also shown in Fig. 1. It can be seen that the same increase in partial conversion of M14 at high S conversion was observed as was reported by Goebel *et al.* [2]. In addition, at low S conversions we obtained negative values for the M14 conversion. We suspect that this may be due to the difficulty of taking representative sample of the emulsion whilst there is still a separate monomer droplet phase present; if the emulsion is not macroscopically homogeneous, the samples taken may contain a relatively small amount of monomer droplets and at the same time a relatively large amount of surfmer.

Goebel *et al.* [2] ascribed the sudden increase in the relative copolymerization rate of the maleate surfmers to the fact that, at 80 °C, the styrene/polystyrene mixture goes through the glass transition at roughly 80% conversion, and that the viscosity increase associated with this transition forced the locus of polymerization to the outer shell. To check this point, we carried out reaction B using KPS and replacing 30% of the S with cyclohexane and keeping

the reaction temperature at 68°C (to minimize loss of cyclohexane by evaporation) so that the system stays above the glass transition temperature during the whole reaction. The results (obtained with UC-MeOH) are also shown in **Fig. 1**, and the data show a similar behaviour as in the case without cyclohexane. The increase in apparent M14 conversion can therefore not be ascribed to the transition to the glassy regime. It can be argued that the use of a water-soluble initiator (KPS) may additionally force the locus of polymerization to the outer shell (with respect to the oil-soluble AIBN), but this effect should be operative during the whole polymerization and not only at the end of the process.

Reaction C (with 30% solids content of S and 2% M14 on monomer basis) was carried out using the water soluble KPS as the initiator. In this reaction the surfmer conversion was determined using two different recovery methods (UC-MeOH and SR-H₂O). When UC-MeOH was used, the results were similar to those in reactions A and B. On the other hand, we found a very high initial conversion of M14, reacting to close to 100% conversion as S reached a conversion of less than 30% (**Fig. 1**), when the unreacted surfmer was recovered with serum replacement with water. These results were in accordance with what was found in the batch aqueous phase reactions and the semi-continuous emulsion terpolymerizations in ref. **1a**, but obviously not with the results of reactions A and B. This indicates that the discrepancy in apparent M14 conversion between the two methods of analysis must reside in the difference in nature of the two recovery methods, or more precisely, due to the difference in the two solvents used, H₂O vs. methanol. With the method of serum replacement with water one can recover all the unreacted surfmer, as was shown by adding a known amount of M14 to a clean latex and subsequent analysis with serum replacement and two-phase titration (TPT) [**1b**]. This suggests that the discrepancy is not due to a difference in amount of desorbed free surfmer, but possibly due to a difference in amount of other components present in the latex, which can be extracted with methanol and be titrated with TPT, or at least influence the titration of free surfmer with TPT. In that respect, it seems logical that, in the case of methanol, more components may desorb from the latex, because methanol is expected to be a better solvent for organic matter. For example, short S chains with a length of up to ca 20 units can dissolve in methanol, and it is not unlikely that the type of material that could affect the titrations is oligomeric. Although the formation of a substantial amount of oligomers with M14 in the present case remains to be proven, it was shown with GPC (using tetrahydrofuran with 5% acetic acid as the eluent) that a sample of the reaction C at a conversion of S of 83%, recovered with UC-MeOH, contained no free surfmer, despite the fact that according to TPT there should have been an amount corresponding to a conversion of approximately 35%. The conclusion therefore is that the M14 surfmer reacts in the beginning of the batch reaction, and not at the end. Possibly the M14 groups become incorporated in oligomers that can be washed out with methanol. If these oligomers are involved in branching reactions at higher conversions, where the amount of free monomer is being depleted, they could become immobilized, which would result in the apparent increase in surfmer conversion in the UC-MeOH method.

The early reaction of the surfmer is further supported by the measurement of the surface coverage of the latex of reaction C carried out by conductimetry. It was found that the number of strong acid groups on the latex surface (i.e. sulfate groups from the KPS and sulfonate groups from the surfmer) corresponds to 45% of the amount of maleate that was added. The maximum amount of sulfate groups coming from the decomposition of KPS can be calculated with the rate constant for decomposition of KPS at 80°C: this results in an amount corresponding to 10% of the number of moles of maleate added. This means that the fraction

of maleate groups that have ended up at the particle surface lies between 0.35 and 0.45. Note that this is contradictory to what was assumed by Stähler, who assumed a total particle surface coverage [3]. However, it would be in agreement with a very high conversion of the surfmer in the beginning of the reaction that can lead to surfmer burying (see below).

In the copolymerization of M14 with S initiated with KPS the initial conversion of the M14 is very high as shown before. In this part of the reaction also the particle nucleation takes place. One could therefore conceive that at least part of the polymerization of M14 is due to the nucleation process. However, upon carrying out a seeded reaction (reaction D) using latex C as the seed latex with M14 conversion close to 100% and a particle size of 78 nm, it can be seen (**Fig. 1**) that the conversion behaviour is very similar to that obtained without a seed latex, *i.e.* a high initial conversion of M14. This suggests that the high consumption rate of M14 is not (solely) due to the kinetic events playing a role in particle nucleation. This is in agreement with the fact that in semi-continuous copolymerizations the instantaneous conversion of the M14 remains high during the whole reaction, provided the particle size is not higher than 100 nm [1b].

In order to see whether the length of the alkyl chain has any drastic effect on the observed behaviour for M14, reactions E and F were carried out, and the results are shown in **Fig. 2**. It can be appreciated that the conversion of M12 relative to that of S is lower in comparison with M14, except at low conversions of S. The lower conversion of M12 can perhaps be attributed to a higher proportion residing in the aqueous phase (the cmc of M12 is some four times larger than that of M14). The final particle sizes of these latices are virtually the same, so an effect of particle size or number can be dismissed. The kinetics of reactions E and F can be seen in **Fig. 3**, where the S and surfmer conversions are plotted versus time. It can be seen that there is hardly a difference between the curves for S, which is not surprising in view of the fact that the particle sizes are virtually the same.

Based on the above presented results, we have the following main observations about the emulsion polymerization between surfmer and S:

- 1) In spite of the apparently low reactivity of M14 with S, M14 reacts quickly, and is virtually depleted when S has reached a conversion of about 25%. This also occurs in a seeded reaction where the initial unswollen particle diameter is 78 nm.
- 2) Ultracentrifugation in methanol indicates the presence of "TPT titratable" species at low and intermediate S conversion, which disappear at high S conversions, whilst serum conversions onwards. This indicates the formation of oligomers during the early stages of the reaction, which become immobilized at high conversions.
- 3) In reaction C the final particle surface is covered with 45% of the total amount of MAL present in the system.

In the following we will try and see if these observations can be explained.

Point 1) must be addressed on the basis of the reactivity ratios and the locus of polymerization. In the very early stage of the reaction (nucleation) the reaction mainly takes place within the micelles, as far as M14 is concerned, because its concentration in the aqueous phase is very low, much lower than that of S. From the results of reaction C one can estimate

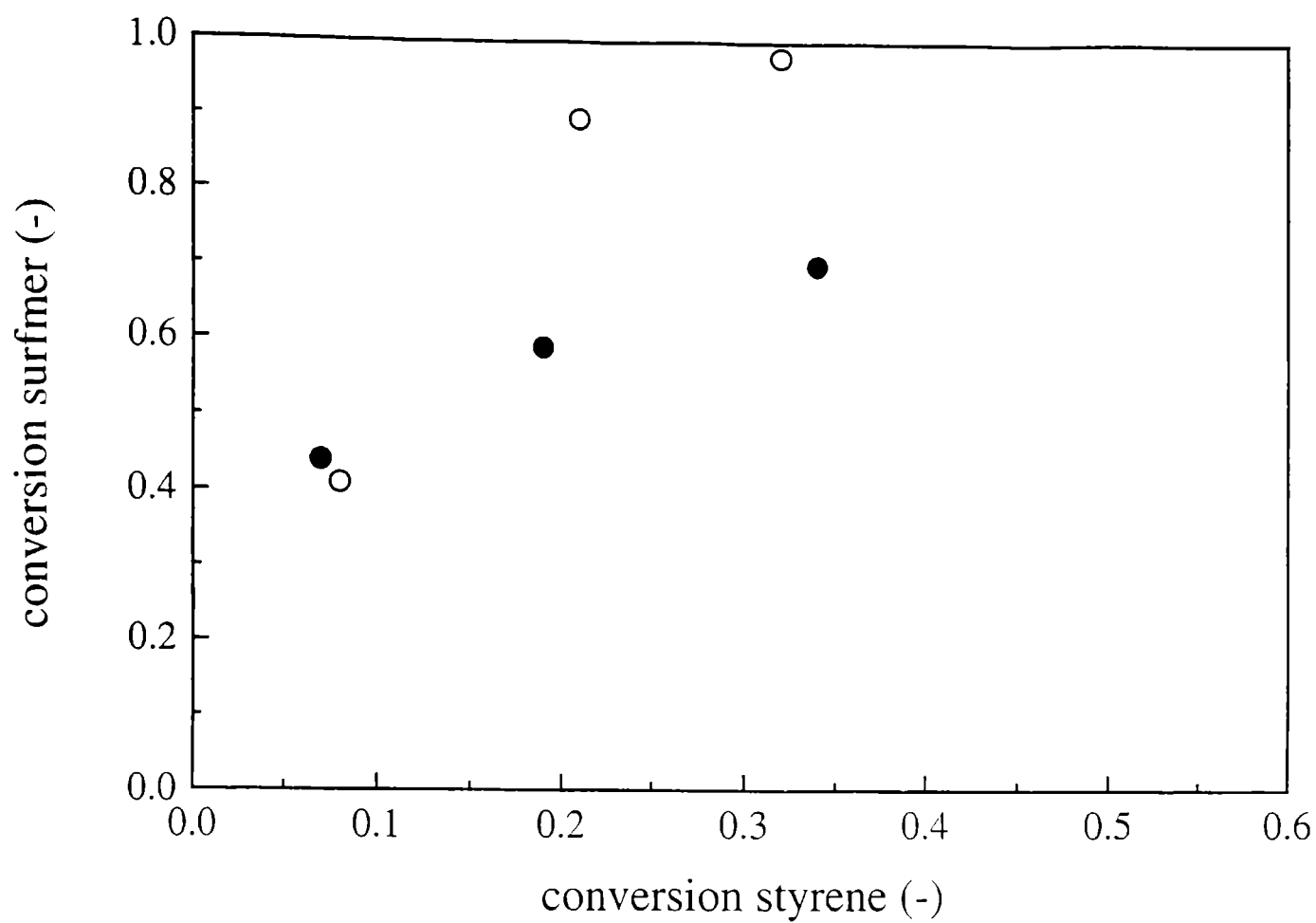


Fig. 2.- Conversion of surfmer versus conversion of S in batch emulsion polymerizations: (O), reaction E (M14); (●), reaction F (M12).

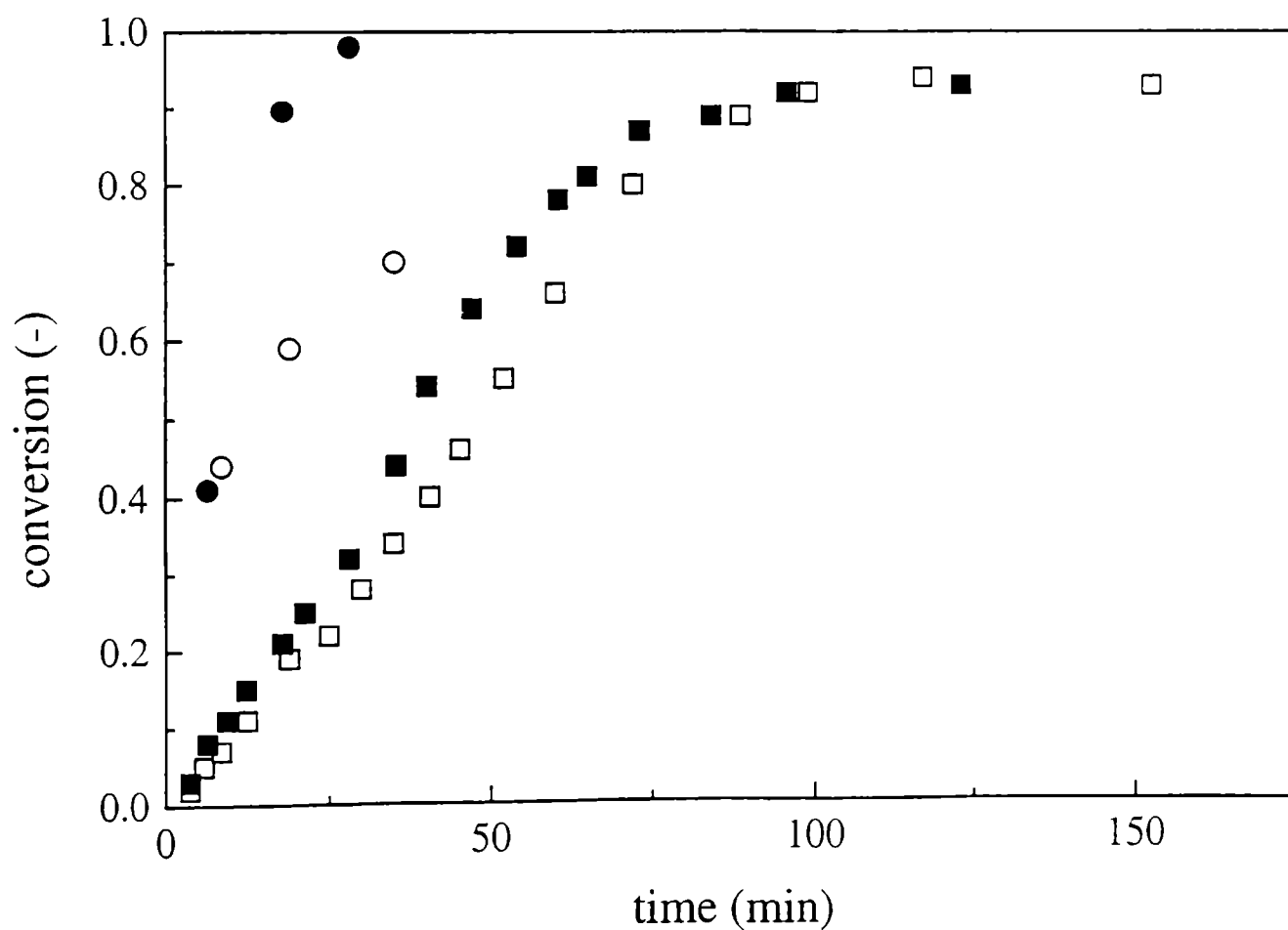


Fig. 3.- Conversion versus time for: reaction E ((■) conversion of S; (●) conversion of M14) and reaction F ((□) conversion of S, (O) conversion of M12).

the initial ratio of incorporation of maleate and S ($= Q_{M14}$, the number of moles of reacted surfmer divided by the number of moles of reacted S) to be approximately 0.06. The overall initial monomer ratio $q_{M14,ov} = 0.014$, the initial monomer ratio in the aqueous phase, $q_{M14,aq} = 0.04$, and an estimate for this ratio within the monomer swollen micelles, $q_{M14,mic}$, using a weight ratio of approximately 1 [4], amounts to 0.25 (the molecular weight of M14 is approximately four times that of S). One can see that in spite of the very low solubility of the maleate in the aqueous phase, both slightly swollen micelles and the aqueous phase are enriched in M14. The reactivity ratio $r_{S,M14}$ can then be estimated using the following equation, based on the well-known copolymerization equation and $r_{M14,S} = 0$:

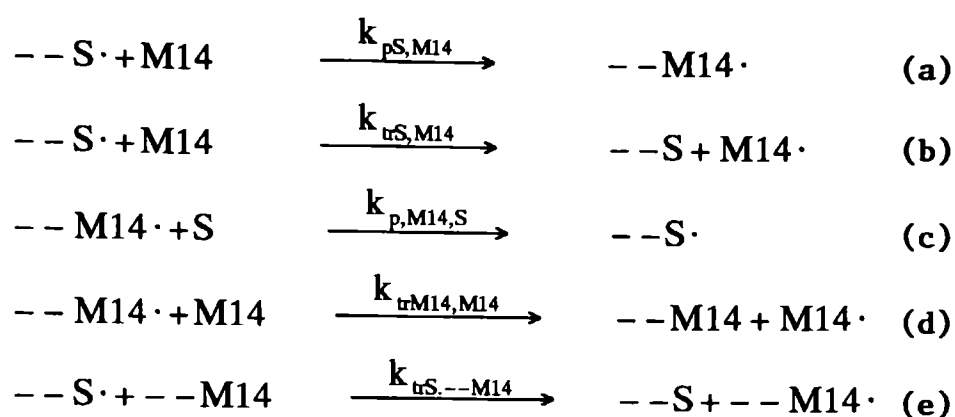
$$r_{S,M14} = q_{M14} \cdot \left(\frac{1}{Q_{M14}} - 1 \right) \quad (1)$$

If q_{M14} is given the value it has in the micelles, it results that $r_{S,M14} = 4$, which compares reasonably with the value given in literature for homogeneous copolymerization of diethyl maleate (DEM) with S: $r_S = 8-10$ and $r_{DEM} = 0$ [5], certainly if we take into account the uncertainty involved with the value of q_{M14} . This indicates that it is possible that M14 has such a high apparent reactivity simply on the basis of propagation, at least when the reaction is taking place in the micelles.

However, this stage will not last very long and the micelles will grow very quickly to become latex particles, whose diameter will increase rapidly. In addition, a high consumption of surfmer was also observed in the seeded emulsion polymerization (reaction D). Normally, incoming radicals from the aqueous phase can propagate into the particle and will encounter monomer in the whole particle. In the present case the overall concentration of M14 in the particles is very small and not be able to account for the high consumption rate of M14 at intermediate S conversion (up to 25%), and therefore a relatively large part the reaction must somehow be taking place at the particle surface, where there is a relatively high concentration of M14.

One can imagine a S radical growing at the surface, after having entered. Addition of M14 to this growing S oligomer has to occur before the oligomer reaches a length high enough to go far into the particle, beyond the shell containing M14. The addition of a charged M14 group keeps the radical near the surface. Note that if every decomposing persulfate molecule would react with at most two M14 molecules (for each initiator fragment) before propagating into the particle, then this cannot account for the high consumption rate of M14. Every incoming radical has to react with many more M14 groups to account for the high surfmer conversion. If we can assume that in the shell the ratio S to M14 is similar to what it is in the swollen micelles, then the average S-block length would be 16 (based in $r_S = 10$). If an oligomer of this size assumes a coil formation, it can be imagined that it is small enough to be able to encounter more molecules of M14. This would keep the radical growing at the surface and keep the consumption rate of M14 relatively high.

The results summarized in point 2) indicate that up to intermediate conversion of S the surfmer is incorporated mainly into oligomers that in the last stages of the polymerization grow in size to become insoluble in methanol. Such behaviour might be explained in terms of transfer reactions, see reaction scheme below,



where $k_{pi,j}$ is a propagation reaction between radical i and monomer j and $k_{tri,j}$ is a chain transfer reaction between radical i and monomer j . $--i\cdot$ represents an oligomer radical. A reaction between a styryl radical and M14 could be propagation and chain transfer ((a) and (b)). In reactions of diethyl maleate (DEM) using the spin trapping technique it was noted by Busfield *et al.* [6] that this monomer was 10 times more susceptible to abstraction of hydrogen from its $-CO-O-CH_2-$ group by a tert-butyloxy radical than addition to that radical. However, the nature of such a radical is different to a styryl radical. An estimation of the rate of chain transfer between an oligostyryl radical and maleate (reaction (b)) could perhaps be given by comparison to the system S-methyl acrylate. In this system a value of $0.05 \text{ dm}^3/\text{mol}\cdot\text{s}$ was found for chain transfer between a polymeric radical with S as the terminal unit and methyl acrylate monomer at 50°C . Ignoring any penultimate effect in the copolymerization of S with a M14 one can estimate the rate constant for addition of M14 to S ((a)) by stating $k_{pS,M14} = k_{pS,S}/r_{S,M14}$. Reliable values for the homopropagation rate constant of S are available [7], and at 60°C it has a value of $350 \text{ dm}^3/\text{mol}\cdot\text{s}$. This gives $k_{pS,M14} \approx 35 \text{ dm}^3/\text{mol}\cdot\text{s}$. With the estimation of $k_{trS,M14} \approx 0.05 \text{ dm}^3/\text{mol}\cdot\text{s}$ (going from 50 to 60°C will not change this value much) it would seem that the preferred reaction between a styryl radical and M14 would be propagation with M14 rather than transfer.

However, the fate of the radical once a M14 group has added is not clear. It could add S monomer ((c)), but rapid chain transfer might occur as well ((d)). In principle one can envisage two possible mechanisms for chain transfer. If transfer as suggested by the data of Busfield *et al.* is by hydrogen transfer from the $-CO-O-CH_2-$ group of a M14 molecule, perhaps the chain transfer constant $k_{trM14,M14}$ ((d)) is more like that of pure methyl acrylate, *i.e.* $\approx 1 \text{ dm}^3/\text{mol}\cdot\text{s}$. An estimation of the rate of addition of S to the M14 radical can be obtained as follows. The reactivity ratio of diethyl fumarate (DEF) in copolymerization with S at 60°C , $r_{DEF,S}$, is 0.02 [8]. With $k_p = 1.35 \cdot 10^{-3} \text{ dm}^3/\text{mol}\cdot\text{s}$ as given by Otsu *et al.* [9] and ignoring the possibility of an penultimate effect, one can calculate the rate of addition of S to a DEF radical by stating $k_{pDEF,S} = k_{pDEF,DEF}/r_{DEF,S} \approx 0.07 \text{ dm}^3/\text{mol}\cdot\text{s}$. It can also be safely assumed that the DEF radical has a structure similar to that of a terminal maleate radical, because of course now the C-C bond, having lost its vinylic character, is (relatively) freely rotatable. Therefore one could set $k_{pM14,S} \approx k_{pDEM,S} \approx k_{pDEF,S} \approx 0.07 \text{ dm}^3/\text{mol}\cdot\text{s}$. If it is assumed that the ratio $[M14]/[S]$ is about 0.25, then from the above follows that $k_{trM14,M14} \cdot [M14]/k_{pM14,S} \cdot [S] \approx 4$ ((c)). In other words it could be possible that the addition of a M14 to a growing S oligomer leads to chain transfer to M14, *i.e.* to oligomer formation. These oligomers would have molecular weights small enough to be extracted by methanol, but probably too high to be extracted by water.

Hydrogen transfer from a M14 group is of course also possible if the M14 group has already been polymerized, although the rate of this reaction might be different. At high conversions, when the the concentration of S has strongly decreased, and no unreacted M14 is present, the reaction between radicals and already incorporated M14 groups may become more important (reactions of type (e), where the M14 group is incorporated in an oligomer), which would lead to an increase of the molecular weight of the oligomers containing M14 groups. This could account for the fact that at higher S conversions these oligomers apparently cannot be abstracted anymore by methanol, whereas this is possible at lower conversions.

Point 3) points out that, at the end of the process, between 35 and 45% of the maleate groups can be retraced at the particle surface. This means that a large part of the maleate groups could not be reached by the protons of the HCl solution that was flushed through the latex. In other words, these maleate groups are buried in the particle interior. This seems only possible if the conversion of the surfmer reaches 100% long before all the S has reacted and before the particle diameter has reached its final value. In **Fig. 4** a line is indicated representing the calculated increase of the swollen particle diameter in reaction C up to a S conversion of about 35%. For the calculation it is assumed that interval 3 starts at 35% conversion, that the maximum swollen diameter is 83 nm, and that particle number is constant. It can be seen that when half the value of the final particle diameter is reached, already about 50% of the maleate has reacted. The polymer formed at a later stage may well be have buried the polymeric material formed earlier. The methanol which extracts the oligomers formed at low conversions, will be able to penetrate the particles, because of the presence of unreacted S, but the protons will certainly not be able to penetrate the particles to any extent.

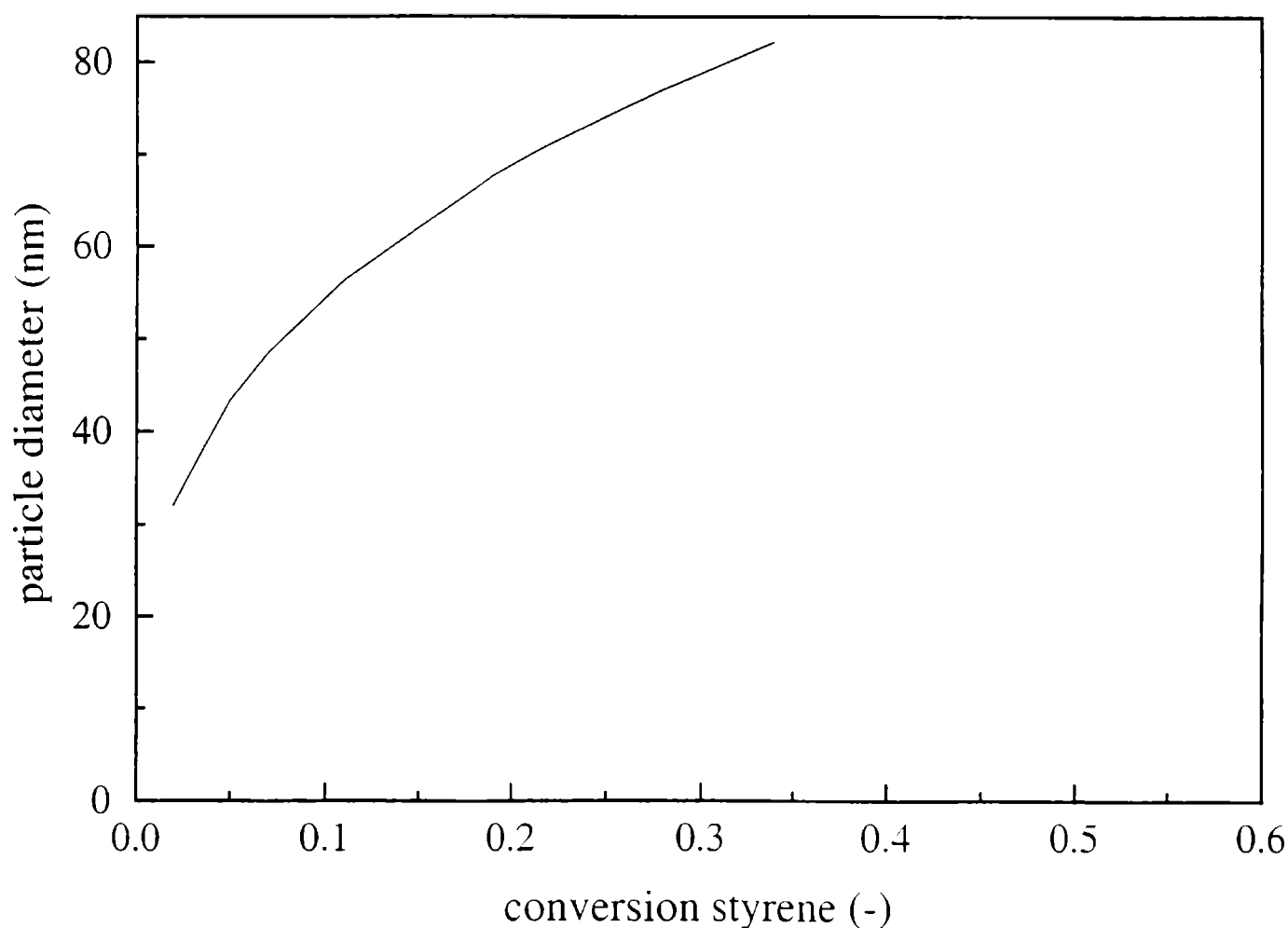


Fig. 4.- Calculated variation of the swollen particle diameter in reaction C.

CONCLUSIONS

The analysis of the free surfmer content with serum replacement with water in batch emulsion polymerizations of styrene with a surfmers based on maleic acid, tetradecyl and dodecyl sulfopropyl maleates, revealed that the surfmer has a very high initial conversion, much higher than that of styrene. This high conversion is not observed if the analysis is performed with methanol (using ultrafiltration to separate the serum from the latex), and this can probably be attributed to the formation of oligomers, which are extracted by the methanol, but not by the water. The high initial conversion, which is accompanied by a relative high degree of burying of surfactant groups, indicates that the reaction takes place in micelles or at the particle surface, which are enriched in surfmer. It is postulated that in the beginning of the emulsion polymerization the relatively high degree of incorporation of surfmer oligomers leads to formation of oligomers due to chain transfer to surfmer and that at the end of the process the main chain transfer process is transfer to surfmer units incorporated into the oligomers. This should increase the molecular weight of the oligomers and render them insoluble in methanol.

ACKNOWLEDGEMENTS

The authors would like to express their gratitude to K. Stähler for providing the M12, and T. Willems at the Eindhoven University of Technology for carrying out the GPC runs. This work was carried out as part of a European Union sponsored network (CHRX CT 930159). MJU was financially supported by the Basque Government. HASS acknowledges a grant of the Training and Mobility of Researchers Programme (ERB4001GT953910). J.I.A acknowledges the fellowship from AECI-UPV.

REFERENCES

- [1] (a) María J. Unzué, Harold A.S. Schoonbrood, José M. Asua, Amaia Montoya Goñi, David C. Sherrington, Katrin Stähler, Karl-Heinz Goebel, Klaus Tauer, Mrie Sjöberg, Kristen Holmberg, "Reactive surfactants in heterophase polymerization for high performance polymersw. VI. Synthesis and screening of polymerizable surfactants (SURFMERS) with varying reactivity in high solids styrene-butyl acrylate-acrylic acid emulsion polymerization", submitted to **J.Appl.Polym.Sci.**
(b) H.A.S. Schoonbrood, M.J. Unzué, O.-J. Beck, J.M. Asua, A. Montoya Goñi, D.C. Sherrington, "Reactive surfactants in heterophase polymerization for high performance polymers. VII. Emulsion copolymerization mechanism of three anionic polymerizable surfactants (SURFMERS) with styrene-butyl acrylate-acrylic acid, submitted to **Macromolecules**.
(c) H.A.S. Schoonbrood and J.M. Asua, "Reactive surfactants in heterophase polymerization for high performance polymers. IX. Optimal surfmer behaviour in emulsion copolymer systems", to be submitted to **Macromolecules**.
- [2] K.- H. Goebel, K. Stähler, **Polym. Adv. Technol.** **6**, 452 (1994).
- [3] K. Stähler, PhD Thesis, Potsdam University, Germany (1994).

- [4] D. Attwood, A.T. Florence "Surfactant systems, their chemistry, pharmacy and biology", Chapman and Hall, London (1983).
- [5] Polymer Handbook, 3rd De., Eds. J. Brandrup and E.H. Immergut, John Wiley & Sons, New York (1989).
- [6] W.K. Busfield, I.D. Jenkins, K. Heiland, **Eur. Polym. J.** **30**, 1259 (1994).
- [7] B.G. Manders, G. Chambard, W.J. Kingma, B. Klumperman, A.M. van Herk, A.L. German, submitted to **J. Polym. Sci.: Part A: Polym. Chem.**
- [8] T. Otsu, A. Matsumoto, K. Shiraishi, N. Amaya, Y. Koinuma, **J. Polym. Sci.: Part A: Polym. Chem.** **30**, 1559 (1992).
- [9] T. Otsu, O. Ito, N. Toyoda, S. Mori, **Makromol. Chem., Rapid Commun.** **2**, 725 (1981).

GAS CHROMATOGRAPHY OF ALIPHATIC AMINES ON DIATOMACEOUS SOLID SUPPORTS MODIFIED BY ADSORPTION AND CROSSLINKING OF POLYETHYLENEIMINES

CROMATOGRAFIA GASEOSA DE AMINAS ALIFATICAS SOBRE SOPORTES SOLIDOS DERIVADOS DE DIATOMEAS MODIFICADAS POR ADSORCION Y ENTRECRUZAMIENTO DE POLI(ETILENIMINAS)

A.M. Nardillo¹ and R.C. Castells¹

SUMMARY

A method for the deactivation of diatomaceous supports based on the adsorption of polyethyleneimine and cross linking by means of a bidentate reagent is described. Aliphatic amines elute as almost symmetrical peaks from columns packed with these supports coated either with Quadrol or with Carbowax 1500. The same columns give good results in the analysis of aliphatic alcohols.

Keywords: *Gas chromatography, supports modification, amines, adsorption of polyethyleneimines*

INTRODUCTION

Adsorption on the solid support surface or on the capillary walls makes gas chromatographic determination of highly basic solutes, specially low molecular weight aliphatic amines, a difficult task. Adsorption processes result in asymmetrical peaks, with consequent superposition, sample size dependent retention times and low precision of signal integration results; in extreme cases they can provoke partial sample loss or non elution. These difficulties are specially grave in the analysis of environmental samples, where alifatic amines need to be detected at the trace level because of health hazards on exposure to their vapours and because of their nauseating odour event at very low concentrations.

Numerous solutions have been offered to avoid the problem of tailing of amine peaks. James et al [1] were the first to suggest the use of alkalies. Decora and Dinneen [2] coated Tide with 10% by weight of potassium hydroxide before applying the stationary phase. Smith and Radford [3] deposited different quantities of KOH from methanolic solutions onto the surfaces of several types of diatomaceous supports, then coating these solids with Apiezon L, Carbowax 20M or silicone fluid DC-710. These authors discovered that packings, whose solid supports had been extracted with water before coating with the stationary phase, gave rise to

¹ Miembro de la Carrera del Investigador del CONICET

asymmetrical peaks, this behaviour pointing out that the beneficial effects of the alkali cannot be explained on the basis of neutralization of acid surface sites alone. Potassium hydroxide deactivation of diatomaceous supports was used by numerous authors in combination with various liquid stationary phases: poly(oxialkylene)ethers [4-9], Penwalt 223 [5,10-14], Apiezon L or M [4,15], Dowfax 9N9 [16], squalane [8], diglycerol, 1,2,3-tris(2-cyanoethoxy) propane and methylsilicones [4]. Other inorganic deactivators (KF, Na_3PO_4 , K_2CO_3 [15,17,18]) and mixtures of tetrahydroxyethylenediamine (THEED) and tetraethylene-pentamine (TEP) [19] that acted both as deactivators and as liquid stationary phases, were also recommended.

Polymeric organic supports, with surfaces supposedly less active than those of siliceous solids, also demand deactivation in amine analysis. With this aim, polyethyleneimine (PEI) and TEP on Porapak Q [20] and KOH on Chromosorb 102 [21] or on Sephabead GHP-1 [22] have been used. Similarly graphitized carbon blacks need deactivation with KOH prior to coating with stationary phase [9,10,13,23-26]. Adsorption phenomena become apparent in glass or fused-silica capillaries also; deactivation has been performed by means of KOH or Na_3PO_4 methanolic solutions [27-29], silylizing with 3-aminopropyl triethoxysilane [30], or by building a polyimide film on the inner wall of the tube [31].

Potassium hydroxide is used in the majority of the columns employed in amine analysis. It is proper to ask if the presence of such a reactive substance is innocuous from the point of view of the column life and of the results of the analysis itself. In first place, silicone depolymerization in the presence of alkalies has been informed by several authors [32-36]; strong bases are used as catalysts in the syntheses and must be meticulously removed from the final products. Polyesters are rapidly decomposed by alkalies [37]. Secondly, columns containing KOH must be protected from moisture; amine-alkali interactions make a contribution to the retention time of amines and, since water is a stronger hydrogen donor, its presence results in a decrease of the amine retention [17]. Finally, solutes decomposition and isomerization has been detected in columns containing potassium hydroxide [28].

Although evidence of the prejudicial effects of KOH is by no means conclusive and a complete and systematic study is lacking, it would undoubtedly be interesting to have available a less aggressive deactivation method for solid supports and capillaries. In this paper a method for the deactivation of siliceous surfaces is described; it is founded on the crosslinking of preadsorbed polyethyleneimine molecules by means of bidentate reagents so as to form an immobile film, insoluble in the liquid stationary phase. Similar synthesis methods were employed with different objectives by Meyers and Royer [38] and by Reigner and col. [39,40]. Thus obtained solids were tested against a group of amines, after coating with appropriate stationary phases, through peak asymmetry measurements.

EXPERIMENTAL

Reagents and materials

Chromosorb P AW, Chromosorb W AW and Chromosorb P AW DMCS, all of them 80/100 mesh, were employed in the preparation of the packings. PEI-6 and PEI-18 were purchased from Analabs, and TEP from Aldrich. Glutaric dialdehyde, GA (Aldrich, 25% aqueous solution) and ethyleneglycol diglycidyl ether, EDGE (Aldrich) were used as

crosslinking reagents. The stationary phases (Apiezon M, OV-17, OV-225, Quadrol, Carbowax 1500, diglycerol) were bought from regular chromatographic suppliers; Fluorad FC-430 was purchased from PCR Inc.

Synthesis of solid supports

A weighed amount of Chromosorb P AW (or Chromosorb W AW) is suspended and stirred in a 5% (w/v) PEI-6 (or PEI-18, or TEP) solution in anhydrous methanol; the mixture was connected to a water pump for about 30 sec to remove air from the pores, and left at room temperature for 1 h without agitation. After filtration, the solid was washed with methanol and transferred to an Erlenmeyer flask where it was contacted for 1 h, under nitrogen atmosphere, with a 0.45% GA solution (recently prepared by dilution of the original reagent using oxygen-free water). The solid is separated, washed with methanol, and suspended again in a 5% PEI solution, now for 30 min; then it is filtered, washed with methanol, suspended in this solvent, and reacted with solid sodium borohydride added in small portions. Finally, the solid after filtration was washed with abundant methanol and dried under vacuum at room temperature. The same technique is used with EDGE, substituting 1,4-dioxane for methanol and extending the reaction time to 3-4 days. Chromatographic packings were prepared in a rotary evaporator, using appropriate volatile solvents with each stationary phase.

Instrumentation

Two gas chromatographs equipped with flame ionization detectors were employed: Hewlett-Packard 5880A level four and Konik 3000 HR GC. Analytical grade nitrogen, previously passed through humidity and oxygen traps (Analabs HGC-145 and HGC-224, respectively), was used as carrier gas at 15-20 mL.min⁻¹. FID's were operated at 180°C and the injection ports at temperatures between 60 and 100°C. The columns were 2 mm i.d. silane treated glass tubing, their lengths ranging between 80 and 180 cm. Solutes were injected in the vapour form, by means of 5 through 250 µL Hamilton syringes, applying the headspace sampling technique; sample sizes were of the order of 100 ng.

RESULTS AND DISCUSSION

A series of guide lines were followed to test the performance of the deactivation method used in this work:

a. Although Chromosorb W AW was used in earlier experiments, most of the work was carried out with Chromosorb P AW; its lower fragility constitutes a definite advantage during deactivation, coating with stationary phases and packing the columns, and its larger specific surface activity represent a more demanding test for the procedures under study. Unmodified Chromosorb P AW and Chromosorb P AW DMCS were also used with comparative purposes.

b. A group of selected stationary phases were coated on the supports at low concentrations (between 5 and 7% W/W).

c. Peak asymmetry, *A*, used in the comparisons, is defined as the ratio of the back width to the front width, measured from a vertical line traced through the peak maximum, at one tenth of its maximum height. Since *A* has strong dependence on sample size, the volume of vapour injected has been kept almost constant for each solute (from 0.8-1 µl for the more volatile, up to several tens of µl for those of higher molecular weight). The more asymmetrical the peak the stronger this dependence; so, in those cases where *A* > 6, we shall simply state “vha”, very high asymmetry.

d. Benzene was injected into all the columns in order to detect other sources of asymmetry, as non uniform distribution of the stationary phase on the solid support or incorrectly packed columns.

PEI-6 gives origin to better supports for the analysis of aliphatic amines than PEI-18 or TEP. On the other hand, no significant differences were detected between the uses of GA or EDGE. An alternative synthesis, consisting in coating Chromosorb P AW with 0.3, 0.5 or 1.0% by weight of PEI-6 and crosslinking with GA, resulted in supports with poor behaviour. The abbreviation MS, modified support, shall be used to identify a solid prepared by the method of the Experimental section, using Chromosorb P AW, PEI-6 and GA.

Symmetrical peaks were obtained with benzene on all the studied packings with the following exceptions: a) diglycerol, 8.1% on MS at 50°C, *A*=1.5; b) OV-225, 6.2% on MS at 65°C, *A*=0.8, and c) Quadrol, 7.1% on Chromosorb P AW DMCS at 55°C, *A*=1.3.

Results obtained for benzene, n-propylamine and n-butylamine on columns containing several stationary phases coated on the MS have been gathered in **Table I**. Very asymmetrical peaks are produced with some of the stationary phases, pointing to the fact that the deactivation is far from complete, and that the stationary phase plays an important role in the process. The best results are obtained by using Quadrol, followed by Carbowax 1500. It is important to mention that no improvement in peak symmetry was obtained by increasing the concentration of Quadrol from 6% to 12%; column efficiency, however, suffered an important drop. On the other side, peaks for methylamine and ethylamine were vha in all the columns studied.

TABLE I
Asymmetry of benzene, n-propylamine and n-butylamine peaks on the modified support coated with several stationary phases

Stationary Phase	Benzene		n-Propylamine		n-Butylamine	
	°C	<i>A</i>	°C	<i>A</i>	°C	<i>A</i>
Quadrol 6.2%	55	1.2	55	2.3	55	2.0
		65	2.2	65	1.6	
Carbowax 1500 6.4%	55	1.0	55	3.8	55	3.0
		65	3.3	65	2.7	
Fluorad FC-430 6.4%	34	1.1	45	vha	45	vha
		65	vha	65	vha	
Diglycerol 8.1%	50	1.5	75	vha	75	vha
		85	vha	85	vha	
Quadrol (*) 6.3%	55	1.2	55	2.4	55	2.1
		65	2.3	65	1.8	

Quadrol (*): support prepared using EDGE
4 feet x 2 mm i.d. silane treated glass columns

The chromatograms obtained at 85°C for three amines on the MS coated with Quadrol or with Fluorad FC-430 are shown in **Figures 1 and 2**, respectively. Fluorad FC-430 is a totally fluorinated polymer for which no special deactivating properties can be predicted. As a matter of fact, Fluorad FC-430 coated on Chromosorb P AW or on Chromosorb P AW DMCS originates amine peaks with very long tails; deactivation with PEI produces a marked improvement, but not totally symmetrical peaks. Better results are obtained with Quadrol on the MS, indicating a deactivation action by the stationary phase. n-Propylamine and n-butylamine peaks with $A > 10$ are obtained in columns containing 6.4% by weight of Quadrol on Chromosorb P AW; worst results are obtained by coating Quadrol on Chromosorb P AW DMCS, very probably as a consequence of a bad distribution of the stationary phase on the silanized support. Also Carbowax 1500 produces better amine peaks on Chromosorb P AW than on the silanized support, and a marked improvement is obtained by using the MS.

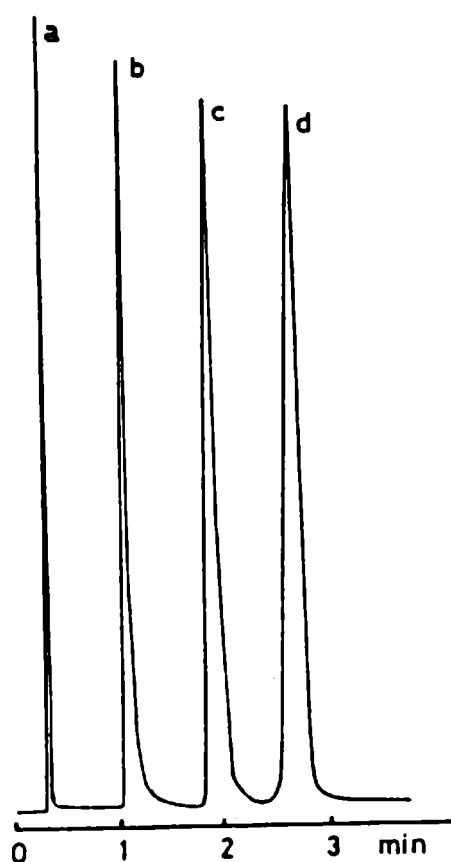


Fig. 1.- Chromatogram on 120 cm x 2 mm y.d. column of 6.3% Quadrol on MS at 85°C. Peak identity: (a) methane, (b) n-propylamine, (c) n-butylamine, (d) 1,3-dimethylbutylamine.

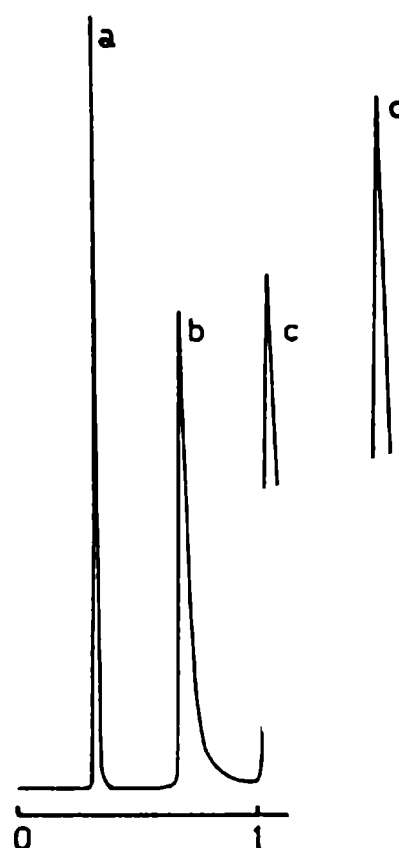


Fig. 2.- Chromatogram on 120 cm x 2 mm i.d. column of 6.4% Fluorad FC-430 on MS at 85°C. For peak identity see Figure 1.

Chromatograms for the same amines mixture at programmed temperature in columns containing MS coated with Quadrol or with Carbowax 1500 are shown in **Fig. 3 and 4**. Quadrol column behaves a little better but the analysis could also be performed on Carbowax 1500.

The supports synthesized in this work were also tested in the analysis of alcohols. **Table II** is a summary of the results obtained with ethanol and n-propyl alcohol. Excellent peaks are obtained using either Quadrol or Carbowax 1500, but this last stationary phase behaves a little better. Methanol, however, produces asymmetrical peaks with both stationary phases.

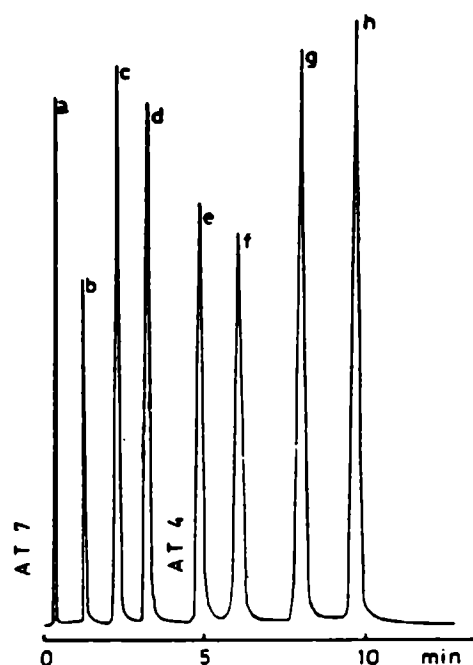


Fig. 3.- Chromatogram on 120 cm x 2 mm i.d. column of 6.3% Quadrol on MS. Isothermal at 75°C for 1 min, programmed to 84°C at 3°C/min, isothermal at 84°C for 1 min, programmed at 108°C at 6°C/min, isothermal at 108°C. Peak identity: (a) methane, (b) n-propylamine, (c) n-butylamine, (d) 1,3-dimethylbutylamine, (e) methylcyclopentylamine, (f) 3-aminoheptane, (g) ethylcyclohexylamine, (h) 2-amino-octane.

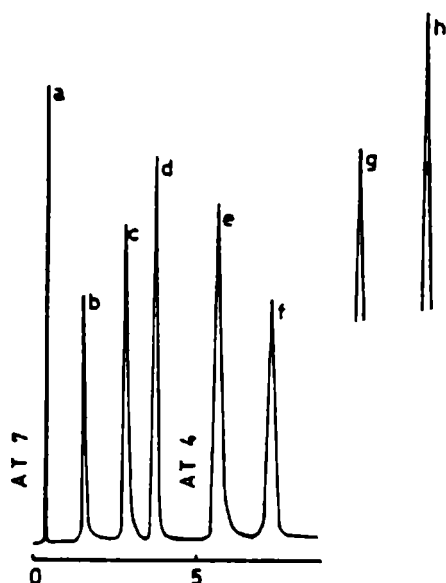


Fig. 4.- Chromatogram on 120 cm x 2 mm i.d. column of 6.4% Carbowax 1500 on MS. Isothermal at 60°C for 1 min, programmed to 68°C at 2°C/min, isothermal at 68°C for 1 min, programmed to 92°C at 4°C/min, isothermal at 92°C. For peak identity see Figure 3.

TABLE II
Asymmetry of ethanol and n-propyl alcohol peaks on the modified support coated with several stationary phases

Stationary phase	Ethanol		n-Propyl Alcohol	
	°C	A	°C	A
Quadrol 6.2% 75	65	1.3	65	1.2
	1.2	75	1.1	
Carbowax 1500	65	1.1	65	1.0
Fluorad FC-430 6.4%	55	2.3	55	1.5
Fluorad FC-430 6.4%/Chromosorb P AW	85	vha	55	3.0

ACKNOWLEDGMENT

This work was supported by the Consejo Nacional de Investigaciones Científicas y Técnicas (CONICET) and by the Comisión de Investigaciones Científicas de la Provincia de Buenos Aires (CIC).

REFERENCES

- [1] A.T. James, A.J.P. Martin and G. Howard Smith.- **Biochem. J.** **52**, 238 (1952).
- [2] A. Decora and G.V. Dinneen.- **2nd. International Symposium, I.S.A.**, Lansing, Mich., 1959, p. 12.
- [3] E.D. Smith and R.D. Radford.- **Anal. Chem.** **33**, 1160 (1961).
- [4] A.A. Anderson, S.P. Yurel and M.V. Shymanska.- **J. Chromatogr.** **95**, 91 (1974).
- [5] W. Lindner.- **J. Chromatogr.** **111**, 331 (1975).
- [6] A.T. Kacprowicz.- **J. Chromatogr.** **269**, 61 (1983).
- [7] A. Tavakkol and D.B. Drucker.- **J. Chromatogr.** **274**, 37 (1983).
- [8] A. Atanasov and M. Atanasova.- **Nauchni Tr.- Plovdivski Univ.** **22**, 199 (1984).
- [9] L. Grönberg, P. Lövkvist and J.A. Jönsson.- **Chromatographia** **33**, 77 (1992).
- [10] L. Mathiasson and P. Lövkvist.- **J. Chromatogr.** **217**, 177 (1981).
- [11] M. Delane, L. Mathiasson and J.A. Jönsson.- **J. Chromatogr.** **207**, 37 (1981).
- [12] G. Audunsson and L. Mathiasson.- **J. Chromatogr.** **315**, 299 (1984).
- [13] J.L. Pons, A. Rimbault, J.C. Darbord and G. Lelvan.- **J. Chromatogr.** **337**, 213 (1985).
- [14] G. Audunsson.- **Anal. Chem.** **60**, 1340 (1988).
- [15] R.V. Golounya, I.L. Zhuravleva and B.M. Polanver.- **J. Chromatogr.** **286**, 79 (1984).
- [16] J.F. O'Donnell and C.K. Mann.- **Anal. Chem.** **36**, 2097 (1964).
- [17] R. Golounya and I.L. Zhuravleva.- **Chromatographia** **6**, 508 (1973).
- [18] S.A. Muylashov, N.N. Kovylyina and E.V. Kovalenko.- **Zavod. Lab.** **52**, 19 (1986).
- [19] Y.L. Sze, M.L. Borke and D.M. Ottenstein.- **Anal. Chem.** **35**, 240 (1963).

- [20] J.R. Lindsay Smith and D.J. Waddington.- **Anal. Chem.** **40**, 522 (1968).
- [21] K. Kuwata, Y. Yamazaki and Uebori.- **Anal. Chem.** **52**, 1980 (1980).
- [22] K. Kuwata, E.Akiyama, Y. Yamazaki, H. Yamasaki, Y. Kuge and Y. Kiso.- **Anal. Chem.** **55**, 2199 (1983).
- [23] A. DiCorcia and R. Samperi.- **Anal. Chem.** **46**, 977 (1974).
- [24] A. DiCorcia, A. Liberti and R. Samperi.- **J. Chromatogr. Sci** **12**, 710 (1974).
- [25] A. DiCorcia, R. Samperi and C. Severini.- **J. Chromatogr.** **170**, 325 (1979).
- [26] S.H. Zeisel, K.A. Da Costa and J.G. Fox.- **Biochem. J.** **232**, 403 (1985).
- [27] E.A. Mistryukov, R.V. Golounya and A.L. Samusenko.- **J. Chromatogr.** **148**, 490 (1978).
- [28] E.A. Mistryukov, A.L. Samusenko and R.V. Golounya.- **J. Chromatogr.** **169**, 391 (1979).
- [29] B. Olufsen.- **J. Chromatogr.** **179**, 97 (1979).
- [30] M. Horká, V. Kahle and M. Krejci.- **J. Chromatogr.** **637**, 96 (1993).
- [31] J. Balla and M. Balini.- **J. Chromatogr.** **299**, 139 (1984).
- [32] D.K. Thomas.- **Polymer** **7**, 99 (1966).
- [33] C.R. Trash.- **J. Chromatogr. Sci.** **11**, 196 (1973).
- [34] A.E. Coleman.- **J. Chromatogr. Sci.** **11**, 198 (1973).
- [35] L. Blomberg.- **J. High Resolut. Chromatogr. Chromatogr. Commun.** **5**, 520 (1982).
- [36] J.A. Yancey.- **J. Chromatogr. Sci.** **23**, 161 (1985).
- [37] D.G. Anderson and R.E. Ansel.- **J. Chromatogr. Sci.** **11**, 192 (1973).
- [38] W.E. Meyer and G.P. Royer.- **J. Am. Chem. Soc.** **99**, 6141 (1977).
- [39] A.J. Alpert and F.E. Regnier.- **J. Chromatogr.** **185**, 375 (1979).
- [40] L.A. Kennedy, W. Kopaciewicz and F.E. Reigner.- **J. Chromatogr.** **359**, 73 (1986).

EXCESS ENTHALPIES OF NITROUS OXIDE + PENTANE AT 308.15 AND 313.15 K FROM 7.64 TO 12.27 MPa

*ENTALPIAS DE EXCESO DE OXIDO NITROSO+PENTANO A 308,15 Y 313,15 K
DESDE 7,64 HASTA 12,17 MPa*

J.A.R. Renuncio¹, C. Pando¹, C. Menduiña¹ and R.C. Castells²

SUMMARY

The excess molar enthalpies H_m^E of nitrous oxide+pentane were measured in the vicinity of the critical locus and in the supercritical region by means of an isothermal flow calorimeter. Smooth representations of the results are presented. Values for H_m^E are similar to those previously found for carbon dioxide+pentane mixtures.

Keywords: *supercritical mixtures, nitrous oxide, pentane, flow calorimetry.*

INTRODUCTION

Nitrous oxide is often used in supercritical fluid extraction, and several authors such as Sakaki (1992) or Alexandrou et al. (1992) have reported that N₂O is a better solvent than carbon dioxide for certain compounds. The measurement of thermodynamic properties such as the excess molar enthalpies (H_m^E) of binary mixtures of nitrous oxide with a hydrocarbon in the vicinity of the critical locus and in the supercritical region would be necessary for understanding the practical uses of N₂O. Pando et al. (1983) reported previously measurements of H_m^E for carbon dioxide + pentane at 308.15 and 323.15 K and pressures up to 12.45 MPa. Castells et al. (1994a,b) reported previously measurements of H_m^E for nitrous oxide + toluene at 308.15, 313.15 and 323.15 K and pressures up to 15.00 MPa. This paper reports values of H_m^E for nitrous oxide + pentane at 308.15 K and 9.49 and 12.27 MPa and at 313.15 K and 7.64, 9.44, and 12.26 MPa. The pressure and temperature conditions of the measurements were chosen to compare results for nitrous oxide + pentane with those previously obtained for carbon dioxide + pentane.

EXPERIMENTAL SECTION

The high-pressure flow calorimeter from Hart Scientific (Model 7501) used for the experiments and the experimental procedure have been described by Christensen and Izatt (1984) and by Gmehling (1993). The calorimeter consists of two thermostated pumps (ISCO, Model LC2600), a thermostated flow cell, and a back pressure regulator. The flow cell with a

¹ Departamento de Química Física I, Universidad Complutense, Madrid, España

² Miembro de la Carrera del Investigador del CONICET, UNLP

pulsed heater, a calibration heater, a Peltier cooler, and a mixing tube wound around a copper cylinder is located in a stainless steel cylinder which is immersed in a thermostat. The combination Peltier cooler/pulsed heater allows the determination of both endothermic and exothermic effects. The flow cell is thermostated in a silicon oil bath (± 0.0005 K) and a manually controlled piston acts as a fine adjustment of the nitrogen pressure over the back pressure regulator. Oscillations in pressure are smaller than ± 0.01 MPa.

The materials employed were nitrous oxide (SEO, 99.99 mol % pure) and pentane (Aldrich, 99+mol % pure, HPLC grade) previously dehydrated with sodium.

All runs were made in the steady-state fixed composition mode. Flow rates were selected to cover the whole mole fraction range. In most cases, the measurements were carried out at a total flow rate of $0.010 \text{ cm}^3 \cdot \text{s}^{-1}$. A few measurements were carried out at a total flow rate of $0.005 \text{ cm}^3 \cdot \text{s}^{-1}$. Reproducibility of results was estimated to be $\pm(1+0.01H_m^E) \text{ J} \cdot \text{mol}^{-1}$. The flow rates measured in cubic centimeters per second were converted to moles per second and to mole fractions using the densities of the two materials estimated as follows. The densities of N_2O at the temperature of the pump and at pressures of 7.64, 9.44, 9.49, 12.26, and 12.27 MPa were calculated by interpolation of the pressure-volume isotherms of the liquid nitrous oxide measured by Couch et al. (1962). The densities of pentane at the temperature of the pump and at pressures of 7.64, 0.44, 9.49, 12.26, and 12.27 MPa were calculated from the densities at atmospheric pressure given in the TRC Thermodynamic Tables (1994) and the isothermal compressibilities obtained from the data of Sage and Lacey (1942).

RESULTS AND DISCUSSION

Excess molar enthalpies were determined for nitrous oxide + pentane over the entire composition range at 308.15 K and 9.49 and 12.27 MPa and at 313.15 K and 7.64, 9.44, and 12.26 MPa. The results are given in **Table I**. For pentane T_c is 469.7 K and p_c is 3.37 MPa, while for nitrous oxide T_c is 309.6 K and p_c is 7.29 MPa (Reid et al., 1988). Owing to the proximity to the nitrous oxide critical point, excess molar enthalpies could not be determined at 308.15 K and 7.64 MPa. Values for H_m^E at each pressure and temperature studied were fitted to the equation

$$H_m^E / (\text{J} \cdot \text{mol}^{-1}) = [x(1-x) / [1 + k(2x-1)]] \sum_{n=0}^N C_n (2x-1)^n \quad (1)$$

where x is the N_2O mole fraction. The coefficients C_n and k are given in **Table II** together with the standard deviations, s , between experimental and calculated H_m^E values and the ratio s/H_{\max}^E of the standard deviation and the maximum absolute value of H_m^E . Values for s/H_{\max}^E are higher than the estimated reproducibility for the flow calorimeter due to the fluctuations in density always present when the critical point is approached.

Figures 1 and 2 are plots of H_m^E against x for the isobars studied at 308.15 and 313.15 K, respectively. Mixtures at 308.15 K and 9.49 and 12.27 MPa and at 313.15 K and 12.26 MPa show moderately endothermic mixing. Mixtures at 313.15 K and 9.44 MPa show moderately endothermic and exothermic mixing in the pentane-rich region and nitrous oxide-rich region, respectively. Mixtures at 313.15 K and 7.64 MPa show very exothermic mixing.

TABLE I

Experimental excess enthalpies H_m^E for $[xN_2O+(1-x)C_5H_{12}]$

x	$H_m^E/(J.mol^{-1})$	x	$H_m^E/(J.mol^{-1})$	x	$H_m^E/(J.mol^{-1})$
308.15 K, 9.49 MPa					
0.049	24	0.388	230	0.744	99
0.098	85	0.440	231	0.788	61
0.145	126	0.492	221	0.847	23
0.191	161	0.543	209	0.894	-24
0.243	196	0.594	174	0.978	-26
0.285	205	0.644	158		
0.343	226	0.670	136		
308.15 K, 12.27 MPa					
0.050	61	0.373	344	0.701	282
0.100	119	0.437	361	0.750	263
0.130	149	0.498	364	0.796	231
0.198	220	0.550	362	0.841	192
0.248	272	0.602	347	0.881	134
0.311	307	0.652	308	0.950	59
313.15 K, 7.64 MPa					
0.044	-81	0.518	-907	0.878	-1642
0.089	-141	0.569	-973	0.922	-1572
0.135	-234	0.623	-1081	0.946	-1511
0.226	-374	0.672	-1195	0.969	-1339
0.324	-547	0.728	-1314	0.989	-929
0.427	-764	0.779	-1478		
0.471	-812	0.835	-1551		
313.15 K, 9.44 MPa					
0.045	22	0.331	105	0.676	-56
0.089	50	0.373	102	0.718	-88
0.090	51	0.376	106	0.721	-93
0.135	72	0.424	91	0.727	-100
0.138	69	0.467	64	0.832	-204
0.140	72	0.474	70	0.836	-205
0.179	82	0.515	38	0.859	-226
0.233	100	0.525	42	0.888	-241
0.280	98	0.571	16	0.948	-177
0.281	111	0.575	27	0.992	-23
0.323	101	0.621	-24		
313.15 K, 12.26 MPa					
0.047	43	0.442	284	0.698	205
0.097	79	0.491	284	0.742	180
0.147	143	0.541	274	0.800	125
0.195	180	0.542	275	0.844	85
0.247	220	0.544	280	0.896	44
0.296	240	0.587	270	0.951	1
0.345	266	0.638	246		
0.439	287	0.695	218		

TABLE II

Coefficients, standard deviation, s , and ratio s/H_{\max}^E for least-squares representation of $H_m^E/(\text{J}\cdot\text{mol}^{-1})$ for nitrous oxide + pentane by eq. 1

	308.15 K		313.15 K		
	9.49 MPa	12.27 MPa	7.64 MPa	9.44 MPa	12.26 MPa
C_0	861.31	1463.3	-3465.4	222.50	1138.0
C_1	474.68	-43.799	417.99	806.91	188.63
C_2	-21.875	-236.09	-354.30	-655.80	-165.44
C_3	366.34			1759.5	292.52
C_4	-1268.9			-1893.7	-810.71
k			0.96972		
$s/\text{J}\cdot\text{mol}^{-1}$	6.5	7.7	33	7.5	4.7
$100s/H_{\max}^E$	2.8	2.1	2.0	3.1	1.6

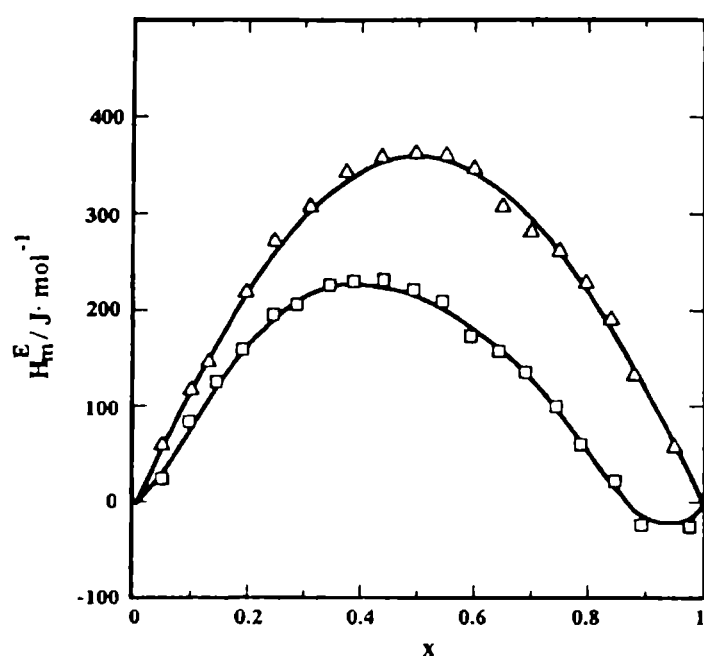


Fig. 1.- Excess molar enthalpies H_m^E against N_2O mole fraction for nitrous oxide+pentane at 308.15 K as a function of pressure: \square 9.49 MPa; Δ 12.27 MPa; — calculated from eq. 1.

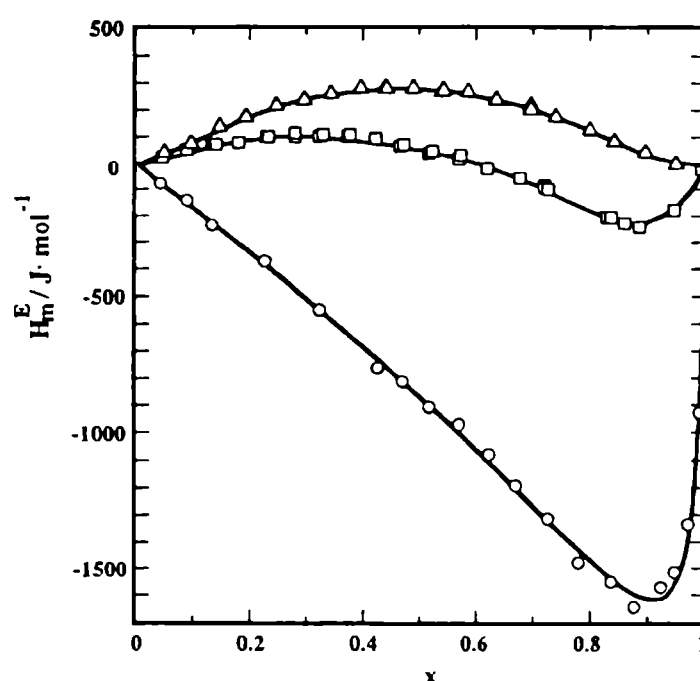


Fig. 2.- Excess molar enthalpies H_m^E against N_2O mole fraction for nitrous oxide+pentane at 313.15 K as a function of pressure: \circ 7.64 MPa; \square 9.44 MPa; Δ 12.26 MPa; — calculated from eq. 1.

Fig. 3 is a plot of p against T for the nitrous oxide + pentane system showing the vapor pressure equilibrium curve of nitrous oxide measured by Couch et al. (1962), the critical locus in the vicinity of the N_2O critical point, and the points at which experimental measurements of H_m^E have been made. Vapor-liquid equilibrium data or critical locus data are not available for nitrous oxide + pentane. The critical locus shown in Fig. 3 has been estimated using the procedure developed by Heidemann and Khalil (1980) and the equation of state proposed by Peng and Robinson (1976).

The changes observed in the excess enthalpy with temperature and pressure may be discussed in terms of liquid-vapor equilibrium and critical constants for the nitrous oxide + pentane mixtures and the densities of N_2O and pentane at the conditions of temperature and pressure of the experiments. A detailed discussion of these changes has been given for carbon

dioxide + pentane by Pando et al. (1983) and for nitrous oxide + toluene by Castells et al. (1994a,b). When the states and densities of the pure components and the mixtures are similar, the values of H_m^E are negative or slightly positive. This is so for the nitrous oxide + pentane mixtures at 308.15 K for isobars at 9.49 and 12.27 MPa and at 313.15 K for isobars at 9.44 and 12.26 MPa when the values of density are similar for N_2O and pentane. When the states and densities of the pure components differ and the resulting mixture is a liquid, large negative values of H_m^E are observed. This is so for the isobar at 313.15 K and 7.64 MPa when a value of 326 kg.m^{-3} is obtained for the N_2O density from the data of Couch et al. (1962), while a value of 615 Kg.m^{-3} is obtained for the pentane density from the TRC Thermodynamic Tables (1994) and the data of Sage and Lacey (1942). The large negative values of H_m^E seem to be a consequence of the nitrous oxide change of state from that of a low-density fluid to that of a liquid mixture component.

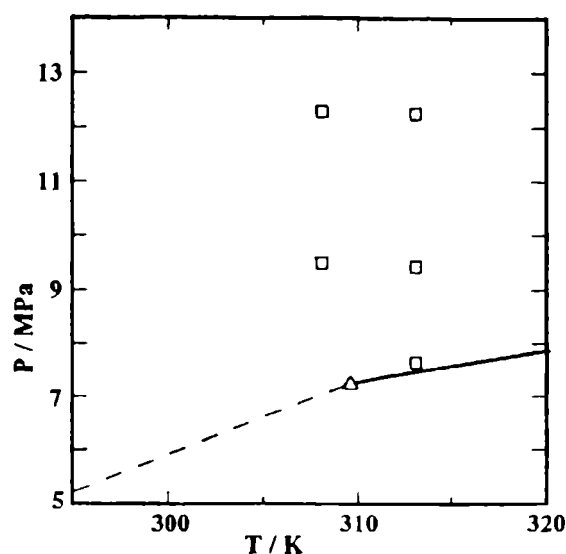


Fig. 3.- Plot of p against T for nitrous oxide + pentane showing the nitrous oxide vapor-liquid equilibrium curve (---) measured by Couch et al. (1962), the nitrous oxide critical point (Δ) taken from Reid et al. (1988), the critical locus (—) estimated using the Peng-Robinson equation of state (Peng and Robinson, 1976), and (T, p) coordinates (\square) where experimental measurements were made.

The shape of the isobars in Figures 1 and 2 denotes a behavior similar to that previously reported for carbon dioxide + pentane by Pando et al. (1983). The critical temperature ($T_c = 304.21 \text{ K}$) and pressure ($p_c = 7.38 \text{ MPa}$) of carbon dioxide are taken from the Carbon Dioxide, IUPAC Thermodynamic Tables of the Fluid State (1976) and are very close to those of nitrous oxide, and the carbon dioxide + pentane and nitrous oxide + pentane critical loci are very similar. The temperature and pressures at which experimental measurements have been made for carbon dioxide + pentane and nitrous oxide + pentane have a similar position with respect to the critical locus in the p against T plot. This may be seen by comparing the plot of Fig. 3 with a similar one shown for carbon dioxide + pentane by Pando et al. (1983) in Fig. 2 of their paper.

ACKNOWLEDGEMENT

We appreciate the aid given to us in estimating the critical locus by Dr. R.A. Heidemann. This work was funded by the Spanish Ministry of Education (DGICYT) Research

Project PB-91-0392. R.C.C. Acknowledges the Universidad Complutense of Madrid for a visiting research professorship at the Department of Physical Chemistry.

LITERATURE CITED

- Alexandrou, N.; Lawrence, M.J.; Pawliszyn, J.- Cleanup of complex organic mixtures using supercritical fluids and selective adsorbents. **Anal. Chem.** **64**, 301-311 (1992).
- Carbon Dioxide IUPAC Thermodynamic Tables of the Fluid State.- Pergamon: Oxford, U.K., 1976.
- Castells, R.C.; Mendiña, C.; Pando, C.; Renuncio, J.A.R.- The excess enthalpies of (dinitrogen oxide + toluene) at the temperature 313.15 K and at pressures from 7.60 MPa to 15.00 MPa. **J. Chem. Thermodyn.** **26**, 641-646 (1994a).
- Castells, R.C.; Mendiña, C.; Pando, C.; Renuncio, J.A.R.- Excess enthalpies of nitrous oxide-toluene in the liquid and supercritical regions. **J. Chem. Soc., Faraday Trans.** **90**, 2677-2681 (1994b).
- Christensen, J.J.; Izatt, R.M.- An isothermal flow calorimeter designed for high temperature, high pressure operation. **Thermochim. Acta** **73**, 117-129 (1984).
- Couch, E.J.; Hirth, L.J.; Kobe, K.A.- Volumetric behavior of nitrous oxide. Pressure-volume isotherms at high pressures. Gas compressibility factors at low pressures. **J. Chem. Eng. Data** **6**, 229-237 (1962).
- Gmehling, J.- Excess enthalpies for 1,1,1-trichloroethane with alkanes, ketones, and esters. **J. Chem. Eng. Data** **38**, 143-146 (1993).
- Heidemann, R.A.; Khalil, A.M.- The calculation of critical points. **AIChE J.** **26**, 769-779 (1980).
- Pando, C.; Renuncio, J.A.R.; Izatt, R.M.; Christensen, J.J.- The excess enthalpies of (carbon dioxide + toluene) at 308.15 and 323.15 K and from 7.58 to 12.45 MPa. **J. Chem. Thermodyn.** **15**, 259-266 (1983).
- Peng, D.-Y.; Robinson, D.B.- A new two-constant equation of state. **Ind. Eng. Chem. Fundam.** **15**, 59-64 (1976).
- Reid, R.C.; Prausnitz, J.M.; Poling, B.E.- **The properties of gases and liquids**. McGraw-Hill, Singapore, 1988.
- Sage, B.H.; Lacey, W.N.- Phase equilibria in hydrocarbon systems. Thermodynamic properties of n-pentane. **Ind. Eng. Chem.** **34**, 730-736 (1942).
- Sakaki, K.- Solubility of β -carotene in dense carbon dioxide and nitrous oxide from 308 to 323 K and from 9.6 to 30 MPa. **J. Chem. Eng. Data** **37**, 249-251 (1992).

**TRC Thermodynamics Tables; TRC data bases for Chemistry and Engineering;
Thermodynamics Research Center of the Texas Engineering Experiment Station, Texas
A&M University System: College Station, TX, 1994.**

EXCESS MOLAR ENTHALPIES OF NITROUS OXIDE-TOLUENE IN THE LIQUID AND SUPERCRITICAL REGIONS

ENTALPIAS MOLARES DE EXCESO DE OXIDO NITROSO-TOLUENO EN LAS REGIONES CORRESPONDIENTES A LIQUIDO Y A FLUIDO SUPERCRITICO

R.C. Castells¹, C. Menduina², C. Pando² and J.A.R. Renuncio²

SUMMARY

The excess molar enthalpies H^E of $[xN_2O + (1-x)C_6H_5CH_3]$ have been measured in the liquid and supercritical regions over the whole concentration range. Mixtures at a temperature of 308.15 K and pressures of 12.27 and 15.00 MPa show moderate endothermic and exothermic mixing in the toluene-rich region and nitrous oxide-rich region, respectively. Mixtures at 308.15 K and 9.49 MPa and at 323.15 K and 12.27 MPa show moderate exothermic mixing. Mixtures at 323.15 K and 7.64 and 9.49 MPa show significant exothermic mixing. The changes observed in the excess enthalpy with temperature and pressure have been discussed in terms of liquid-vapour equilibrium and critical constants for nitrous oxide-toluene. The experimental values of H^E at 308.15 and 323.15 K and those previously reported at 313.15 K have been analysed using the Peng-Robinson equation of state.

Keywords: Supercritical mixtures, nitrous oxide, toluene, flow calorimetry.

INTRODUCTION

In the last decade, thermodynamic properties such as the excess molar enthalpies of carbon dioxide-hydrocarbon mixtures have been extensively studied in the near critical and supercritical regions because of their anomalous behaviour in the vicinity of the critical locus and because of their practical importance in high-pressure technology [1,2]. Carbon dioxide has been employed commonly in supercritical fluid extraction because of its low toxicity, safety and low critical temperature. It has been reported that N_2O is a better solvent than CO_2 for certain molecules [3,4]. The nitrous oxide and carbon dioxide molecules are isoelectronic and have the same molar mass and very close critical points. For CO_2 T_c is 302.21 K and p_c is 7.38 MPa [5], while for N_2O T_c is 309.6 K and p_c is 7.24 MPa [6]. N_2O has a weak dipole moment of 0.166 D ($1\text{ D} \approx 3.33564 \times 10^{-30}\text{ Cm}$) [7], while CO_2 has none. This fact seems to be related to the higher affinity shown by N_2O to certain molecules.

¹ Miembro de la Carrera del Investigador del CONICET, UNLP

² Departamento de Química Física I, Universidad Complutense, Madrid, España

We reported previously measurements of the excess molar enthalpies H^E for carbon dioxide-toluene at temperatures of 308.15, 358.15, and 413.15 K and pressures up to 12.67 MPa [8] and for nitrous oxide-toluene at 313.15 K and pressures up to 15.00 MPa [9]. The results for carbon dioxide-toluene could be fitted to the Peng-Robinson equation of state [10,11]. This equation is a cubic equation of state of the form

$$p = \frac{RT}{v - b} - \frac{a(T)}{v(v + b) + b(v - b)} \quad (1)$$

For pure components, a and b are expressed in terms of the critical properties and the acentric factor α

$$a(T) = 0.45724\alpha(T)(R^2 T_c^2 / p_c) \quad (2)$$

$$b = 0.07780(R T_c / p_c) \quad (3)$$

$$\alpha(T) = \{1 + \kappa[1 - (T/T_c)^{1/2}]\}^2 \quad (4)$$

$$\kappa = 0.37464 + 1.54226\omega - 0.26992\omega^2 \quad (5)$$

For mixtures, a and b are given by

$$a = \sum_i \sum_j x_i x_j (1 - \delta_{ij})(a_i a_j)^{1/2} \quad (6)$$

$$b = \sum_i x_i b_i \quad (7)$$

where $\delta_{ij} = \delta_{ji}$ is the binary interaction parameter which is usually determined from experimental binary data.

Flow calorimetric measurements of H^E covering the whole concentration range for nitrous oxide-toluene at 308.15 and 323.15 K and 7.64, 9.49, 12.27, and 15.00 MPa are reported here. H^E for these mixtures are calculated using the cubic equation of state mentioned above and the resulting values are compared with experimental values. The pressure and temperature conditions of the measurements were chosen in order to compare results for nitrous oxide-toluene with those previously obtained for carbon dioxide-toluene [8].

EXPERIMENTAL

The measurements were made using the flow mixing apparatus and the experimental procedure described previously [9]. The chemicals were pumped into the calorimeter by two thermostatted ISCO pumps (model LC2600). The calorimeter cell was thermostatted in a silicon oil bath (± 0.0005 K) and the pressure was controlled by a back-pressure regulator. A manually controlled piston acts as a fine adjustment of the nitrogen pressure over the back-pressure regulator. Oscillations in pressure were smaller than ± 0.01 MPa.

TABLE I

Experimental and calculated excess enthalpies H^E for $[xN_2O + (1-x)C_6H_5CH_3]$

$H^E/(J\ mol^{-1})$			$H^E/(J\ mol^{-1})$			$H^E/(J\ mol^{-1})$		
x	expt.	calc.	x	expt.	calc.	x	expt.	calc.
308.15 K, 9.49 MPa								
0.050	1.6	-3.8	0.505	-165	-172	0.822	-425	-430
0.101	-1.4	-7.6	0.551	-223	-211	0.874	-426	-427
0.151	-18	-13	0.601	-271	-257	0.898	-418	-410
0.202	-24	-21	0.649	-298	-301	0.927	-373	-366
0.302	-60	-49	0.701	-359	-350	0.949	-307	-307
0.401	-85	-98	0.749	-386	-389	0.980	-168	-162
0.451	-120	-131	0.802	-405	-422			
308.15 K, 12.27 MPa								
0.052	14	17	0.457	16	17	0.851	-200	-200
0.102	32	31	0.504	-5.4	-2.1	0.876	-202	-201
0.153	49	42	0.551	-21	-26	0.900	-194	-195
0.203	44	49	0.606	-54	-58	0.907	-190	-191
0.257	52	52	0.653	-86	-88	0.929	-176	-173
0.308	50	50	0.754	-161	-156	0.950	-142	-144
0.353	46	45	0.761	-163	-160	0.981	-69	-72
0.407	32	33	0.805	-184	-185			
308.15 K, 15.00 MPa								
0.053	32	32	0.463	112	111	0.854	-69	-73
0.104	56	57	0.510	100	101	0.879	-79	-80
0.156	82	79	0.558	86	86	0.890	-81	-81
0.207	92	95	0.612	63	63	0.902	-83	-82
0.262	108	108	0.665	37	35	0.909	-80	-81
0.358	120	119	0.719	-0.1	2.8	0.931	-78	-76
0.386	120	119	0.766	-29	-27	0.952	-63	-64
0.413	118	118	0.809	-51	-52	0.981	-34	-32
0.438	114	115						
323.15 K, 7.64 MPa								
0.050	-223	-249	0.496	-2587	-2673	0.798	-4291	-4359
0.099	-580	-535	0.546	-2953	-2960	0.848	-4482	-4561
0.151	-792	-833	0.549	-3016	-2979	0.892	-4435	-4307
0.204	-1142	-1123	0.603	-3354	-3285	0.953	-2099	-2108
0.252	-1320	-1364	0.649	-3471	-3534	0.970	-1255	-1258
0.300	-1635	-1604	0.698	-3833	-3798	0.975	-968	-996
0.352	-1872	-1872	0.750	-4125	-4086	0.990	-155	-351
0.399	-2155	-2119						
325.15 K, 9.49 MPa								
0.051	-113	-100	0.405	-850	-884	0.707	-1598	-1595
0.103	-176	-205	0.406	-922	-885	0.754	-1694	-1687
0.154	-338	-313	0.478	-1062	-1059	0.806	-1796	-1764
0.205	-419	-423	0.510	-1126	-1137	0.876	-1718	-1780
0.258	-546	-540	0.547	-1207	-1225	0.929	-1620	-1616
0.306	-668	-651	0.557	-1265	-1251	0.950	-1443	-1433
0.347	-729	-745	0.654	-1474	-1479	0.971	-1139	-1114
0.348	-749	-743						
323.15 K, 12.27 MPa								
0.054	-12	-18	0.464	-305	-300	0.722	-553	-543
0.106	-32	-40	0.468	-300	-304	0.759	-581	-569
0.211	-102	-97	0.504	-358	-338	0.762	-563	-571
0.213	-104	-98	0.515	-340	-349	0.812	-576	-591
0.266	-131	-134	0.516	-341	-350	0.829	-573	-592
0.267	-127	-135	0.562	-396	-395	0.892	-559	-554
0.271	-141	-138	0.568	-403	-401	0.900	-561	-543
0.318	-170	-173	0.597	-422	-430	0.949	-444	-405
0.357	-198	-205	0.613	-450	-446	0.952	-385	-388
0.366	-210	-212	0.617	-463	-450	0.982	-195	-198
0.391	-250	-234	0.670	-498	-499	0.990	-118	-117
0.416	-267	-256	0.690	-513	-517	0.991	-104	-101
0.418	-249	-257	0.715	-529	-538			
323.15 K, 15.00 MPa								
0.054	0.3	1.6	0.418	-69	-77	0.857	-316	-320
0.105	1.6	0.8	0.440	-87	-88	0.881	-314	-310
0.106	2.5	0.7	0.444	-85	-90	0.891	-302	-303
0.159	-2.8	-3.0	0.465	-110	-102	0.904	-299	-291
0.211	-11	-10	0.515	-127	-131	0.932	-256	-250
0.264	-29	-21	0.559	-163	-160	0.935	-240	-243
0.294	-28	-29	0.583	-186	-177	0.936	-236	-241
0.362	-49	-53	0.667	-238	-236	0.972	-142	-138
0.363	-61	-53	0.714	-277	-269	0.982	-95	-98
0.387	-62	-63	0.720	-263	-273	0.982	-87	-98
0.390	-66	-65	0.767	-300	-300	0.998	-4.9	-12
0.415	-71	-76	0.812	-312	-318			

The materials employed were nitrous oxide (SEO 99.99 mol % pure) and toluene (Merck 99.5 mol % pure) previously dehydrated with sodium.

All runs were made in the steady-state fixed composition mode. Flow rates were selected to cover the whole mole fraction range. In most cases, the measurements were carried out at a total flow rate of $0.010 \text{ cm}^3 \text{ s}^{-1}$. A few measurements were carried out at a total flow rate of $0.005 \text{ cm}^3 \text{ s}^{-1}$. Flow rates range from 5.0×10^{-5} to $2.0 \times 10^{-4} \text{ mol s}^{-1}$. The reproducibility of the results was $\pm 1 \%$. The flow rates measured in $\text{cm}^3 \text{ s}^{-1}$ were converted to mol s^{-1} and to mole fractions using the densities of the two materials estimated as follows. The densities of N_2O at the temperature of the pump and at pressures of 7.64, 9.49, 12.27, and 15.00 MPa were calculated by interpolation of the pressure-volume isotherms of the liquid nitrous oxide measured by Couch et al. [12]. The densities of toluene at the temperature of the pump and at pressures of 7.64, 9.49, 12.27, and 15.00 MPa were calculated from the densities and isothermal compressibilities of Garbajosa et al. [13] and Aicart et al. [14].

RESULTS

Excess molar enthalpies were determined for $[\text{xN}_2\text{O} + (1-\text{x})\text{C}_6\text{H}_5\text{CH}_3]$ over the entire composition range at 308.15 K and 9.49, 12.27 and 15.00 MPa and at 323.15 K and 7.64, 9.49, 12.27, and 15.00 MPa. The results are given in Table I. Values for H^E at each temperature and pressure studied were fitted to the equation:

$$H^E / \text{J mol}^{-1} = \text{x}(1 - \text{x}) \frac{\sum_{n=0} C_n (2\text{x} - 1)^n}{1 + \sum_{k=1} B_k (2\text{x} - 1)^k} \quad (8)$$

The coefficients C_n and B_k are given in Table II together with the standard deviations, s , between experimental and calculated H^E values.

TABLE II

Coefficients and standard deviation, s , for least-squares representation of $H^E/\text{J mol}^{-1}$ for $[\text{xN}_2\text{O} + (1-\text{x})\text{C}_6\text{H}_5\text{CH}_3]$ by eqn. (8)

coefficients	T = 308.15 K			T = 323.15 K			
	9.49 ^a	12.27 ^a	15.00 ^a	7.64 ^a	9.49 ^a	12.27 ^a	15.00 ^a
C_0	-672.50	-1.0886	414.66	-10776.7	-4449.1	-1340.7	-487.70
C_1	1036.5	895.99	728.85	—	752.96	820.66	851.63
C_2	-199.83	-271.33	-350.32	—	—	—	-285.19
C_3	-329.81	—	223.46	—	—	—	—
B_1	0.84701	0.73508	0.55148	1.0787	0.92391	0.83657	0.73433
B_2	—	—	—	0.13777	—	—	—
B_3	—	—	—	-0.43665	—	—	—
B_4	—	—	—	-0.98008	—	—	—
B_5	—	—	—	0.43122	—	—	—
B_6	—	—	—	1.24735	—	—	—
s	10	3.2	2.0	83	25	11	5.8

^a p/MPa

Fig. 1 and 2 are plots of H^E against x for the isobars studied at 308.15 and 323.15 K, respectively. **Fig. 3** is a plot of p against T for $[xN_2O + (1-x)C_6H_5CH_3]$ showing the vapour-pressure equilibrium curve of nitrous oxide [12], the critical locus in the vicinity of the N_2O critical point, and the points at which experimental measurements of H^E have been made. For toluene T_c is 591.8 K and p_c is 4.10 MPa [6]. Vapour-liquid equilibrium data or critical locus data are not available for $[xN_2O + (1-x)C_6H_5CH_3]$. The critical locus shown in **Fig. 3** has been estimated using the procedure developed by Heidemann and Khalil [15] and the Peng-Robinson equation of state [10].

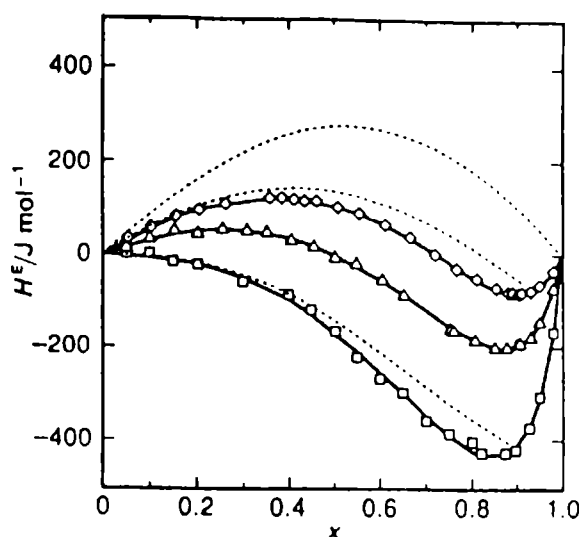


Fig. 1.- Plot of H^E against x for $[xN_2O + (1-x)C_6H_5CH_3]$ at 308.15 K as a function of pressure: \square 9.49; Δ 12.27; \diamond 15.00 MPa; (—) calculated from eqn. (8); (---) calculated from eqn. (1).

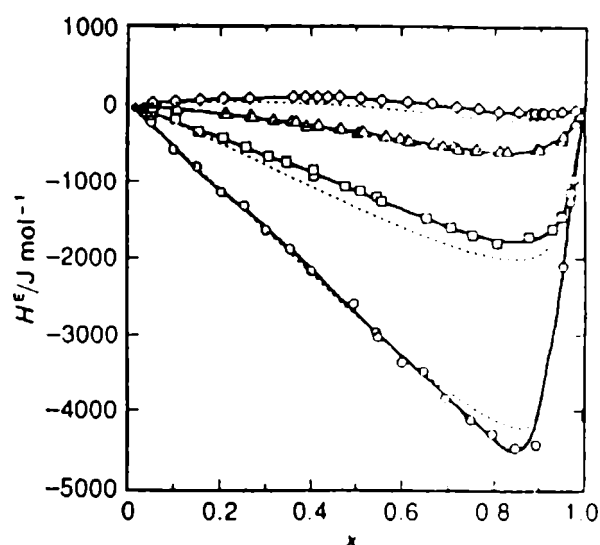


Fig. 2.- Plot of H^E against x for $[xN_2O + (1-x)C_6H_5CH_3]$ at 323.15 K as a function of pressure: \circ 7.60; \square 9.49; Δ 12.27; \diamond 15.00 MPa; (—) calculated from eqn. (8); (---) calculated from eqn. (1).

The densities of N_2O and toluene at the temperatures and pressures of the experiments are listed in **Table III**. Values for N_2O densities were taken from Couch et al. [9] and from Langenfeld et al. [16]. Values for toluene densities were calculated from the coefficients of the Tait equation given by Takagi [17]. The toluene enters the calorimeter as a liquid because the temperature is lower than the critical temperature of this component and the pressures are always higher than its critical pressure. The values of the density of toluene shown in **Table III** are typical of a liquid and change very little with pressure. At 308.15 K the nitrous oxide also enters the calorimeter as a liquid because the temperature is lower than the critical temperature of this component and the pressures are always higher than its critical pressure. The values of the density of nitrous oxide at 308.15 K shown in **Table III** are those typical of a liquid and change very little with pressure. At 323.15 K the nitrous oxide enters the calorimeter as a supercritical fluid because the temperature and pressures studied are always greater than those defining its critical point. However, this N_2O fluid may be a low-density (gas-like) fluid or a high-density (liquid-like) fluid depending on the pressure. The values of the density of nitrous oxide at 323.15 K change as the pressure increases from those typical of a gas at 7.64 and 9.49 MPa to those typical of a liquid at 12.27 and 15.00 MPa. The resulting $[xN_2O + (1-x)C_6H_5CH_3]$ may be liquid, gas-like fluid, or liquid-like fluid, depending on the critical temperature and pressure of the particular mixture. The phase diagram for $[N_2O + C_6H_5CH_3]$ belongs to class I in the classification of van Konynenburg and Scott [18]. The critical locus predicted by the Peng-Robinson equation [10] for $[N_2O + C_6H_5CH_3]$ is similar to the critical locus for the $[CO_2 + C_6H_5CH_3]$ [8]. The critical line goes through a maximum at $p \approx 17.5$ MPa and $T \approx 435$ K and returns to the toluene critical point ($T_c = 591.8$ K, $p_c = 4.10$ MPa). Since the temperatures

and pressures studied are far from those defining the critical point of toluene, $[x\text{N}_2\text{O} + (1-x)\text{C}_6\text{H}_5\text{CH}_3]$ is a liquid from $x = 0$ to $x \approx 0.95$, and is a fluid only in a narrow composition range in the N_2O -rich region. Owing to the transition from a liquid to a fluid mixture, there is also a two-phase region between the liquid and the fluid mixture regions. This is detected by a high-slope linear section in the N_2O -rich region of the isobars shown in Fig. 1 and 2. Unfortunately, the vapour and liquid equilibrium-phase compositions cannot be determined from these plots.

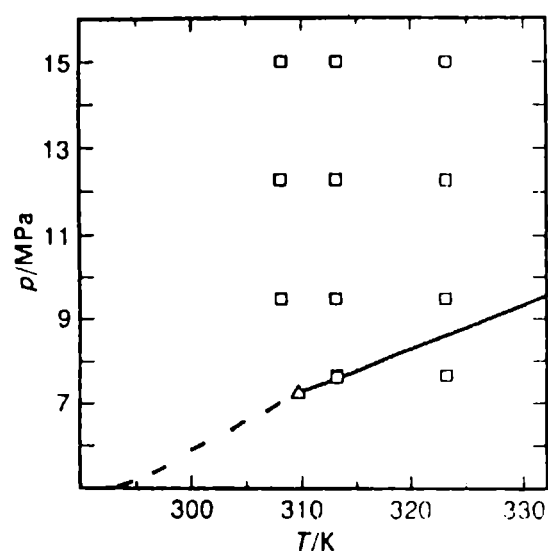


Fig. 3.- Plot of p against T for $[x\text{N}_2\text{O} + (1-x)\text{C}_6\text{H}_5\text{CH}_3]$ showing the vapour-liquid equilibrium curve (---) and critical point (Δ) of nitrous oxide, the critical locus (—) from $x = 1.00$ to 0.97 , and (T, p) coordinates (\square) where experimental measurements were made.

TABLE III

Densities of N_2O and toluene under the temperature and pressure conditions of the experiments

p/MPa	$\rho/\text{Kg m}^{-3}$			
	N_2O		toluene	
	308.15 K	323.15 K	398.15 K	323.15 K
7.64	---	222	---	846
9.49	740	437	861	848
12.27	790	664	863	850
15.00	819	727	865	852

When the states and densities of the pure components and the mixture are similar (liquid or liquid-like fluid nitrous oxide and liquid toluene forming a liquid or liquid-like fluid mixture), the values of H^E are negative or slightly positive. This is so at 308.15 K for isobars at 9.49, 12.27 and 15.00 MPa and at 323.15 K for isobars at 12.27 and 15.00 MPa when the density values are similar for N_2O and toluene. When the states and densities of the pure components differ (gas-like fluid nitrous oxide and liquid toluene), and the resulting mixture is

a liquid, large negative values of H^E are observed. This is so at 323.15 K for the isobars at 7.60 and 9.49 MPa when the density of N_2O is much lower than that of toluene.

The shape of the isobars in **Fig. 1** and **2** denotes behaviour similar to that previously reported for $[xCO_2 + (1-x)C_6H_5CH_3]$ [8]. The critical point of carbon dioxide is very close to that of nitrous oxide and the $[xC_2O + (1-x)C_6H_5CH_3]$ and $[xN_2O + (1-x)C_6H_5CH_3]$ critical loci are very similar. The temperature and pressures at which experimental measurements have been made for $[xCO_2 + (1-x)C_6H_5CH_3]$ and $[xN_2O + (1-x)C_6H_5CH_3]$ have a similar position with respect to the critical locus in the p against T plot. This may be seen by comparing the plot of **Fig. 2** with a similar one shown for $[xCO_2 + (1-x)C_6H_5CH_3]$ in **Fig. 3** of ref. 8.

Calculation of the excess molar enthalpy

The excess molar enthalpy of a binary mixture is given by

$$H^E = [H - H^*]_{\text{mix}} - \sum_i x_i [H - H^*]_i \quad (9)$$

where $[H - H^*]_{\text{mix}}$ is the residual molar enthalpy of the mixture and $[H - H^*]_i$ is that of components 1 and 2, respectively. The residual molar enthalpy is given by

$$H - H^* = RT(z - 1) + \int_{\infty}^v \left\{ T \left[\frac{\partial p}{\partial T} \right]_v - p \right\} dv \quad (10)$$

where z is the compressibility factor. For a fluid which follows the Peng-Robinson equation of state, eqn. (10) becomes

$$H - H^* = RT(z - 1) + \frac{T \frac{da}{dT} - a}{2^{3/2} b} \ln \left[\frac{z + 2.414B}{z - 0.414B} \right] \quad (11)$$

where B is given by

$$B = \frac{b}{RT} \quad (12)$$

Comparison of the Peng-Robinson equation of state with experiment

Excess enthalpies for the nitrous oxide-toluene system were calculated at 308.15, 313.15 and 323.15 K from 7.60 to 15.00 MPa using the expressions given in the previous section. The experimental values of H^E at 313.15 K were reported in a previous paper and are shown in **Fig. 4**. The values used for the critical constants are those already given. Values for the acentric factor were taken from Reid et al. [6]. The binary interaction parameter was adjusted to give the best fit to the experimental H^E values at 308.15, 313.15 and 323.15 K. A

value of 0.1018 was obtained for δ_{12} . Since the vapour and liquid equilibrium-phase compositions are unknown, H^E values were calculated only in the one-phase region. The curves of long dashes shown in Fig. 1, 2 and 4 are H^E values calculated using this value for δ_{12} . Although better results could be obtained if δ_{12} was adjusted to give the best fit at each temperature, we prefer to make comparison with experiment using a single value for the interaction parameter. For the 9.49, 12.27 and 15.00 MPa isobars at 308.15, 313.15 and 323.15 K the mean deviation of the calculated values of H^E from experiment is 80 J mol^{-1} . For the 7.64 MPa isobar at 323.15 K the mean deviation is 100 J mol^{-1} . This is in good agreement if we take into account the fact that this isobar exhibits a minimum of -4500 J mol^{-1} . The agreement is not good for the 7.60 MPa isobar at 313.15 K which exhibits a minimum of -2300 J mol^{-1} (the mean deviation is 600 J mol^{-1}). This discrepancy between experimental measurements and the calculated curve seems to arise from the failure of the Peng-Robinson equation of state to give the correct value for the compressibility factor of nitrous oxide under these conditions of temperature and pressure. Couch et al. [12] reported experimental values for the nitrous oxide compressibility factor for a wide range of temperature and pressure. The agreement between this values for z and those calculated by means of the Peng-Robinson equation or by means of the Kubic equation [19] is good except at 7.60 MPa and 313.15 K when we are in the vicinity of the nitrous oxide critical point.

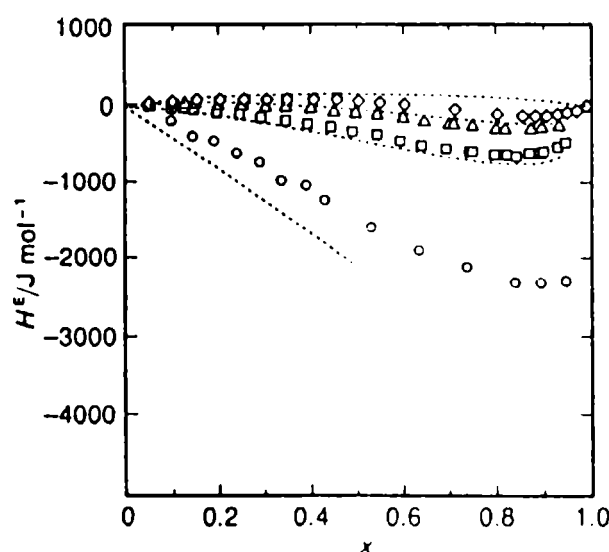


Fig. 4.- Plot of H^E against x for $[x\text{N}_2\text{O} + (1-x)\text{C}_6\text{H}_5\text{CH}_3]$ at 313.15 K as a function of pressure: O 7.60; \square 9.49; Δ 12.27; \diamond 15.00 MPa; (---) calculated from eqn. (1).

Wormald and co-workers [20-24] have successfully used the Kubic equation of state to fit excess enthalpies of several binary mixtures at high pressures. H^E data for the $[\text{N}_2\text{O}-\text{C}_6\text{H}_5\text{CH}_3]$ system were also analysed using this equation. Results from this calculation are not reported in this paper because values for the deviation between experimental and calculated H^E are higher than those obtained for the Peng-Robinson equation of state.

ACKNOWLEDGEMENT

This work was funded by the Spanish Ministry of Education (DGICYT) Research Project PB-91-0392. We appreciate the aid given to us by Dr. R.A. Heidemann in estimating

the critical locus. R.C.C. acknowledges the Universidad Complutense of Madrid for a visiting research professorship at the Department of Physical Chemistry.

REFERENCES

- [1] *Supercritical Fluid Technology*.- Ed. T.J. Bruno and J.F. Ely, CRC Press, Boca Raton, FL, 1991.
- [2] G. Morrison, J.M.H. Levelt Sengers, R.F.Chand and J.J. Christensen.- *Supercritical Fluid Technology*, De. J.M.L. Penninger, M. Radosz, M.A. McHugh and V.J. Krukonis, Elsevier, Amsterdam, 1985.
- [3] K. Sakaki.- **J. Chem. Eng. Data** **37**, 249 (1992).
- [4] N. Alexandrou, M.J. Lawrence and J. Pawliszyn.- **Anal. Chem.** **64**, 301 (1992).
- [5] *Carbon Dioxide, IUPAC Thermodynamic Tables of the Fluid State*.- Pergamon, Oxford, 1976.
- [6] R.C. Reid, J.M. Prausnitz and B.E. Poling.- *The Properties of Gases and Liquids*, McGraw-Hill, Singapore, 1988.
- [7] D.E. Stogryn and A.P. Stogryn.- **Mol. Phys.** **11**, 371 (1966).
- [8] C. Pando, J.A.R. Renuncio, R.S. Schofield, R.M. Izatt and J.J. Christensen.- **J. Chem. Thermodyn.** **15**, 747 (1983).
- [9] R.C. Castells, C. Menduiña, C. Pando and J.A.R. Renuncio.- **J. Chem. Thermodyn.** **26**, 641 (1994).
- [10] D-Y. Peng and D.B. Robinson.- **Ind. Eng. Chem. Fundam.** **15**, 59 (1976).
- [11] A.G. Casielles, C. Pando and J.A.R. Renuncio.- **Thermochim. Acta** **154**, 57 (1989).
- [12] E.J. Couch, L.J. Hirth and K.A. Kobe.- **J. Chem. Eng. Data** **6**, 229 (1962).
- [13] G. Garbajosa, G. Tardajos, E. Aicart and M. Diaz Peña.- **J. Chem. Thermodyn.** **14**, 671 (1982).
- [14] E. Aicart, G. Tardajos and M. Diaz Peña.- **J. Solution Chem.** **11**, 557 (1982).
- [15] R.A. Heidemann and A.M. Khalil.- **AIChE J.** **26**, 769 (1980).
- [16] J.J. Langenfeld, S.B. Hawthorne and D.J. Miller.- **Anal. Chem.** **64**, 2263 (1992).
- [17] T. Takagi.- **Rev. Phys. Chem. Jpn.** **48**, 17 (1978).

- [18] P.H. Van Koynenberg and R.L. Scott.- **Phil. Trans. R. Soc.** **298**, 495 (1980).
- [19] W.L. Kubic.- **Fluid Phase Equilibria**, **9**, 79 (1982).
- [20] C.N. Colling, N.M. Lancaster, M.J. Lloyd, M. Masucci and C.J. Wormald.- **J. Chem. Soc. Faraday Trans.** **89**, 77 (1993).
- [21] M. Masucci and C.J. Wormald.- **J. Chem. Soc. Faraday Trans.** **89**, 1345; 3375 (1993).
- [22] M. Masucci, C.J. Wormald and L. Yan.- **J. Chem. Soc. Faraday Trans.** **89**, 4193 (1993).
- [23] C.J. Wormald and C.N. Colling.- **J. Chem. Thermodyn.** **25**, 599 (1993).
- [24] C.J. Wormald and M.J. Lloyd.- **J. Chem. Thermodyn.** **26**, 101 (1993).

SEPARATION OF LOW-BOILING PYRIDINE BASES BY GAS CHROMATOGRAPHY

SEPARACION DE BASES PIRIDINICAS DE BAJO PUNTO DE EBULLICION POR CROMATOGRAFIA GASEOSA

M.C. Titon¹ and A.M. Nardillo²

SUMMARY

The analysis of the low-boiling pyridine and its alkyl derivatives is a difficult task for gas chromatography due to their close vapor pressures and polarities. The methods described in the paper employ columns packed with N,N,N',N'-tetrakis(hydroxyethyl)ethylenediamine and metal transition compounds on diatomaceous supports which permit a rapid and reliable separation.

Keywords: *Pyridines, gas chromatography, THEED, metallic stearates.*

INTRODUCTION

Owing to the importance of applications in chemical industries of pyridine and its alkyl derivatives considerable attention has been given to their chromatographic separation and determination. The analysis of the low-boiling tar base fraction, the β -picoline fraction, is a complex problem in gas chromatography. On account of their close vapor pressures and polarities it is difficult to separate some compound pairs, i.e. 4-methyl- and 3-methylpyridine.

The use of capillary columns and adequate stationary phases diminish these difficulties. Polar liquids such as N,N-bis(hydroxyethyl)trimethylenediamine [1] have produced an acceptable separation but with tailing peaks. Pretreatment or addition of strong bases, i.e. potassium hydroxide, to Carbowax 1540 [2] or to β -cyanoethylpolysiloxane [3] have allowed better symmetries but without the necessary selectivities. Other applications include the use of non-polar phases [4-7] and a wide variety of polar phases such as Amine-220 [8,9], amine-treated Carbowax 20M [6,10] and Reoplex 400 [4,5,8]. According to Novročíková et al. [5] a soft sodium-calcium glass column with Reoplex 400 can resolve, with identification purposes, 72 pyridine alkyl homologues, except three pairs and one triad compounds.

Numerous chromatographic papers have been published using packed columns [11-25]. Since the first steps of chromatography it has been well known that glycerol, triethanolamine and polyethyleneglycol [11,12] were used as liquid phases to separate a few pyridine bases mixtures. In most of these studies the solid support was deactivated by means of surface

¹ División Química Analítica, Facultad de Ciencias Exactas, UNLP

² Miembro de la Carrera del Investigador del CONICET, UNLP

silylation, additions of non-volatile organic compounds or potassium hydroxide in order to improve the symmetry of the peaks, but they suffer from long analysis times, partially resolved pairs or, in some cases, tailing. It is important to point out the high selectivities of 4-methyl-/3-methylpyridine on glycerol and on benzoic acid derivative [19].

Finally, metal transition stearates or oleates [20,26], or their mixtures with Apiezon M [27,28] have been exploited as stationary phases for pyridine bases separation. Studies of systems such as Co-phthalocyanine supported on carbon black, in packed and porous-layer open tubular columns [29]; squalane plus Ni- β -ketoamine complexes [30] and 1,2,3-tris(2-cyanoethoxy)-propane plus cupric chloride [31] were tried with limited success.

The industrial-scale fractionation of pyridine bases is carried out by distillation, consequently the β -picoline fraction could contain compounds whose boiling points are lower than 150°C as principal components and small quantities of other alkylpyridines, i.e. lutidines or collidines. The aim of the present work is to develop a suitable packed column for a rapid and reliable separation of components of the β -picoline fraction and of binary samples of 4-methyl- and 3-methylpyridine when one of them is in a higher ratio concentration.

EXPERIMENTAL

Konik 3000 and Hewlett-Packard 5880A gas chromatographs equipped with flame ionization detectors were used in this study. The columns were $\frac{1}{4}$ in. O.D. x 2 mm I.D. (1 in. = 2.54 cm) silanized glass tubing, with lengths ranging between 1 and 2 m. Analytical-grade nitrogen, previously passed through humidity (Analabs HGC-145) and oxygen (Analabs HGC-224) traps, was used as carrier gas at 15-20 ml min⁻¹. The flame ionization detector was operated at 150°C and the injector port at 140°C. Samples of 0.5 μ l of 0.5% (w/w) solutions were injected by means of 5- or 10- μ l syringes (Hamilton 75N or 701N).

The pyridine (Py), 2,4,6-collidine (2,4,6-C) and six lutidines or dimethylpyridines (2,3-; 2,4-; 2,5-; 2,6-; 3,4-; and 3,5-L) were from Aldrich and picolines or methylpyridines (2-MP; 3-MP and 4-MP) and 2-ethylpyridine (2-EtP) were from Fluka; analytical-grade n-hexane (Merck) was used to prepare sample solutions. The solid support, Chromosorb P AW, 100-120 mesh, was from J. Manville. The stationary phases were from various suppliers.

Metallic stearates were prepared as described by Whitmore and Lauro [32] from stearic acid and inorganic metal salts, all analytical reagents. Column packings were prepared by mixing a solid support with a solution which contains the required quantity of stationary phase in an adequate solvent, chloroform for a single liquid phase; chloroform plus benzene for a binary phase; and methanol for N,N,N',N'-tetrakis(hydroxyethyl)ethylenediamine (THEED) plus cupric chloride. The solvent was slowly removed in a rotary evaporator (Büchi) under a nitrogen stream and gentle heating.

The column performance has been compared by means of the following parameters: (1) the symmetry of the pyridine peak, defined as the ratio of the back width and the front width of the peak, measured from a vertical line traced through the peak maximum, at one tenth of the peak maximum; and (2) the number of theoretical plates/m for pyridine and its alkyl derivatives.

TABLE I
Selectivities of pyridine bases on liquid stationary phases

	SELECTIVITY											
	100°C				90°C				80°C			
	Cd	Ni	Zn	THEED	Cd	Ni	Zn	THEED	Cd	Ni	Zn	THEED
Pyridine	1.26	1.26	1.32	1.22	1.30	1.29	1.36	1.26	1.33	1.33	1.40	1.30
2-MP	1.22	1.22	1.22	1.09	1.25	1.26	1.25	1.12	1.29	1.23	1.29	1.16
2,6-L	1.13	1.13	1.13	1.12	1.14	1.13	1.13	1.11	1.14	1.13	1.12	1.10
2-EtP	1.24	1.27	1.19	1.34	1.24	1.26	1.18	1.32	1.23	1.24	1.16	1.30
3-MP	1.12	1.13	1.11	1.12	1.12	1.13	1.11	1.13	1.13	1.14	1.12	1.13
4-MP	1.10	1.08	1.17	1.08	1.12	1.11	1.20	1.11	1.14	1.14	1.24	1.14
2,5-L	1.12	1.13	1.12	1.15	1.13	1.13	1.13	1.16	1.13	1.14	1.13	1.16
2,4-L	1.04 ^a	1.04 ^a	1.04 ^a	1.03 ^a	1.04 ^a	1.04 ^a	1.04 ^a	1.03 ^a	1.04 ^a	1.04 ^a	1.04 ^a	1.03 ^a
2,3-L	1.16	1.17	1.18	1.05	1.19	1.23	1.21	1.09	1.23	1.23	1.25	1.12
2,4,6-C	1.35	1.36	1.26	1.34	1.34	1.33	1.23	1.30	1.33	1.31	1.20	1.27
3,5-L	1.42	1.45	1.42	1.46	1.44	1.47	1.43	1.48	1.46	1.49	1.45	1.50
3,4-L												
t' _R 3,4-L (min)	15.1	10.4	12.4	12.3	22.4	15.4	18.0	18.3	34.5	22.6	26.7	29.1

Columns Cd 2 m x 2 mm I.D., 3.2% THEED plus cadmium stearate (0.16 mol fraction); Ni 1.5 m x 2 mm I.D., 3.1% THEED plus nickel stearate (0.16 mol fraction); Zn 6 ft x 2 mm I.D., 3.1% THEED plus zinc stearate (0.16 mol fraction); THEED 2 m x 2 mm I.D., 4.1% THEED.

^a Selectivities were determined injecting binary mixtures of 2,5-L plus 2,4-L and 2,5-L plus 2,3-L.

RESULTS AND DISCUSSION

Peak shape and column efficiency improved when siliceous solid supports were deactivated by means of a liquid stationary phase or treated with a silanizing reagent or with an adequate additive. For those purposes, in the first stage of the present work, we have employed a series of high-polarity phases such as glycerol, diglycerol, AT-220, Quadrol and THEED, all of them between 2 and 6% (w/w).

Asymmetries lower than 1.2, measured at 90°C, were observed with AT-220 (the best), THEED and Quadrol, and the numbers of theoretical plates were approximately the same, 2500-2200 theoretical plates/m. A good balance between peak symmetry, relative retention, analysis time and temperature was obtained with 4% liquid phase. The results with the use of THEED are expressed as selectivities and they are summarized in **Table I**. At 70°C all pairs between pyridine and 2,5-L gave satisfactory results, except 2,6-L/2-EtP, but the analysis time was very long, approximately 20 min. At higher temperature an improved resolution of the above-mentioned pair was obtained. However, large drops in selectivities were observed with 2-MP/2,6-L and 4-MP/2,5-L; obviously, analysis time decreased considerably.

We intended to improve selectivities by adding transition metal organic salts. Several columns containing 3% THEED plus increased cadmium stearate [$\text{Cd}(\text{St})_2$] concentrations ($X = 0.023, 0.045, 0.086$ and 0.16 ; where X denotes mol fraction) were studied. The best separations were obtained at higher metal salt concentrations. So a better balance was reached between selectivity and temperature for the pairs mentioned above compared to the results we obtained with THEED. The selectivities are summarized in **Table I**. The efficiency of binary liquid phases presented a small drop with increased metal salt concentration.

Nickel stearate and THEED mixtures behaved similarly as cadmium salt (**Table I**). Therefore, both mixtures of stearates (Ni or Cd) plus THEED can be used for separation of the β -picoline fraction components with a packed column 1.5 m long, at temperatures between 80 and 90°C. **Fig. 1** shows a typical chromatogram, obtained for a sample of seven pyridine bases on an 1.5 m column packed with 3.1% THEED plus $\text{Ni}(\text{St})_2$ ($X = 0.16$) at 90°C. The behavior described above was compared to that obtained for a Carbowax Amine fused-silica capillary column [33,34]. The results indicate that our packed column has had a good performance.

The zinc stearate as liquid phase has been specially indicated for its high selectivity [26,35]. However, its mixture with THEED did not lead to important improvements with respect to cadmium and nickel salts. The results in **Table I** show higher selectivities for Py/2-MP and 4-MP/2,5-L and lower for 2-EtP/3-MP. Furthermore, it was observed that efficiency drops to 1500 theoretical plates/m at $X = 0.16$.

It is relevant to point out that with the studied metal stearates it was possible to get a better separation of the β -picoline fraction, but the improvement in selectivity, respect of pure THEED, was not obtained for 4-MP/3-MP pair.

In aqueous solution pyridine interaction with cupric ion is higher than with Ni(II) and Cd(II); thus, the logarithms of the equilibrium constants are 2.41, 1.78 and 1.27 respectively [36] and its o-alkyl derivatives are strongly affected by steric impediments. A mixture of $\text{Cu}(\text{St})_2$ ($X = 0.22$) in 3% THEED as liquid phase reverse the gas chromatographic retentions of Py, 2-MP and 2,6-L, but selectivities were not high enough for separation and the 4-MP/3-

MP pair selectivity reached 1.4. However, this behavior was blurred by an unstable retention, which remained although the column was maintained 100 h at 100-120°C. A mixture of cupric chloride ($X = 0.16$) plus 4.1% THEED has produced: (1) a better retention stability ($\pm 4\%$ fluctuation in a period of 8 h); (2) a low efficiency, only 1200-1300 theoretical plates/m, and (3) selectivities for the 4-MP/3-MP pair of 1.29 and 1.27 at 80°C and 90°C, respectively. **Fig. 2** shows a chromatogram obtained for a solution of 3-MP (Fluka, purity higher than 98%) in n-hexane on a column packed with the above-mentioned binary stationary phase at 85°C. This column failed when applied to a 2,3- and 2,4-L mixture, it provided a higher retention for 2,4-L (an inverted behavior of Cd, Ni and Zn salts plus THEED) and a 1.08 selectivity at 70-90°C. Higher cupric chloride concentrations packings have produced columns of lower efficiency; at present we continue working with another cupric organic salts to improve selectivity and retention stability.

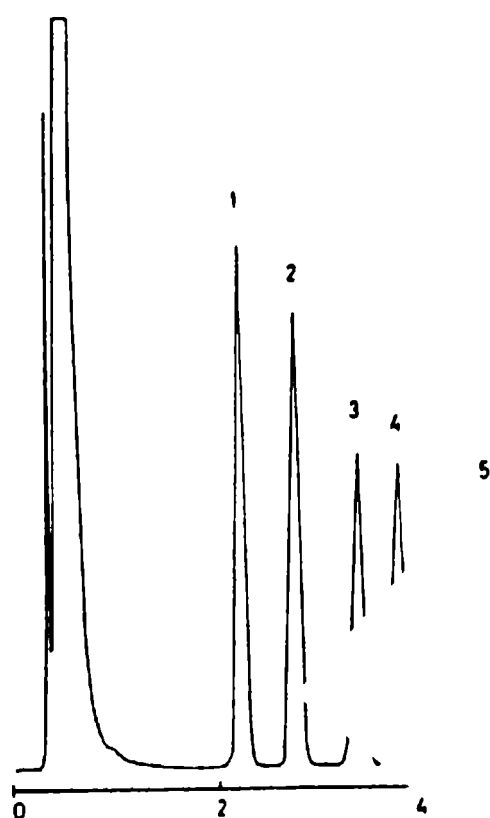


Fig. 1.- Chromatogram on 1.5 m x 2 mm I.D. glass column of 3.1% THEED plus nickel stearate (0.16 mol fraction) on Chromosorb P AW, 100-120 mesh, at 90°C. Peaks: 1=Py; 2=2-MP; 3=2,6-L; 4=2-EtP; 5=3-MP; 6=4-MP; 7=2,5-L.

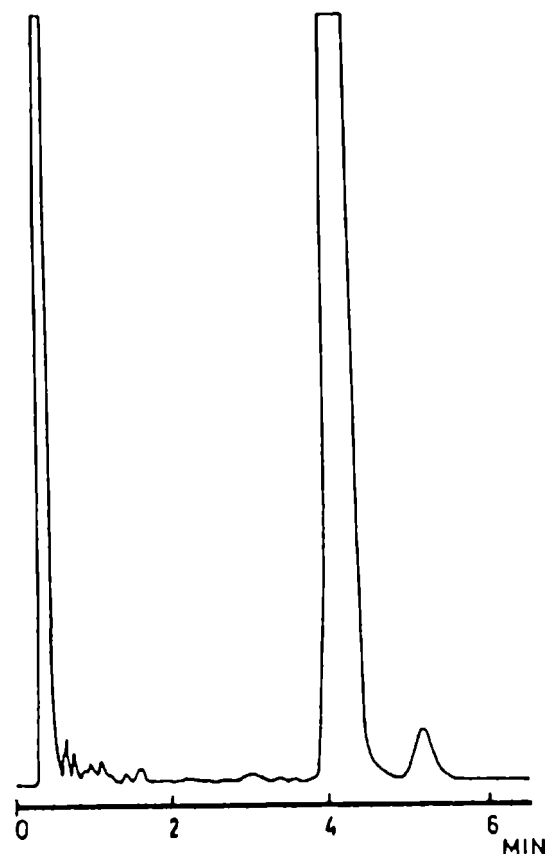


Fig. 2.- Chromatogram on 4 ft. x 2 mm I.D. glass column (1 ft. = 30.48 cm) of 4.1% THEED plus cupric chloride (0.16 mol fraction) on Chromosorb P AW, 100-120 mesh, at 85°C. Sample 0.5 μ l of 4% solution of 3-MP (Fluka, purity higher than 98%) in n-hexane.

ACKNOWLEDGMENT

This work was sponsored by the Consejo Nacional de Investigaciones Científicas y Técnicas (CONICET) and by the Comisión de Investigaciones Científicas de la Provincia de Buenos Aires.

REFERENCES

- [1] K. Heyns, R. Stute and J. Winkler.- *J. Chromatogr.* **21**, 302 (1960).

- [2] E.W. Cieplinski.- **Anal. Chem.** **38**, 928 (1966).
- [3] E.L. Ilkova and E.A. Mistryukov.- **Chromatographia** **4**, 77 (1971).
- [4] J. Oszezapowicz, J. Golab and H. Pines.- **J. Chromatogr.** **64**, 1 (1972).
- [5] M. Novrocíková, J. Novrocík and J.Vimetal.- **Collect. Czech. Chem. Commun.** **48**, 3270 (1983).
- [6] J.E. Premeez and M.E. Ford.- **J. Chromatogr.** **388**, 23 (1987).
- [7] E.B. Caramao, L.M.F. Gomes, M.D. de Oliveira and F.M. Lancas.- **J. High Resolt. Chromatogr. Chromatogr. Commun.** **10**, 579 (1987).
- [8] K. Tesarik and S. Ghyczy.- **J. Chromatogr.** **91**, 723 (1974).
- [9] J. Macák, , V.M. Nabivach, P. Buryan and J.S. Berlizov.- **J. Chromatogr.** **209**, 472 (1981).
- [10] M. Horká, V. Kahle and M. Krejčí.- **J. Chromatogr.** **637**, 96 (1993).
- [11] W.J. Murray and A.F. Williams.- **Chem. Ind. (London)** **38**, 1020 (1956).
- [12] V.T. Brooks and G.A. Collins.- **Chem. Ind. (London)** **38**, 1021 (1956).
- [13] A.W. Decora and G.U. Dinneen.- **Anal. Chem.** **32**, 164 (1960).
- [14] W.E. Golding and C.A. Townsend.- **Chem. Ind. (London)** **42**, 1476 (1960).
- [15] J.S. Fitzgerald.- **Aust. J. Appl. Sci.** **12**, 51 (1961).
- [16] A.A.F. van der Meeren and A.L.T. Verhaar.- **Anal. Chim. Acta** **40**, 343 (1968).
- [17] M. Anwar, C. Hanson and A.N. Patel.- **J. Chromatogr.** **34**, 529 (1968).
- [18] Y. Kaburaki, Y. Mikami, Y. Okabayashi and Y. Saida.- **Bunseki Kagaku** **18**, 1100 (1969); **Chem. Abstr.** **72**, 75794 (1970).
- [19] M. Kremser and L. Premru.- **J. Chromatogr.** **89**, 131 (1974).
- [20] V.D. Shatts, A.A. Avots and V.A. Belikov.- **Zh. Anal. Khim.** **32**, 797 (1977).
- [21] L.G. Sednevets and A.G. Pankov.- **Zh. Anal. Khim.** **32**, 1039 (1977).
- [22] V.M. Nabivach and L.A. Venger.- **J. Chromatogr.** **144**, 118 (1977).
- [23] V.M. Nabivach and L.A. Venger.- **J. Chromatogr.** **159**, D8 and D11 (1978).
- [24] A. Bhattacharjee and D. Guha.- **J. Chromatogr.** **298**, 161 (1984).

- [25] J. Martín and L. Gascó.- **An. Quím.** **64**, 775 (1968); **Chem. Abstr.** **70**, 43666 (1969).
- [26] D.H. Desty.- **Nature (London)** **181**, 604 (1958).
- [27] D.W. Barber, C.S.G. Phillips, G.F. Tusa and A. Verdin.- **J. Chem. Soc.** 18 (1959).
- [28] A.A. Anderson, P. Mekss and M.V. Shimanskaya.- **Symp. Biol. Hung.** **34**, 141 (1986); **Chem. Abstr.** **107**, 228100 (1987).
- [29] J.J. Franken, C. Vidal-Madjar and G. Guiochon.- **Anal. Chem.** **43**, 2034 (1971).
- [30] J. Maslowska and G. Bazylak.- **Collect. Czech. Chem. Commun.** **54**, 1530 (1989).
- [31] L.D. Turkova, A.G. Vitenberg and G.G.Belen'kii.- **Neftekhimiya** **7**, 458 (1967); **Chem. Abstr.** **68**, 65462 (1968).
- [32] W.F. Whitmore and M. Lauro.- **Ind. Eng. Chem.** **22**, 646 (1930).
- [33] **General Catalog 1991**.- Chrompack, Middelburg, 1991, p. 37.
- [34] **The Supelco Reporter**.- Vol. XI, No. 2, Supelco, Bellefonte, PA, 1992, p. 4.
- [35] H. Rotzsche.- **Stationary Phases in Gas Chromatography**, Elsevier, Amsterdam, 1991, p. 282.
- [36] J. Bjerrum.- **Chem. Rev.** **46**, 381 (1950).

EVALUATION OF THE SURFACE TREATMENT EFFECT ON THE CORROSION PERFORMANCE OF PAINT COATED CARBON STEEL

EVALUACION DEL EFECTO DEL TRATAMIENTO SUPERFICIAL SOBRE EL COMPORTAMIENTO FRENTE A LA CORROSION DE ACERO AL CARBONO PINTADO

D.M. Santágata¹, P.R. Seré,² C.I. Elsner³ and A.R. Di Sarli⁴

SUMMARY

Electrochemical impedance spectroscopy studies were carried out for plasticized chlorinated rubber coated carbon steel sheets under free corrosion conditions when exposed to artificial sea water. Four different sample types were used changing the surface treatment procedures (sandblasted, pickling, pickling + phosphatized and phosphatized + wash primer). The EIS data has been interpreted considering the values of the distinct equivalent electrical circuit models, whose components allowed a quantitative evaluation of the long term corrosion behaviour for the different pretreated coated steel specimens. Furthermore, from impedance data the water content of the paint on the steel substrate was calculated by the Brasher expression and the progress of the coating delamination process by the also empirical expression relating the measured/specific double layer capacitance ratio. On the basis of both the electrochemical and the visually monitored test results it was concluded that the best corrosion performance was provided by pickling + phosphated painted steel surfaces followed by the pickling ones. This result has been attributed to the fact that such surface treatments can improve the barrier protection and the steel/paint adhesion properties or reduce the osmotic pressure effect, respectively.

INTRODUCTION

The surface preparation and/or pretreatment is always important to obtain satisfactory coatings performance, being particularly critical for immersion or high humidity conditions, which are unforgiving of mistakes in surface preparation and coating application. Coatings must be able to form a barrier in order to break the metal-electrolyte connection for delaying or stopping the metallic substrate corrosion reaction. By this characteristic and other laterly mentioned based on the film strong properties, it is little wonder that the chlorinated rubber, compound formed by reacting natural rubber with chlorine, has over the years found so much

¹ Becario de la CIC

² Becario de la CIC, UNLP

³ Miembro de la Carrera del Investigador del CONICET, UNLP

⁴ Miembro de la Carrera del Investigador de la CIC

use as a maintenance coating vehicle. Thus, coatings made from chlorinated rubber that have been blended with highly chlorinated additives provide toughness, water impermeability and chemically resistant properties. In consequence, heavy-duty coating systems based on this polymer have been used extensively in the protection and decoration of chemical plants, refineries, pipelines, bridges, power generation and many other (power transmission, harbor, marine, etc.) facilities. In addition, traffic and floor paints, concrete and swimming pools and reservoirs as well as fire retardant coatings using chlorinated rubber based binder have also been prepared. As there is no paint being indestructible, all the organic coatings will undergo normal deterioration with time, however, its rate can be slowed significantly by choosing a top quality coating and/or using the appropriate surface preparation and application technique.

Water and oxygen can permeate, at least to some extent, through any organic film although it has no intrinsic structural defects such as cracks and/or pores through the film. Water and oxygen travel through the film by jumping from one free volume hole to others.

As part of a program aimed to define a lifetime prediction model for steel sheets coated with an organic film, an investigation related with the role played by the surface pretreatment given to the substrate on the global deterioration of such systems has been started. Therefore, the purpose of the present paper was to study differences on the corrosion protection and coating disbondment provided by a chlorinated rubber paint applied to previously treated [sandblasted (S), pickling (P), pickling + phosphated (PPh) or sandblasted + wash primer (SWP)] carbon steel sheets in artificial sea water. This steel was particularly chosen because it is a commonly used structural material which requires protection against corrosive environments. EIS measurements were carried out with a view to understand the effect, if any, of the surface preparation method on the corrosion protective properties afforded by a chlorinated rubber paint (30 and 80 μm in thickness), plasticized with chlorinated paraffin and pigmented with titanium dioxide.

EXPERIMENTAL PROCEDURE

Each sample substrate consisted of a (10x10x0.3 cm) carbon steel test panel, whose percentual chemical composition was: C (0.16); Mn (0.54); Si (0.05); S (0.01); P (0.01), Fe being the difference. The surface treatment procedures for steel were: 1) sandblasted to ASa 2 1/2-3 (Swedish Standard SIS 05 59 00/67) and its roughness, measured with a Hommel Tester mod. T 1000, was $2.04 \pm 0.24 \mu\text{m}$; 2) pickling in inhibited HCl + phosphated, using a bath based in ZnO and $\text{H}_3\text{PO}_4\text{-HNO}_3$ mixture at 95°C for 30min; 3) pickling in inhibited HCl or 4) sandblasted + wash primer. Then, the steel sheets were cleaned with toluene to ensure surface uniformity and coated with a commercially available chlorinated rubber prepared by addition of 70% chlorinated rubber 20cP, plasticized by addition of 30% chlorinated paraffin and pigmented with TiO_2 . Specimens were coated using a Bird applicator, which gave uniform coating thicknesses. The average dry film thicknesses (30 or 80 μm for thin and thick films, respectively) were measured using an Elcometer mod. 300 electromagnetic gauge, **Table I**. Two acrylic tubes used as electrolyte vessels were fixed to the intact coated steel sheet, using an epoxy adhesive. The geometrical area for each cell exposed to the electrolyte was 15.9 cm^2 . A Pt-Rh mesh and the Saturated Calomel (SCE) were used as counter- and reference electrodes, respectively. The cell was filled with artificial sea water prepared according to the ASTM Standard D-1141/94 to a depth of 9 cm.

TABLE I
Coatings thickness / μm

Sample	thickness	Sample	thickness	Sample	thickness	Sample	thickness
P₁	30	S₁	30	PPh₁	30	SWP₁	30
P₃		S₃		PPh₃		SWP₂	
P₅		S₅		PPh₆		SWP₃	
P₇		S₇		PPh₈		SWP₅	
P₉				PPh₁₀		SWP₇	
P₂	80	S₂	80	PPh₂	80	SWP₄	80
P₄		S₄		PPh₄		SWP₆	
P₆		S₆		PPh₅		SWP₈	
P₈				PPh₇		SWP₁₀	
P₁₀				PPh₉			

All impedance spectra in the frequency range $10^{-3} \text{ Hz} \leq f \leq 3.10^5 \text{ Hz}$ were performed in the potentiostatic mode at the corrosion potential, as a function of the exposure time to the electrolyte solution, using the 1255 Solartron Frequency Response Analyzer and the 1286 Solartron Electrochemical Interface, the amplitude of the applied AC voltage was 10 mV peak to peak. Data processing was accomplished with a PC and a set of programs developed at the CIDEPINT [1] and by Boukamp [2].

EXPERIMENTAL RESULTS

Water uptake

Water absorption by an organic coating leads to changes in the film mechanical and electrical properties since, for example, reduces adhesion and/or cohesion forces as well as the electrical resistance. Many authors [3-5] have studied the water uptake process using impedance measurements, for evaluating the organic coating capacitance trend when immersed in an aqueous solution. The significance of such evaluation arises from the fact that this phenomenon is related to the corrosion protection properties, which can be determined from EIS data.

As the water permeates, the dielectric constant of the polymer changes and, therefore, the coating capacitance (C_1) does too. In this way, the coating capacitance evolution allows the water uptake evaluation using, for instance, an expression derived by Hartshorn, Megson and Rushton [6] and employed by Brasher [7] to obtain the following empirical equation:

$$X = \frac{\log C_1(t) / C_{1,0}}{\log 80}$$

where:

- X** volume fraction of water absorbed.
- $C_{1,0}$; $C_1(t)$** the organic coating capacitance measured just after immersion ($t=0$) and at any time t , respectively.
- $\log 80$** logarithm of the water dielectric constant or water permittivity at 25°C.

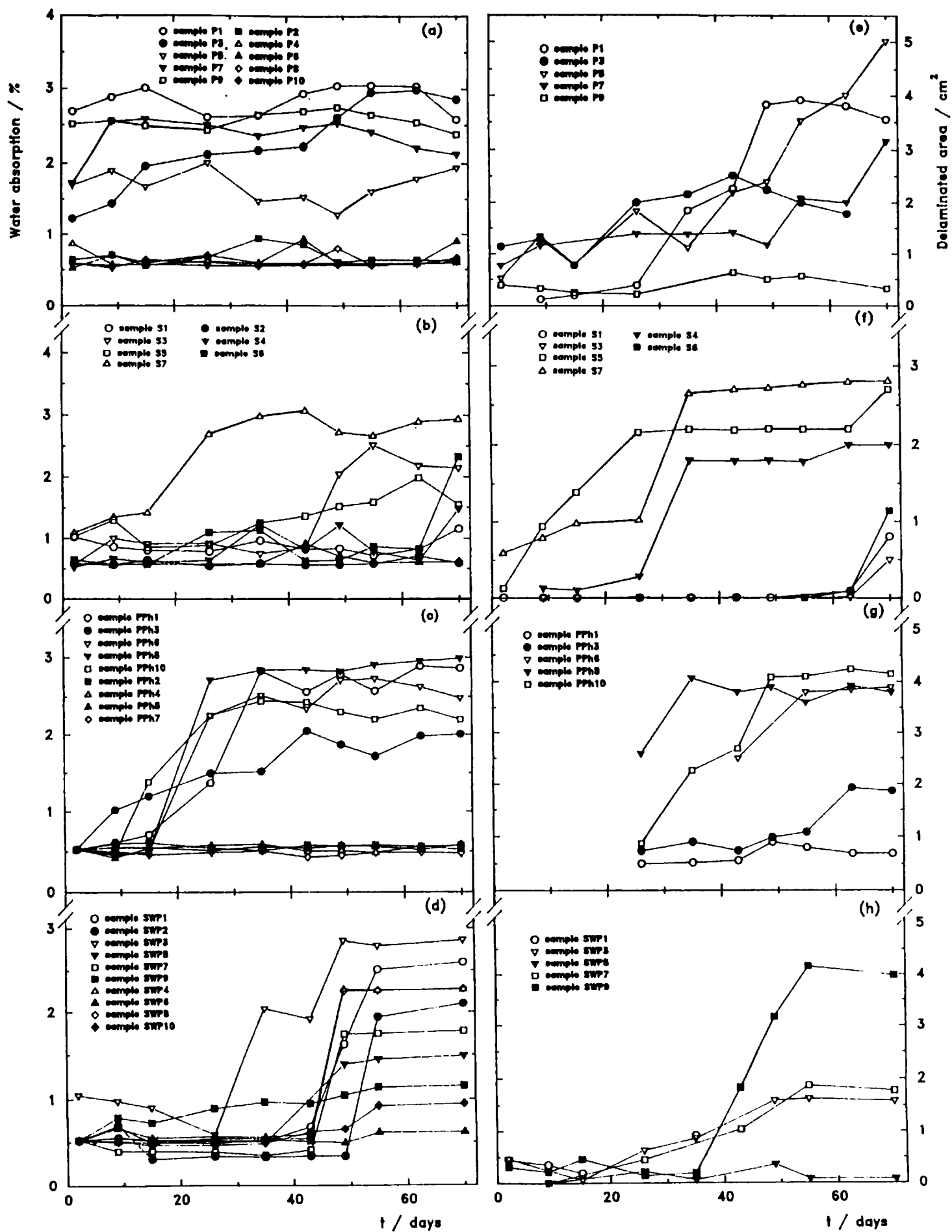


Fig. 1.- (a-d) Percentage of water absorption (%) and (e-h) Delaminated area vs. exposure time (t) for the carbon steel/chlorinated rubber/artificial sea water tested systems.

Fig.1a-d shows the water absorption of chlorinated rubber coatings of 30 μm and 80 μm in thickness deposited on steel sheets subjected to different surface preparation procedures and exposed to artificial sea water. From these data it was possible to obtain values of water uptake saturation ranging between 0.5-3%.

Corrosion potential

Fig.2a-d illustrates the corrosion potential (E_{corr}) changes measured in the coated steel sheets for 70 days of exposure. It is evident that, in general, the potential of the pickling (P), pickling + phosphated (PPh) and sandblasted + wash primer (SWP) samples, coated with the thicker (80 μm) paint films remained almost unvariable and close to 0 ± 0.1 V/SCE, while the potential corresponding to samples subjected to the same type of surface preparation but coated with a thinner (30 μm) chlorinated rubber film as well as all the sandblasted (S) samples exhibited values which either remained at or varied to the normal E_{corr} for unprotected steel under these experimental conditions of -0.6 ± 0.1 V/SCE, reflecting certain area of exposed metal; in essence, the more negative the measured potential becomes, the more susceptible to corrosion is the underlying steel surface.

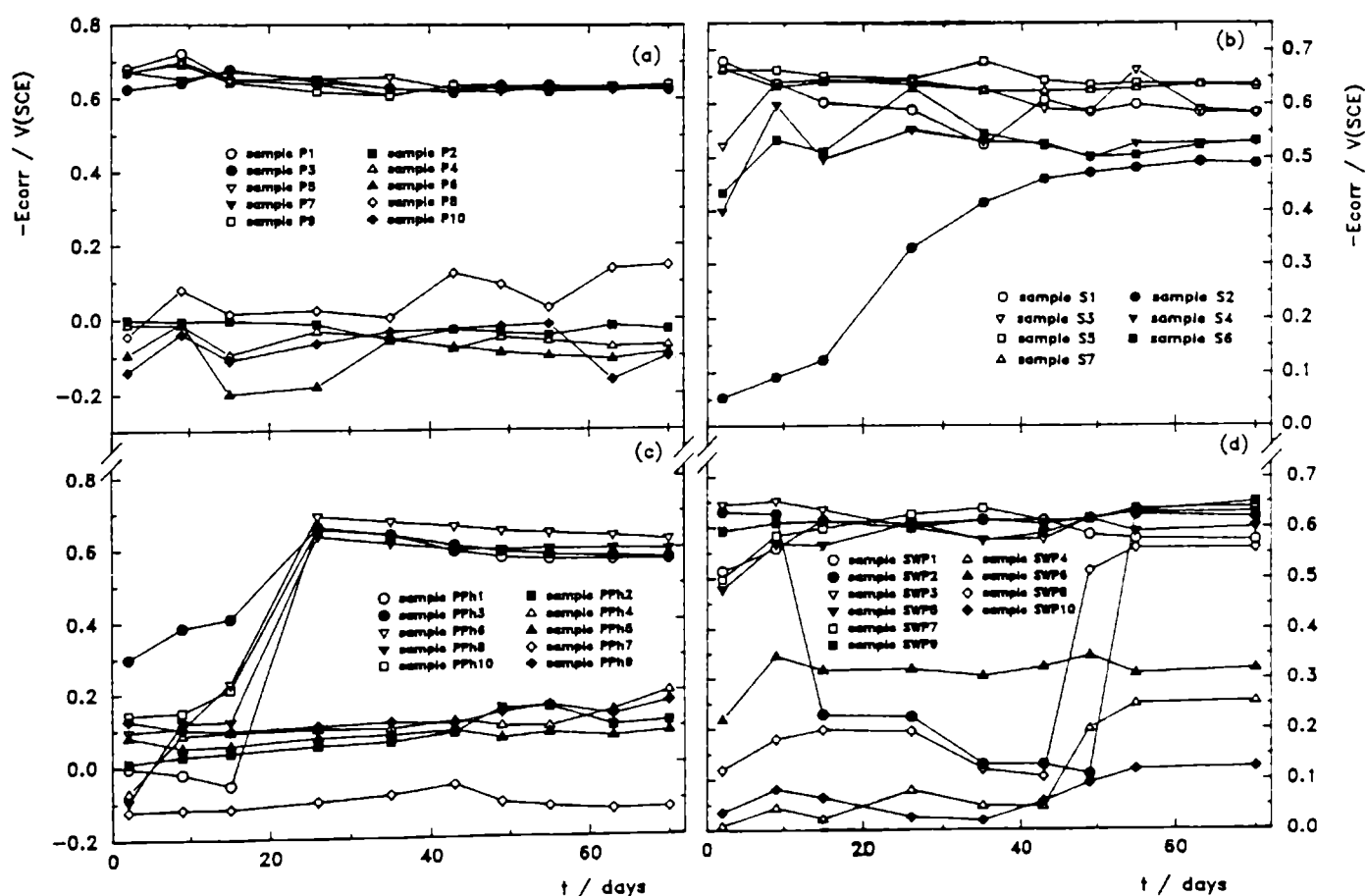


Fig. 2.- (a-d) Corrosion potential (E_{corr}) vs. exposure time (t) for the carbon steel/chlorinated rubber/artificial sea water tested systems.

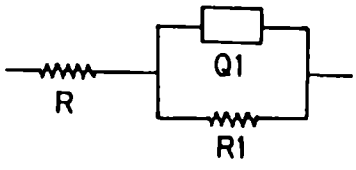
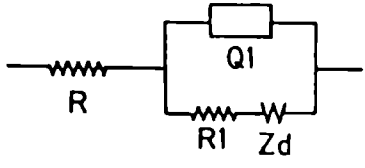
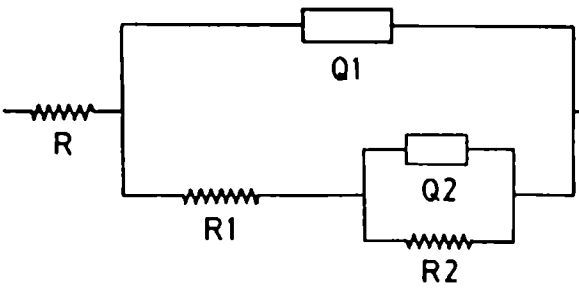
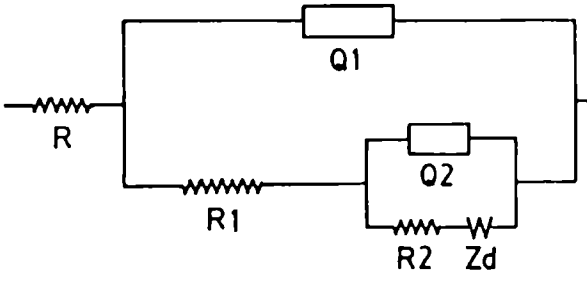
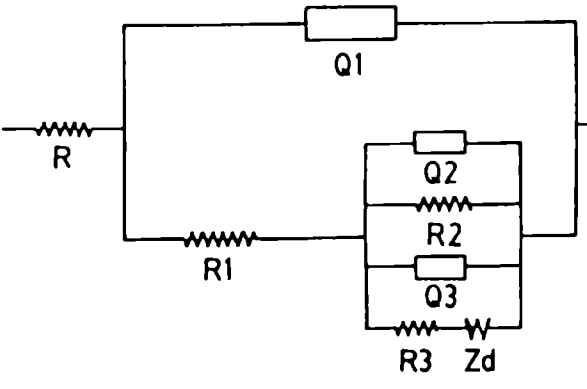
Equivalent circuit models

Impedance spectra provide important information related with both the organic coating deterioration evolution and the kinetics of the corrosion process suffered by the underlying steel substrate. The dynamic character of both the membrane conductivity and the corrosion products (basically rust) formation as well as the shifts in the disbonded area account for changes of the coated steel/electrolyte systems impedance spectra throughout the immersion time. In order to give a physical explanation of such changes as well as to obtain a more accurate and less consuming time curve fitting procedure of experimental impedance data, the equivalent circuit models shown in **Table II** had to be used. They represent the parallel and/or series connection of a number of resistors and capacitors, simulating a heterogeneous arrangement of electrolytically conducting paths. In addition, the numbers included in the rows of the table display the times that the corresponding equivalent circuit had to be used to obtain the best experimental data fitting. At the beginning of the exposure, there was no solution at the steel/paint interface, therefore, neither electrochemical double layer nor faradaic reaction occurred and the information coming from impedance data was associated with the organic coating properties. Thus, R represents the electrolyte resistance between the reference(SCE) and working (coated steel) electrodes, R_1 is the resistance to the ionic flux -describing paths of lower resistance to the electrolyte solution penetration shortcircuiting the organic coating- whose value is being usually used as a criterion of coating integrity, and $Q_1 \equiv C_1$ is the dielectric capacitance- whose value is associated with the membrane water uptake [8], **circuit A**. As the exposure time goes on, permeated corrodent species such as water, oxygen and ions increase the coating conductivity in such a way that not only the R_1 and C_1 but also a diffusional component Z_d - which was related to the relaxation of a mass transport process linked with the oxygen reduction reaction [9]- became measurable; the latter masking completely the initial corrosion attack taking presumably place at a highly localized steel area, **circuit B**. Then, once the permeating species reach more significant electrochemically active areas of the substrate, the corrosion process became to be measurable so that the electrochemical double layer ($Q_2 \equiv C_2$) and the charge transfer resistance R_2 -proper of the faradaic process- could be estimated, **circuit C**; in turn, this circuit could be connected with the diffusional component Z_d in series with R_1 , **circuit D**.

Sometimes, when the time constants (RC or RQ couples) corresponding to the anodic and cathodic reactions did not overlap, these components together with the diffusional one had to be used in order to get the best data fit, **circuit E**.

Distortions observed in the resistive-capacitive contributions indicate a deviation from the theoretical models in terms of a time constants distribution caused by either the lateral penetration of the electrolyte at the steel/chlorinated rubber paint interface (usually started at the base of the coating defects), underlying steel surface heterogeneities (topological, chemical composition, surface energy) and/or diffusional processes that could take place along the test [10, 11]. By fitting the transfer function associated to the most probable equivalent circuit, these factors were taken into consideration through the constant phase element Q_i ; however, difficulties in providing an accurate physical description of the occurred processes were sometimes found. In such cases, the standard deviation value of the fitting procedure was used as final criterion to define the most probable circuit.

TABLE II

Circuit	S	P	PPh	SWP
<p>(A)</p> 	27	45	62	50
<p>(B)</p> 	3	17	1	10
<p>(C)</p> 	22	5	19	15
<p>(D)</p> 	7	18	3	10
<p>(E)</p> 	16	7	5	6

Impedance results

The time dependent values of the equivalent circuit elements corresponding to the steel pretreated/chlorinated rubber paint/artificial sea water systems modeled by some of the impedance networks shown in **Table II**, are summarized in **Fig.3a-h**, **Fig.4a-h** and **Table III**.

The loss of the barrier protective properties, particularly faster in the thinner polymer films, caused that either decreasing or very low R_1 values were observed in the case of P, PPh and SWP as well as in almost all the S samples, **Fig.3a-d**. At initial times, most of the R_1 values for the thicker coatings were at or above $10^7 \Omega\text{cm}^2$, regardless of the pretreatment applied, while the corresponding values to the thinner ones were highly variable ranging between 10^3 and $10^8 \Omega\text{cm}^2$. As the test proceeded, however, except the R_1 of the thicker coatings applied on PPh samples which did not change, the ionic resistance decreased to a magnitude depending on the steel surface pretreatment; this being indicative of an increasing coating layer ionic conductivity, and presumably a lower protective capacity caused by the electrolyte penetration. For instance, **Fig.5** summarizes the time dependence of the coating resistance R_1 and capacitance Q_1 , the coated steel E_{corr} , charge transfer resistance R_2 and electrochemical double layer capacitance Q_2 , the membrane water absorption percentage and the delaminated area for the pickling + phosphated painted steel. Whether the metal substrate was coated with a thick or a thin paint film, R_1 started at a value of about $10^7 \Omega\text{cm}^2$, but in the latter case it dropped to $\approx 10^4 \Omega\text{cm}^2$ in 25 days of exposure; the Figure also shows that these changes correlate well with the E_{corr} displacement towards more active values as well as with the increase in the coating capacitance and the amount of water absorbed. Furthermore, it is interesting to denote that from the time the mentioned changes occurred, the R_2 and Q_2 values became to be calculable, indicating not only the presence of a significant corrosion process but also the end of an effective coating barrier protection and the point from which the delaminated corroding area A_d (**Fig.1e-h**) could be estimated by means of the following empirical equation:

$$A_d = \frac{Q_2(t)}{20}$$

where:

A_d delaminated area. (cm^2)

$Q_2(t)$ electrochemical double layer capacitance measured at any time t . (μF)

20 typical value of the bare steel double layer capacitance, adopted to estimate the underlying metallic active surface. (μFcm^{-2})

and its cyclic behaviour is typical for defective coatings with a permanent change of plugged and free pores [12-16].

With regard to the electrochemical parameters R_2 and Q_2 and the delaminated area evolution, **Fig.1-4** illustrate that once the barrier protection of the coating was lost, the E_{corr} reached (or remained at) a "plateaux" near to $-0.6 \pm 0.05 \text{ V/SCE}$ and R_1 stabilized between 10^3 - $10^4 \Omega\text{cm}^2$ but the changes in the electrochemical interface behaviour may be significant leading, in most cases, to highly delaminated (i.e. electrochemically active) areas and, therefore, underlying steel corrosion. Along the exposure test, the kinetics and magnitude of both the resistive and capacitive changes associated with the corrosion process taking place at

TABLE III

t / days	2	9	15	26	35	43	49	55	63	70
Sample S1										
$R_3 10^3 / \Omega \text{cm}^2$						3.29	13.70		0.28	0.36
$Q_3 10^3 / \text{Fcm}^{-2}$						0.79	2.68		3.22	1.30
$Z_4 10^3 / F$	1.90	3.19	5.14	13.60					156	
Sample S3										
$R_3 10^3 / \Omega \text{cm}^2$		0.74	6.15	3.13		1.55				0.08
$Q_3 10^3 / \text{Fcm}^{-2}$		3.46	3.82	8.29		13.40				17.20
$Z_4 10^3 / F$		2.07	5.07							20.70
Sample S4										
$R_3 10^3 / \Omega \text{cm}^2$				31.00					0.10	7.55
$Q_3 10^3 / \text{Fcm}^{-2}$				0.34					2.05	4.10
$Z_4 10^3 / F$							7.82			
Sample S5										
$R_3 10^3 / \Omega \text{cm}^2$	12.50					0.72	0.40			
$Q_3 10^3 / \text{Fcm}^{-2}$	5.22					24.30	3.52			
$Z_4 10^3 / F$					7.31			8.50		
Sample S6										
$R_3 10^3 / \Omega \text{cm}^2$						23.80				7.68
$Q_3 10^3 / \text{Fcm}^{-2}$						0.16				120
$Z_4 10^3 / F$				5.69						
Sample S7										
$R_3 10^3 / \Omega \text{cm}^2$				20.30		8.22		7.29		
$Q_3 10^3 / \text{Fcm}^{-2}$				1.35		3.17		2.59		
Z_4 / F										
Sample P1										
$R_3 10^3 / \Omega \text{cm}^2$			7.07					7.41		
$Q_3 10^3 / \text{Fcm}^{-2}$			15.60					7.55		
$Z_4 10^3 / F$	34.50						6.02			
Sample P3										
$R_3 10^3 / \Omega \text{cm}^2$	27.00	3.13	0.03	0.36	7.25	4.08	9.85		1.20	
$Q_3 10^3 / \text{Fcm}^{-2}$	0.20	2.51	5.59	5.78	6.79	16.8	14.9		9.18	
$Z_4 10^3 / F$					8.69			2.82		
Sample P5										
$R_3 10^3 / \Omega \text{cm}^2$			0.70	1.16	2.92					
$Q_3 10^3 / \text{Fcm}^{-2}$			3.94	2.66	1.17					
Sample P7										
$R_3 10^3 / \Omega \text{cm}^2$								3.70	1.53	
$Q_3 10^3 / \text{Fcm}^{-2}$								2.83	4.66	
$Z_4 10^3 / F$			2.12	4.30	8.05					
Sample P9										
$R_3 10^3 / \Omega \text{cm}^2$			696				462			9.06
$Q_3 10^3 / \text{Fcm}^{-2}$			8.17				47.6			40.1
$Z_4 10^3 / F$		23.8			1.93	0.22		7.95		2.03
Sample PPh1										
$R_3 10^3 / \Omega \text{cm}^2$									4.51	3.92
$Q_3 10^3 / \text{Fcm}^{-2}$									3.70	5.04
Sample PPh3										
$R_3 10^3 / \Omega \text{cm}^2$						1.43				1.21
$Q_3 10^3 / \text{Fcm}^{-2}$						2.43				1.58
$Z_4 10^3 / F$							3.65	3.10		
Sample PPh6										
$R_3 10^3 / \Omega \text{cm}^2$									3.70	
$Q_3 10^3 / \text{Fcm}^{-2}$									2.90	
$Z_4 10^3 / F$					9.93					
Sample PPh8										
$R_3 10^3 / \Omega \text{cm}^2$						3.22			9.15	
$Q_3 10^3 / \text{Fcm}^{-2}$						2.72			1.07	
Sample PPh10										
$R_3 10^3 / \Omega \text{cm}^2$						13.30				3.86
$Q_3 10^3 / \text{Fcm}^{-2}$						5.61				2.69
$Z_4 10^3 / F$				2.92						
Sample SWP1										
$Z_4 10^3 / F$						0.31	0.41	930		
Sample SWP3										
$R_3 10^3 / \Omega \text{cm}^2$			3.49		20.90		0.70			
$Q_3 10^3 / \text{Fcm}^{-2}$			0.84		1.51		3.62			
$Z_4 10^3 / F$						0.03		575		
Sample SWP5										
$Z_4 10^3 / F$		0.11	0.10		0.18	0.26	3190			
Sample SWP7										
$R_3 10^3 / \Omega \text{cm}^2$				1.00						
$Q_3 10^3 / \text{Fcm}^{-2}$				9.37						
$Z_4 10^3 / F$		0.11	0.17		0.16			7800		
Sample SWP9										
$R_3 10^3 / \Omega \text{cm}^2$		3.78			5.90					
$Q_3 10^3 / \text{Fcm}^{-2}$		4.08			12.30					
$Z_4 10^3 / F$			4.64							

the steel/chlorinated rubber paint interface showed a certain dependence on the substrate surface treatment. Thus, the R_2 and Q_2 values either fluctuated between 3-4 orders of magnitude or else stayed almost steady, showing a well differentiated dynamic of the delamination growth. These results, together with the sometimes appearing Q_3 and R_3 components linked in series with the diffusional Z_4 one -see **Tables II and III**- suggest the presence of a mixed diffusion and charge transfer controlled process; it was assumed that such components would be intimately related with the bad corrosion performance of the coated steel but, particularly, with the kinetics of the reaction/(s) occurring at the cathodic areas, mainly the oxygen diffusion through the film, its reduction reaction and/or the OH^- diffusion through the film defects. As in order to obtain further insights about the correct physical and electrochemical interpretation of such a circuit more investigations are currently in progress, no further explanations are intended here.

Comparatively, the experimental results arisen from the differently surface treated steel sheets/80 μm chlorinated rubber paint/artificial sea water systems showed that the P and PPh samples remained unchanged and displaying a high corrosion protection level throughout the test, with values of E_{corr} near to $0 \pm 0.1 \text{ V/SCE}$, $R_1 \geq 10^7 \Omega\text{cm}^2$, $Q_1 \leq 10^{-9} \text{ Fcm}^{-2}$, water absorption $\leq 1\%$ and of Q_2 and R_2 tending to zero and infinite, respectively. However, as can be seen in **Fig.1-4** the SWP samples, but mainly the S ones, did not provide a good protective performance. Therefore, under the current experimental conditions a ranking of the corrosion protection as a function of the different pretreatments leads to the following results: $\text{PPh} \geq \text{P} \geq \text{SWP} > \text{S}$ for thick chlorinated rubber films and $\text{PPh} > \text{P} > \text{S} \approx \text{SWP}$ for the thin ones.

DISCUSSION

Tests accomplished under free corrosion conditions showed the influence of both the paint coating barrier effect and the surface preparation procedure on the protective capacity. A large amount of diverse data has been gathered using an electrochemical technique, then fitted by means of mathematical algorithms arisen from electrical equivalent circuit models, and interpreted on the bases of their correlation with physicochemical processes occurred in pretreated steel/chlorinated rubber paint/artificial sea water systems.

Thus, examination of the experimental results, coming from such freely corroding systems and summarized in **Figs.1-4** and **Table III**, show that the extent of protection at any stage was much higher and stable when the thick polymer film was applied on P and PPh than on S and SWP samples. This was attributed to a good barrier protection provided by the paint film -which reduces enough the permeation of corrosion inducing chemicals such as water, oxygen and ions through the film to impede, if not eliminate, a continuous cathodic reaction-improved by the following mechanisms:

a) on surfaces cleaned by acid derusting (i.e. samples P), all the rust particles are removed causing not only an enhancement on the metal/coating adhesion but also the absence of a salt water soluble layer on the steel surface which will undoubtedly retard the formation of an electrolytic layer at the metal/coating interface (due to a reduced, if any, osmotic effect) during immersion; and

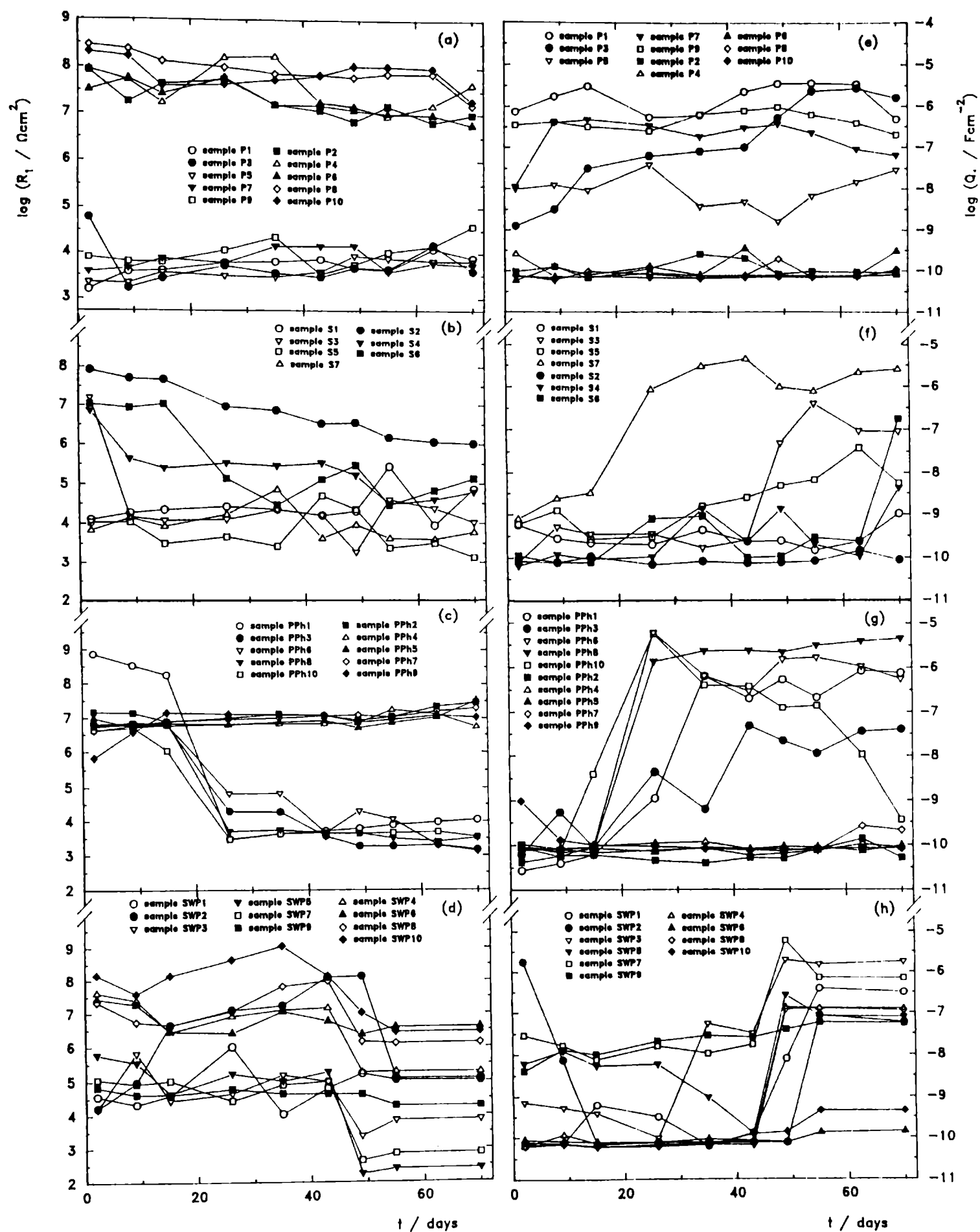


Fig. 3.- (a-d) Logarithm of the ionic resistance (R_i) and (e-h) of the dielectric capacitance (Q_1), corresponding to the applied chlorinated rubber paint coatings vs. exposure time (t) in artificial sea water.

b) on samples PPh, the phosphate coating forms complex metallic compounds with the steel substrate having good ability to resist corrosion [17]. This phosphated provides high surface roughness allowing to get stronger mechanical adhesion forces at the phosphated/paint interface and, therefore, also enhances the resistance to coating delamination.

In agreement with these mechanisms, it was assumed that the steel surface stayed effectively isolated from the electrolyte solution throughout the exposure time. Referring to the same type of steel sheets coated with thinner more defective paint films, the **Figures** also report: 1) a less significant difference among the samples behaviour and 2) all the electrical and electrochemical parameters evolution account for a more or less severe coating deterioration and corrosive attack whose kinetics was dependent on the type of surface preparation used and 3) the lost of corrosion protective properties through a series of physicochemical processes turned all these samples unsuitable for exposure conditions similar to the actual experimental ones. It is important to denote that samples PPh exhibited a delay time since for the first 20-25 days immersion neither corrosion nor disbonding could be detected, nevertheless, although, as occurred with the rest of the samples, once this process started it advanced at a rate which either increased with time or became zero, **Fig.1g**. Such a delay time was attributed to the above mentioned temporary corrosion resistant properties of the porous phosphated layer. The disbonding growth was probably due to the cathodic reaction process, which was mainly the oxygen reduction reaction forming hydroxyl ions that have been suggested to destroy the interfacial bond [18].

It is interesting to compare the water absorption values of the different samples in artificial sea water and the corrosion protection properties. Thus, the higher absorption values together with the anomalous polymer capacitance trend, strongly increased as the immersion time elapsed (**Fig.3e-h** and **Fig.1a-d** respectively), can be justified by assuming water penetration into the paint/treated steel interface; besides, these results correlate quite well with the trend of both the delaminated area (**Fig.1e-h**) and the E_{corr} of the coated steel (**Fig.2**) as well as with the chlorinated rubber coating film ionic resistance R_1 one as a function of the exposure time, **Fig.3**. Such a relationship can also be observed with the charge transfer resistance R_2 (associated with the underlying steel corrosion rate) and the double layer capacitance Q_2 contributions which vary inversely and directly, respectively, with the extent of the metallic active area, as can be seen in **Fig.4**. Furthermore, the substrate corrosion is accompanied by an activated transport of species through the organic coating film so that the electroneutrality condition can be performed. If the ionic current through the film is concentrated at this active area, it may be assumed that the R_1 value is influenced not only by the amount of water absorbed (**Fig.1 e-h**) -which diminishes the barrier energy in order that the mass transport process takes place-, and the amount of electrical charge developed into the no hydrophilic tested chlorinated rubber films -which makes they behave like a semipermeable membrane [19]- but also by the extent of the delaminated area.

Despite of some uncertainties which caused difficulties to interpret univocally the different combination of elements in the equivalent circuit models used for describing the dynamically changing impedance data corresponding to freely corroding coated steel interfaces, the agreement between the experimental evidence and the samples state observed during the periodic visual inspection, provided a figure of merit for the susceptibility of pretreated and coated steel surfaces to both corrode and delaminate.

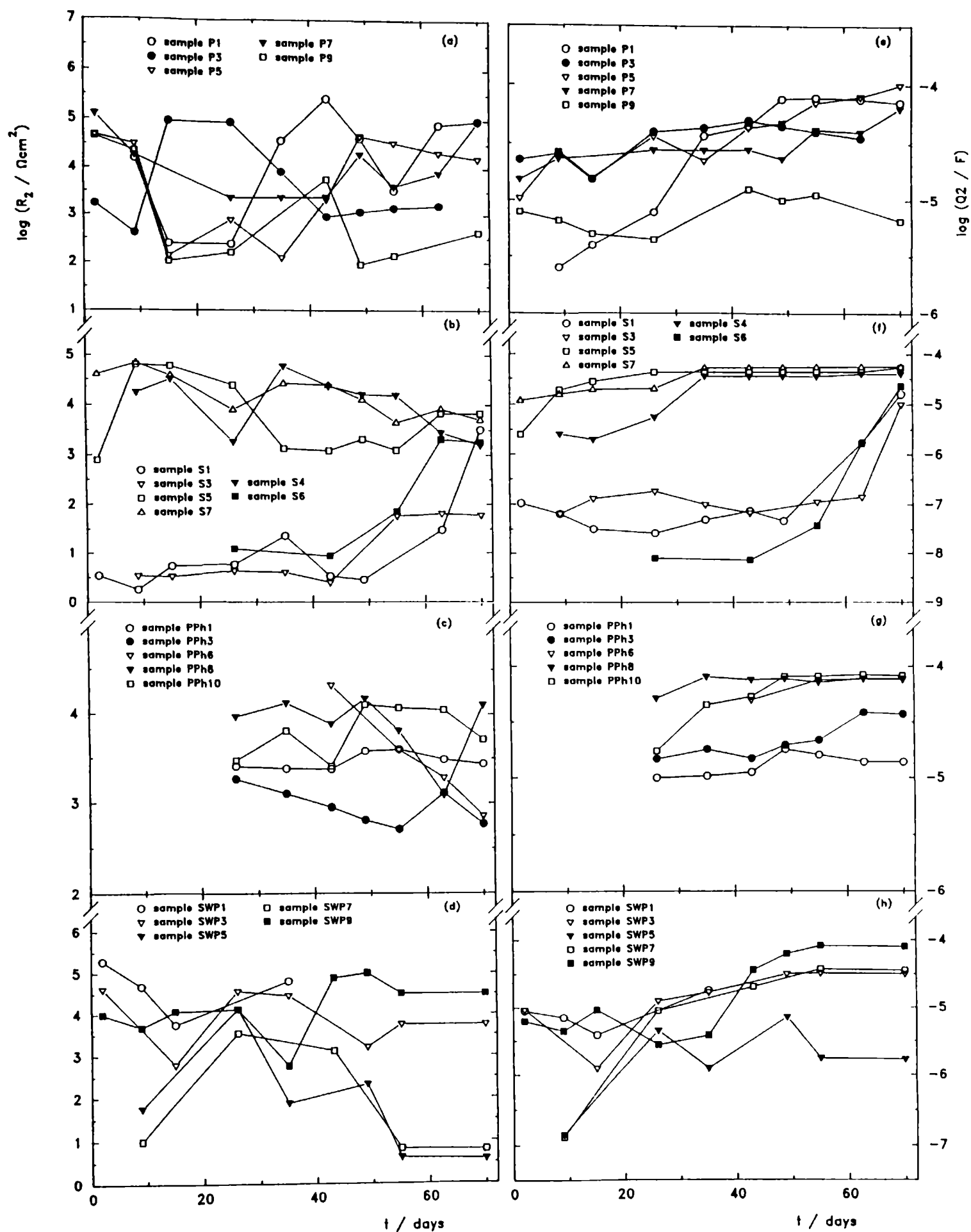


Fig. 4.- (a-d) Logarithm of the charge transfer resistance (R_2) and (e-h) of the double layer capacitance (Q_2) of the coated carbon steel sheets vs. exposure time (t) in artificial sea water.

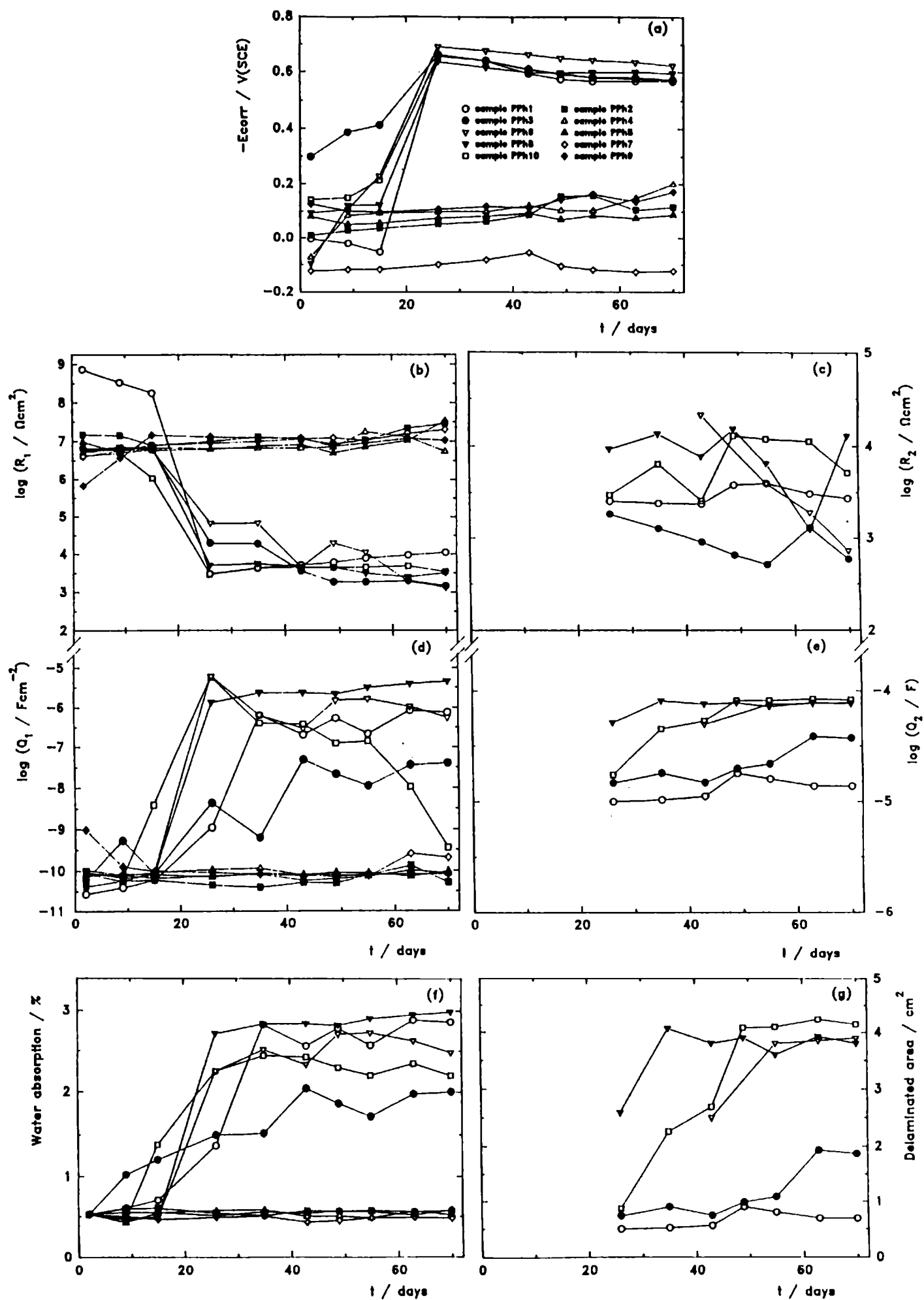


Fig. 5.- Time dependence of the different parameters characterising the pickling + phosphated painted steel/artificial sea water system performance.

CONCLUSIONS

The agreement between electrochemical and periodic visual inspection results demonstrated that the impedance measurements are sensitive enough to report changes introduced on the coated steel corrosion performance when different surface preparation techniques are used. Furthermore, it was also showed that interpretation of experimental data fitted using equivalent circuit models turned increasingly complicated as the dynamic changes in the physicochemical processes occurring at the coated metal/electrolyte solution interface did. Therefore, more efforts are being developed in order to obtain insights related not only with the kinetics parameters characterization but also with the intrinsic nature of such processes.

The corrosion behaviour of chlorinated rubber painted steel exposed to artificial sea water correlates well with the water absorption percentage, the delaminated area and the membrane ionic resistance performance. Among the surface preparation techniques tested, the best corrosion protection level was provided by pickling + phosphated painted steel surfaces followed by the pickling ones. By comparing these results with those corresponding to the sanblasted and sandblasted + wash primer samples, it was concluded that not only if a stable, corrosion resistant and adhesion enhancing layer forms on but also when a free of rust treated steel surface is obtained, the metallic structure useful life can be highly lengthened when a permselective and thick enough to provide significant barrier protection organic coating film is applied, at least, under exposure conditions including aqueous solutions containing high chloride concentrations.

ACKNOWLEDGEMENTS

The authors gratefully acknowledge the Comisión de Investigaciones Científicas de la Provincia de Buenos Aires and the Consejo Nacional de Investigaciones Científicas y Técnicas (CONICET) for their financial support to this research work.

REFERENCES

- [1] V.M. Ambrosi and A.R. Di Sarli.- **Anti-Corrosion**, October, 9 (1993).
- [2] B.A. Boukamp.- Report CT88/265/128, CT89/214/128, University of Twente, The Netherlands, 1989.
- [3] G.W. Walter.- **Corros. Sci.**, **32**, 1059 (1991).
- [4] H. Leidheiser, Jr.- **J. Coat. Technol.**, **63**, 21 (1991).
- [5] P.R. Seré, D.M. Santágata, C.I. Elsner and A.R. Di Sarli.- **Surf. Coat. International**. In press
- [6] L. Hartshorn, N.J.L. Megson and E. Rushton.- **J. Soc. Chem. Ind.**, **56**, 266T (1937).

- [7] D.M. Brasher and A.H. Kingsbury.- **J. Appl. Chem.**, **4**(2), 62 (1954).
- [8] H. Leidheiser, Jr. and M.W. Kendig.- **Corrosion**, **32**, 69 (1976).
- [9] R.A. Armas, S.G. Real, C. Gervasi, A.R. Di Sarli and J.R. Vilche.- **Corrosion**, **48**, 379 (1992).
- [10] T. Szauer and A. Brandt.- **J. Oil Col. Chem. Assoc.**, **67**, 13 (1984).
- [11] D.J. Frydrych, G.C. Farrington and H.E. Townsend.- **Corros. Protection by Organic Coatings** (ed. M.W. Kendig & H. Leidheiser, Jr.), vol. 87-2, p.240. The Electrochem. Soc., Pennington, NJ, (1987).
- [12] G.W. Walter.- **J. Electroanal. Chem.**, **118**, 259 (1981).
- [13] N. Pébere, T. Picoud, M. Duprat and F. Dabosi.- **Corros. Sci.**, **29**, 1073 (1989).
- [14] J. Titz, G.H. Wagner, H. Spähn, M. Ebert, K. Jüttner and W.J. Lorenz.- **Corrosion**, **46**, 221 (1990).
- [15] G. Reinhard and U. Rammelt.- **Plaste Kautsch**, **31**, 312 (1984).
- [16] J.C. Rowlands and D.J. Chute.- **Corros. Sci.**, **23**, 331 (1983).
- [17] ASM Handbook, *Corrosion*, vol.13, ed. ASM International, 1992.
- [18] H. Leidheiser, Jr.- **Prog. Org. Coatings**, **7**, 79 (1979).
- [19] D.Y. Perera and P.M. Heertjes.- **J. Oil Col. Chem. Assoc.**, **54**, 313 (1971); Ibid. **54**, 395 (1971); Ibid. **54**, 546 (1971); Ibid. **54**, 774 (1971).

ANEXO

**PUBLICACIONES CIENTIFICAS Y TECNICAS
REALIZADAS POR EL CIDEPINT
(Período 1990-1996)**

*SCIENTIFIC AND TECHNICAL PAPERS
PUBLISHED BY CIDEPINT
(Period 1990-1996)*

AÑO 1990

1. *Relación entre la fijación de micro y macro "fouling" y los procesos de corrosión de estructuras metálicas.*
M. Stupak, M. Pérez, A.R. Di Sarli.
Revista Iberoamericana de Corrosión y Protección, **21** (6), 219-225 (1990).
2. *Influence of micaceous iron oxide pigmentation on the protective capacity of sealants.*
B. del Amo, A.R. Di Sarli, C. Gervasi.
Corrosion Prevention and Control, **37** (6), 145-151 (1990).
3. *Evaluating antifouling paints.*
B. del Amo, C.A. Giúdice, G. Villoria.
European Coatings Journal, (1), 8-14 (1990).
4. *Viscosity adjustment in high build antifouling paints.*
B. del Amo, C.A. Giúdice.
Pitture e Vernici, **66** (5), 22-27 (1990).
5. *Evaluation of anticorrosive paint binders by means of AC techniques. Influence of chemical composition.*
A.R. Di Sarli, E. Schwiderke, J.J. Podestá.
Journal of the Oil and Colour Chemists' Association, **73** (1), 18-23 (1990).
6. *Potentiometric behaviour of the copper electrode in aqueous copper (II) perchlorate solutions containing sodium chloride.*
R. Romagnoli, V.F. Vetere.
Analytica Chimica Acta, **234**, 331-338 (1990).
7. *Regression against temperature of gas-chromatographic retention data.*
R.C. Castells, E.L. Arancibia, A.M. Nardillo.
Journal of Chromatography, **504**, 45-53 (1990).
8. *Contribution of alkalies by aggregates to alkali aggregate reaction in concrete.*
R.O. Batic, J.D. Sota, R. Iasi.
Petrography applied to concrete and concrete aggregates. ASTM-STP 1061. Bernard Erlin and David Stark, Editors, ASTM, Philadelphia, mayo 1990.
9. *High-build soluble matrix antifouling paints tested on raft and ship's bottom.*
V. Rascio, C.A. Giúdice, B. del Amo.
Progress in Organic Coatings, **18** (4), 389-398 (1990).
10. *Binders for self-polishing antifouling paints.*
J.C. Benítez, C.A. Giúdice, V. Rascio.
European Coatings Journal, (11), 618-631 (1990).

11. *Thermodynamics of hydrocarbon solutions using GLC.*
R.C. Castells, E.L. Arancibia, A.M. Nardillo, C.B. Castells.
Journal of Chemical Thermodynamics, **22**, 269-277 (1990).

AÑO 1991

12. *Influence of some variables on behaviour of zinc-rich paints based on ethyl silicate and epoxy binders.*
B. del Amo, C.A. Giúdice.
American Paint and Coatings Journal, **76** (11), 36-43 (1991).
13. *Formulation and elaboration of vinyl sealers pigmented with micaceous iron oxide.*
C.A. Giúdice.
American Paint and Coatings Journal, **75** (55), 36-46 (1991).
14. *Dispersion of cuprous oxide in soluble matrix antifouling paints. Rheology and efficiency.*
C.A. Giúdice.
Pitture e Vernici, **67** (1), 5-13 (1991).
15. *Study of complexation equilibrium employing polarized metallic electrodes.*
V.F. Vetere, R. Romagnoli.
The Analyst, **116**, 937-940 (1991).
16. *Influence of binder composition on the behaviour of self-polishing antifouling paints.*
J.C. Benítez, C.A. Giúdice.
Pitture e Vernici, **67** (9), 9-20 (1991).
17. *Analysis of the influence of plasticizer on the degradation of metal/chlorinated rubber/seawater systems.*
A.R. Di Sarli.
Corrosion Prevention and Control, **38** (4), 96-100 (1991).
18. *Flame retardant paints (I).*
C.A. Giúdice, B. del Amo.
European Coatings Journal, (11), 740-755 (1991).
19. *Analysis of isomeric cresols by gas chromatography.*
A.M. Nardillo, R.C. Castells, C.B. Castells.
Chromatographia, **32**, 457-460 (1991).

AÑO 1992

20. *Anticorrosive protection by zinc-ethyl silicate paints. A review.*
R. Romagnoli, V.F. Vetere.
Corrosion Reviews, **10** (3-4), 337-366 (1992).

21. *High efficiency antifouling paints.*
C.A. Giúdice.
European Coatings Journal, (3), 88-98 (1992).
22. *Fire retardant paints.*
C.A. Giúdice.
European Coatings Journal (5), 248-258 (1992).
23. *Flame retardant paints. II.*
C.A. Giúdice, B. del Amo.
European Coatings Journal, (1-2), 8-14 (1992).
24. *Thermodynamics of tetra-n-octyltin + hydrocarbon systems by liquid chromatography.*
R.C. Castells, C.B. Castells.
Journal of Solution Chemistry, **21**, 129-146 (1992).
25. *Zinc rich paints on steels in artificial sea water by electrochemical impedance spectroscopy.*
R.A. Armas, C. Gervasi, A.R. Di Sarli, S.G. Real, J.R. Vilche.
Corrosion, **48**, 379-383 (1992).
26. *An impedance spectroscopy study of anodized aluminium and aluminium-manganese substrates.*
C.A. Gervasi, J.R. Vilche.
Electrochimica Acta, **37**, 1389-1394 (1992).
27. *Coatings in Argentina: Present and future.*
C.A. Giúdice.
European Coatings Journal, (6), 377-384 (1992).
28. *Thermodynamics of tri-n-octyltin chloride + hydrocarbon mixtures by gas-liquid chromatography.*
R.C. Castells, C.B. Castells.
Journal of Solution Chemistry, **21**, 1081 (1992).
29. *Characterization of anodically formed porous and barrier oxide layers on aluminium using electrochemical impedance.*
R.C. Rocha-Filho, C. Gervasi, S.G. Real, J.R. Vilche.
Journal of the Brazilian Chemical Society, **3** (3), 120-123 (1992).
30. *Tratamiento de aguas industriales en la década del 90. Uso del ozono para el control de la biocorrosión y del biofouling. Preservación del medio ambiente.*
M. Viera, H.A. Videla.
Revista Iberoamericana de Corrosión y Protección, **23** (3-4), 66-70 (1992).
31. *Influence of coating thickness on the barrier effect of marine paints' binders. An assessment using impedance measurements.*
A.R. Di Sarli, C.I. Elsner.
Journal of Coating Technology and Biotechnology, **55** (3), 285-292 (1992).

32. *Resistant lamellar micaceous iron oxides.*
C.A. Giúdice.
European Coatings Journal, (3), 134-144 (1993).
33. *Heavy duty offshore protection.*
C.A. Giúdice.
European Coatings Journal, (5), 344-354 (1993).
34. *Binders for marine paints.*
A.R. Di Sarli.
European Coatings Journal, (4), 252-258 (1993).
35. *Electrochemical testing of anticorrosion systems.*
A.R. Di Sarli.
European Coatings Journal, (10), 706-712 (1993).
36. *An electrochemical impedance spectroscopy study of zinc rich paints on steels in artificial sea water by a transmission line model.*
S.G. Real, A.C. Elías, J.R. Vilche, C.A. Gervasi, A.R. Di Sarli.
Electrochimica Acta, **38**, 2029-2035 (1993).
37. *The use of electrochemical impedance measurements to assess the performance of organic coating systems on naval steel.*
E. Cavalcanti, O. Ferraz, A.R. Di Sarli.
Progress in Organic Coatings, **23**, 183-198 (1993).
38. *Evaporation of the liquid phase during drying of oleoresinous emulsion binders.*
J.J. Caprari, O. Slutzky, P. Pessi.
Pitture e Vernici, **69** (9). 17-20 (1993).
39. *A phenomenological approach to ionic mass transfer at rotating disc electrodes with a hanging column of electrolyte solutions.*
C.I. Elsner, P.P. Schilardi, S.L. Marchiano.
Journal of Applied Electrochemistry, **23**, 1181-1186 (1993).
40. *Kinetics of the electroreduction of anodically formed cadmium oxide layers in alkaline solutions.*
J.I. de Urraza, C.A. Gervasi, S.B. Saidman, J.R. Vilche.
Journal of Applied Electrochemistry, **23**, 1207-1213 (1993).
41. *The mechanism of the anti-corrosive action of zinc ethyl silicate paints.*
R. Romagnoli, V.F. Vetere.
Journal of the Oil and Colour Chemists' Association, **76**, 208-213 (1993).
42. *Halomethanes in tri-n-octyllamine and squalane mixtures at infinite dilution.*
R.C. Castells, E.L. Arancibia, A.M. Nardillo.
Journal of Solution Chemistry, **22**, 85-94 (1993).

43. *Use of EIS to characterize the performance of naval steel/organic coating systems in NaCl solution.*
A.R. Di Sarli, E. Cavalcanti, O. Ferraz.
Corrosion Prevention and Control, **40** (3), 66-70 (1993).
44. *Development of a mathematical treatment for electrochemical impedance data obtained from coated metals: Part 2.*
V. Ambrosi, A. Di Sarli.
Anti-Corrosion, October, 9-13 (1993).
45. *Binder dissolution in antifouling.*
C.A. Giúdice, D.B. del Amo.
European Coatings Journal, (1-2), 16-23 (1993).

AÑO 1994

46. *Zinc hydroxy phosphite for corrosion protection.*
C.A. Giúdice, D.B. del Amo.
European Coatings Journal, (7-8), 490-496 (1994).
47. *The role of calcium acid phosphate as a corrosion inhibitive pigment.*
V.F. Vetere, R. Romagnoli.
British Corrosion Journal, **29** (2), 115-119 (1994).
48. *Adhesion of lamellar iron oxide vinyl paints.*
C.A. Giúdice, B. del Amo.
European Coatings Journal, (5), 292-299 (1994).
49. *Pulsating diffusional boundary layers. III. A redox electrochemical reaction under intermediate kinetics control involving soluble species in solution. Theory and experimental test.*
C.I. Elsner, L. Rebollo Neira, W.A. Egli, S.L. Marchiano, A. Plastino, A.J. Arvía.
Acta Chimica Hungarica - Models in Chemistry, **131** (2), 121 (1994).
50. *The influence of cathodic currents on biofouling attachment to painted metals.*
M. Pérez, C.A. Gervasi, R. Armas, M.E. Stupak, A.R. Di Sarli.
Biofouling, **8**, 27-34 (1994).
51. *Evaluation of electrical and electrochemical parameters for painted steel/artificial sea water systems by using EIS.*
V. Ambrosi, A.R. Di Sarli.
Bulletin of Electrochemistry, **10** (2-3), 91-95 (1994).
52. *The excess enthalpies of (dinitrogen oxide + toluene) at the temperature 313.15 K and at pressures from 7.60 MPa to 15.00 MPa.*
R.C. Castells, C. Menduina, C. Pando, J.A.R. Renuncio.
Journal of Chemical Thermodynamics, **26**, 641 (1994).

53. *Fireproof pigments in flame retardant paints.*
B. del Amo, C.A. Giúdice.
European Coatings Journal, (11), 826-832 (1994).
54. *Heterogeneous reaction between steel and zinc phosphate.*
R. Romagnoli, V.F. Vetere.
Corrosion (NACE), **51**, 116-122 (1994).
55. *Influence of the composition of zinc-ethyl silicate paints.*
R. Romagnoli, V.F. Vetere, R.A. Armas.
Journal of Applied Electrochemistry, **24**, 1013-1018 (1994).
56. *Rheology of pigment dispersion during paint manufacture.*
C.A. Giúdice, J.C. Benítez.
Pitture e Vernici, **11**, 33-36 (1994).
57. *Comparison between electrochemical impedance and salt spray tests in evaluating the barrier effect of epoxy paints.*
C.I. Elsner, A.R. Di Sarli.
Journal of the Brazilian Chemical Society, **51**, 15-18 (1994).
58. *Corrosion protection of steel in artificial sea water using zinc rich alkyd paints. An assessment of the pigment-content effect by EIS.*
C.A. Gervasi, A.R. Di Sarli, E. Cavalcanti, O. Ferraz, E.C. Bucharsky, S.G. Real, J.R. Vilche.
Corrosion Science, **36**, 1963-1972 (1994).
59. *Elektrochemische und in situ Rastertunnelmikroskopische Untersuchungen in den systemen HOPG(0001)/Ag⁺.*
G.A. Gervasi, R.T. Pötzschke, G. Staikov, V.J. Lorenz.
Wiss. Abschlussber. Int. Sem. Univ. Karlsruhe, **29**, 34-46 (1994).
60. *Combined action of oxidizing biocides for controlling biofilms and MIC.*
H.A. Videla, M.R. Viera, P.S. Guimmet.
Corrosion/94, paper N° 260 (1994).
61. *Corrosión en la Industria Naval. Guía Práctica de la Corrosión.*
V. Rascio.
CYTED - Programa Iberoamericano de Ciencia y Tecnología para el Desarrollo. 32 pp (1994).
62. *Excess molar enthalpies of nitrous oxide-toluene in the liquid and supercritical regions.*
R.C. Castells, C. Meduina, C. Pando, J.A.R. Renuncio.
J. Chem. Soc. Faraday Trans., **90**, 2677-2681 (1994).
63. *Pinturas antiincrustantes vinílicas tipo alto espesor basadas en resina colofonia desproporcionada.*
J.C. Benítez, C.A. Giúdice.
Rivista di Merceologia, **33** (I), 1-15 (1994).

AÑO 1995

64. *Evaluation of zinc rich paint performance by electrochemical impedance spectroscopy.*
E.C. Bucharsky, S.G. Real, J.R. Vilche, A.R. Di Sarli, C.A. Gervasi.
Journal of the Brazilian Chemical Society, **6** (1), 39-42 (1995).
65. *The characterization of protective properties for some naval steel/polymeric coatings/3% NaCl solution systems by EIS and visual assessment.*
O. Ferraz, E. Cavalcanti, A.R. Di Sarli.
Corrosion Science, **38** (8), 1267-1289 (1995).
66. *Electrochemical evaluation of the oxygen permeability for anticorrosive coating films.*
C.I. Elsner, R.A. Armas, A.R. Di Sarli.
Portugaliæ Electrochimica Acta, **13**, 5-18 (1995).
67. *Corrosion monitoring of ZRP on steel by EIS to evaluate the performance of different coating formulation.*
C.A. Gervasi, R. Armas, A.R. Di Sarli, E.C. Bucharsky, S.G. Real, J.R. Vilche.
Materials Science Forum, **192-194**, 357-362 (1995).
68. *Non-pollutant inhibitive pigments: Zinc phosphate and modified zinc phosphate. A review.*
R. Romagnoli, V.F. Vetere.
Corrosion Reviews, **13** (1), 45-64 (1995).
69. *Coatings for corrosion prevention of seawater structures.*
C.A. Giúdice, J.C. Benítez.
Corrosion Reviews, **13** (2-4), 81-190 (1995).
70. *Study of the heterogeneous reaction between steel and zinc phosphate.*
R. Romagnoli, V.F. Vetere.
Corrosion (NACE), **51** (2), 116-122 (1995).
71. *Infinite dilution activity coefficients of hydrocarbons in tetra-n-alkyltin solvents between 313.15 K measured by gas-liquid chromatography.*
R.C. Castells, C.B. Castells.
Journal of Solution Chemistry, **24**, 285 (1995).
72. *Excess enthalpies of nitrous oxide + pentane at 308.15 K from 6.64 to 12.27 MPa.*
J.A.R. Renuncio, C. Pando, C. Mendiña, R.C. Castells.
Journal of Chemical Engineering Data, **40**, 642 (1995).
73. *Thermodynamic consideration of the retention mechanism in a poly(perfluoroalkyl ether) gas chromatographic stationary phase used in packed columns.*
R.C. Castells, L.M. Romero, A.M. Nardillo.
Journal of Chromatography, **715**, 299 (1995).

74. *Separation of low-boiling pyridine bases by gas chromatography.*
M.C. Titón, A.M. Nardillo.
Journal of Chromatography, **699**, 403-407 (1995).
75. *Electrochemical characterization of anodic passive layers on cobalt.*
E.B. Castro, C.A. Gervasi, J.R. Vilche, C.P. Fonseca.
Journal of the Brazilian Chemical Society, **6** (1), 43-47 (1995).

AÑO 1996

76. *Semicontinuous emulsion polymerization of methyl methacrylate, ethyl acrylate, and methacrylic acid.*
J.I. Amalvy.
Journal of Applied Polymer Science, **59**, 339-344 (1996).
77. *High build antifouling paints based on disproportionated calcium resinate.*
C.A. Giúdice, J.C. Benítez.
Corrosion Reviews, "Special Issue on Industrial Paints for Corrosion Control", **14** (1-2), 1-14 (1996).
78. *Anticorrosive paints with flame retardant properties.*
C.A. Giúdice, B. del Amo.
Corrosion Reviews, "Special Issue on Industrial Paints for Corrosion Control", **14** (1-2), 35-46 (1996).
79. *Influence of the hydrolysis degree of the binder on the electrochemical properties of zinc-ethyl silicate paints.*
R. Romagnoli, C.A. Aznar, V.F. Vetere.
Corrosion Reviews, "Special Issue on Industrial Paints for Corrosion Control", **14** (1-2), 59-71 (1996).
80. *Macrofouling community at Mar del Plata harbor along a year (1991-1992).*
Pezzani, M. Pérez, M. Stupak.
Corrosion Reviews, "Special Issue on Industrial Paints for Corrosion Control", **14** (1-2), 73-86 (1996).
81. *Study of commercially available epoxy protective coatings by using non-destructive electrochemical techniques.*
P.R. Seré, D.M. Santágata, A.R. Di Sarli, C.I. Elsner.
Corrosion Reviews, "Special Issue on Industrial Paints for Corrosion Control", **14** (1-2), 87-97 (1996).
82. *Application of powder coatings. A bibliographic review to obtain a calculation system for the design of a conventional fluidized bed.*
J.J. Caprari, A.J. Damia, M.P. Damia, O. Slutzky.
Corrosion Reviews, "Special Issue on Industrial Paints for Corrosion Control", **14** (1-2), 99-120 (1996).

83. *Study of the anticorrosive properties of micronized zinc phosphate and zinc molybdophosphate in alkydic paints.*
B. del Amo, R. Romagnoli, V.F. Vetere.
Corrosion Reviews, "Special Issue on Industrial Paints for Corrosion Control", **14** (1-2), 121-133 (1996).
84. *Effect of the cathodic protection on coated steel/artificial sea water systems.*
D.M. Santágata, C. Morzilli, C.I. Elsner, A.R. Di Sarli.
Corrosion Reviews, "Special Issue on Industrial Paints for Corrosion Control", **14** (1-2), 135-144 (1996).
85. *Preliminary study of the biofouling of the Parana river (Argentina).*
M. Stupak, M.C. Pérez, M.T. García, E. García Solá, A. Leiva Azuaga, A. Mendivil, G. Niveyro.
Corrosion Reviews, "Special Issue on Industrial Paints for Corrosion Control", **14** (1-2), 145-155 (1996).
86. *The surface condition effect on adhesion and corrosion resistance of carbon steel/chlorinated rubber/artificial sea water systems.*
P.R. Seré, A.R. Armas, C.I. Elsner, A.R. Di Sarli.
Corrosion Science, **38** (6), 853-866 (1996).
87. *Influence of aluminium pretreatment on coating adhesion.*
C. Giúdice, B. del Amo, M. Morcillo Linares.
Corrosion Prevention and Control, **43** (1), 15-20 (1996).
88. *Coating systems for underwater protection.*
C. Giúdice, B. del Amo.
Corrosion Prevention and Control, **43** (2), 43-47 (1996).
89. *Gas chromatographic measurement of the activity coefficients of hydrocarbons at infinite dilution in di-n-octyltin dichloride. Comparison of results obtained in other alkyltin solvents.*
A.M. Nardillo, B.M. Soria, C.B. Castells, R.C. Castells.
Journal of Solution Chemistry, **25**, 369 (1996).
90. *Gas chromatographic separation of low-boiling pyridine bases.*
M.C. Titon, F.R. González, A.M. Nardillo.
Chromatographia, **42**, 465 (1996).
91. *Thermodynamics of solutions of hydrocarbons in low molecular weight poly(isobutylene): a gas chromatographic study.*
R.C. Castells, L.M. Romero, A.M. Nardillo.
Macromolecules, **29**, 4278 (1996).
92. *Vibrational spectroscopic study of distribution of sodium dodecyl sulfate in latex films.*
J.I. Amalvy and D.B. Soria.
Progress in Organic Coatings, **28**, 279-283 (1996).

AÑO 1990

1. *High build antifouling paints based on calcium resinate.*
C.A. Giúdice, V. Rascio.
Proc. 11th International Corrosion Congress, Vol. 2, 335-345 (1990).

AÑO 1991

2. *Research and development of antifouling paints.*
C.A. Giúdice.
Anales de la "Giornata di Studio", 31º Salone Nautico Internazionale, Génova (Italia), 1-14 (1991).
3. *Anticorrosive and antifouling protection in seawater.*
C.A. Giúdice.
Anales del Workshop "Corrosione e Protezione di Materiali Metallici in Mare", Istituto Sperimentale Talossografico/Centro Sviluppo Materiali, Taranto (Italia), junio (1991).

AÑO 1992

4. *Influencia de la dureza del material a tratar en el resultado de las operaciones de limpieza con chorro de abrasivos.*
J.J. Caprari, O. Slutzky, P.L. Pessi, C. Lasquibar.
Anales 4º Congreso Iberoamericano de Corrosión y Protección, 2, 555-567 (1992).
5. *Pinturas antiincrustantes tipo matriz soluble basadas en resina colofonia desproporcionada.*
C.A. Giúdice, J.C. Benítez.
Anales 4º Congreso Iberoamericano de Corrosión y Protección, 2, 653-667 (1992).
6. *Inhibidores de corrosión en fase acuosa para utilizar en operaciones de hidroarenado.*
J.J. Caprari, O. Slutzky, M.J. Chiesa, R.D. Ingeniero.
Anales 4º Congreso Iberoamericano de Corrosión y Protección, 2, 761-776 (1992).
7. *Characterization of the atmospheric corrosion products formed on low carbon steel, aluminium, copper, and zinc specimens.*
S.L. Granese, E.S. Ayllón, B.M. Rosales, F.E. Varela, C.A. Gervasi, J.R. Vilche.
Proceedings 1st Pan American Corrosion and Protection Congress, 1, 191-210 (1992).
8. *Zinc rich paint coatings characterization on naval steel by electrochemical impedance spectroscopy.*
A.C. Elías, S.G. Real, J.R. Vilche, R.A. Armas, C.A. Gervasi, A.R. Di Sarli.
Proceedings 1st Pan American Corrosion and Protection Congress, 2, 529-540 (1992).

AÑO 1993

9. *Algunas variables que influyen sobre la concentración crítica de pigmento en volumen (CPVC) de una pintura anticorrosiva.*
J.C. Benítez, C.A. Giúdice.
Anales de las II Jornadas Argentinas en Ciencia de los Materiales, I, 53-56 (1993).
10. *Reología en pinturas. Esfuerzo de corte involucrado en el fenómeno de escurrimiento.*
B. del Amo, J.C. Benítez.
Anales de las II Jornadas Argentinas en Ciencia de los Materiales, I, 57-60 (1993).

AÑO 1994

11. *Influence del electrolito en los procesos difusionales a través de películas de pintura.*
C.I. Elsner, R.A. Armas, A.R. Di Sarli.
Anales de las Jornadas SAM'94, Bahía Blanca, Argentina, 7-10 de junio (1994).
12. *An EIS analysis of gradual deterioration of zinc rich paint coatings in sea water by a transmission line model.*
S.G. Real, J.R. Vilche, C.A. Gervasi, A.R. Di Sarli.
Symposium on Electrochemical Impedance Analysis of Geometrically Awkward and Mathematically Complex Structures, San Francisco, California, EE.UU., 22-27 de mayo (1994).
13. *Derniers developpements en peintures antisalissures autopolissantes en Argentine.*
J.C. Benítez, C.A. Giúdice, V. Rascio.
Proceedings 22nd FATIPEC Congress, Vol. III, 214-225 (1994).
14. *Propiedades físicas y mecánicas de productos para la impermeabilización de mampostería y mortero.*
A.C. Aznar, J.J. Caprari, J.F. Meda.
Anales 1º Simposio Argentino de Impermeabilización, Mar del Plata, 17-18 de noviembre, pp. 35-44 (1994).

AÑO 1995

15. *Correlación de parámetros magnéticos con la concentración de óxido ferroso en sedimentos cuaternarios de la localidad de Hernández, La Plata, Provincia de Buenos Aires.*
J.C. Bidegain, R.R. Iasi, R.H. Pérez, R. Pavlicevic.
Anales Cuartas Jornadas Geológicas y Geofísicas Boanerenses, Junín, 15-17 de noviembre (1995).

16. *Influence of binders used in the formulation of zinc rich paints (ZRP) on the performance of the final coatings on naval steel in sea water.*
J.R. Vilche, E.C. Bucharsky, S.G. Real, A.R. Di Sarli.
Proceedings Symposium on Marine Corrosion (T-7C), NACE, Orlando, Florida, EE.UU., 26-31 de marzo (1995).
17. *Electrochemical testing to assess some protective properties of vinyl coatings.*
P. Seré, E.I. Elsner, A.R. Di Sarli, E. Cavalcanti.
Proceedings 18º Congreso Brasileiro de Corrosión, Río de Janeiro, Brasil, 20-24 de noviembre (1995).
18. *Electrochemical evaluation of steel/plasticized chlorinated rubber/sea water systems.*
E. Cavalcanti, O. Ferraz, C.I. Elsner, A.R. Di Sarli.
Proceedings 18º Congreso Brasileiro de Corrosión, Río de Janeiro, Brasil, 20-24 de noviembre (1995).

AÑO 1996

19. *Evaluación electroquímica de los criterios de protección catódica del acero en el hormigón.*
V.F. Vetere, R.O. Batic, R. Romagnoli, I.T. Lucchini, J.D. Sota, R.O. Carbonari
Anales Jornadas SAM'96, San Salvador de Jujuy, Argentina, 11-14 de junio (1996)
20. *Protección anticorrosiva por medio de imprimaciones reactivas a base de taninos.*
V.F. Vetere, R. Romagnoli, J.I. Amalvy, O.R. Pardini
Anales VII Jornadas Argentinas de Corrosión y Protección, Mendoza, Argentina, 17-19 de setiembre (1996).
21. *Variación de la adherencia en la interfase acero-mortero de cemento portland en probetas protegidas catódicamente en función del potencial aplicado.*
O.R. Batic, V.F. Vetere, R. Romagnoli, J.D. Sota, R.O. Carbonari, I.T. Lucchini
Anales VII Jornadas Argentinas de Corrosión y Protección, Mendoza, Argentina, 17-19 de setiembre (1996).
22. *Evaluación de modelos teóricos de soluciones de no-electrolitos en la predicción de índices de retención de Kováts de parafinas en escualano.*
R.C. Castells, C.B. Castells
Anales XXI Congreso Argentino de Química, Bahía Blanca, Argentina, 18-20 de setiembre (1996).
23. *Efecto de la diferencia de viscosidad entre la fase móvil y el pulso inyectado sobre el perfil de elución de un pico de cromatografía líquida.*
R.C. Castells, C.B. Castells
Anales XXI Congreso Argentino de Química, Bahía Blanca, Argentina, 18-20 de setiembre (1996).

24. *Cromatografía gaseosa con temperatura y presión programadas en etapas múltiples.*
F.R. González, A.M. Nardillo
Anales XXI Congreso Argentino de Química, Bahía Blanca, Argentina, 18-20 de setiembre (1996).
25. *Control de la corrosión de estructuras metálicas en ambientes agresivos por medio de sistemas de recubrimiento.*
V. Rascio
Anales Jornadas Especializadas sobre la Corrosión, Buenos Aires, Argentina, 5-6 de setiembre (1996).
26. *Susceptibilidad magnética y concentraciones de FeO en Loess y paleosuelos cuaternarios como indicadores de cambios paleoambientales y paleoclimáticos.*
J.C. Bidegain, R. Pavlicevic, R.R. Iasi, R.H. Pérez
Anales III Congreso de Exploración de Hidrocarburos, Buenos Aires, Argentina, 13-18 de octubre (1996).
27. *Comportamiento anticorrosivo de pinturas vinílicas pigmentadas con fosfato de cinc.*
B. del Amo, R. Romagnoli, V.F. Vetere, L.S. Hernández
Anales XII Congreso Iberoamericano de Electroquímica y IX Encuentro Venezolano de Electroquímica, Mérida, Venezuela, 24-29 de marzo (1996).
28. *Recent developments in miniemulsion polymerization.*
I. Aizpurua, J.I. Amalvy, M.J. Barandiaran, J.C. de la Cal, J.M. Asua
Proceedings IUPAC 2nd International Symposium on Free Radical Polymerization: Kinetics and Mechanisms, Santa Margherita Ligure, Génova, Italia, 26-31 de mayo (1996).
29. *Anticorrosive behavior of paints pigmented with zinc phosphate with EIS.*
B. del Amo, L.S. Hernández, C. López
Proceedings Simposio 13 del International Materials Research Congress, Cancún, México, 1-6 de setiembre (1996).
30. *The use of polymerisable surfactants in emulsion copolymerisation for coatings application.*
J.I. Amalvy, M.J. Unzué, H.A.S. Schoonbrood, J.M. Asua
Proceedings 16th Conference on Waterborne, High Solids and Radcure Technologies, Frankfurt, Alemania, 11-13 de noviembre (1996).

AÑO 1990

1. *Experiencias de cria en laboratorio de **Balanus amphitrite**.*
M. Stupak, M.C. Pérez.
CIDEPINT-Anales, 105-118 (1990).
2. *Revisión de conceptos relacionados con protección catódica y su compatibilidad con esquemas de pintado.*
C. Gervasi, A.R. Di Sarli.
CIDEPINT-Anales, 33-69 (1990).
3. *Análisis de la respuesta potenciométrica de una electrodo metálico bajo diferentes tratamientos para ser empleado en el campo de la Química Analítica.*
R. Romagnoli, V.F. Vetere.
CIDEPINT-Anales, 267-278 (1990).
4. *Parámetros que condicionan el rendimiento de diferentes tipos de arena empleados en operaciones de arenado.*
J.J. Caprari, O. Slutzky, P.L. Pessi, R.E. Pavlicevich.
CIDEPINT-Anales, 71-103 (1990).
5. *La espectrometría de absorción atómica. Conceptos, instrumentación y técnicas.*
R.R. Iasi.
CIDEPINT-Anales, 119-156 (1990).
6. *Granitoides. Depósitos coluviales y desarrollo de suelos complejos en el Cerro El Sombrero, Partido de Lobería, Provincia de Buenos Aires.*
M.C. Camilión, M.A. Zárate, R.R. Iasi.
Ciencia del Suelo, 8 (2), 211-221 (1990).

AÑO 1991

7. *Evaluación de propiedades de piezas de aluminio anodizado aplicando técnicas electroquímicas.*
A.R. Armas, C. Gervasi, A.R. Di Sarli.
CIDEPINT-Anales, 97-106 (1991).
8. *Desarrollo de un sistema para el tratamiento matemático de datos de impedancia.*
V. Ambrosi, A.R. Di Sarli.
CIDEPINT-Anales, 107-158 (1991).

9. *Listado de trabajos sobre corrosión, propiedades y tecnología de pintruas realizados en LEMIT y CIDEPINT, 1948-1990.*
M.I. López Blanco, V.M. Ambrosi.
CIDEPINT-Anales, I-LVIII (1991).
10. *Guía del usuario de un sistema de búsqueda bibliográfica.*
V.M. Ambrosi.
CIDEPINT-Anales, LIX-LXXXIX (1991).
11. *Industria de la pintura y afines.*
V. Rascio, J.J. Caprari.
CIDEPINT-Anales, XCI-CXX (1991).
12. *Estudio de las características de pinturas ricas en cinc aplicando técnicas electroquímicas.*
R.A. Armas, C.A. Gervasi, A.R. Di Sarli, S. Real, J.R. Vilche.
CIDEPINT-Anales, 97-106 (1991).

AÑO 1992

13. *Estudio de la influencia del material a tratar en el resultado de las operaciones de limpieza con chorro de arena.*
J.J. Caprari, O. Slutzky, P.L. Pessi.
CIDEPINT-Anales, 53-79 (1992).
14. *Development of a system for the treatment of electrochemical impedance data.*
V.M. Ambrosi, A.R. Di Sarli.
CIDEPINT-Anales, 81-128 (1992).
15. *A kinetic study of the electroreduction of anodically formed cobalt oxide layers.*
C.A. Gervasi, S.R. Biaggio, J.R. Vilche, A.J. Arvia.
CIDEPINT-Anales, 141-165 (1992).
16. *Pinturas antiincrustantes tipo matriz soluble; influencia de la relación tóxico principal/tóxico de refuerzo sobre larvas de *Balanus amphitrite* y *Polydora ligni*.*
M.C. Pérez, M. Stupak.
CIDEPINT-Anales, 195-211 (1992).
17. *Influencia de la composición del ligante sobre el comportamiento de pinturas antiincrustantes autopulimentables.*
J.C. Benítez, C.A. Giúdice.
Color y Textura, 27, 21-24 (1992).

AÑO 1993

18. *Pinturas antiincrustantes basadas en resinas colofonia y colofonia modificada, esterificadas con óxido de tributil estaño.*
J.J. Caprari, O. Slutzky.
CIDEPINT-Anales, 49-59 (1993).
19. *Chemical and biocidal properties of the cuprous thiocyanate antifouling pigment.*
V.F. Vetere, M.C. Pérez, R. Romagnoli, M.E. Stupak.
CIDEPINT-Anales, 161-172 (1993).
20. *Los fondos difíciles... Pintado y protección del acero galvanizado.*
B. del Amo.
Color y Textura, **31**, 8-10 (1993).

AÑO 1994

21. *Polimerización en emulsión semicontinua del sistema metacrilato de metilo, acrilato de etilo y ácido metacrílico. Caracterización, propiedades del látex y su empleo en la formulación de pinturas emulsionadas.*
J.I. Amalvy.
CIDEPINT-Anales, 147-162 (1994).
22. *Propuesta de un método para la determinación de tensión de adhesión y cohesión de materiales termoplásticos para la demarcación de pavimentos.*
A.C. Aznar.
CIDEPINT-Anales, 215-226 (1994).
23. *Pinturas. Aspectos ecológicos relacionados con su empleo. Impacto ambiental producido por los disolventes, componentes del ligante y aditivos.*
J.J. Caprari.
CIDEPINT-Anales, 227-248 (1994).
24. *Velocidad de evaporación de la fase líquida durante el proceso de secado de ligantes oleorresinosos emulsionados.*
J.J. Caprari, O. Slutzky, P.L. Pessi.
Color y Textura, **32**, 15-18 (1994).
25. *Gas chromatography of aliphatic amines on diatomaceous solid supports modified by adsorption and crosslinking of polyethyleneimines.*
A.M. Nardillo, R.C. Castells.
Anales de la Asociación Química Argentina, **82** (5), 337-345 (1994).
26. *Estudio de la fase líquida de morteros afectados por la reacción alcali agregado.*
O.R. Batic, R. Iasi, R. Pérez, J.D. Sota
Hormigón, **27**, 19-28 (1994).

AÑO 1995

27. *Comportamiento anticorrosivo de pinturas vinílicas pigmentadas con fosfato de cinc.*
B. del Amo, R. Romagnoli, V.F. Vetere, L.S. Hernández.
CIDEPINT-Anales, 157-168 (1995).
28. *Análisis teórico del comportamiento y de métodos electroquímicos utilizados para caracterizar sistemas metal/recubrimiento orgánico/electrolito acuoso.*
A.R. Di Sarli.
CIDEPINT-Anales, 181-251 (1995).
29. *Pinturas retardantes del fuego. Ensayos y clasificación de materiales.*
C.A. Giúdice.
Casa Nueva, Edición N° 84, 72-74, Julio (1995).
30. *Los fondos difíciles... Pintado y protección del acero galvanizado.*
B. del Amo.
Casa Nueva, Edición N° 86, 68-70, Setiembre (1995).
31. *Procesos de corrosión y su relación con el proyecto y diseño de edificios e instalaciones.*
V. Rascio.
Casa Nueva, Edición N° 88, 70-74, Noviembre (1995).
32. *Pinturas. Aspectos ecológicos relacionados con su empleo. Impacto ambiental producido por los disolventes, componentes del ligante y aditivos.*
J. J. Caprari.
Industria y Química, **319**, 31-33 (1995).
33. *Parámetros de utilidad para la medición del comportamiento de pinturas.*
V. Rascio.
Industria y Química, **320**, 46-49 (1995).
34. *Toxicidad en relación con la elaboración y empleo de pinturas. 1ª parte.*
C.A. Giúdice, D.B. del Amo.
Industria y Química, **321**, 38-41 (1995).
35. *Toxicidad en relación con la elaboración y empleo de pinturas. 2ª parte.*
C.A. Giúdice, D.B. del Amo.
Industria y Química, **322**, 22-24 (1995).

AÑO 1996

36. *Effect of the paint application method on adhesion and corrosion resistance of an alkyd coated steel.*
P.R. Seré, D.M. Santágata, C.I. Elsner, A.R. Di Sarli
CIDEPINT-Anales 1996, 1-16.

37. *Study of formulation variables of thermoplastic reflecting materials for traffic marking.*
A.C. Aznar, J.J. Caprari, J.F. Meda, O. Slutzky.
CIDEPINT-Anales 1996, 17-26.
38. *Chemical and electrochemical assessment of tannins.*
V.F. Vetere, R. Romagnoli
CIDEPINT-Anales 1996, 27-40.
39. *Dilute-solution viscosimetry and solution properties of colloidal polymers.*
J.I. Amalvy
CIDEPINT-Anales 1996, 41-52.
40. *Revisión sobre los aspectos biológicos del "fouling".*
M.C. Pérez, M.E. Stupak
CIDEPINT-Anales 1996, 95-154
41. *Comparative corrosion behaviour of 55aluminium-zinc alloy and zinc hot-dip coatings deposited on low carbon steel substrates.*
P.R. Seré, M. Zapponi, C.I. Elsner, A.R. Di Sarli
CIDEPINT-Anales 1996, 175-195.
42. *Reactive surfactants in heterophase polymerization of high performance polymers. VIII. Emulsion polymerization of alkyl sulfopropyl maleate polymerizable surfactants (surfmers) with styrene.*
H.A.S. Schoonbrood, M.J. Unzué, J.I. Amalvy, J.M. Asua
CIDEPINT-Anales 1996, 197-208.
43. *Evaluation of the surface treatment effect on the corrosion performance of paint coated carbon steel.*
D.M. Santágata, P.R. Seré, C.I. Elsner, A.R. Di Sarli
CIDEPINT-Anales 1996, 243-258.
44. *Pinturas. Riesgos involucrados en la elaboración y empleo.*
C.A. Giúdice, B. del Amo
Casa Nueva, Edición N° 90, 70-74, Enero (1996).
45. *Pigmentos inhibidores de la corrosión de bajo impacto ambiental: fosfato de cinc y fosfatos de cinc modificados.*
R. Romagnoli, V.F. Vetere
Industria y Química, **323**, 22-30 (1996).
46. *Métodos para estudiar la corrosión de metales recubiertos con materiales poliméricos.*
A.R. Di Sarli
Industria y Química, **324**, 36-41 (1996).
47. *Demarcación para seguridad del tránsito en rutas y ciudades.*
A.C. Aznar
Revista de Ingeniería, Centro de Ingenieros de la Provincia de Buenos Aires, **136**, 25-29 (1996).

Teniendo en cuenta que algunos trabajos han sido publicados en Anales y en Revistas Internacionales o en Anales y Proceedings de Congresos, se deja constancia que en cada caso se lo menciona sólo una vez, considerando la cita de mayor relevancia.

Se incluyen trabajos realizados en colaboración con investigadores de otros organismos de ciencia y técnica.

(05)
PINT
C37
2807

**ESTE EJEMPLAR SE TERMINO
DE IMPRIMIR EL DIA 30 DE
NOVIEMBRE DE 1996**

CIDEPINT
Centro de Investigación y Desarrollo
en Tecnología de Pinturas
CIC - CONICET
52 e/ 121 y 122 (1900) La Plata

SERVICIOS CALIFICADOS
QUE PRESTA EL CENTRO

- Estudios y asesoramiento sobre problemas de corrosión de materiales en contacto con medios agresivos.
- Estudios y asesoramiento sobre protección de los mencionados materiales por medio de cubiertas orgánicas (pinturas), inorgánicas (silicatos) o metálicas (galvanizado, cromado, niquelado).
- Estudios sobre protección de metales, maderas, hormigones, plásticos, etc., empleados en estructuras de edificios, puentes, diques, instalaciones industriales, instalaciones navales, etc.
- Estudio de medios agresivos.
- Asesoramiento sobre diseño de estructuras y selección de los materiales a utilizar.
- Diseño de esquemas de protección de acuerdo a las diferentes condiciones de servicio.
- Formulación de recubrimientos, para protección de superficies y estructuras.
- Suministro de información sobre tecnología de preparación de superficies metálicas y no metálicas.
- Estudio de operaciones y procesos involucrados en la preparación de pinturas y revestimientos protectores.
- Preparación, a requerimiento de usuarios, de pinturas en escala de laboratorio o de planta piloto.
- Normalización, en casos especiales no cubiertos por IRAM.
- Formación y perfeccionamiento de personal científico calificado.
- Transferencia de conocimientos a la industria, organismos estatales, universidades, etc. a través del dictado de conferencias, cursos, etc.

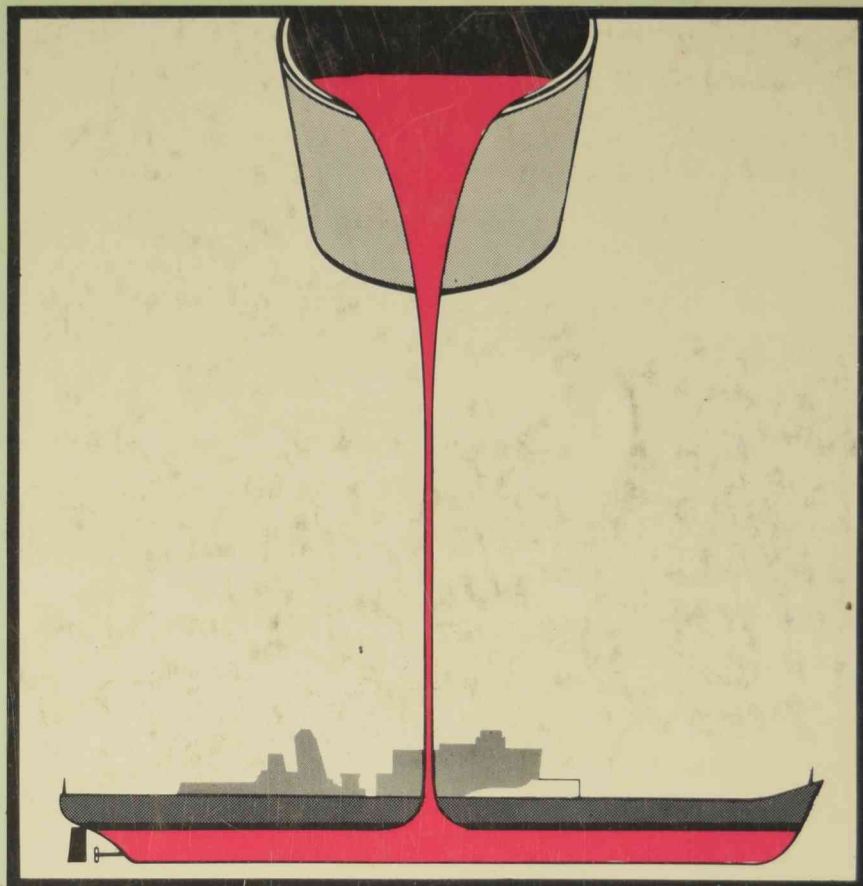
SERVICIOS NO CALIFICADOS

- Control de calidad para la industria de pinturas (pigmentos, aceites, resinas, aditivos, etc.).
- Control de calidad de pinturas, barnices y materiales para revestimiento, a requerimiento de fabricantes o usuarios.
- Ensayos de resistencia a agentes corrosivos o de envejecimiento acelerado.
- Control de calidad de materiales para señalización vial.
- Suministro de documentación a través del servicio de reprografía del Centro.
- Análisis de metales, cementos, cales y materiales para edificios, materiales refractarios y arcillas, minerales, etc.

ci de pint

**Centro de Investigación y
Desarrollo en Tecnología
de Pinturas (CIC-CONICET)**

52 entre 121 y 122
1900 La Plata (Argentina)
Teléfonos (021) 3-1141/44
(021) 21-6214
Télex: CESLA 31216 AR
FAX: 54-21-250471



Investigación y Desarrollo de pinturas anticorrosivas, antiincrustantes y productos especiales para protección industrial, en escala de laboratorio y planta piloto; estudios electroquímicos aplicados a problemas de corrosión de materiales y estructuras.

Control de calidad para la industria de pinturas y materiales afines, asesoramientos, peritajes, etc.